FIELDIANA

Geology

NEW SERIES, NO. 47

The Mammalian Faunas of the Washakie Formation, Eocene Age, of Southern Wyoming. Part IV. The Uintatheres

William D. Turnbull

December 31, 2002
Publication 1519

PUBLISHED BY FIELD MUSEUM OF NATURAL HISTORY

Information for Contributors to Fieldiana

General: *Fieldiana* is primarily a journal for Field Museum staff members and research associates, although manuscripts from nonaffiliated authors may be considered as space permits.

The Journal carries a page charge of $65.00 per printed page or fraction thereof. Payment of at least 50% of page charges qualifies a paper for expedited processing, which reduces the publication time. Contributions from staff, research associates, and invited authors will be considered for publication regardless of ability to pay page charges, however, the full charge is mandatory for nonaffiliated authors of unsolicited manuscripts. Three complete copies of the text (including title page and abstract) and of the illustrations should be submitted (one original copy plus two review copies which may be machine copies). No manuscripts will be considered for publication or submitted to reviewers before all materials are complete and in the hands of the Scientific Editor.

Manuscripts should be submitted to Scientific Editor, *Fieldiana,* Field Museum of Natural History, Chicago, Illinois 60605-2496, U.S.A.

Text: Manuscripts must be typewritten double-spaced on standard-weight, 8½- by 11-inch paper with wide margins on all four sides. If typed on an IBM-compatible computer using MS-DOS, also submit text on 5¼-inch diskette (WordPerfect 4.1, 4.2, or 5.0, MultiMate, Displaywrite 2, 3 & 4, Wang PC, Samna, Microsoft Word, Volkswriter, or WordStar programs or ASCII).

For papers over 100 manuscript pages, authors are requested to submit a "Table of Contents," a "List of Illustrations," and a "List of Tables" immediately following title page. In most cases, the text should be preceded by an "Abstract" and should conclude with "Acknowledgments" (if any) and "Literature Cited."

All measurements should be in the metric system (periods are not used after abbreviated measurements). The format and style of headings should follow that of recent issues of *Fieldiana.*

For more detailed style information, see *The Chicago Manual of Style* (13th ed.), published by The University of Chicago Press, and also recent issues of *Fieldiana.*

References: In "Literature Cited," book and journal titles should be given in full. Where abbreviations are desirable (e.g., in citation of synonymies), authors *consistently* should follow *Botanico-Periodicum-Huntianum* and *TL-2 Taxonomic Literature* by F. A. Stafleu & R. S. Cowan (1976 *et seq.*) (botanical papers) or *Serial Sources for the Biosis Data Base* (1983) published by the BioSciences Information Service. Names of botanical authors should follow the "Draft Index of Author Abbreviations, Royal Botanic Gardens, Kew," 1984 edition, or *TL-2.*

References should be typed in the following form:

Croat, T. B. 1978. Flora of Barro Colorado Island. Stanford University Press, Stanford, Calif., 943 pp.

Grubb, P. J., J. R. Lloyd, and T. D. Pennington. 1963. A comparison of montane and lowland rain forest in Ecuador. I. The forest structure, physiognomy, and floristics. Journal of Ecology, **51:** 567–601.

Langdon, E. J. M. 1979. Yagé among the Siona: Cultural patterns in visions, pp. 63–80. In Browman, D. L., and R. A. Schwarz, eds., Spirits, Shamans, and Stars. Mouton Publishers, The Hague, Netherlands.

Murra, J. 1946. The historic tribes of Ecuador, pp. 785–821. In Steward, J. H., ed., Handbook of South American Indians. Vol. 2, The Andean Civilizations. Bulletin 143, Bureau of American Ethnology, Smithsonian Institution, Washington, D.C.

Stolze, R. G. 1981. Ferns and fern allies of Guatemala. Part II. Polypodiaceae. Fieldiana: Botany, n.s., **6:** 1–522.

Illustrations: Illustrations are referred to as "figures" in the text (not as "plates"). Figures must be accompanied by some indication of scale, normally a reference bar. Statements in figure captions alone, such as "×0.8," are not acceptable. Captions should be typed double-spaced and consecutively. See recent issues of *Fieldiana* for details of style.

All illustrations should be marked on the reverse with author's name, figure number(s), and "top."

Figures as submitted should, whenever practicable, be 8½ by 11 inches (22 × 28 cm) and may not exceed 11½ by 16½ inches (30 × 42 cm). Illustrations should be mounted on boards in the arrangement to be obtained in the printed work. This original set should be suitable for transmission to the printer as follows: Pen and ink drawings may be originals (preferred) or photostats; shaded drawings must be originals, but within the size limitation; and photostats must be high-quality, glossy, black and white prints. Original illustrations will be returned to the corresponding author upon publication unless otherwise specified.

Authors who wish to publish figures that require costly special paper or color reproduction must make prior arrangements with the Scientific Editor.

Page Proofs: *Fieldiana* employs a two-step correction system. The corresponding author will normally receive a copy of the edited manuscript on which deletions, additions, and changes can be made and queries answered. Only one set of page proofs will be sent. All desired corrections of type must be made on the single set of page proofs. Changes in page proofs (as opposed to corrections) are very expensive. Author-generated changes in page proofs can only be made if the author agrees in advance to pay for them.

♾ This paper meets the requirements of ANSI/NISO Z39.48-1992 (Permanence of Paper).

FIELDIANA

Geology

NEW SERIES, NO. 47

The Mammalian Faunas of the Washakie Formation, Eocene Age, of Southern Wyoming. Part IV. The Uintatheres

William D. Turnbull

Curator Emeritus
Department of Geology
Field Museum of Natural History
1400 So. Lake Shore Drive
Chicago, Illinois 60605-2496
U.S.A.

Accepted December 10, 1999
Published December 31, 2002
Publication 1519

PUBLISHED BY FIELD MUSEUM OF NATURAL HISTORY

ISSN 0096-2651
PRINTED IN THE UNITED STATES OF AMERICA

The beautifully preserved Funderburk skull of *Uintatherium anceps,* PM 53933 (FMNH neg. nos. GEO 85354 and 85355).

Table of Contents

PREFACE 1
INTRODUCTION 6
MATERIAL AND ABBREVIATIONS 13
METHODS, SYSTEMATICS, MORPHOLOGY, AND MATERIALS 14
Methods 14
Systematics 15
Morphology 15
Holotype 15
Distribution 15
Revised Diagnosis 15
Materials 19
Uintatherium anceps 19
Skull, Jaws, and Dentition 19
Skull and Upper Dentition 21
Basicranium, Ear Region, and Endocranial Features, *Uintatherium* and *Eobasileus* 46
Jaws and Lower Dentition 60
Postcranium (Both Taxa) 76
Axial Skeleton 76
Appendicular Skeleton 80
Eobasileus cornutus 93
Holotype 93
Distribution 93
Diagnosis 93
Skull and Upper Dentition 93
Jaws and Lower Dentition 104
Feces 112
The Status of *Tetheopsis* 116
PALEOBIOLOGY 117
Estimating Uintathere Body Size 119
Pachyostosis: Another Partial Analogue? 123
SUMMARY AND CONCLUSIONS 128
ACKNOWLEDGMENTS 133
LITERATURE CITED 134

List of Illustrations

Frontispiece: Anterolateral and ventrolateral views of the Funderburk skull (PM 53933)

1. Distribution map 2
2. Skull lengths 4
3. Skull proportions 8
4. Strata 10
5. *Uintatherium anceps* skull (PM 53933) 16
6. Skull and jaw measurements 18
7. Method of cheek tooth measurements ... 20
8. Stereographic view of ventral side of partial skull of a newborn *U. anceps* specimen, PM 3896 23

9 and 10. Medial, lateral, and two X-ray views of newborn *U. anceps* skull, PM 3896 ..... 24, 25

11. Juvenile skull of *U. anceps,* PM 8019 26
12. Partial skull of juvenile *U. anceps,* PM 55406A 28
13. Jaw fragments, upper dentition, PM 53933 31
14. Ventral and dorsal views of a vandalized *U. anceps* skull, PM 1666 32
15. Right lateral, dorsal, and ventral views of *U. anceps,* PM 1667 34
16. Fragmentary skull and jaws of an adult *U. anceps,* PM 55406B, associated with one of the juvenile specimens 36
17. Dorsal and ventral views of fragment of *U. anceps* skull, PM 53921, associated with a disarticulated partial skeleton 38
18. Associated nasals and lower incisor teeth, PM 8020, and an isolated right M2 from the Piceance Creek Basin 39
19. Ventral and left lateral views of AMNH 1664 (skull); right lateral and ventral views of AMNH 1694 (skull) 40
20. Ventral and left ventrolateral views of AMNH 1671 (skull) 41
21. Ventral and left lateral views of AMNH 2366 (skull); right lateral and ventral views of AMNH 1689 (skull) 42
22. Dorsal, right lateral, and ventral views of AMNH 1693 (skull) 43
23. Right lateral and ventral views of skull of *Tinoceras* (*Laoceras*) *pugnax* Marsh, 1885 (synonym of *U. anceps*): YPM 11044 44
24. Ventral, right lateral, and dorsal views of PUM 10298, the Princeton skull of *Elachoceros parvum* Scott, 1886 45
25. Plots of upper cheek teeth (length × anterior width) of *U. anceps.* 47
26. Stereo view of basicranial region of skull of holotype of *U. robustum* Leidy, 1872 (synonym of *U. anceps*), ANSP 12607 50
27. Basicranial region of a Field Museum partial skull of *U. anceps,* PM 1667 52
28. Stereo view of basicranial region of two specimens of *U. anceps*: USNM

18599 (partial skull) and Funderburk skull (PM 53933) 54
29. Basicranial region of *Eobasileus cornutus*, P 12170 56
30. Basicranial region of *U. anceps*, PUM 10298 and AMNH 2366 58
31. Juvenile jaws of *U. anceps*, AMNH 1678 62
32. Occlusal view of lower jaws of *U. anceps*, PM 54801 and PM 55174 64
33. Partial left ramus of a subadult specimen of *U. anceps* 65
34. Jaws of of *U. anceps*, AMNH 13151 and PM 53933 66
35. Edentulous symphyseal fragment of *U. anceps*, PM 38781 67
36. Jaws of a young adult, probably female, *U. anceps* specimen, PM 55827 68
37. Fragmented jaws of *U. anceps* with fair cheek dentition 69
38. Two American Museum specimens of *U. anceps*, AMNH 1664A and B. AMNH 1664A, shown in C, is edentulous. AMNH 1664B, shown in A and B, has its left ramus lacking teeth, its right with p3-m3. 70
39. Mandibular rami of *Tinoceras pugnax* (synonym of *U. anceps*), YPM 11044; p4–m3 of UM 101209 71
40. Bivariate plots (length × anterior width) of lower cheek teeth dimensions in *U. anceps* 77
41. Early-stage unfused vertebral elements of *U. anceps*, PM 3896 78
42. Early-stage unfused elements of *U. anceps*, PM 3896 80
43. Cervical and other vertebrae of the articulated, partial adult skeleton of *U. anceps*, PM 55423 82
44. Articulated portion of rib cage of PM 55423 84
45. Articulated right front limb of PM 55423 85
46. Scapula of newborn *U. anceps* specimen, PM 3896; Humerus of adult specimen, PM 2079 86
47. Articulated forelimb of *U. anceps*, PM 39393 87
48. Dorsal view of articulated partial left manus of *Eobasileus cornutus*, PM 3212 88
49. Left ilium of newborn *U. anceps*, PM 3896 89
50. Adult pelvis and sacrum of *U. anceps*, PM 3894; tibia of an adult, PM 38782 90
51. Dorsal view of adult *U. anceps* pelvis, PM 53921, and associated femur 91
52. Articulated partial right hind limb of PM 55423 94
53. Articulated partial hind foot of *E. cornutus*, PM 3212; articulated partial hind limb of *U. anceps*, PM 39393 95
54. Ventral and left lateral views of Cope holotype specimen of *E. cornutus*, AMNH 5040 96
55. Right lateral and ventral views of the Abbott/Riggs *E. cornutus* skull from the Uinta Basin, P 12710 98
56. Partial skull of *E. cornutus* from the Uinta Basin, P12164; isolated teeth from the Washakie Fm. 100
57. University of Wyoming's *E. cornutus* skull, UWM 13644; University of Washington's Burke Museum specimen, UWBM 59204 101
58. Pieces of AMNH 13149 in a previously unopened jacket 102
59. Anterolateral view of skull and jaws of *Uintacolotherium blayneyi* Cook (= *E. cornutus*), DMNH 496 105
60. Partial skull and jaws of *Tinoceras annectens* Marsh (= *E. cornutus*), YPM VP 11043 106
61. Bivariate plots (length × anterior width) of upper cheek teeth of *E. cornutus* 107
62. Lower jaws and dentition of *E. cornutus*, PM 1737 108
63. Lower jaw of *E. cornutus*, UCMP 81356 110
64. Occlusal view of mandible of E. cornutus with a worn dentition, CMNH 29493 111
65. Bivariate plots (length × posterior width) of lower cheek teeth of *E. cornutus* 113
66 and 67. Comparisons of plots of upper and lower cheek teeth of *U. anceps* and *E. cornutus* 114
68. Fecal mass, probably from *E. cornutus*, PM 59510 116
69. Damuth's body cylinder concept 120
70 and 71. Cheek tooth comparisons of large living mammals with *U. anceps* .. 124
72. Midshaft cross section of *U. anceps* femur, PM 39393, showing early pachyostosis 126

73. Three modern sirenians: *Trichechus* (small, bunolophodont cheek teeth), *Dugong* (small hypsodont teeth), and *Hydrodamalis* (no teeth) 130
74. Uintathere habit and habitat cartoon 132

List of Tables

1. Skull measurements for *U. anceps* 140
2. Jaw measurements for *U. anceps* 142
3. Skull measurements for *E. cornutus* 144
4. Jaw measurements for *E. cornutus* 146
5. Measurements of upper teeth of *U. anceps* 148
6. Measurements of lower teeth of *U. anceps* 154
7. Rib measurements of *U. anceps,* PM 55423 165
8. Measurements of scapula and humerus of *U. anceps* and *E. cornutus* 166
9. Measurements of radius and ulna of *U. anceps* and *E. cornutus* 168
10. Measurements of pelvis and femur of *U. anceps* and *E. cornutus* 170
11. Measurements of patella, tibia, and fibula of *U. anceps* and *E. cornutus* 173
12. Measurements of astragalus and calcaneum of *U. anceps* and *E. cornutus* 176
13. Measurements of upper teeth of *E. cornutus* 178
14. Measurements of lower teeth of *E. cornutus* 180
15. Upper dentitions of specimens from the transition zone compared with those of *U. anceps* and *E. cornutus* 182
16. Pelvic width measurements of *U. anceps* compared with those of elephants, mammoth, mastodon, several rhinoceroses, and hippopotami 183
17. Skull, jaw, and cheek-tooth-row lengths of *U. anceps* and *E. cornutus* compared with the same suite of gigantic mammals as in Table 16 184
18. Long bone dimensions of *U. anceps* and *E. cornutus* compared with the same suite of gigantic mammals as in Table 16 187
19. Head–body length 189

Related Publications

Prior numbers in this series are:

Part I. Introduction, by W. D. Turnbull. Fieldiana: Geology, **33**(30): 569–601, 1978.

Part II. *Protoptychus hatcheri* Scott, 1895, by W. D. Turnbull. Fieldiana: Geology, n.s., **21**: 1–33, 1991.

Part III. Perissodactyls from the Washakie Formation (middle-late Eocene) Washakie Basin, Wyoming, by S. M. McCarroll, J. J. Flynn, and W. D. Turnbull. Fieldiana: Geology, n.s., **33**: 1–38, 1996.

Other related contributions have included:

1. W. D. Turnbull. 1972. The Washakie Formation of Bridgerian-Uintan Ages, and the related faunas, pp. 20–31. *In* Field Conference, Tertiary Biostratigraphy, Southern and Western Wyoming, ed. R. M. West. Garden City, New York.
2. J. J. Flynn. 1986. Correlation and geochronology of Middle Eocene strata from the western United States. Palaeogeography, Palaeoclimatology, Palaeoecology, **55**: 335–406.
3. L. Krishtalka, M. C. McKenna, R. M. West, C. C. Black, M. R. Dawson, J. J. Flynn, W. D. Turnbull, R. K. Stucky, T. M. Bown, D. J. Golz, and J. A. Lillegraven. 1987. Eocene biochronology of North America, pp. 77–117. *In* Cenozoic Mammals of North America: Geochronology and Biostratigraphy, ed. M. O. Woodburne. University of California Press, Berkeley.
4. W. D. Turnbull and D. M. Martill. 1988. Taphonomy and preservation of a monospecific titanothere assemblage from the Washakie Formation (Late Eocene), Southern Wyoming: An ecological accident in the fossil record. Palaeogeography, Palaeoclimatology, Palaeoecology, **63**: 91–108.
5. S. M. McCarroll, J. J. Flynn, and W. D. Turnbull. 1993. Biostratigraphic and magnetic polarity correlations of the Washakie Formation, Washakie Basin, Wyoming. Journal of Vertebrate Paleontology, **13**(Suppl. 3), Abstracts, 49a.
6. W. D. Turnbull. 1993. Additions to knowledge of the uintatheres of the Washakie Formation and aspects of their biology. Journal of Vertebrate Paleontology, **13**(Suppl. 3), Abstracts, 60a.
7. S. M. McCarroll. 1994. Perissodactyls from the Washakie Formation (Middle-Late Eocene), Washakie Basin, Wyoming. Journal of Vertebrate Paleontology, **14**(Suppl. 3), Abstracts, 37A.
8. W. D. Turnbull. 1995. The problem of the uintatherium molars (once more), pp. 261–265. In R. J. Radlanski and H. Renz, eds., Proceedings of the 10th

International Symposium on Dental Morphology. C & M Brünne Gbr., Berlin.
9. S. M. McCarroll. 1995. An early Uintan fauna from the upper unit of the Adobetown Member, Washakie Formation, Washakie Basin, Wyoming. Journal of Vertebrate Paleontology, **15**(Suppl. 3), Abstracts, 42A.
10. S. M. McCarroll, J. J. Flynn, and W. D. Turnbull. 1996. A review of the biostratigraphic and magnetic polarity correlations of the Washakie Fm. (Bridgerian and Uintan Ages), Washakie Basin, Wyoming, pp 25–39. *In* D. Prothero and R. J. Emry, eds., The Terrestrial Eocene-Oligocene Transition in North America. Cambridge University Press, Cambridge, 688 pp.
11. D. S. G. Covey and S. M. McCarroll. 1996. The artiodactyl fauna of the Washakie Formation, Eocene Age, of southwestern Wyoming. Journal of Vertebrate Paleontology, **16**(Suppl. 3), Abstracts, 29A.
12. S. M. McCarroll and W. D. Turnbull. 1996. A Late Bridgerian fauna from the Kinney Rim Member of the Washakie Formation, Washakie Basin, Wyoming. Journal of Vertebrate Paleontology, **16**(Suppl. 3), Abstracts, 51A–52A.
13. S. E. Foss, W. D. Turnbull, and L. Barber. 2001. Observations on a new specimen of *Achaenodon* (Mammalia, Artiodactyla) from the Eocene Washakie Formation of southern Wyoming. Journal of Vertebrate Paleontology, **21**(3), Abstracts, 51A.

The Mammalian Faunas of the Washakie Formation, Eocene Age, of Southern Wyoming. Part IV. The Uintatheres

William D. Turnbull

Preface

Few fossil mammals have had as bizarre a history as the uintatheres. They are truly unique in their own right as one of the earliest land mammals to reach gigantic size and because of their distinctive morphology. Misinterpreted from the start, these end members of the dinoceratan line became the focus of a lifelong rivalry between two famous paleontologists that fostered much hasty publication and left a legacy of taxonomic confusion.

Uintatheres have been known since Othniel C. Marsh described the first specimen (1871), which he understandably mistook for a new titanothere (*Titanotherium ? anceps*).[1] The following year, Joseph Leidy (1872a,b) named *Uintatherium robustum* on August 1, and on August 19, both Edward Drinker Cope (1872a) and Marsh (1872a) published new names for uintatheres, *Lefalophodon* (= *Loxolophodon* for the species *L. cornutus, L. furcatus,* and *L. pressicornis,* all = *Eobasileus cornutus*) and *Tinoceras grande* (= *U. anceps*), respectively. Within less than a year, Cope and Marsh had entered into a competitive race to name the greatest number of new taxa: according to Wheeler (1961), each published 16 "really different" articles on the extinct Order Dinocerata, the order to which the uintatheres belong. Wheeler went on to state that "Leidy, Cope and Marsh each proposed two genera. Leidy proposed two species, Cope three, and Marsh four" (p. 5). In this whirlwind of publication, objectivity often got lost. The feud that developed between Cope and Marsh began with, and centered on, the uintatheres and prevailed throughout much of their subsequent work. Another study by Wheeler (1960) reports this unfortunate yet fascinating episode in considerable detail, as does one by Romer (1964), which gives a slightly different perspective.

The origins of the Dinocerata are unclear. Being one group within the early specialized adaptive radiations of the placental mammals, they began as midsized animals (derived from smaller ancestors) and ended in the gigantic descendant species that are my direct concern here. The Order Dinocerata, which died out in the late Eocene, has no close living relatives. Nor do any extant mammals serve as good biological analogues. Schoch and Lucas (1985), the most recent reviewers of the order, essentially follow Wheeler (1961), the prior reviewer, who gave a thorough accounting of all of the then known taxa. Prior to that study, the Marsh monograph (1886) was the work to turn to, and still is for its descriptive anatomy and illustrations. The Schoch and Lucas (1985) work filled the gap between their report and Wheeler's (1961) revision, documenting new materials and extending their study to include within its systematic section a cladistic analysis that formally united the Orders Dinocerata and Xenungulata within their new Mirorder Uintatheriamorpha. I have nothing new to offer in this regard and so merely refer the reader to that work for the full details.

The same can be said for coverage of the geographic distribution and geochronologic occurrence of the order. For my purpose here, it will suffice to note that Uintatheres have been found on two continents, Asia and North America, and that the distribution is disjunct (Fig. 1), there being no reported remains thus far from either western Canada or Alaska, on the one hand, or from western Asia and Europe or eastern North America on the other. Figure 1 is modified from Schoch and Lucas (1985), combining their figures 1 and 2, where each of the areas is identified. The starred dot in the Wyoming portion of the North American section of Figure 1 indicates the Washakie Basin. The earliest identified Uintathere remains are from Upper Paleocene deposits of both regions (Late Paleocene age), when they had already diversified into three genera. All of the terminal genera, *Gobiatherium, Uintatherium, Tetheopsis,* and *Eobasileus,* are from Mid-Upper Eocene deposits of Mid-Late Eocene age. Of these,

[1] For further details see Wheeler (1961).

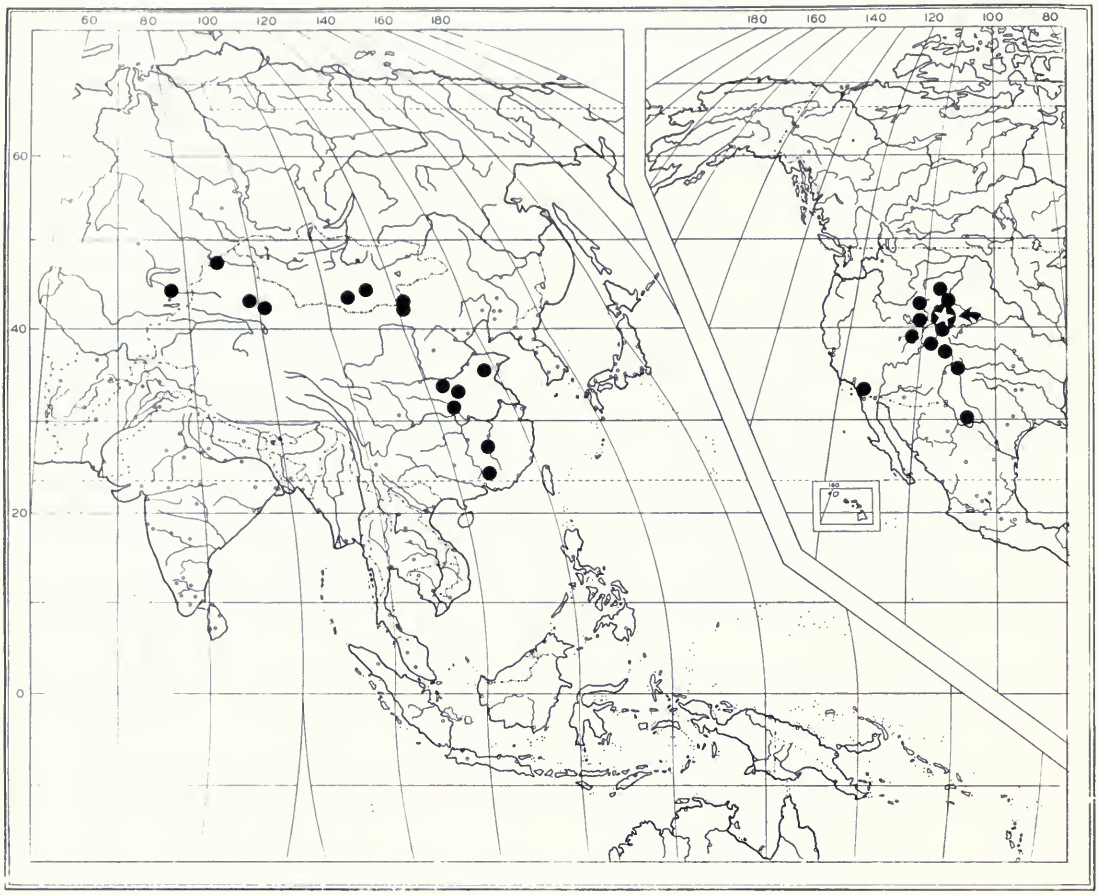

FIG. 1. Distribution map for the Dinocerata, modified from Schoch and Lucas (1985). They provide details for each of the Asian and North American localities. The one important here, the Washakie Basin of southwestern Wyoming, is starred.

Note the disjunct nature of the distribution—approaching halfway around the world in either east or west direction at the present time. In the Paleocene and Eocene, however, the European connection was much closer than it is today because the North Atlantic was just beginning to form, yet there are no records from either eastern North America or western Asia or Europe, a gap of about 180° (i.e., between over 105°W and almost 75°E), which would be expected if the European route was the one used. The present 125° gap between 120°E and 115°W, across Beringia, is also a great distance with no record.

the first two (*G.* and *U.*) are from Asia. The last three (*U., T.,* and *E.*), which were accepted by both recent reviewers, are from North America. The Washakie Basin is the only place where all three are reported together. In their study, Schoch and Lucas (1985, p. 44) criticized Wheeler (1961) for neglecting "to either justify his synonymies or to describe the morphology of the taxa in any detail. For example, Wheeler (1961) considered no less than twenty-eight named species of large North American uintatheres to be synonyms of *Uintatherium anceps* without ever explicitly documenting these synonymies." This was fair for the species-level taxonomy, the point of the Schoch and Lucas (1985) criticism. Previously, Wheeler (1955, p. 1699) had given his brief characterization of the genera as follows:

> *Uintatherium* Leidy, 1872, is a large middle Eocene form with a mesocephalic[2] skull. *Tetheopsis* Cope, 1885, a very large form from the uppermost middle Eocene and lowermost upper Eocene, has a dolichocephalic skull. *Eobasileus* Cope, 1872, from the upper Eocene, is the largest uintathere known and has the most dolichocephalic skull.

Wheeler was trying to sort out and cope with the many hastily named, often poorly documented, and usually misinterpreted materials. Essentially, what Wheeler did was to focus on the species of the three genera with remains that he believed to be adequate to base diagnoses upon. This accomplished, he was able to differentiate the genera on skull size and horn and cranial crest development and proportions—a tremendous advance over the prior confusion, even if a bit naive in some respects (see below). Schoch and Lucas (1985) closed their paragraph as follows: "However, it appears that at a generic level, Wheeler's (1961) revision is valid and we accept the genera that he recognized and defined as valid, although they may be in need of revision at the specific level" (p. 44).

It is against this background that I treat the Washakie uintatheres which are, in the Schoch and Lucas (1985) scheme, all within the Tribe Uintatheriini, Subfamily Uintatheriinae of the Family Uintatheriidae (see below). Three genera constitute this tribe, *Uintatherium, Tetheopsis,* and *Eobasileus.* All are reported in the Washakie Formation, and they are all truly large, about the size of the largest living rhinoceroses. The three genera each show strong sexual dimorphism, with the males being larger and heavier, especially in their cranial protruberances or "horns" and related crests. Both sexes have inframandibular processes, which are reported to be well developed in the males of all three genera and in females of *Uintatherium* but rudimentary in *Tetheopsis* and *Eobasileus* females. Whether this is a primary condition for those females or a reversion is uncertain, for in other regards those genera are considered to be more specialized than *Uintatherium.*

I began this study by plotting skull lengths for all 34 of the adult specimens listed by Wheeler (1961, p. 78, chart 3) onto a standard distribution chart (Simpson & Roe, 1939). This gave two peaks (Fig. 2A).The group of short skulls had a peak at the 5th decile class, composed of 27 or 28 specimens (including one, possibly two, that Wheeler assigned to *Tetheopsis*). The group of larger skulls, composed of six or seven specimens (including three, possibly four of Wheeler's *Tetheopsis*), had a peak in the 10th decile class. All of the skulls Wheeler considered to belong to *Uintatherium* were within the shorter group, and those considered to be *Eobasileus* were in either the 8th or 10th decile classes at the large end of the chart. The five *Tetheopsis* skulls fell into deciles 5, 7, and 10, the first two with one specimen each and the last with three (Fig. 2A).

How to interpret this picture? I began to suspect that something was amiss with *Tetheopsis.* The peaks suggest that the three that fall into the 10th decile class could be *Eobasileus,* while the smallest could be *Uintatherium.* That leaves only one specimen in the 7th decile class, which could be either but would most probably be *Uintatherium* if indeed the five *Tetheopsis* skulls should be reidentified. Figure 2B shows the same graph with added FMNH specimens (three juveniles and one adult), and a previously undescribed adult skull, UW 13644.

Turning next to Wheeler's (1961, p. 26) analysis of cranial proportions based on skull length and horn positions, I initially believed this to be a great advance. My instant enthusiasm for the scheme had to be tempered somewhat when I realized that because of the nature of the heterogonic growth directions and rate patterns, the neat diagnostic relationships between the regions A, B, and C was somewhat less clear-cut than Wheeler stated it to be. This is because in youth, maxillary and parietal horns grow away from one another; then, throughout most of adulthood, they grow more nearly straight upward; and in senility they

[2] I consider them all to be dolichocephalic, with *Eobasileus* being the most and *Uintatherium* the least so.

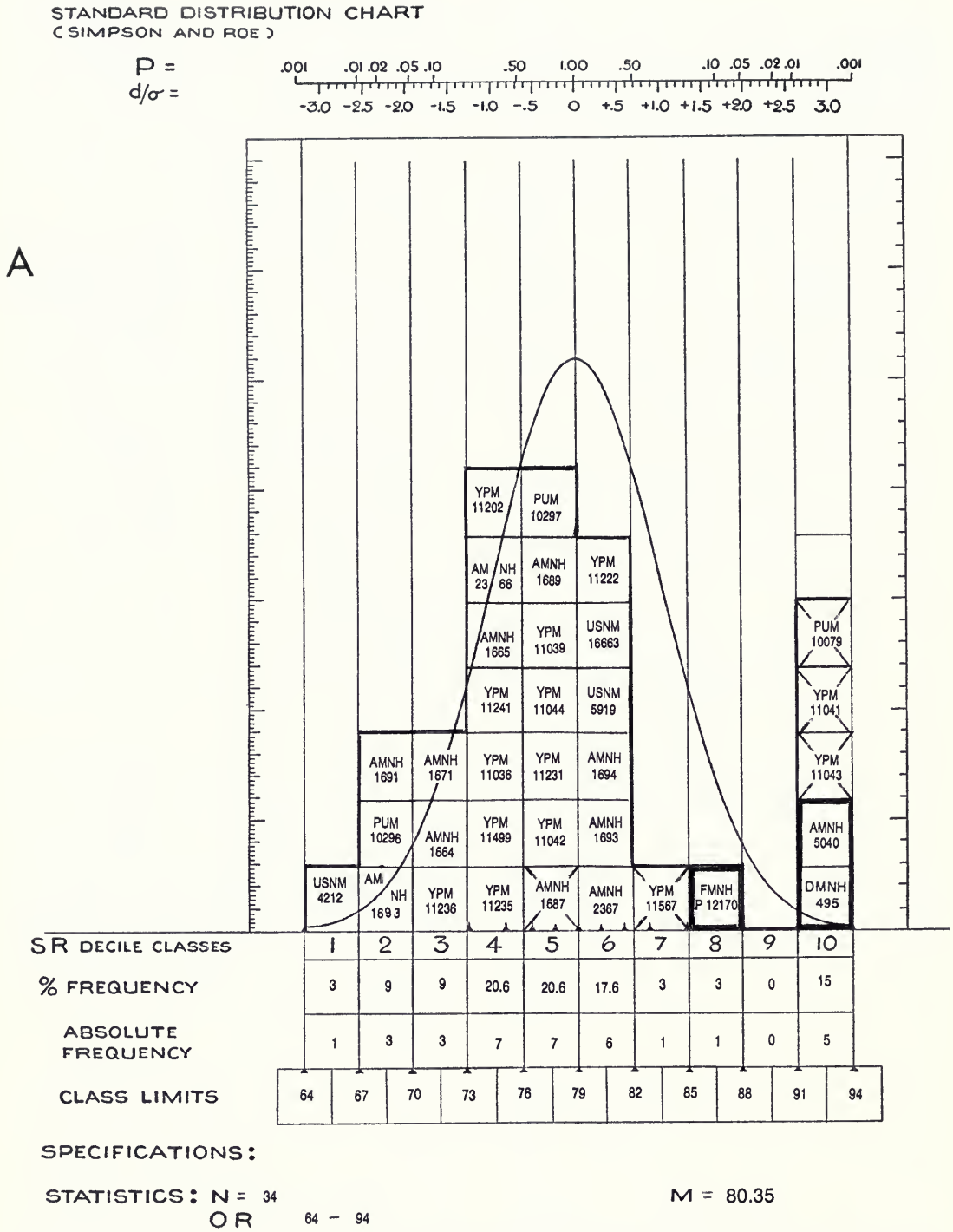

FIG. 2. **A,** Skull lengths of all 34 of the then-known adult skulls of the three terminal North American genera as given by Wheeler (1961), plotted on a standard distribution chart. This shows two distinct peaks, not three (although one of them is broad enough to be blending two together), and not the normal curve to be expected if all had been from a single species. Most specimens (26 in all) are *Uintatherium* by Wheeler's assignments (the blocks with only specimen numbers), all of which fall within the decile classes 1–6. A few (three) are *Eobasileus* (blocks with dark outline), in decile classes 8 and 10, at the upper end of the scale. *Tetheopsis* (blocks with X) is suspect; its five

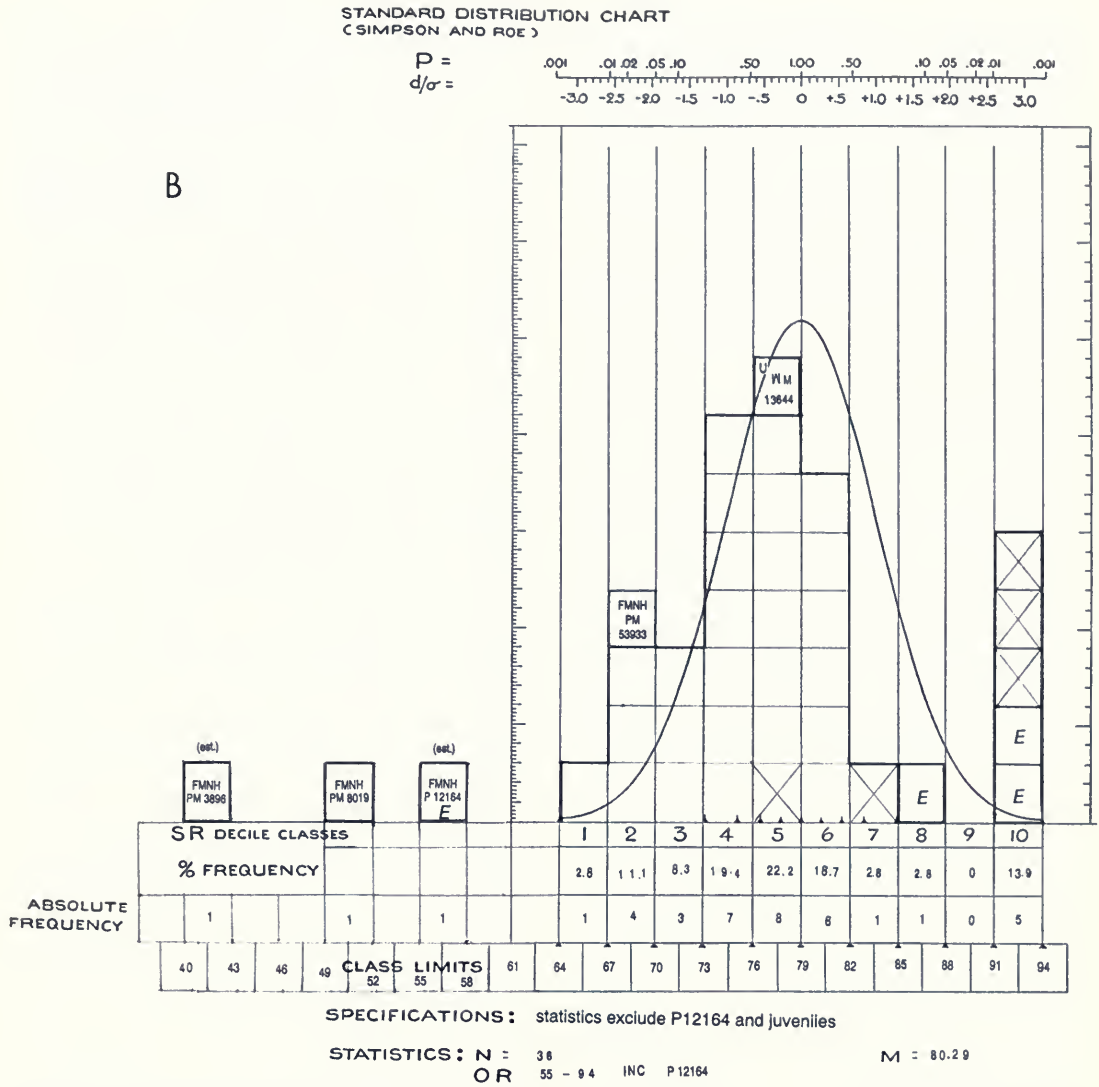

FIG. 2 (*Cont.*) specimens fall as follows: three with the *Eobasileus* in decile class 10, one well within *Uintatherium* in decile class 5, and one in between the others in class 7.

B, The same, but with a slightly increased adult sample size of 37 and the addition of two juveniles. The three added adult specimens are the complete FMNH young adult skull (PM 53933), the new University of Wyoming skull with a heavily worn dentition (UW 13644), and the cranially aberrant specimen that Wheeler had assigned to *Eobasileus* on the basis of tooth dimensions (P 12164). It was not included in either Wheeler's chart or in (**A**) above. I include it here (its length being minimally estimated) along with the two juvenile specimens (PM 3896, a near-newborn whose length is also estimated, and PM 8019). Neither the juveniles nor P 12164 are included in the adult statistics for reasons given in the text. The UW specimen is remarkable in that it falls clearly within the *Uintatherium* peak for skull length, whereas most of its dentition falls within the plots of *Eobasileus* teeth, as do its skull proportion ratios (see text).

begin to approach one another, thus tending toward restoration of the youthful proportions (Fig. 3). As far as I can tell, the blurring of these cranial proportions is not extreme enough to be a problem because the values for the two genera are too far apart for this to be a significant factor. Curiously, Wheeler's figure 1 (modified here in my Figure 3) is somehow incorrect in that he states that it is based on the outline of a specimen of *U. anceps,* which should, according to Wheeler, have a B/A ratio between 1.5 and 2.2. The figure itself has a B/A ratio of 3.0.

Introduction

I have three main goals in mind with this work: (1) to document all of the Field Museum materials of the North American terminal genera of the Order Dinocerata, as well as most of the heretofore unreported specimens in other collections, especially the more important of them; (2) to expand our understanding of the morphology and systematics of those genera; and (3) to learn as much as possible about their biology as can be inferred from their remains and from consideration of partial analogues among living large terrestrial ungulates and sirenians.

The uintatheres of the Washkie Formation (Bridgerian- and Uintan-age deposits within the Washakie Basin, Sweetwater County, southwest Wyoming) occur within the deposits of both ages, with the greatest frequency in the Lower Brown Sandstone unit of Granger (1909). Several workers have made detailed studies of the formation, documenting its stratigraphy, general geologic features, and its faunas: Bradley (1945, 1964); Cope (1884); Flynn (1983, 1988); Granger (1909); Hayden (1873, 1874—both with Cope contributions); Johannsen (1914); King (1878); Marsh (1872a,b, 1886); Matthew (1909); Maugher (1977); McCarroll (1995); McCarroll, et al. (1996a,b); Osborn (1907, 1909); Osborn and McMaster (1881); Osborn and Speir (1879); Roehler (1969, 1972, 1973, 1985, 1992a,b); Scott (1937); Sinclair (1909); Sullivan (1980); Turnbull (1972, 1978, 1991, 1993); Turnbull and Martill (1988); Wheeler (1961); and Wortman (1901).

The Washakie Basin is a 2,500 square mile (6,475 square kilometer), high, structural and topographic intermontane Tertiary basin in SW Wyoming (Bradley, 1945; Love, 1961; Roehler, 1972, 1992a,b; Turnbull, 1978). It has been a structural basin at least since Late Cretaceous times, with Lance, Fort Union, Wasatch, and Green River Formations (Fms.) underlying the Bridgerian-Uintan-age Washakie Fm. The Hartt Cabin Bed of the Laney Member of the Green River Fm. intertongues with the Kinney Rim Member of the Washakie Fm. Late Pleistocene-Holocene deposits (not shown) are scattered between the crests of more resistant older deposits in a thin covering veneer (alluvium and dunes). Stratigraphic detail has been presented by Granger (1909), Wheeler (1961), Roehler (1969, 1972, 1985, 1992a,b), and Turnbull (1978). The concepts of the latter two authors in the mid-1970s were summarized in Turnbull (1978), in which Roehler's cross section of the basin is given (pp. 574–575), along with a correlation chart that related the Granger and Roehler-Turnbull interpretations to Eocene provincial ages and their subdivisions.

That chart is greatly modified here (Fig. 4) to show both Roehler's (1992b) correlations of Middle and Upper Eocene lithostratigraphic units of Washakie and Green River Basins (left side) and to expand the Washakie Fm. portion of the Eocene so as to stress its major marker units (dark bars, with Roehler's designated bed numbers). The marker beds that I have found to be the most useful are emphasized in black: Flock of Sheep Limestone (Bed 502) in the uppermost part of the Laney; Light-Gray Tuff (515) and Tan-White Tuff (540) in the Kinney Rim Member (Roehler, 1973); Robin's Egg Blue (579) and Middle Red (596-604) in the lower part of the Adobe Town Member; and Granger's Bed 11 (= 622), and Rose Red (644) in the middle part. All can be traced for at least 2 miles to more than 10 miles in continuous outcrop, and for even greater distances across eroded or covered gaps. Granger's Bed 11, the Middle Red, and the Rose Red are the most extensive, and four of the marker beds (515, 540, 579, 622) have major ashfall components to their makeup.

It should be noted here that the marker beds are the only ones that can be closely related to either provincial age or paleomagnetic boundaries. For correlation, most intervening bed assignments for specimens or localities, unless they are on or very close to the measured sections, are estimates based on proportional distances from (above, below, or between) recognized marker bed(s). This has to be the case because there is much dune and sage cover, and because within the units themselves in these fluviatile deposits, few beds are traceable laterally for any great distance. Either

they pinch out, to be replaced by a different bed, or they change in their lithology. Also, I have added my best estimate of relationships to the geomagnetic polarity time scale.

The chart shows the lowest member of the Washakie Fm., which Roehler (1973) named the Kinney Rim Member and which I (Turnbull, 1978) designated TWkK (for Tertiary, Washakie Fm., Kinney Rim Member). The greatest section we found measured 893.9 ft (272.5 m) from the bottom of Roehler's Bed 515 to an unconformity at the top of Bed 568 (Flynn, 1983). There are two marker beds within the unit. That which Roehler called Tan-White Tuff (Bed 515) is within the member at its base and is of some help on the Kinney Rim; and the other is the White Tuff Marker bed (540), near the middle of the member. Just beneath the unit at the top of the Green River Fm., the Cathedral Limestone (Bed 514) is helpful; and about 120 ft (36.58 m) lower down a section in the Laney, the Flock of Sheep Limestone (Bed 502), also can be helpful because it is one of the more easily recognized and widespread beds. Hence, I show it as well, and here point out that it may even correlate with a Hartt Cabin unit, the Barrel Springs White layer. (This was a theory from Roehler, which seems to be both logical and likely.)

Above this is the Adobe Town Member (variously written as Adobetown, 'dobetown, or 'Dobe Town), which includes both Lower Washakie (= Washakie A) and Upper Washakie (= Washakie B) of most workers following Granger (1909) through Wheeler (1961). This "old" Washakie A portion I had designated TWkA1 (for Tertiary, Washakie Fm., Adobe Town Member, Division 1). Our measure for it is 877.8 ft (267.6 m) from the base of Bed 569 to the top of Bed 620 (at the base of Granger's Bed 11). Three markers aid in tracing this unit: the Robin's Egg Blue (Bed 579), which is above the top of the Lower Brown Sandstone itself; the Middle Red (Beds 596–604); and Beds 620–622 (= Granger's Bed 11). The latter marks the boundary between TWkA1 and TWkA2 and is most useful because it can be easily traced for the greatest distance. Its whitest part, Bed 622, immediately overlies the unit (Bed 621) that is just above the basal bed (620) of Washakie B (TWkA2).

The "old" Washakie B division of the Adobe Town Member is designated TWkA2 (for Tertiary, Washakie Fm., Adobe Town Member, Division 2). Our measure for it is 1,100.7 ft (335.6 m). Traditionally, it included Beds 620 (the base of Granger's Bed 11) through 675 (Granger's Bed 22 at the top of the Mammoth Buttes). The main marker beds are Granger's Bed 11, which is traceable for the greatest distance around the Basin, and Bed 644 (Rose Red) higher up, which can be traced for about 20 miles (32 km) on the E and NE sides of the Basin.

The situation is more complicated, however, as can be seen by tracing the deposits to the south–southwest (from Sec. 28, T16N, R97W, Manuel Gap Quadrangle) along the crest of the Adobe Town Rim (to Sec. 25, T15N, R98W, Cow Creek Reservoir Quadrangle). All along this stretch, the sediment column gradually climbs at least an estimated several hundred feet higher to where three green ash beds[3] occur (in Secs. 24 and 25, T15N, R98W, Kinney Spring and Cow Creek Reservoir Quadrangles). One of these green, shaly, ash deposits (eagle-nest ash) has been dated at 45.1 ± 1.7 MYBP (potassium-argon, Krueger B7667 the biotite fraction), a date I now consider to be reasonable on both faunal and stratigraphic grounds. The hornblende fraction (A7667) gave a date decidedly too old (51.4 ± 2.8 MYBP), probably caused by some detrital contaminant; and because of this inconsistency, I had hesitated to publish them. I do so now, because I think that the biotite date should be made known.

Farther to the south, in the southern part of the axis of the Basin, still higher units are present. Stratigraphically these lie above the "old" Washakie B, and in their lower part they extend the upper portion of TWkA2 upward (i.e., they are well above the top of Granger's section). The uppermost part of these higher beds constitutes the ill-defined highest unit, which I designated TWkA3 in 1978. Independently, both Roehler (unofficially) and I had recognized this unit, which he measured at 341.0 ft (104.0 m), much of it fine lake bed clays, and he (Roehler, 1985) simply added it to the top of TWkA, because he did not divide up the Adobetown Member in that work. Taken together, the three green "ash" beds

[3] The X-ray diffraction patterns for all three of these ash beds are very much alike, suggesting that the source of the ash was the same for the three in spite of the time intervals between adjacent ones, represented by ~60 ft (~18 m between the bottom and middle ashes, and ~75 feet (~23 m) between the middle and top pair. All of the peaks for Clinoptilolite coincide, and there is a decided (amorphous) hump in the 15°–40° range of the background curve, indicative of glass. I thank Dr. Paul Predecki of the University of Denver and his students for the diffraction work, and Dr. Predecki for help with the interpretation.

SKULL PROPORTIONS

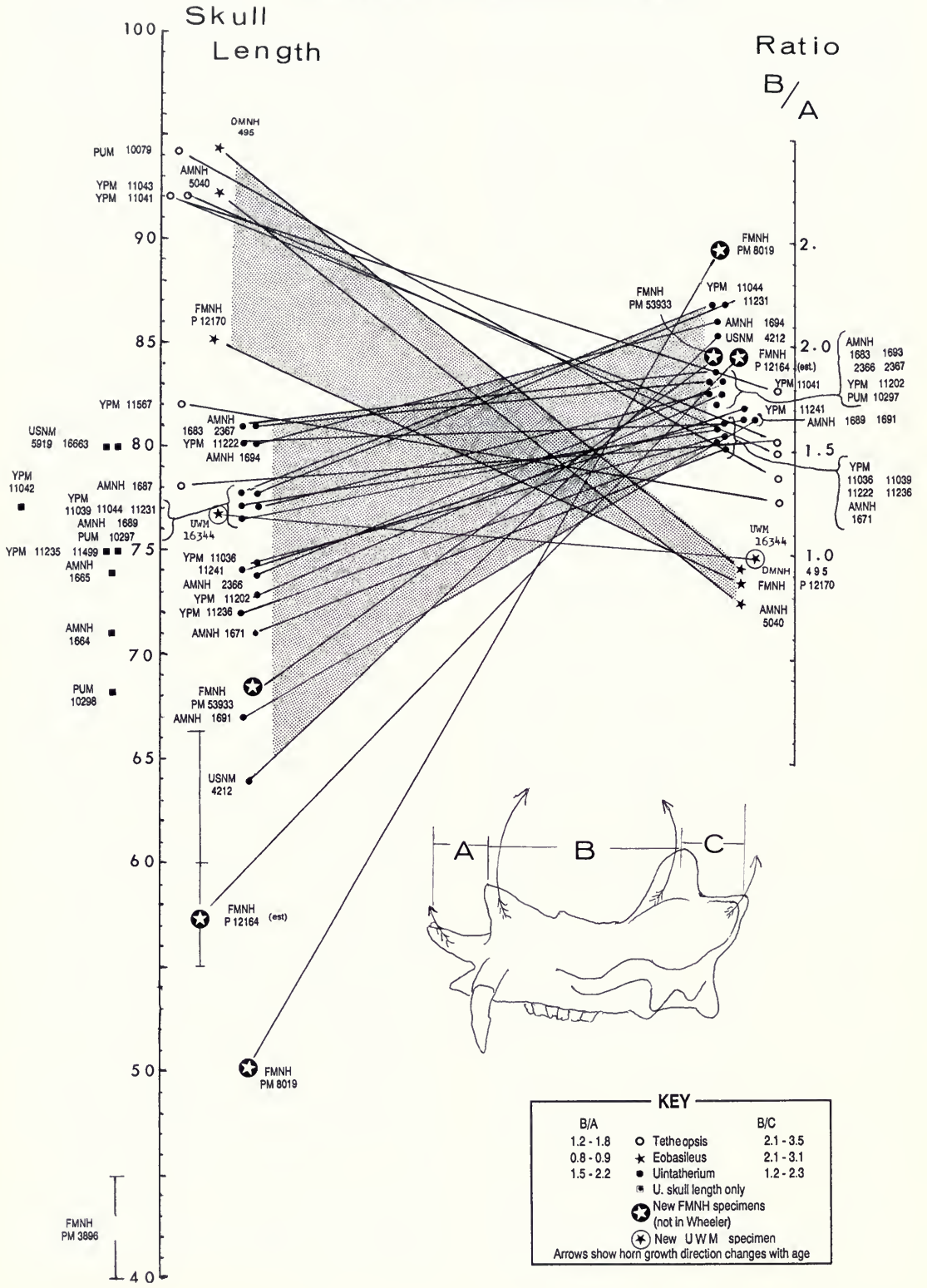

provide a sort of dividing marker unit, enabling us to separate in one area TWkA2 from the largely pond or lake sediments of the uppermost unit, TWkA3. In the upper half of TWkA3, in sections 30 (T15N, R97W); 6 and 7 (T14N, R97W); and 1, 12, 13, 14, 23, 24, 25, and 26 (T14N, R98W), the exposures to the east of the high ground are the clays, while the largely covered exposures to the west are more varied in their lithology, being mainly sandstone channels, overbank deposits, and some lake bed clays. To date, the fossil record of TWkA3 is poor, and it has no good traceable marker unit. Nonetheless, in addition to the mentioned green ash beds near its base, higher up near the very top, in the area north of Turtle Butte (Secs. 13, 14, 23 and 24), there are two thin (~1 ft [0.3 m] thick), ochre-colored, fine sandstone beds about 20 ft (6.1 m) apart vertically, which are traceable for about a mile (1.6 km). At Turtle Butte itself, erosion has removed both of the sandstone beds, but on the higher ground to the SSE of the Butte, the lower of those two sandstones is again exposed for more than half a mile (0.8 km) on both east and west sides of the butte. Hence, that bed can be traced for about 3 miles (~4.8 km) and thus serves as a marker near the top of TWkA3. Unit TWkA3 is in need of additional study. Both Roehler (1973) and Turnbull (1978) considered Beds 676–708 possibly to be of Uinta C age, based on the lithologic differences, but as yet no fossils have been found that either support or refute that notion. I now consider it to be unlikely, because the clays are now seen as a local lake deposit, not as the typical Uinta C beds. TWkA3 appears to intertongue in its lowermost half with the upper, coarser, deltaic units of TWkA2, but cover has thus far prevented resolution of the extent of the overlap or any of its details.

The magnetic polarity data shown in Figure 4 are from Flynn (1986) and are my choice of the most likely of the several alternative interpretations suggested by Flynn. For the most recent as-

←

FIG. 3. Cranial proportions of the same taxa as shown in Figure 2A (data from Wheeler, 1961) are given here for relating skull lengths and the B/A cranial ratios as used by Wheeler to separate the genera. In addition to the Wheeler data, the new Field Museum (white stars in black circles) and University of Wyoming (black stars in white circles) specimen data are added, as in Figure 2B. Note that the B/A ratios for adults of *Eobasileus* are lower than all of the others, while skull length does not serve to separate *Tetheopsis* from the other genera. Whereas Wheeler detected only one juvenile specimen—a jaw—in all of the materials he examined, the new FMNH materials include six such specimens, among them two skulls that are complete enough to appear here. Also, eight additional skull length values are included (the black squares to the left of the skull length line), but their ratio values could not be ascertained.

The many lines between the length and ratio scales connect the same specimens. The shaded areas set off specimens Wheeler assigned to *Eobasileus* and *Uintatherium*. The fact that the *Tetheopsis* specimens, which on skull-length criteria alone show two clusters, are more tightly grouped on the B/A ratio scale would tend to support the notion that genus is valid. However, when plotted in this manner, the slopes of the lines for *Eobasileus* and *Uintatherium* are reversed, and most *Tetheopsis* specimens follow the slope of the former genus. The estimated skull length of the very aberrant *E. cornutus* specimen, FMNH P 12164, is about 67 cm. The star representing it on the length scale was deliberately placed low (at 57.5 cm) to keep it outside the range of *U. anceps* specimens. Skull length, horn development, and B/A ratio suggest that it was either a juvenile (but its dentition is far too worn for that to be the case) or an aberrant female (conclusion of both Wheeler and me).

In the cranial vignette, below, arrows schematically show changes in (heterogonic) growth directions of the horns and crests with advancing age, so that there is a tendency for individuals of advanced age to take on more youthful proportions. Fortunately, the ratios are different enough that usually this is not a problem.

→

FIG. 4. Details of the stratigraphic units of the Washakie Fm. Shown on the left side, slightly modified from Roehler (1992b), are the chronostratigraphic units of the Eocene and the lithostratigraphic units of the Green River and Washakie Basins. On the right side the Washakie Fm. is expanded for greater detail and modified from Roehler–Turnbull sections. In conjunction with it, I give my assessment of relationship to the geomagnetic polarity time scale. For emphasis, the marker beds useful for stratigraphic understanding and correlation are set off in black. The upper boundary of TWkA2 with the overlying unit (TWkA3) is an interfingering one that is quite uncertain (see text). Unit TWkA3 is made up largely of lake bed clays that were deposited near the axis of the basin. I also call attention to the fact that the exact correlations with Chrons 19R and 20N are somewhat doubtful, as is indicated by question marks and dashed lines. An unconformity is indicated by the wavy line between the Kinney Rim and Adobe Town Members.

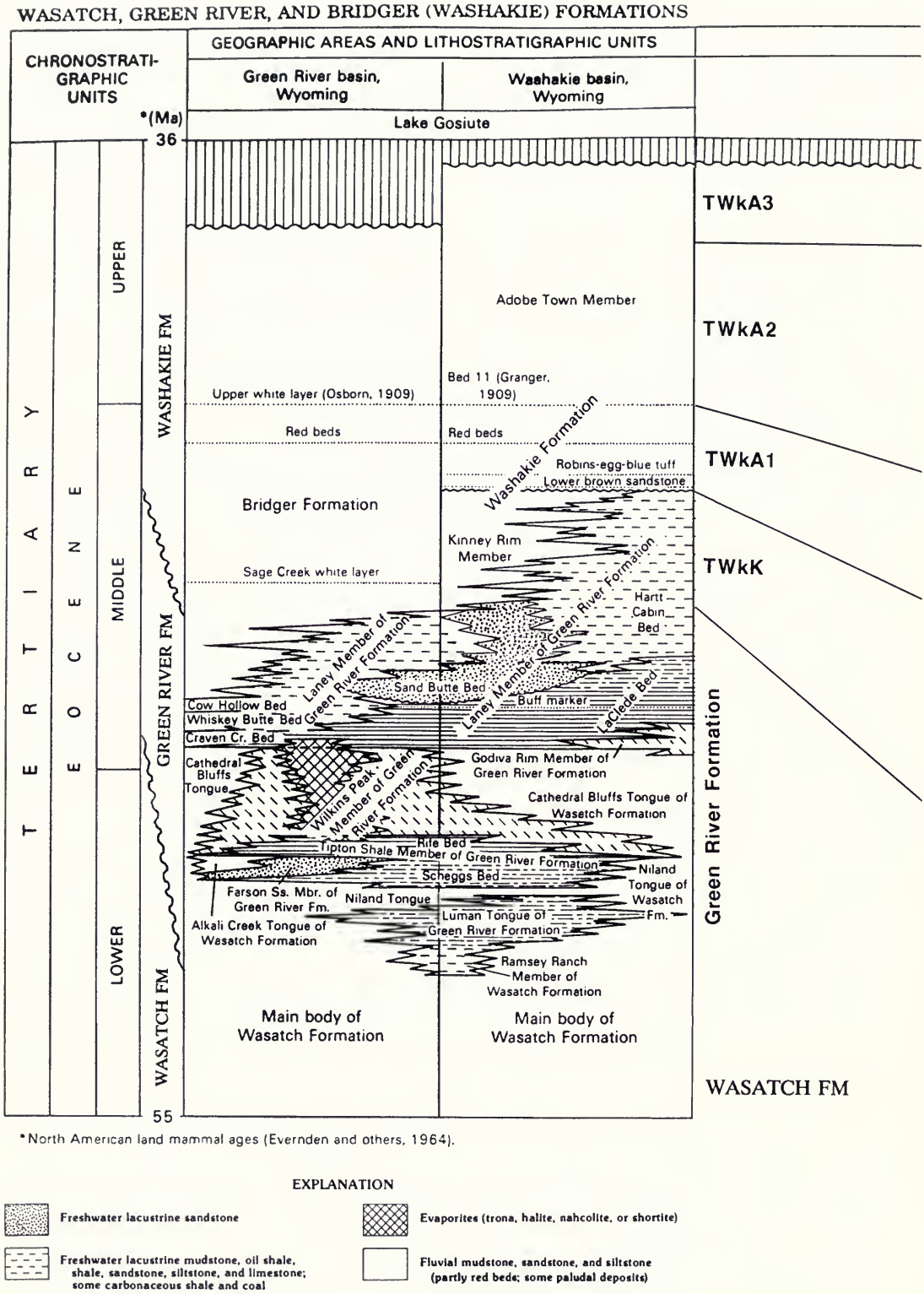
WASATCH, GREEN RIVER, AND BRIDGER (WASHAKIE) FORMATIONS
CHRONOSTRATI-GRAPHIC UNITS
GEOGRAPHIC AREAS AND LITHOSTRATIGRAPHIC UNITS
Green River basin, Wyoming
Washakie basin, Wyoming
*(Ma)
36
55
Lake Gosiute
TERTIARY
EOCENE
UPPER
MIDDLE
LOWER
WASHAKIE FM
GREEN RIVER FM
WASATCH FM
TWkA3
TWkA2
TWkA1
TWkK
Green River Formation
WASATCH FM
Adobe Town Member
Bed 11 (Granger, 1909)
Upper white layer (Osborn, 1909)
Red beds
Red beds
Washakie Formation
Robins-egg-blue tuff
Lower brown sandstone
Bridger Formation
Kinney Rim Member
Sage Creek white layer
Laney Member of Green River Formation
Hartt Cabin Bed
Sand Butte Bed
Buff marker
LaClede Bed
Cow Hollow Bed
Whiskey Butte Bed
Craven Cr. Bed
Cathedral Bluffs Tongue
Wilkins Peak Member of Green River Formation
Godiva Rim Member of Green River Formation
Cathedral Bluffs Tongue of Wasatch Formation
Rife Bed
Tipton Shale Member of Green River Formation
Scheggs Bed
Niland Tongue of Wasatch Fm.
Farson Ss. Mbr. of Green River Fm.
Niland Tongue
Alkali Creek Tongue of Wasatch Formation
Luman Tongue of Green River Formation
Ramsey Ranch Member of Wasatch Formation
Main body of Wasatch Formation
Main body of Wasatch Formation
*North American land mammal ages (Evernden and others, 1964).
EXPLANATION
Freshwater lacustrine sandstone
Evaporites (trona, halite, nahcolite, or shortite)
Freshwater lacustrine mudstone, oil shale, shale, sandstone, siltstone, and limestone; some carbonaceous shale and coal
Fluvial mudstone, sandstone, and siltstone (partly red beds; some paludal deposits)

FIGURE 4.

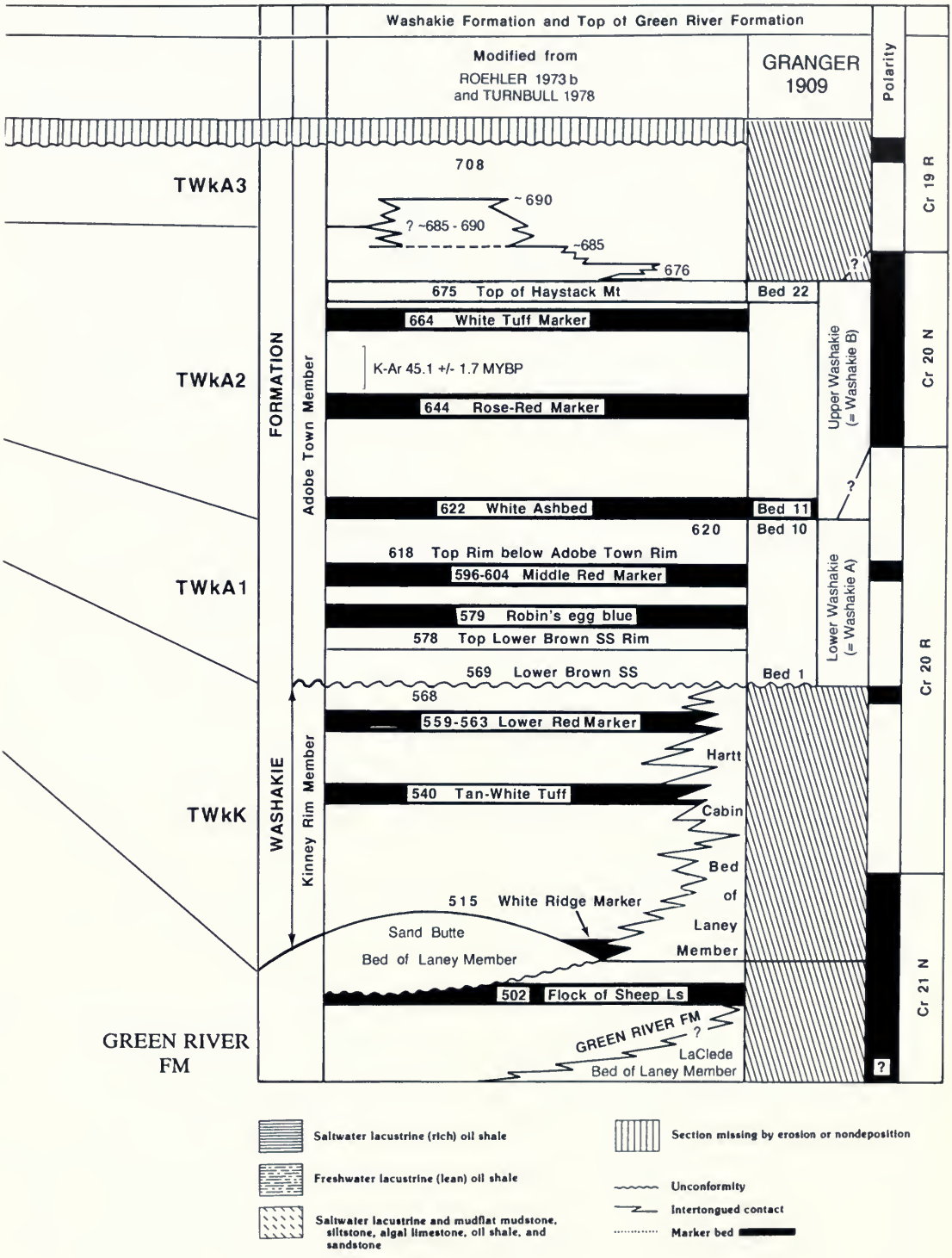
Washakie Formation and Top of Green River Formation
Modified from
ROEHLER 1973 b
and TURNBULL 1978
GRANGER
1909
Polarity
TWkA3
TWkA2
TWkA1
TWkK
GREEN RIVER
FM
FORMATION
WASHAKIE
Adobe Town Member
Kinney Rim Member
708
~690
? ~685 - 690
~685
676
675 Top of Haystack Mt
Bed 22
664 White Tuff Marker
K-Ar 45.1 +/- 1.7 MYBP
644 Rose-Red Marker
622 White Ashbed
Bed 11
620
Bed 10
618 Top Rim below Adobe Town Rim
596-604 Middle Red Marker
579 Robin's egg blue
578 Top Lower Brown SS Rim
569 Lower Brown SS
Bed 1
568
559-563 Lower Red Marker
Hartt
540 Tan-White Tuff
Cabin
Bed
of
Laney
Member
515 White Ridge Marker
Sand Butte
Bed of Laney Member
502 Flock of Sheep Ls
GREEN RIVER FM
?
LaClede
Bed of Laney Member
Upper Washakie
(= Washakie B)
Lower Washakie
(= Washakie A)
Cr 19 R
Cr 20 N
Cr 20 R
Cr 21 N
Saltwater lacustrine (rich) oil shale
Freshwater lacustrine (lean) oil shale
Saltwater lacustrine and mudflat mudstone, siltstone, algal limestone, oil shale, and sandstone
Section missing by erosion or nondeposition
Unconformity
Intertongued contact
Marker bed

FIGURE 4.

sessment, see McCarroll et al. (1996a,b,c), where these alternatives are discussed.

The vast majority of the uintatheres of the Washakie Fm. come from TWkA1 and TWkA2, the old Washakie A and B units (= Lower and Upper Washakie). None have been found in the uppermost unit, TWkA3, and only indeterminate scraps have come from the Kinney Rim Member (TWkK). Wheeler (1961) reviewed the geology in some detail, and more recently Roehler (1992a,b) has given us the definitive treatment. The reader should refer to those works if more information is desired. Wheeler concluded his section on the Washakie Fm. thus:

> *Uintatherium* is an abundant fossil in certain areas of the Washakie A faunal zone (plate 6). *Eobasileus,* a rare fossil, is known from Washakie B. The few known specimens of the genus *Tetheopsis* are all from the Washakie formation, occurring in both faunal zones (p. 15).

Here I need to add a few caveats with regard to some locality names in the older literature. First, Cope (1873, p. 526) used the term "Haystack Mt."[4] to designate the last high butte at the E-SE end of the 7-mile (11-km) arc of his "Mammoth Buttes." Subsequently, most workers, and indeed the USGS topographic maps, have used the name "Haystack Mt." to designate all of this 7-mile arc of higher ground, not Cope's original "Mammoth Buttes" term. Second, there have been several places designated "Dug Springs," one being Tadpole Spring or Tadpole Stage Station; and at least one other is indicated as being "high on Haystack Mt.," and still another "near Haystack," but lower in the section. A third ambiguous locality name used at different times by different persons is simply "Haystack" or "Haystack Mt." Not only is this imprecise geographically, it is imprecise stratigraphically, because more than 100 ft (32 m) of the top of Washakie A of Granger is at the base of both Haystack proper and the Mammoth Buttes, but only part of Washakie B is within Haystack, while all of it is to be found within the Mammoth Buttes (in the Granger section). Wheeler did his best to sort this out, but some uncertainty is bound to remain and should not be dismissed, for, as with all older reports, there may well be other similar problems as yet undetected.

I should note here also that in my notes and specimen labeling in the late 1950s, I was in the habit of designating the specimens from the mostly lower-lying Upper Washakie deposits in Secs. 1, 2, 11, and 12 of T16N, R97W, at the western end of the Mammoth Buttes, as coming from "the northwest flank of Haystack." It was (and still is) a term of convenience, beginning in those days before the USGS topographic maps were available for the area and Haystack was used as a synonym for Mammoth Buttes (mea culpa).

Also it is necessary to understand the use of the established names of the various rims: these

---

[4] It is a real pity that this obscure work has not been more readily available. Had it been, the misnaming of these topographic-geologic features probably would not have happened, nor would we miss out on some of Cope's sometimes flowery, sometimes charming writing, his vivid descriptions of geologic features, or his insightful impressions. The irony is that Cope caused the problem himself. He belatedly came to realize that he had erred in details of the anatomy of Uintatheres in his hasty restoration, and he reacted with equal haste in trying to recall and destroy all copies of the released work. He nearly succeeded, but fortunately a few copies were beyond recall (the American Museum Library has a copy, which the late Morris Skinner photocopied for me). Wheeler (1960, p. 3) reproduced Cope's illustration from it. It shows Cope's initial visualization of uintatheres as a kind of antlered elephant, including an elephant's trunk. Of course, they were not elephants, or even close relatives; they were not antlered, nor did they bear elephant-sized trunks. Nevertheless, they did have some elephant-like attributes that greatly impressed Cope. This is apparent from his description of his finding of *Eobasileus cornutus*, "the Monster of Mammoth Buttes," in the Washakie badlands. A quote from that work gives the flavor of Cope's writing and makes his reaction understandable: "Here was the fountainhead. Pick, sledge, and chisel soon exposed an enormous skull with a perfect set of teeth, a huge polished tusk of saber form, curving downward from the jaw, and a pair of massive horns rising from each eyebrow. Removing a mass of rock, the shoulder-blade was exposed, a huge plate from two to three feet wide, and close alongside his pelvis, nearly complete. When I had laid the hip-bones bare their expanse measured about four and [a] half feet." Clearly, the girdles are elephantine in their proportions, and Cope when describing the beast was near the mark in stating, "a head . . . terminating in a short trunk, somewhat similar to that of the elephant . . . its body like that of the elephant, with high withers and a sloping rump, terminating in a short tail: its limbs rather shorter than those of the living elephant, but with the same short, stubby toes, and the knee below the body as in the elephant, bear and monkey." Mostly these were fair observations, but then, carried away, he went on, "The same ambling gait, the same huge ears, and the little twinkling eyes, all betrayed in life the elephantine kinship, while the hollow forehead and its surrounding horns, if not bearing the stamp of the elephant's wisdom, marked him as a king, and his shining weapons showed his ability to maintain the claim."

are loose stratigraphic-geographic terms. The Kinney Rim is situated on the west side of the basin and exposes Wasatch and Green River Fms. on its steep west side, and the Kinney Rim Member, Washakie Fm., on its eastern dip slopes. Antelope Canyon separates this structure from its northern equivalent, the DeLaney Rim (usually called Laney Rim). To the south, the Kinney Rim merges with the Cherokee Rim, which has many faults. The east side of the Basin is more openly eroded, and there is no distinct, continuous equivalent rim, but the Flat Tops are its outliers. Within this "circle" in ascending order are the Lower Brown Sandstone Rim, the Rim Below the Adobe Town Rim ('Dobe Town Rim) on the west side of the Basin = the Willow Creek Rim on the east side (sometimes referred to as the middle rim), and the Adobe Town Rim. The first of these conforms reasonably well with the Lower Brown Sandstone at its base. The middle rim, designated by its stratigraphic position, is usually capped by a resistant, broad, cobble-covered bench (? possibly in places including some Bishop Conglomerate residuals) 10–15 ft (3–4.5 m) below Granger's Bed 11. The Adobe Town Rim exposes ever higher beds as one follows it from north to south through the upper part of TWkA2 and most if not all of TWkA3. Somewhere within Section 12, T14N, R98W, Cow Creek Reservoir Quadrangle, or nearby, the dips become reduced; and then, when one proceeds farther south, they take on a more northern component, which increases progressively as one proceeds down-section all the way to the Cherokee Ridge.

Material and Abbreviations

Listings of all Washakie Fm. uintathere specimens known to me are available according to institution from the author and the Department of Geology, Field Museum of Natural History (FMNH). In each case I indicate whether or not I have seen the specimen. I do the same for Wheeler: If he saw the specimen, I indicate the page in Wheeler's 1961 revision where it is referred to. In addition to specimens in the Field Museum of Natural History, I have examined most of the mid- to late Eocene uintatheres in the following collections:

Academy of Natural Sciences, Philadelphia (ANSP)
American Museum of Natural History (AMNH)
Denver Museum of Natural History (DMNH)
Princeton University Museum (PUM); now included in the Yale collection (YPM)
United States National Museum (USNM)
University of California Museum of Paleontology (UCMP)
University of Colorado Museum (UCM)
Utah Field House (UFH)
Yale, Peabody Museum of Natural History (YPM and PUM)
Other smaller collections:
Carnegie Museum of Natural History (CMNH), University of Michigan Museum of Paleontology (UMMP), University of Washington, Burke Museum (UWBM), Collection of Fossil Vertebrates, Department of Geology and Geophysics, University of Wyoming (UW or UWM)

PM or P denotes the FMNH fossil mammal collection. Other abbreviations either are standard or are provided in the text or figure captions upon the first instance of their use.

Measurements are given in English and metric units (millimeters and centimeters are given in metric units only). I should state at this point that one of the main purposes of this work is to document all of the FMNH uintathere materials, especially those from the Washakie Fm. I will not repeat the anatomical descriptions that are covered in the Marsh (1886) monograph and in Wheeler (1961) beyond whatever is necessary to fill in gaps in our understanding and to describe and illustrate the more significant of them, including mostly heretofore unreported Washakie specimens.

In the text following each heading, I discuss only the more important of the new materials. Because I recognize only *Uintatherium* and *Eobasileus* as valid genera, I indicate my assignment of each specimen to either *U. anceps* or *E. cornutus,* or as being indeterminate.

The Field Museum's Washakie specimens of these taxa (except for one collected in 1947 by R. Zangerl) were collected by me and my field crews between the years 1956 (when I started to systematically collect in the formation) and the present, and by J. Flynn and his crews since 1989. They consist of more than 75 specimens, three of them being partial skeletons, eight of which are skulls or significant portions of skulls, three of which are fragmentary skull pieces, and seven of which are jaws. All are from Sweetwater County, Wyoming. Together they contribute considerably to

our understanding of the genus *Uintatherium,* and to a lesser extent to *Eobasileus.*

Most important of the lot are PM 53933 (frontispiece; Fig. 5), a young adult (the Funderburk skull); PM 3896, a newborn; and PM 8019 and PM 54406A, two juvenile skulls; all four are assigned to *Uintatherium anceps.* Also previously unreported is a skull in the University of Wyoming collection (UW 13644) originally considered to belong to this species but which has the dental proportions of *E. cornutus.*

Other previously unreported important specimens are (1) PM 1737, a pair of jaw rami, (2) a left mandibular ramus in the University of California collection, UCMP 81356, and (3) a partial mandible of *U. anceps* in the Carnegie Museum collection, CMNH 29493 (all three are from the Washakie Fm. The first two expand the record of *E. cornutus,* the taxon with the fewest specimens); (4) an excellent skull and a pair of jaws (unassociated) from the Bridger Fm., recently collected by a party from Sierra College, California; and (5) a nearly complete skeleton from the Uinta Fm. of Colorado. The Field Museum has a cast of the skull and jaws of this skeleton, PM 60171. The specimen is now in the Gunma Prefecture Museum.

Methods, Systematics, Morphology, and Materials

Methods

With the publication of his *Revision of the Uintatheres,* Wheeler (1961) did a great service for mammalian paleontology. He reduced the chaotic plethora of named genera and species to a reasonable number—a formidable task, considering the inadequacies of the descriptions, often of the types themselves, and because of the needless synonyms resulting from hasty and careless early publications. Except for *Tetheopsis,* he has in my opinion done a most adequate job, and, as noted earlier, Schoch and Lucas (1985) accepted the generic assignments and synonymies, although expressing some uncertainty about the need for further species revisions.

Skull and jaw measurements of *Uintatherium anceps* and *Eobasileus cornutus* are given in Tables 1 through 4, and are illustrated in Figure 6. One thing that may be expected to improve our understanding of species distinctions, and which neither Wheeler nor Schoch and Lucas have done, is to see whether measurements of individual teeth can better define the species. Wheeler (1961) did utilize total upper and lower cheek-tooth row lengths, with limited success (see his charts 5 and 6). Frequently, individual tooth measurements have proved useful in many other groups when other criteria have failed. Tables 5 and 6 give these data, and in Figure 7 the measures themselves are illustrated. In addition, I present more details of dental features, including information on the deciduous teeth and dental formulas, and I provide scattered supplementary anatomical details wherever the Washakie materials offer new information. To make them more useful for future functional analysis, I designate a few dental features differently than did Wheeler (compare Wheeler's figs. 2 and 3 with my Fig. 7A and 7B).

Crown features of molars of advanced uintatheres are labeled and diagrammed, and the scheme for individual cheek-tooth measurements is given in Figure 7. These measures also differ from the more usual ones in that anterior and posterior widths (AW and PW) are the greatest tooth widths measured through the long dimension of each of the major lophs and lophids (i.e., along functional crests). Thus, for the upper teeth, AW measures the distance from crown base to crown base aligned through the protoloph; PW is the measurement aligned through the metaloph. In the lower teeth, AW is measured along the metalophid and PW is measured along the line from metastylid to hypoconid (hypolophid). Length measures are more standard and obvious.

In using this work, it will be essential for the serious student of the uintatheres to have at hand the Marsh Dinocerata monograph (1886), with its many fine osteological illustrations, and the Wheeler (1961) revision. The former provides an excellent, detailed, osteological-anatomical base for comparative purposes for skull, jaws, and postcranium. The latter is useful both for its reasoned discussion and taxonomic revision and for the photographic coverage it provides for nearly all of the better specimens. To duplicate either set of these illustrations is unnecessary and costly, so I illustrate only the more important, new, or previously unreported or unillustrated materials, mostly those of the Field Museum, but I also include several belonging to the American Museum, Carnegie Museum, Denver Museum, University of California Museum of Paleontology, University of Wyoming Museum, and the Utah State Fieldhouse.

Systematics (following Schoch and Lucas, 1985)

Mirorder Uintatheriamorpha Schoch & Lucas, 1985
- Order Xenungulata Paula Couto 1952
  - *Carodina* Simpson 1935
- Order Dinocerata Marsh 1873a
  - Family Prodinoceratidae Flerov 1952
    - *Prodinoceras* Matthew, Granger, Simpson 1929
  - Family Uintatheriidae Flower 1876 (1873)
    - Subfamily Gobiatheriinae Flerov 1952
      - *Gobiatherium* Osborn & Granger 1932
    - Subfamily Uintatheriinae Flower 1876 (1873)
      - Tribe Bathyopsini Osborn 1898
        - *Bathyopsis* Cope 1881
      - Tribe Uintatheriini Flower 1876 (1873)
        - *Uintatherium* Leidy 1872 (including in part, *Tetheopsis* Cope 1885); type species of the genus is *U. robustum* = *Titanotherium* ? *anceps* Marsh, 1871
        - *Eobasileus* Cope 1872b (including in part, *Tetheopsis* Cope 1885); type species of the genus is *Loxolophodon cornutus* Cope, 1872b

At present, only two North American species within the Uintatheriini are recognized unequivocally, *Uintatherium anceps* (Marsh) and *Eobasileus cornutus* (Cope). As indicated earlier, I suspected that the two named species of *Tetheopsis, T. speirianus* (Osborn) and *T. ingens* (Marsh), may more properly be assigned to one or the other of the two taxa, and in this study that suspicion is confirmed and those reassignments are made.

Uintatherium anceps (Marsh) is based on *Titanotherium* ? *anceps* Marsh, 1871, p. 35 (holotype YPM 11030), and *U. robustum* Leidy, 1872a, pp. 168–169, and 1873 (holotype ANSP 12607, 12609, 12610, 12611, 12612, 12613, 12619, and 12622). Wheeler provides a full synonymy listing and documents most of the materials he assigned as *U. anceps* (Wheeler, 1961, pp. 27–47), and the reader is referred to that work for the full list. Junior synonyms include *U. latifrons* and *U. segne*; *Tinoceras ingens, T. vagus, T. affine, T. pugnax, T. grande, T. annectans, T. crassifrons, T. hians, T. longiceps,* and *T. stenops*; *Dinoceras mirabile, D. distans, D. agreste, D. laticeps, D. lucare*; and *Elachoceras parvum.*

Eobasileus cornutus (Cope) is based on *Lefalaphodon discornatus* Cope 1872a, *E. cornutus* Cope 1872b, and *Loxolophodon cornutus* Cope 1872c (the holotype of both is AMNH 5040). Again, Wheeler (1961, pp. 52–53) gives the details.

Morphology

Uintatherium anceps (Marsh, 1871) (the only species of the genus)
- *Titanotherium* ? *anceps* Marsh, 1871, p. 35
- *Uintatherium robustum* Leidy, 1872a, pp. 168–169
- *Uintamastix atrox* Leidy, 1872a p. 169

An additional 26 species are listed in Wheeler's synonymy listing:
- Two of *Loxolophodon* by Cope, 1872b,
- Nine of *Tinoceras,* all by Marsh between 1872 and 1886,
- Eight of *Dinoceras,* all by Marsh between 1872 and 1886,
- *Eobasileus galeatus* Cope, 1873b, pp. 1–2
- *U. leidianum* and *princeps* by Osborn, Scott and Speir, 1887, pp. 63–82
- *U. latifrons* and *signe* by Marsh, 1885, pp. 262 and 276: 1886, pp. 40, 220–222
- *Elachoceras parvum* and *U. alticeps,* Scott, 1886, pp. 304–307
- *Tetheopsis speirianus* (Osborn, 1881)

Holotype—YPM 11030 is illustrated by Wheeler (1961; pl. 8, fig. 1).

Distribution—Middle Eocene, Upper Bridgerian of Bridger and Washakie Basins of SW Wyoming, within the Adobetown Member, in TWkA1 of the latter. Also questionably in the lower part of the Uinta Fm. of the Uinta Basin, Utah, and the lower part of the Sand Wash Basin of NW Colorado. Scanty remains have been recovered in the Piceance Creek Basin of W Colorado, the Friars Fm. of S California, and the Pruett Fm. of West Texas.

Revised Diagnosis—A large uintathere, larger and more dolichocephalic than its predecessors *Bathyopsis* and *Probathyopsis,* but smaller than and nearly as dolichocephalic as its successor *Eobasileus.* Skull length of adults between 69 and 85 cm; upper cheek-tooth row P2–M3, 143–169 mm long. It is distinguished from *E. cornutus* by

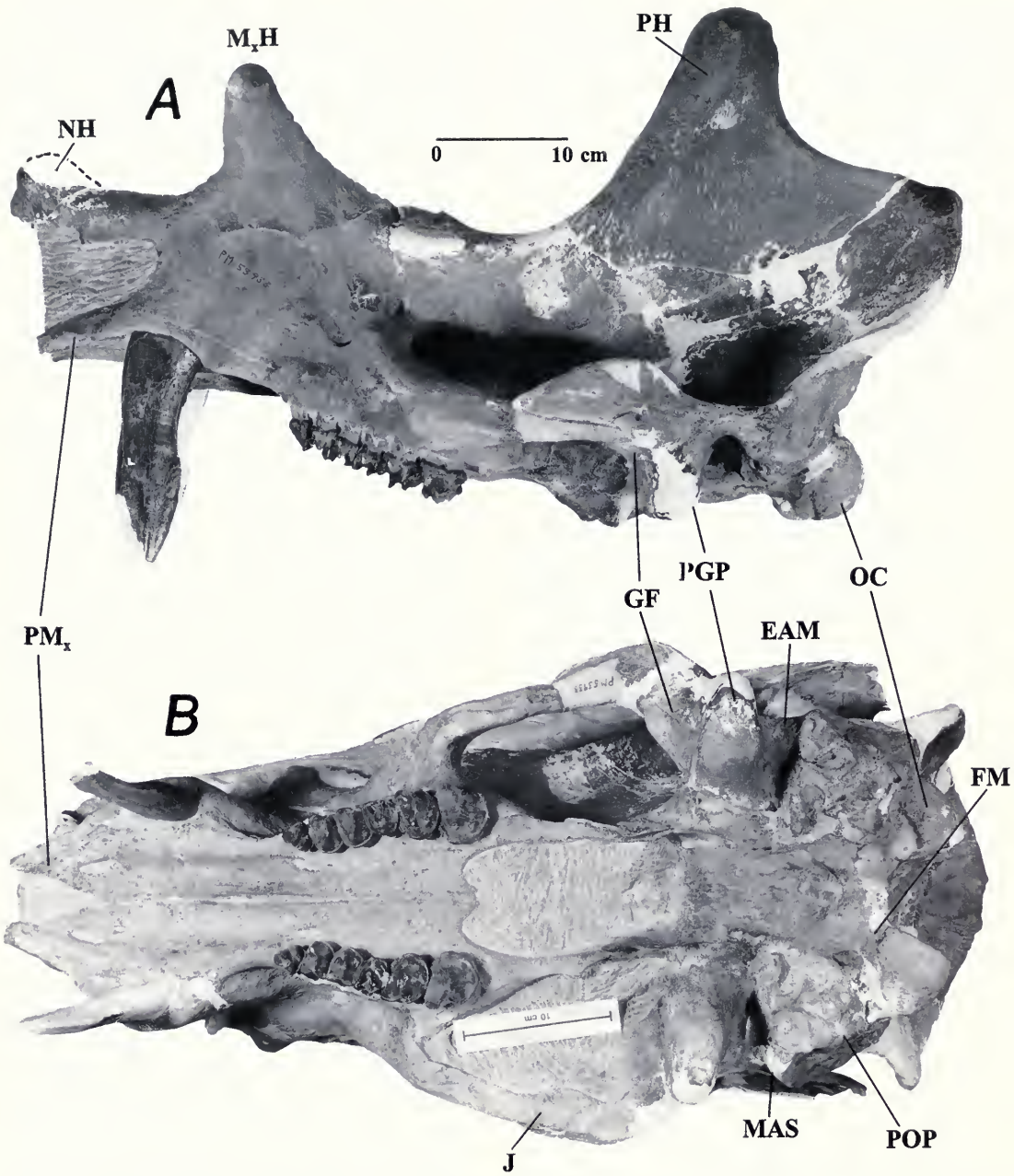

FIG. 5. **A,** Left lateral, **B,** ventral, **C,** dorsal, and **D,** inverted posterior views of the most complete adult *Uintatherium anceps* skull in the Field Museum's Washakie collection, the well-preserved Funderburk skull, PM 53933. The skull is that of a young adult male that is lacking only a minor bit here and there and most of its right canine tusk. Its cheek teeth are nearly unworn except for the M1s, on which the enamel of the lophs is breached, but the greater part of the structure of each loph remains. The relatively short horns and low parietal–occipital crests are further testimony to its young age state. It was discovered by the late Tom Funderburk, collected in 1984, and donated to the Museum in 1989. Abbreviations are identified in the captions to Figures 8 and 9, and others as needed. Scale for C is the same as for A and B (FMNH neg. nos. GEO 85689 (A), 85690 (B), 85799.1 (C), and 85799.2 (D)).

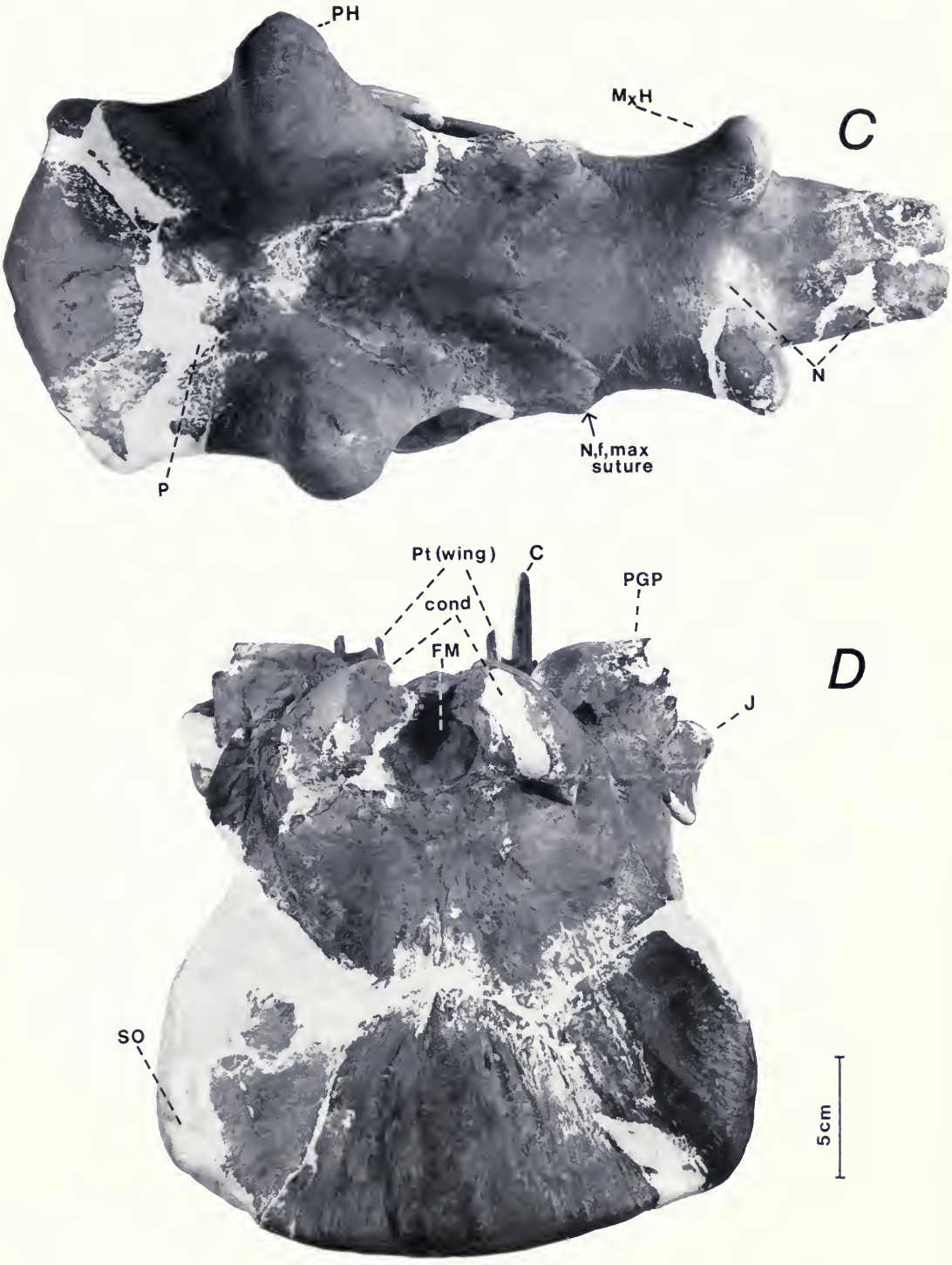

FIG. 5. *Continued.*

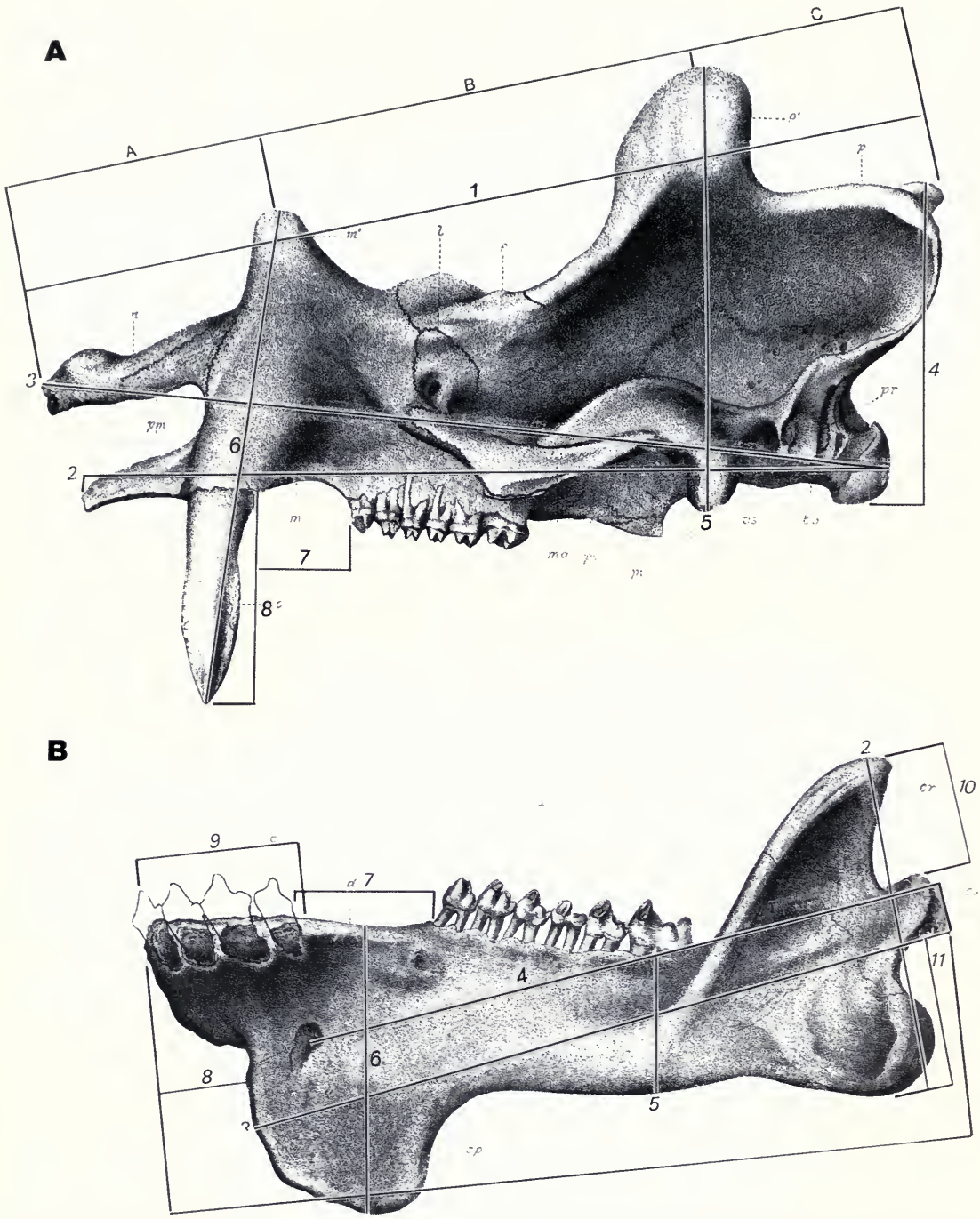

FIG. 6. Drawings of skull and jaws that show how some of the more useful measurements were taken: **A,** Skull measures are shown overlain on Marsh's (1886) pl. II of *Dinoceras mirabile* (= *U. anceps*); **B** shows his pl. XIX, the jaw of *Tinoceras pugnax* (= *U. anceps*) with the jaw measurements indicated. In **A,** the basis for Wheeler's cranial proportion ratios is shown by the small capital letters A, B, and C. The numerals in drawings **A** and **B** correspond to those numbers in Tables 1–4.

the ratios of the horn spacings in the Wheeler (1961) scheme, where distance from nasal tip to maxillary horn is called A, that from maxillary horn to parietal horn is called B, and that from parietal horn to rear of occipital crest is called C. The B/A ratio is about 1½ to 3 and the B/C ratio is about 1 to 2⅓ (to be compared with *E. cornutus*, where B/A is about 1 and B/C is between about 2 and 3). (It is of interest that Leidy (1873), without explicitly giving these details, stated that skull proportions separated the genera.)

Certainly one of the least distorted, most complete, and well preserved of known uintathere skulls is PM 53933 (frontispiece and Fig. 5), discovered by the late Tom Funderburk in 1984 and collected by him (with the help of his son, Dave Funderburk) at a locality near the center of the NW ¼, Sec. 8, T15N, R94W, Salazar Butte Quadrangle, Sweetwater County, Wyoming (FMNH Loc. FM-2-85-KL/WDT). The specimen is complete except for the jaws and a few minor pieces of the skull that were broken off as that part of the specimen, which was nearly entirely encased in a massive sandstone block, fell and tumbled down 50 feet (16 m) after being pushed from its precariously balanced in situ position on a narrow promontory ridge to its resting spot at the base of the Lower Brown Sandstone Rim. The block surely weighed ca. 250–300 lb (115–135 kg), for the prepared skull minus the jaws, and with all surrounding matrix prepared away but with internal cavities still matrix-filled, weighs more than 125 lb (56 kg). Preparation was begun by Tom Funderburk and continued until Mr. Murray Daniels[5] suggested, then insisted, that further preparation would require professional help. Final preparation by William Simpson was done at the Field Museum; and in 1989, at my request, Mr. Funderburk donated the skull to the Museum.

Apparently at least parts of the jaws and postcranial skeleton also had been preserved, although at the time nothing else was found. During the years following its discovery, I have collected much float from beneath the promontory. Other parts of the skeleton (three in situ ribs) came from the same horizon 9–12 feet (3–4 m) behind the location of the skull, at the point where the promontory joined the main bluff. From the proximity of this block and the skull, I assume both to be parts of the same individual. The additional scraps were recovered on the slopes beneath the promontory where the skull and these other in situ parts had lain. They include a mix of bones, some of which surely belonged to the specimen (the symphysis and rear portions of both rami, six vertebrae, fragments of the pelvis and sacrum, three complete ribs, and rib pieces). Other more dubious bits may belong, but among them are at least three pieces that do not: an occipital condyle and the rear of the jaw of another, smaller uintathere, and a fragment of the mandibular symphysis of a titanothere. Also, a great many turtle bone fragments were found.

Materials

Uintatherium anceps

Skull, Jaws, and Dentition—In 1923, H.E. Wood contributed an analysis of the molar crown features of *U. anceps* that cleared up a confusion begun earlier by Cope (1884) with his contorted "ectoloph rotation hypothesis" and was soon thereafter further supported and modified by Osborn (1898). The problem Wood set for himself was to reanalyze the molar crown features in order to clarify cusp homologies and to gain insight into the relationships of uintatheres to other mammals. He thereby overturned the thinking of the two giants in the field and arrived at a more logical and straightforward interpretation, which I have briefly remarked on elsewhere (Turnbull, 1995). Suffice it to say that Wood interpreted the three main cusps of the upper molars to be protocone, paracone, and metacone (i.e., the usual cusps of the normal trigon of Cope-Osborn terminology) and to be connected by lophs. It then follows that the primary cusps of the lower molars are protoconid, paraconid (reduced), and metaconid, with the protolophid weak, metalophid strong, and the hypoconid (and hypolophid) well developed. The other lower molar cusps present are the entoconid and hypoconulid, and a metastylid closely associated with the metaconid. All of these features are shown in Figure 7A and B, and this terminology is followed throughout the work. Tables 5 and 6 give dental measurements

[5] The late Mr. Murray Daniels and his wife, Mary Jane, and family, long friends of the Field Museum, have been extremely helpful to me and my field crews since the mid-1960s, when we first met. From their years of exploring the Washakie desert, they all became quite knowledgeable about both the geology of the basin and its fossils. They came to know its geography intimately. Fortunately, Murray's advice to Tom was heeded, and this certainly saved the dentition from further unnecessary damage.

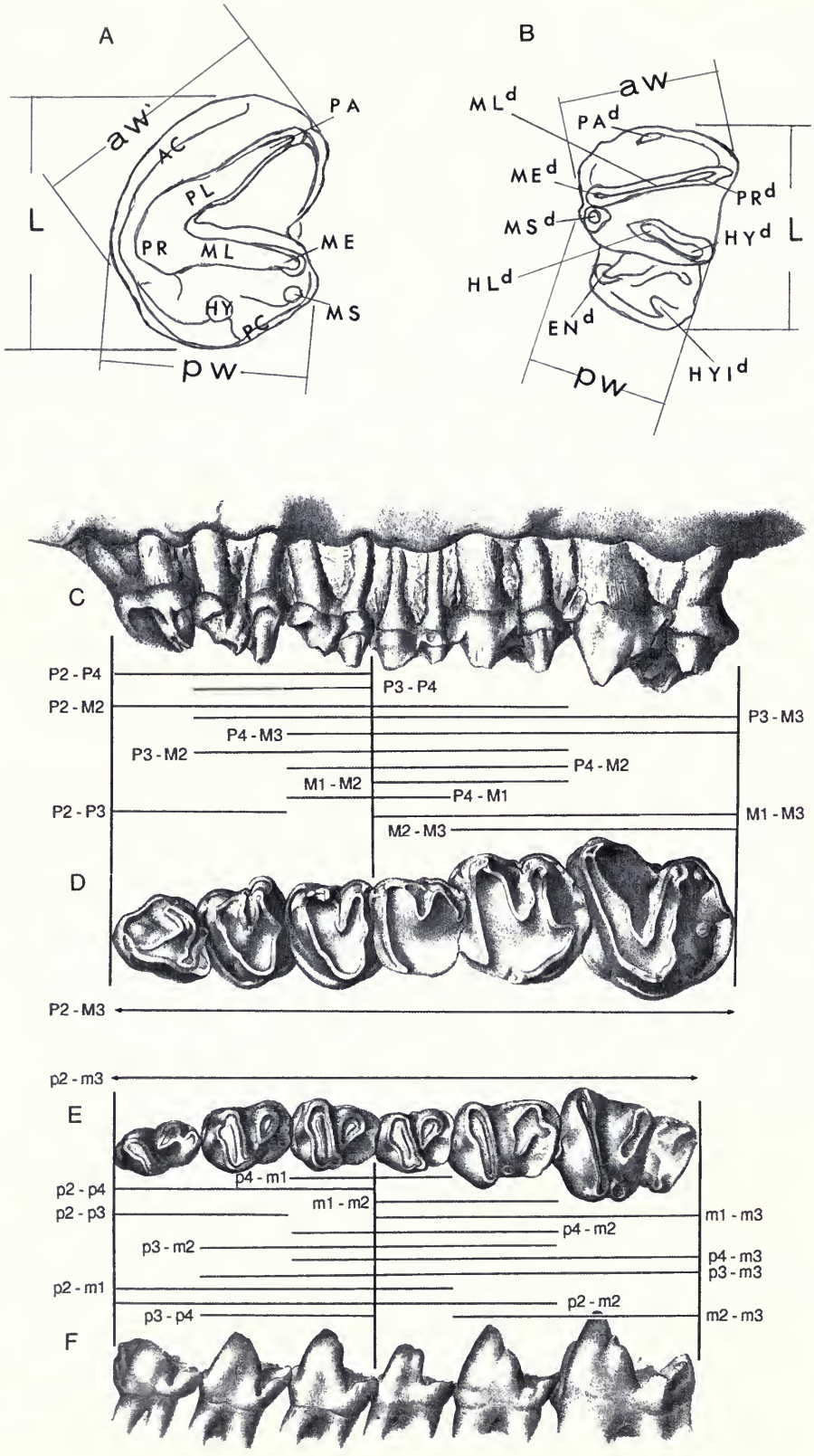
A
aw
AC
PA
PL
L
PR
ML
ME
HY
PC
MS
pw
B
MLd
aw
PAd
MEd
PRd
MSd
HYd
L
HLd
ENd
pw
HYId
C
P2 - P4
P3 - P4
P2 - M2
P3 - M3
P4 - M3
P3 - M2
P4 - M2
M1 - M2
P4 - M1
P2 - P3
M1 - M3
M2 - M3
D
P2 - M3
p2 - m3
E
p4 - m1
p2 - p4
m1 - m2
p2 - p3
m1 - m3
p4 - m2
p3 - m2
p4 - m3
p3 - m3
p2 - m1
p2 - m2
p3 - p4
m2 - m3
F

for specimens assigned to *Uintatherium anceps* and for those two smaller specimens that Wheeler assigned to *Tetheopsis* (here considered to belong to *U. a.*).

Of the 11 skulls or partial skulls in the Field Museum collection, the Funderburk specimen is no. 1, PM 53933 (frontispiece, Figs. 5, 13, and 27C–D). With it, as noted above, are some jaw fragments and a few associated postcranial elements. The frontispiece shows the skull in two left-side, slightly anterolateral views, the top view showing features of the skull roof, the bottom those of the palate. The others are (2) the left maxillary of a very young individual and part of its skeleton, PM 3896, probably nearly a newborn (Figs. 8–10), which because of its age provides the most new information; (3) a nearly complete juvenile skull, PM 8019 (Fig. 11), found by Rocky Joe Potter, son of the late Wise Potter, then manager of the Eversole Ranch, in 1958; (4) a partial skull of another, older, juvenile, PM 54406A (Fig. 12); (5, 6) two partial skulls, PM 1666 and PM 1667 (Figs. 14, 15), that, according to the late Roy Eversole (founder of the Eversole Ranch), had been largely destroyed by "a curious sheep herder with a sledge." Also included are four other less important Field Museum skull specimens: (7) PM 54406B (Fig. 16), a laterally crushed, badly preserved skull and associated left jaw ramus; (8) PM 53921, consisting of the nasal bones, other skull fragments, and about half of the postcranial skeleton (Fig. 17); (9) PM 8020 (Fig. 18), consisting of only the nasal bones with their short oval nasal horns, two lower incisors, a lower canine, and part of an upper canine; (10) PM 39393, a very fragmentary bit of skull associated with various postcranial elements, including five thoracic vertebrae and articulated front and rear feet; and (11) PM 55467, a partial skull that includes the right parietal horn and both maxillary horns.

The University of Wyoming now has a specimen (UW 13644), an aged adult with a heavily worn dentition (Fig. 56). It is unique in that it measures both with *Uintatherium* on skull length criteria and with *Eobasileus* on other cranial features and on most of its dentition. Hence, I only mention it here and discuss it at greater length in the *Eobasileus* section, where I assign it.

Among the many specimens (in addition to PM 1667 and PM 53933) that preserve the basicranium, two of the more easily transported are of particular interest. Both are illustrated and discussed in the section on the ear region. They are ANSP 12607 (Fig. 26) and USNM 18599 (Fig. 27A–B).

SKULL AND UPPER DENTITION—Without doubt, the "newborn" specimen, PM 3896 (Figs. 8–10), provides the most new information.[6] Its maxillary

[6] It is curious that among all of the then-known specimens studied by Wheeler (1961), only one, a jaw, was recognized as being that of a juvenile. Yet Marsh (1886, p. 51) clearly implied that other juveniles were known. In addition to this, I suspect that differences in the collectors' approaches had something to do with this apparent bias. I have made it a policy to collect everything that preserved a recognizable boney surface feature, regardless of how fragmentary or insignificant it appeared to be initially. Of the cranial specimens I have collected, four are juvenile, a far higher proportion than seen in the earlier collections. Probably the earlier collectors, who were looking for fine materials, may have overlooked or dismissed a few of the scrappier juvenile specimens, whose bones tend to be less mineralized and thus were less frequently (or less well) preserved.

←

FIG. 7. Uintathere cheek teeth and the method of measurement used. **A–B:** Outline diagrams of uintathere molars, which also will serve for the posterior two premolars. **A,** A left M3, and **B,** a right m3, are shown, along with most crown features and measurement details. The three terminal North American genera are similar enough for these diagrams to serve for all, and the anterior molars and posterior premolars have the same basic form, although the more anterior usually are simpler and smaller. The unconventional way in which width measurements were taken is indicated. This is necessary because I have chosen functionally related width measurements (involving the major lophs and lophids) that differ from the simple width measures more commonly used. Abbreviations: Upper molar: aw = greatest width through protoloph (PL); pw = greatest width through metaloph (ML); L = greatest length of tooth crown; cusps PR, PA, ME, MS, HY = protocone, paracone, metacone, metastyle, and hypocone, respectively. Lower molar: aw = greatest width through metalophid (MLd); pw = greatest width through hypolophid (HLd, and including the metastylid when present); cusps PRd, PAd, MEd, MSd, HYd, ENd and HYId = protoconid, paraconid, metaconid, metastylid, hypoconid, entoconid and hypoconulid, respectively.

C–D: Left upper cheek teeth of *Tinoceras ingens* (= *U. anceps*) shown in labial (**C**) and occlusal (**D**) aspects (from Marsh, 1886, pl. XVIII). Various combinations of multiple cheek teeth length measurements are shown here and in E–F. I think this full array will prove useful because most specimens are scrappy; having many combinations of measurements should help with identification of such material.

E–F: Right lower cheek teeth of *T. pugnax* (= *U. anceps*) shown in occlusal (**E**) and lingual (**F**) aspects (from Marsh, 1886, pl. XIX).

horn is merely a small lump of bone on the anterodorsal edge of the maxillary (Fig. 9). The high form of the maxillary is evident (Figs. 9, 10) in both lateral (9B) and medial (9A) views. The infraorbital foramen is clearly visible on the lateral view, as is the swollen area within which the still unmineralized permanent canine had been developing. The great height of the nasal passage is indicated by the broad, smooth surface beneath the large sculptured suture for the nasal bone, features that can be seen in the medial view. The extensive midline suture and sutures for the premaxillary and malar bones are also clear.

Some of the details of the deciduous dentition are indicated by alveoli or roots (Figs. 8–10). The dC appears to have been double-rooted, to judge from the X-ray (Fig. 10) and the shape of the two alveoli situated in the proper position for that tooth (Figs. 8, 9A), where there is an intervening saddle-shaped connection between them. There is a single alveolus for dP1 (Figs. 8, 9A, 10B), and there are three alveoli (or roots) for each of the other deciduous upper premolars, with the lingual being the largest, the anterobuccal intermediate, and the posterobuccal the smallest. The palate is narrow (Fig. 8); the midline sutural ridge stands high off the deep palatal groove, which extends from the canine area to the middle of the premolar region. Most palatal features are a bit distorted because of compression. Its posterior portion, from mid-premolar area to the rear of M1, is relatively small and flat, and a bit of the anterior edge of the posterior palatine foramen is preserved at the rear edge.

In X-rays of the specimen (Fig. 10) the forming canine is indicated by the formation of its large, discrete crypt seen in the expected position within the swollen anterior edge of the maxillary. Because no mineralization of its enamel or dentine had yet occurred, only the limits of the pocket are seen. The formed but still encrypted P4, which is visible in the prepared specimen, can also be seen on the X-rays, and there is a faint trace of a forming P3 among the roots of the dP3. The tip of the protocone of the P3 is just visible through a small resorption window in the bone ahead of the lingual root of the dP3. The M1, with its broken crown, can be seen on the specimen and on the X-rays, but I cannot make out any trace of the forming M2 on the X-rays, although remnants of it are evident behind the M1 on the specimen (Figs. 8, 9). A smooth shallow pocket behind the area of the M2 is a portion of the anterior wall of the crypt of the M3, the only indication of the presence of that forming tooth in this juvenile maxillary. This specimen came from Bed ~569–570 (TWkA1), at locality FM-7-58-WDT in SW ¼, SE ¼, Sec. 22, T16N, R95W, Salazar Butte Quadrangle.

Another juvenile, but more mature, animal is represented by a nearly complete skull of *U. anceps,* PM 8019 (Fig. 11). Shown in dorsal view (Fig. 11A), the maxillaries, frontals, parietals, and much of the left nasal are preserved, with the paired frontals and parietals fused with no trace of a midline suture. The frontoparietal suture is closed but visible. The maxillary and parietal horns are seen to be mere buds. The sutures between the nasals, maxillaries, and with the frontals are open, and at this threefold junction the decided bulge seen in this area in most other skulls is already a marked feature. A definite low ridge runs transversely across the top of the skull between the parietal horns. In Figure 11B, the ventral view, the dentition, the maxillaries, and the maxillary part of the palate are seen, as are the basicranium, most of both squamosals, and the left malar. This specimen preserves the alveolus for the posterior root of the dC immediately behind the permanent tooth, which had been about to errupt.

In the basicranium of this juvenile, the glenoids (GL in Fig. 11) and postglenoid processes (PGP) are prominent features. Much of the ear region is missing; there are no traces of petrosals or tympanics. The external auditory meatus (EAM) is a broad, vaulted opening situated immediately behind the postglenoid process, which serves as its anterior border. It is roofed by the squamosal (SQ), which sends down a stout, short mastoid process behind the opening, but no mastoid foramen is to be seen. On the dorsal surface of the basicranial elements (not shown), the floor supporting the medulla is seen leading forward from the foramen magnum to near the rear of the basisphenoid, where a smooth circular pit for the pituitary (PIT) is located. Its dimensions are about 1.75 cm (or ⅔ inch) from front to rear by about 1.6 cm (less than ⅗ inch) from side to side.

Figure 11C shows a horizontal section through the braincase (looking up). It shows the oblique suture between the alisphenoid (SAS) and the parietal (P), the supraoccipital (SO), parts of each frontal (F) and parietal (P), a bit of the vomer (V), and the dorsal side of the remarkably smooth braincase, most of which seems to be the area of the cerebrum (C). At this age stage, it is undivided (i.e., there is hardly a sign of division between

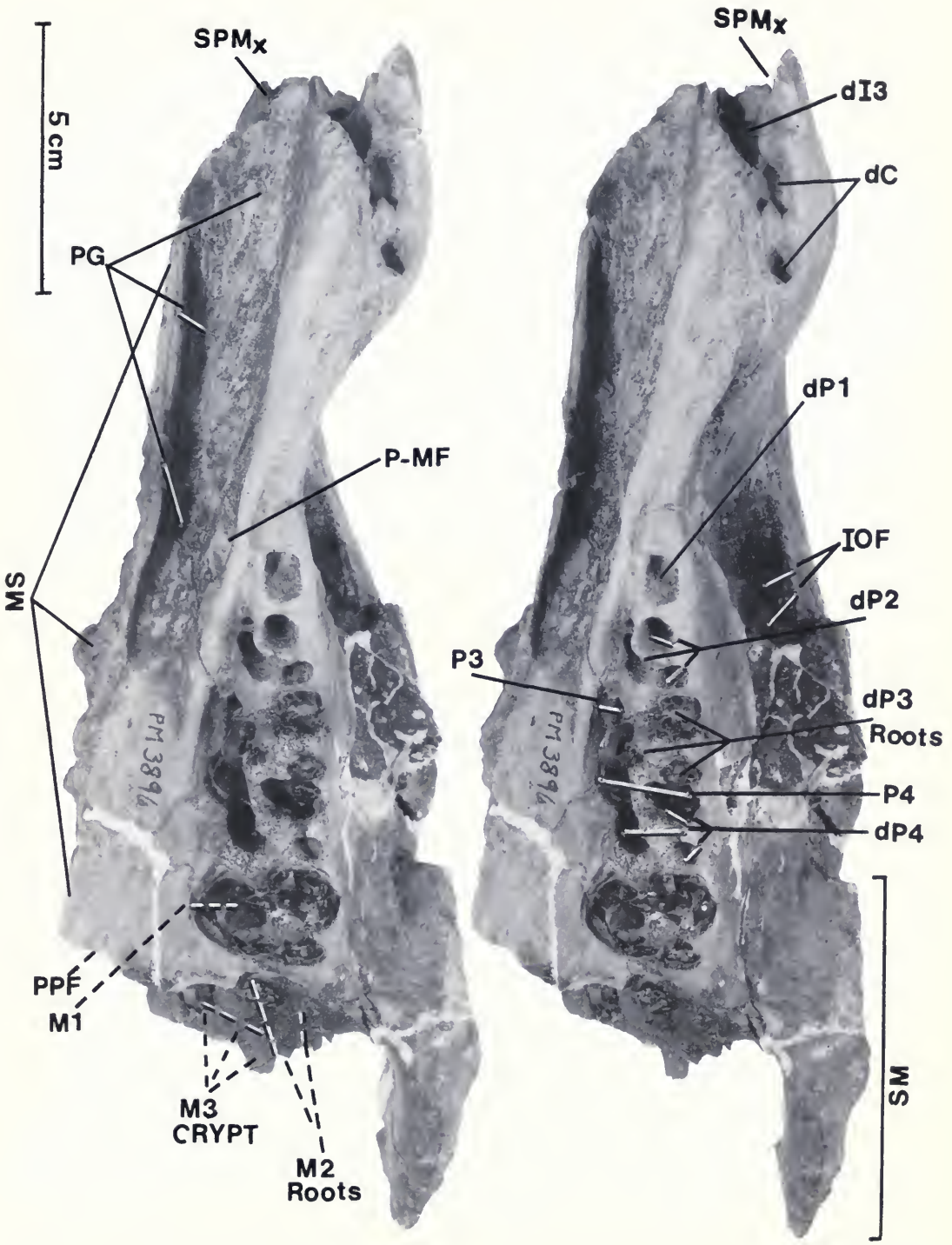

FIG. 8. Stereo pair showing the left maxillary in ventral view of a near-newborn specimen of *Uintatherium anceps*, PM 3896. Details of the palate and portions of both deciduous and permanent dentitions can be seen. Abbreviations: IOF = infraorbital foramen, MS = midline suture of the palate, P-MF = palato-maxillary foramen, PPF = posterior palatine foramen, PG = palatal groove or trough, SM = hidden suture for malar (jugal), SPMx = suture for premaxillary (a hidden groove). Dental abbreviations are standard; dI3, dC, dP1–2 and dP4 all indicated by their alveoli; dP3 and M2 are roots only; M1 consists of roots and much of the crown base, P3–4 can be seen through the open alveoli of their deciduous predecessors, and M3 was probably formed, as the anterior wall of its crypt is preserved behind and above the roots of M2 (FMNH neg. nos. GEO 85337.1 and 85337.2).

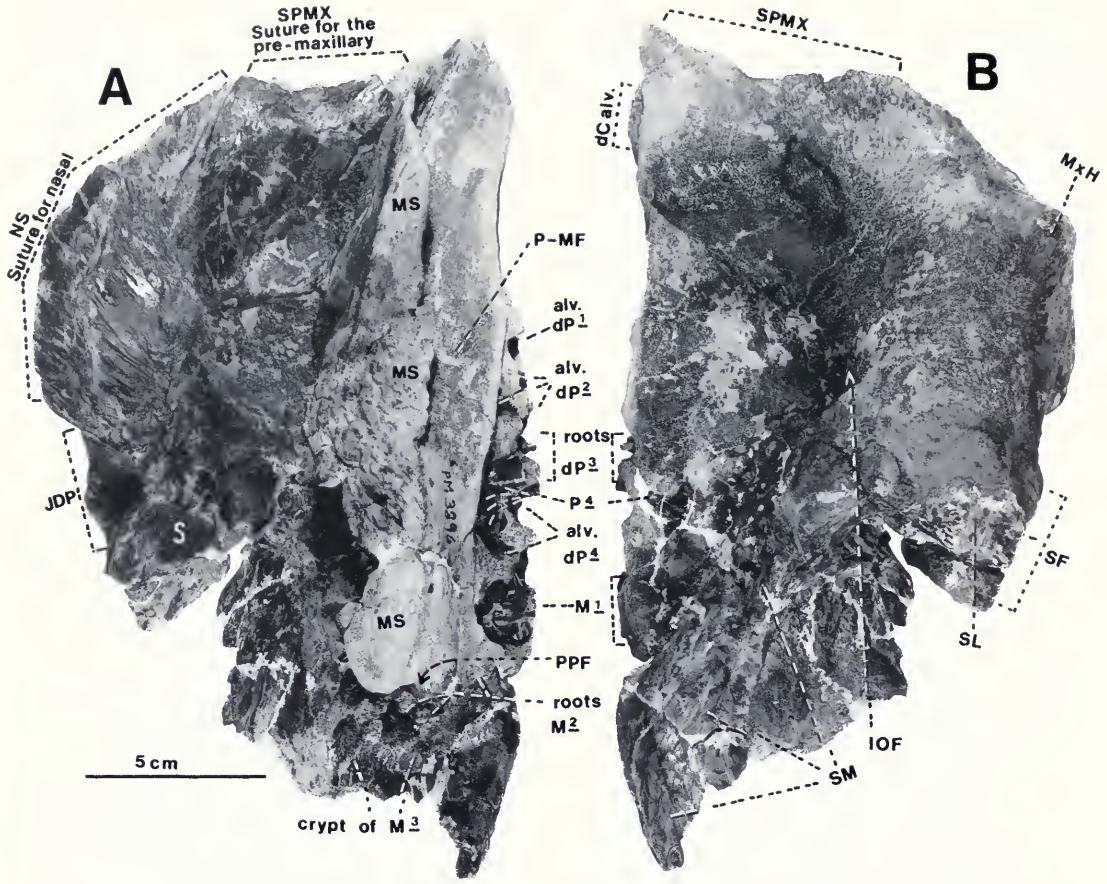

FIG. 9. Medial (**A**) and lateral (**B**) views of the same left maxillary as in Figure 8, PM 3896, showing the considerable depth of the skull in this region, the very immature maxillary horn bud, the extensive sutures for the nasal and premaxillary bones, as well as the near-midline suture of the palate. By comparing this "near-newborn" maxillary with the other juvenile and young adults, I estimate the skull length at about 40 to 45 cm. Associated with this specimen are many postcranial elements, including a scapula, an ilium, and vertebral elements (Figs. 46, 49 and 41, 42). The teeth, alveoli, and other tooth features are labeled using standard dental abbreviations. Other abbreviations are: J-DP = juvenile-dorsal pit (of uncertain significance), IOF = infraorbital foramen, MS = midline palatal suture, MxH = maxillary horn bud, NP = nasal passage, P-MF = palato-maxillary foramen, S = sinus cavity, SF = suture for frontal, SL = suture for lacrimal, SM = suture for malar, SN = suture for nasal, SPMx = suture for premaxillary (groove) (FMNH neg. nos. GEO 85779 and 85780).

→

FIG. 10. Direct prints of X-ray films of the juvenile maxillary, PM 3896, in which the forming canine, P3, and P4 can be seen. The orientation of both is as in Figure 9B. Two penetration levels, the greater in **A,** the lesser in **B,** are shown to aid in seeing various features that are either under- or overexposed in the opposite view. In the case of the canine, the large maxillary inflation needed to allow the tooth to begin its (later) formation is readily seen (both exposures), but little or no mineralization had occurred (greater exposure). Tips of the crowns of P3 and P4 can be seen in the greater exposure, and alveoli of dI3 (or I3 ?), dC, dP1, 2, 4 can be seen in the lesser. Figures 9 and 10 have been placed opposite one another to facilitate comparisons. a = artifact (probably a break); other abbreviations as in Figures 8 and 9.

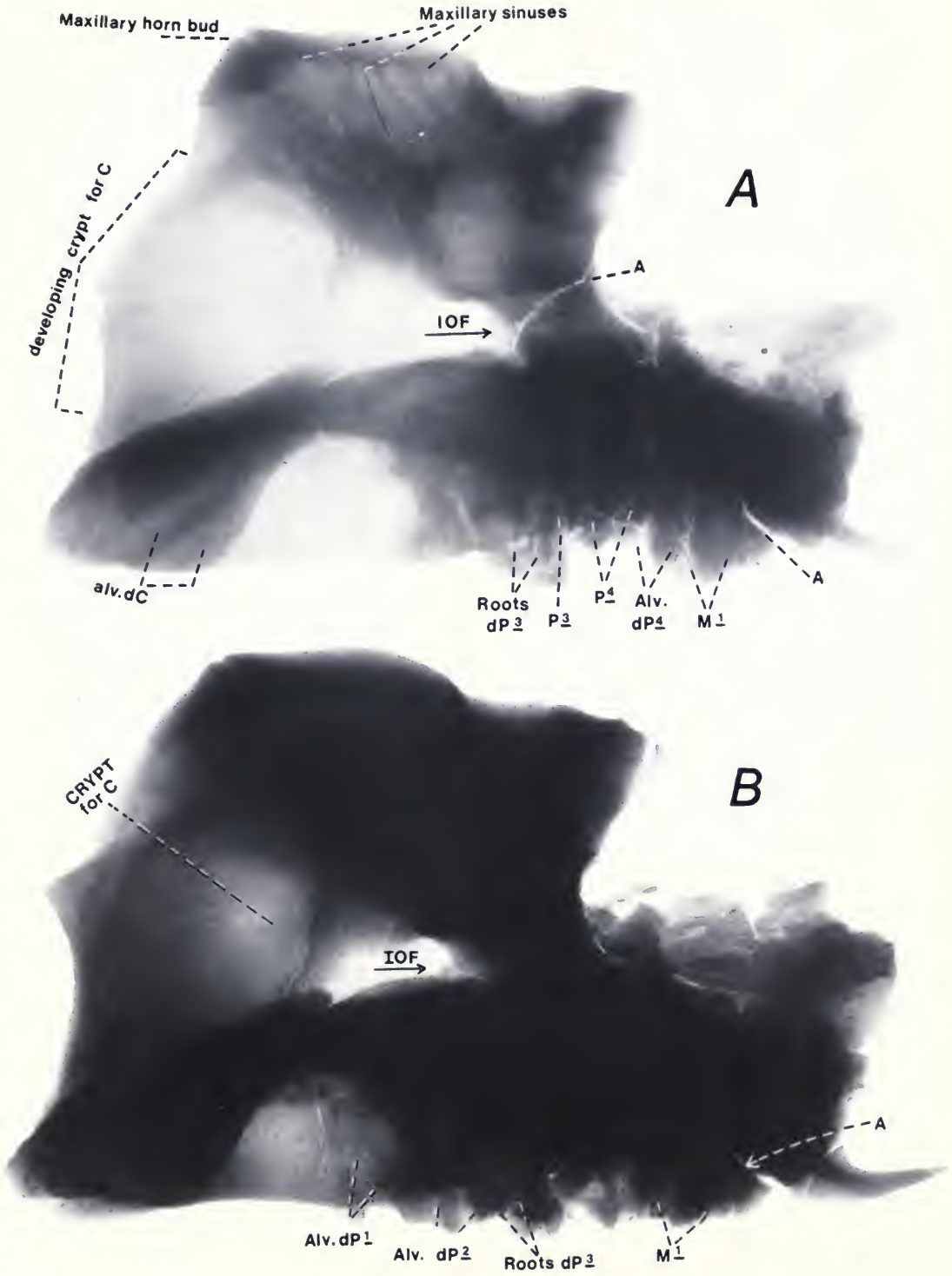
Maxillary horn bud
Maxillary sinuses
developing crypt for C
A
A
IOF
alv.dC
Roots dP3
P3
P4
Alv. dP4
M1
A
B
CRYPT for C
IOF
A
Alv. dP1
Alv. dP2
Roots dP3
M1

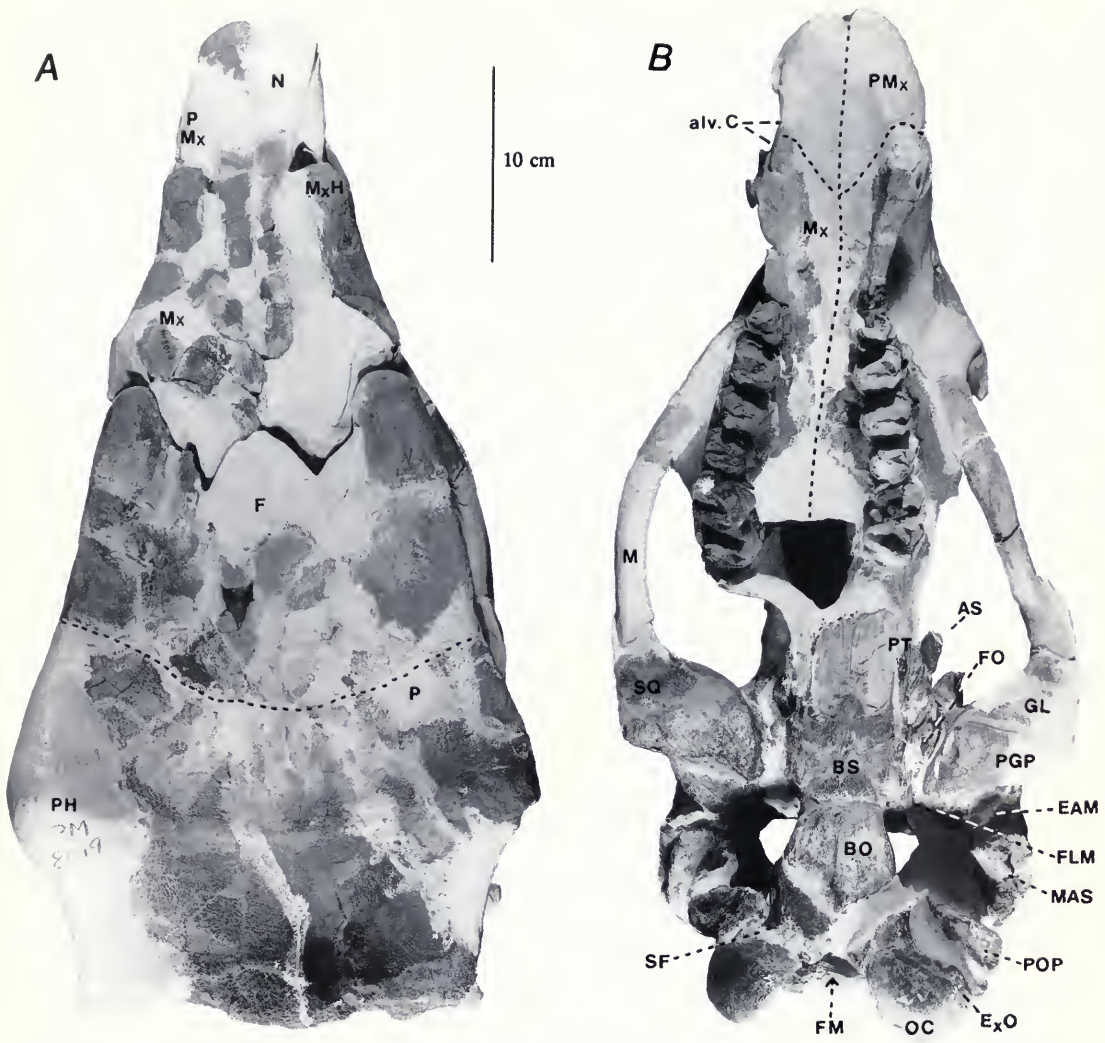

FIG. 11. PM 8019, skull of a juvenile *Uintatherium anceps* shown in dorsal (**A**), ventral (**B**), and ventral from within the cranium (**C**) views. In **D,** the upper dentition and palate are shown enlarged. This specimen represents another juvenile age stage in which the horns are still in the "bud" stage (A), whereas the dentition (B, D) has advanced to the point of complete eruption of the P2s through M2s, with M3s formed but still encrypted. Nonetheless, this skull probably was only slightly larger than that of the "newborn," to judge by the distance between the notch behind the anterior buttress of the zygomatic arch and the tip of the maxillary. The right canine is seen through breaks in the maxillary bone. It appears to have been beginning to erupt. Most of the dorsal cranial sutures are visible, as is the transverse ridge between the budding parietal horns (A), a feature that Marsh (1886) had noted. In B, some basicranial features are shown; in C, the simple, relatively smooth dorsal surface of the braincase is seen with a few features identified. Abbreviations as in Figures 8 and 10, others as follows: AS = alisphenoid, BO = basioccipital, C = cerebrum, CF = condyloid foramen, ExO = exoccipital, FM = foramen magnum, F = frontal, GL = glenoid, HF = hypoglossal foramen, MAS = mastoid, Mx = maxillary, OB = olfactory bulb, OC = occipital condyle, P = parietal, PH = parietal horn bud, Pin = pineal pit, PMx = premaxillary, POP = paroccipital process, PT = pterygoid, SAS = suture for alisphenoid, and SO = supraoccipital (FMNH neg. nos. GEO 85687, 85705, and 85706).

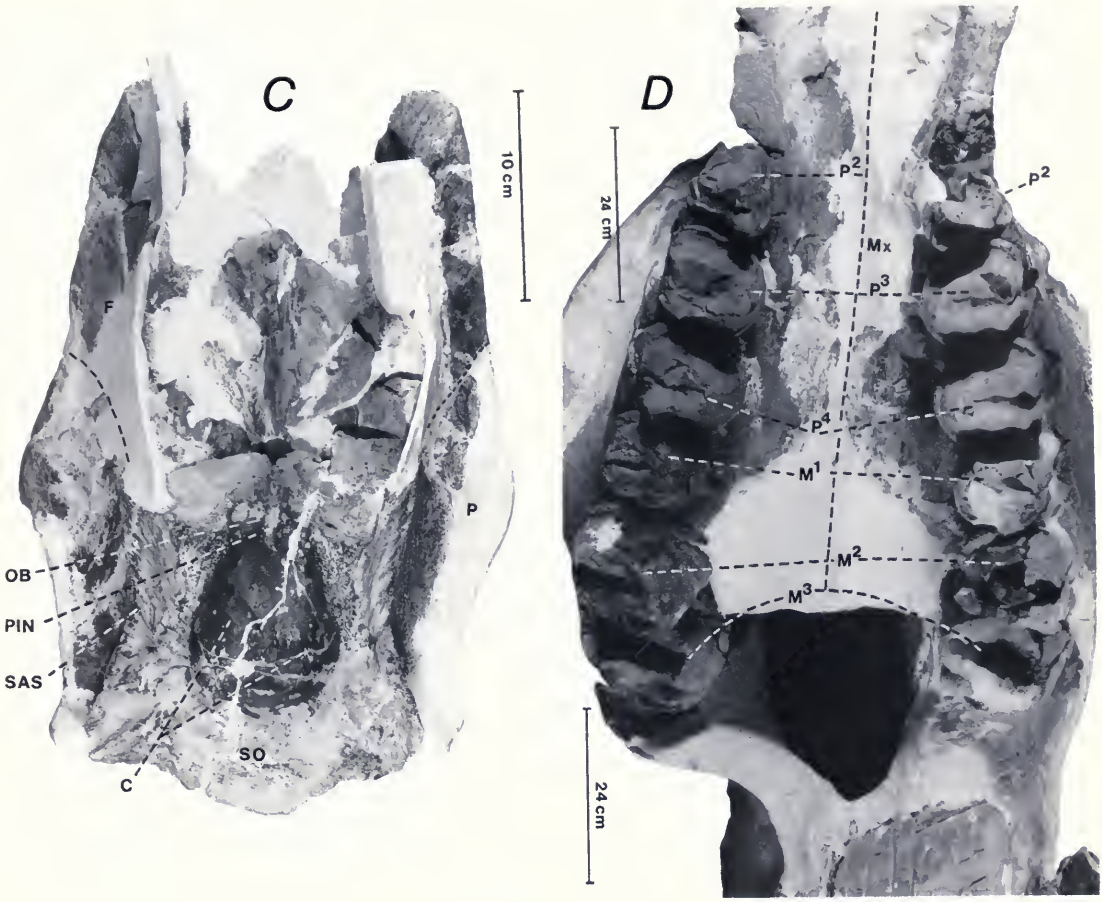

FIGURE 11. *Continued.*

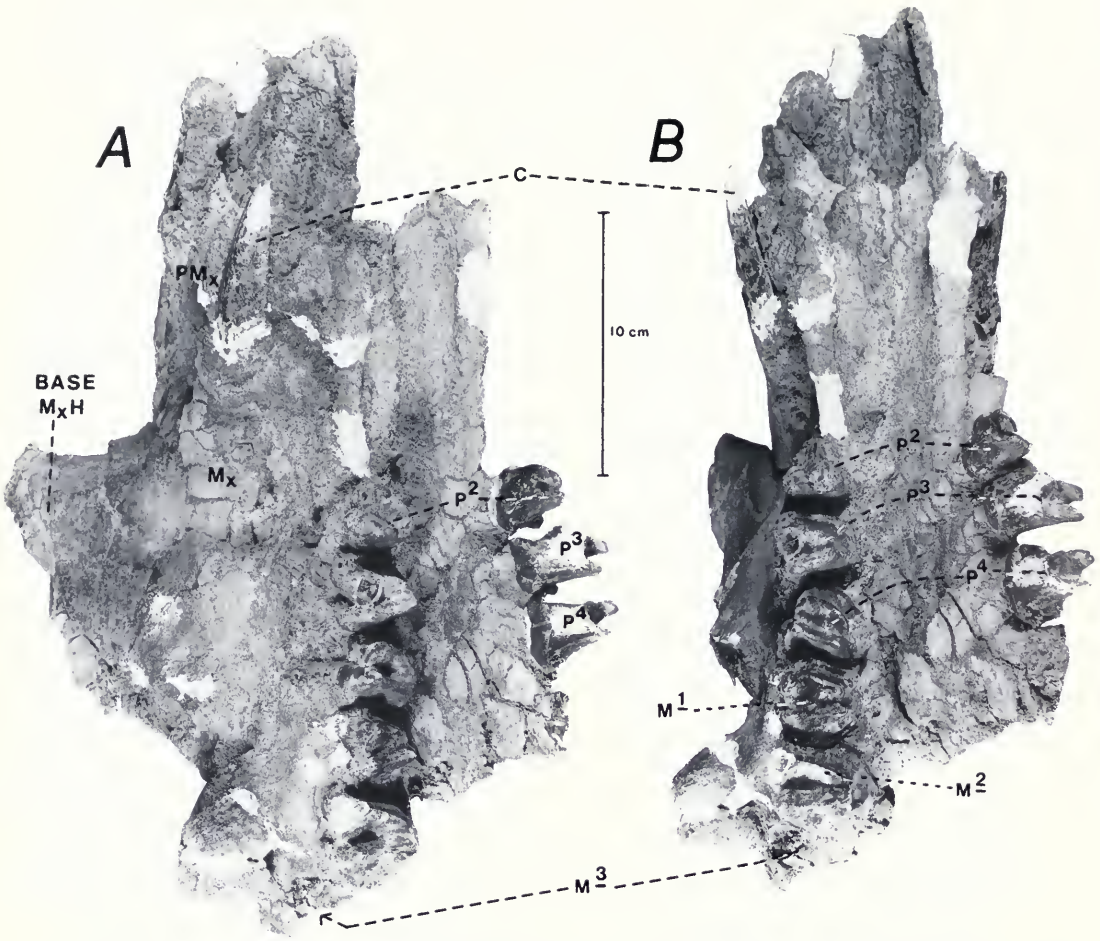

FIG. 12. PM 54406A, the partial skull of another juvenile specimen of *Uintatherium anceps,* shown in right ventrolateral (**A**) and ventral (**B**) views. I am uncertain of its sex. Its very narrow canine tusks are formed but still unerupted or just beginning to erupt. From their extremely slender proportions, I suspect the specimen to be female, and from the eruption stages of the cheek teeth, it must have been young, probably about the same age as PM 8019 when it died. Nonetheless, its maxillary horn appears to have been more developed than that of PM 8019 or the "newborn" because the base for it is expanded, which suggests that it may be a male. It is also possible that the "canines" are in fact deciduous teeth, but that seems highly unlikely, because other decidedly younger specimens had already shed their apparently smaller dCs (FMNH neg. nos. GEO 85701 and 85702).

right and left portions of the cerebrum), but, as can be seen in endocasts of fully grown individuals such as Marsh showed (1886, pl. VI), the adult condition does have a weak dorsal division between the two hemispheres. PM 8019 has dorsal margins of both olfactory bulbs (OB), and the pineal pit (PIN) is preserved.

Figure 11D is a close-up of the palate and cheek teeth, P2–M3 of both sides. An interesting feature preserved in this specimen is the posterior alveolus of the right deciduous canine, just behind the permanent tooth, which was beginning to erupt. The medial wall of the anterior alveolus can also be seen. So this specimen shows the same double-rooted condition of the dC as the "newborn" specimen. Skull and dental measurements are given in Tables 1 and 5. The M1s are the only teeth showing any wear. Both M3s are fully formed, have a surrounding cingulum except in the region of the paracone, but are still within their crypts. Both P2s are broken, but between them their morphology is clear: a loph extends from the anteromedial cusp diagonally backward and laterally to a lower single external cusp. A smaller posterointernal cusp is present, and a cingulum surrounds the entire crown. Left M1–2 are broken but largely present. M2–3 each have a small hypocone. The specimen was recovered from the grassy flat just below the base of the Lower Brown Sandstone rim, about 200 yards NNE of the old Eversole Ranch house. Its horizon is about beds 569–571 (TWkA1), the locality is FM-1-59-WDT in NW ¼, Sec. 12, T15N, R99W, Sand Butte Rim SE Quadrangle.

The partial skull, PM 54406A (Fig. 12), is that of another older juvenile, or early subadult, of about the same dental age stage as the prior specimen but with a more developed maxillary horn, to judge from its broken horn base. It preserves most of the nasals and maxillaries, left and right P2–P4; the right M1–2 is erupted, and the M3 is fully formed but still in its crypt. From the cheek teeth, it is essentially at the same age stage as PM 8019. The distal 6 cm of the right canine is exposed (unerupted), as is a similar but lesser part of the left. Both are relatively very small and very slender: the anteroposterior length of the right measures only 24 mm at its widest exposed part, suggesting that the specimen is female, but the more developed horn base suggests otherwise. Hence, I am uncertain as to its sex. None of the teeth other than the M1 show any wear, and that on the M1 is slight. I believe that both it and PM 8019 represent late juvenile developmental stages.

The canines were about ready to erupt and are partially exposed by damage. They are very slender, just the tips of the forming teeth, which suggests that the specimen is probably a female (the left one is split lengthwise, and part of its anterior half is missing). They are not deciduous teeth, for even though the cheek teeth are but little, if at all, advanced over those of the two prior specimens, the canine teeth are larger than milk teeth would be expected to be. Further, it is significant that the maxillary horn appears to be advanced well beyond the nubbin stage. Left and right P2–P4s are present in unworn condition, and the lophs are high and crested. The P2 has a small cusp that I take to be the protocone (it is in that area) with both anterior and posterior crests. The anterior crest extends anterolabially to join a weak ridge near the base of the paracone. The posterior crest runs directly laterally to meet a ridge from the metacone. The surrounding cingulum is complete except where it climbs onto the base of the protocone and disappears. Thus, in this specimen, the three primary cusps are in their usual positions. P4 is not fully erupted; its posterior cingulum is wedged beneath the anterior cingulum of the M1. The right M1–M2 are in place, the former showing some wear, the latter being unworn; and the M3 is formed within its crypt. The hypocone present on M1–2 is minute, but is more prominent on M3. The specimen is from locality FM-1-85-KL/WDT, ~Bed 591 (TWkA1), in NE ¼, NW ¼, Sec. 26, T15N, R95W, Powder Mountain NE Quadrangle. It is one of a number of uintathere elements (PM 54401–54408, 54421, and 54676) discovered by Bureau of Land Management (BLM) crews and reported to me. Initially thought to be part of PM 54406B, it has proved to be otherwise (see below).

Most of the complete adult skulls of *U. anceps* are to be found in the collections of Yale University (including the Princeton materials), the American Museum, and the U.S. National Museum. At the Field Museum, we have only one such specimen, PM 53933 (frontispiece and Fig. 5), which is much like those described and beautifully illustrated by Marsh in his 1886 monograph, the first extensive, definitive treatment of the terminal uintatheres. That study, as noted earlier, is an essential accompanying work to have at hand when dealing with uintathere anatomy. However, most differences that Marsh took to be of a specific nature I consider to be a combination of age, sex, and individual variation, following Wheeler (1961) and Schoch and Lucas (1985).

Some of the sutures of this young adult were already closed, often without much of a trace. Those that are clear are the midline sutures of all three bones that make up the palate (premaxillary, maxillary, and palatine), and the maxillary–premaxillary, –nasal, –palatine, –frontal, frontoparietal, and squamosal–malar sutures. Others that cannot be followed completely but may be glimpsed in places are maxillary–malar, maxillary–lacrimal, parieto-occipital, supraoccipital–exoccipital, and most of the basicranial sutures. I am unable to locate any of the sutures of the alisphenoid and most of those for the squamosal. Figure 5A shows the skull viewed from the left side. The still relatively small nasal horns are indicated (buried in the cradle), but the growing maxillary and parietal horns and the extent of occipital crest development are readily seen, as is the barely worn canine tusk. Figure 5B shows the ventral aspect of the skull, where the palate, most of the basicranium, the left zygomatic arch, and the cranial wall all have been prepared free of matrix. The sandstone matrix has been left in the interior, and to support the right arch. Figure 5C shows the dorsal aspect in which the crests connecting parietal horns and the occipital crest are apparent. Figure 5D, the posterior aspect (inverted, resting on its dorsum) shows the great extent of the occipital region and the crests for attachment of the nuchal musculature, as well as the condyles and foramen magnum. The ear region is reported in a separate section below.

The adult upper dentition is well illustrated by the Funderburk skull, PM 53933 (Figs. 13A and 5A–B). It consists of the complete left upper canine, partial right canine, and both left and right P2–M3s. The virtually complete left upper canine is oval in cross section (5.63 mm × 2.94 mm) where it leaves the maxillary. It protrudes 18 cm from the alveolar edge to its tip. Its lanceolate shape is as Marsh described it for his specimen of *D. mirabile* (his pls. I and II), but the lanceolate shape is more extreme than Marsh (1886, pp. 43–45) shows it to be in his illustrations. I assume that individual variation, differing age stages of the adult males, and degree of wear account for the differences. Marsh's (1886, pp. 47–49) descriptions of the upper cheek teeth of *T. stenops* serve about as adequately as does the FMNH *U. anceps* specimen, PM 53933. The teeth in the FMNH specimen are less worn, so that their cusps and lophs are more clearly delineated, even those on the M1s. Each molar has a small hypocone; the left P4 has a distinct one, and even the right P3–4 each have a minute one. PM 53933 differs slightly from Marsh's illustration for *T. stenops* (1886, p. 47). In the Marsh specimen, the protoloph and metaloph of the M3 meet in a U shape, while in FMNH PM 53933 the union takes on a V shape. On the left side, just ahead of the P2, there is a faint suggestion of a nearly filled remnant of the alveolus for the P1; on the right side, either it has been filled without a trace or no P1 ever formed. Others have found this sort of variation for this tooth position (Schoch & Lucas, 1985). Such minor differences I consider to be well within the range of individual variation. The locality it came from, FM-2-85-KL/WDT, is near the center of NW ¼, Sec. 8, T15N, R94W, Salazar Butte Quadrangle. It is from Bed 569 (TWkA1).

The two partly destroyed adult skulls, PM 1666 and PM 1667, in spite of the extensive damage they have suffered, do provide some information, as follows. In its dorsal aspect, PM 1666 can be seen to preserve, either as bone or as a cast of the bone impression taken from recovered and fitted matrix blocks, most of the nasals, maxillaries, and frontals (Fig. 14B). There is enough evidence from matrix impressions and bone scraps to enable one to say that the maxillary horns were developing but were not yet large. They were more developed than just horn buds, and there is a weak transverse bony ridge between them. The most complete of the parietal horns (right) is also only somewhat developed. In ventral view (Fig. 14A), the anterior part of the palate (premaxillary and maxillaries into the diastemal region) is preserved, including the left canine broken off at the alveolar margin. None of the cheek teeth remain, but the right zygomatic arch and glenoid and part of the left are preserved, as is some of the pterygoid. There is an 8-cm-long part of the broken-off tusk and much of the ? occipital crest among the many other scraps, including an intriguing bit, the fill of a canal of some sort (probably vascular), but with both anastomosing and diverging laterals to the main tract. This suggests that it might have served both vascular and nervous pathways. All indications suggest that this was the skull of a young adult or advanced subadult individual. It came from locality FM-13-56-WDT, in NW ¼, Sec. 12, T16N, R98W, Ft. LaClede Quadrangle, from Bed 569 (TWkA1).

PM 1667 was facing out from the cliff base at the same horizon, ~50 yards (~46 m) north of the previous specimen, when I found it. The front half had been almost totally vandalized, but the rear part was largely still in situ. In dorsal aspect,

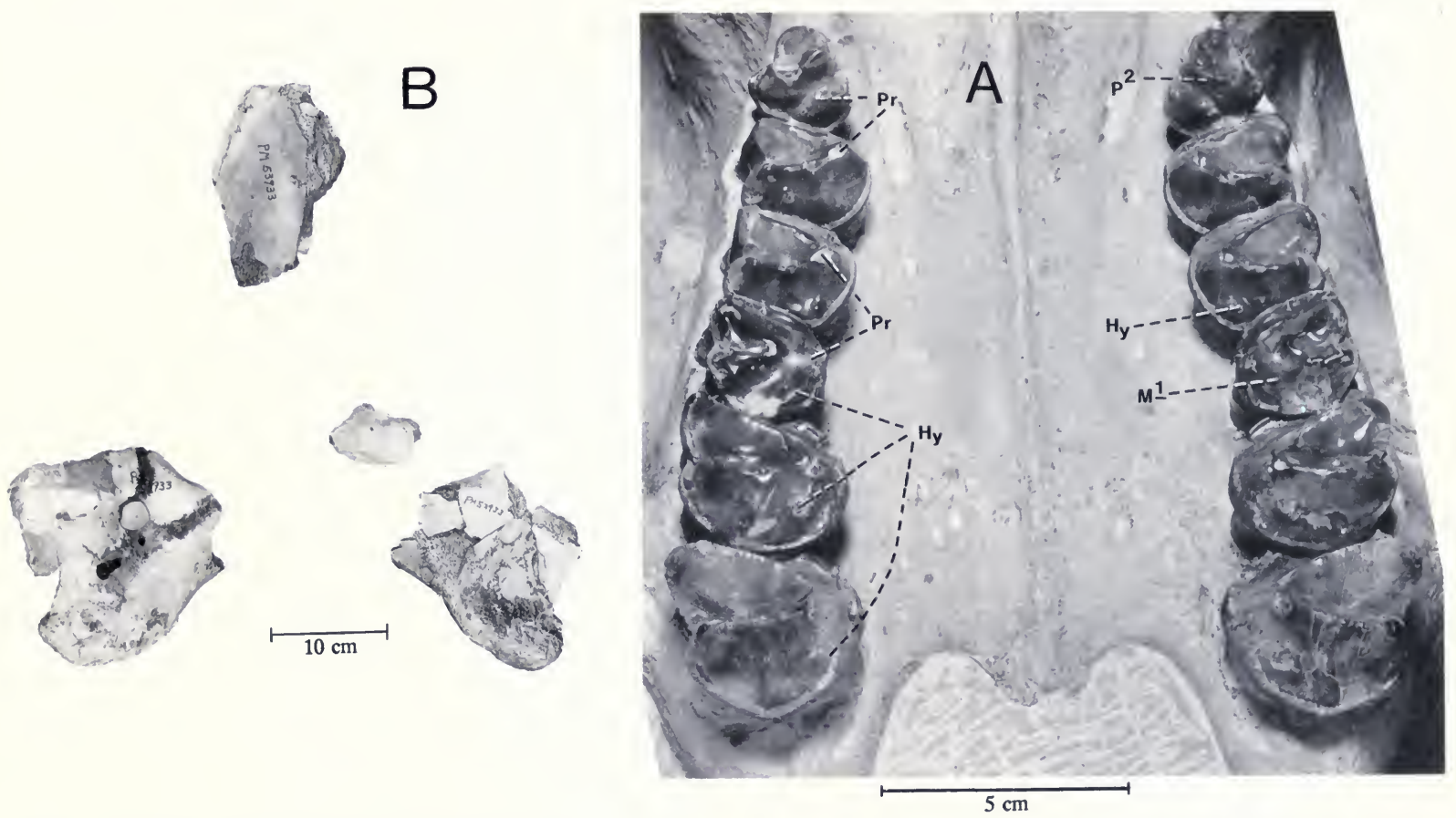

FIG. 13. PM 53933, *Uintatherium anceps,* the Funderburk specimen. In **A,** the palate and upper dentition (left and right P2–M3) are shown enlarged over that of Figure 5. Tooth abbreviations are standard: Hy = hypocone, M1 = 1st molar, P2 = 2nd premolar, Pr = protocone. In **B,** fragments of the once articulated jaws, including most of the symphysis, both coronoid processes, and the right condyle, are shown. In the symphyseal piece the alveoli for i1–4 and c are visible (see also Fig. 34B) (FMNH neg. nos. GEO 85689 and 85926).

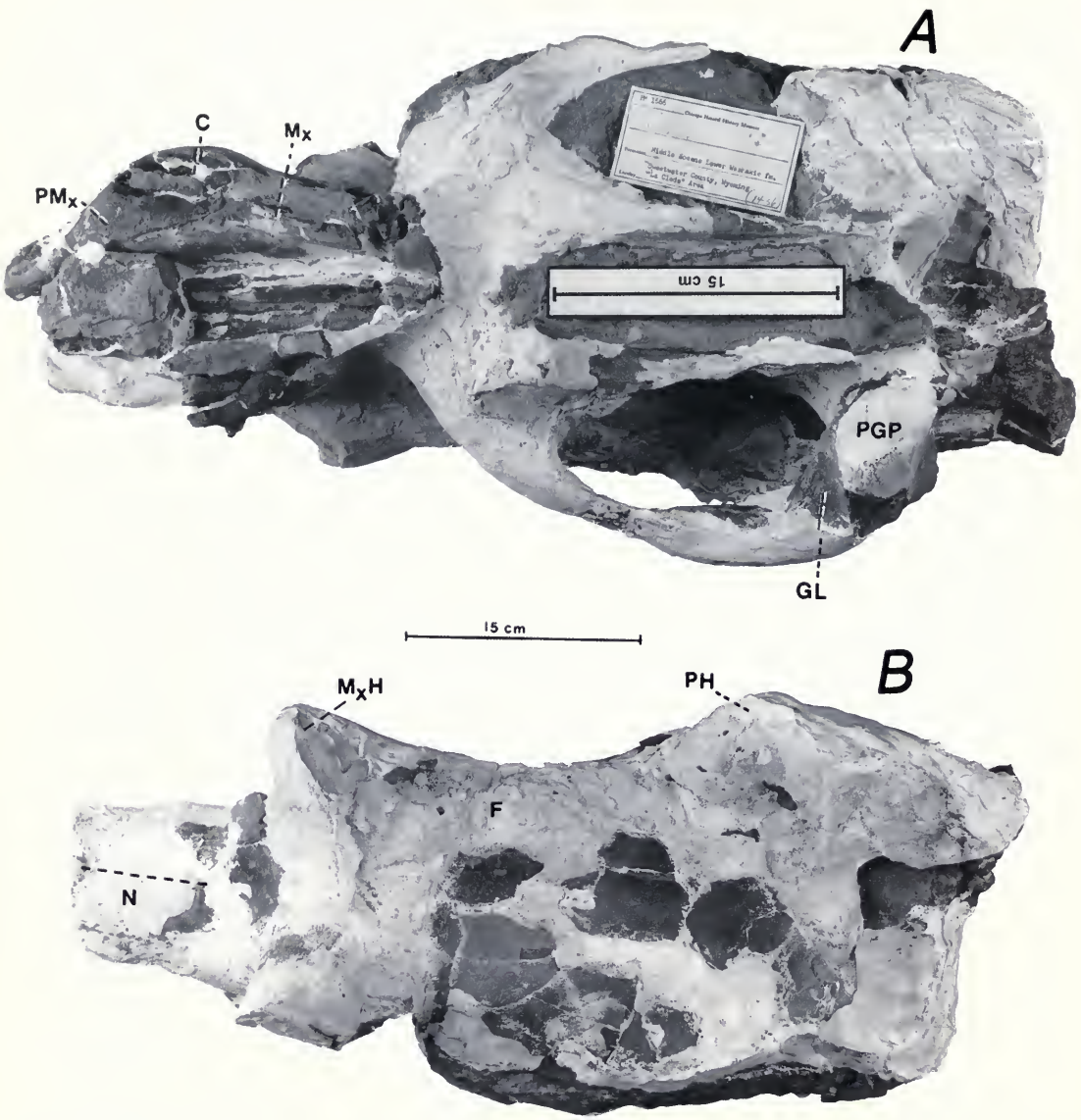

FIG. 14. PM 1666, one of two vandalized skulls of *Uintatherium anceps,* is shown in ventral (**A**) and dorsal (**B**) views, as restored by fitting bony breaks and casts from natural molds in matrix impressions. The extent of horn development and the remnant of its permenant tusk both indicate that it most probably was a young adult. The only tooth preserved in the skull is the base of the left canine broken off at the alveolar margin. There is an 8-cm-long piece of it (or its opposite) among the many scraps we have not been able to fit into their proper positions (FMNH neg. nos. GEO 85791 (A) and 85794 (B)).

frontals and parietals are represented mostly by bone, somewhat by casts of the entombing matrix (Fig. 15B). The occipital crest is well delineated, but not high, and there is a low transverse bridge of bone between the bases of the parietal horns. In right lateral view (Fig. 15A), much of the temporal fossa and part of the rear of the zygomatic arch, the glenoid and postglenoid process, as well as the external meatus, mastoid, and occipital condyle, are visible. The skull is somewhat crushed dorsoventrally. In ventral view (Fig. 15C), the basicranium is seen to be well preserved from pterygoids to condyles. Behind the postglenoid process and the superficies meatus, many features of the ear region are preserved. The paroccipital process is weakly developed and the mastoid process, while larger, is not as prominent as either the postglenoid processes or the occipital condyles. The anterior tip of the ? petrosal can be seen ahead of the anterior crux of the tympanic process of the mastoid, an irregularly curved, bulbous structure behind and lateral to the meatus (see below, section on the ear region). A number of foramina can be identified (f. magnum, hypoglossal f., f. lacerum posterium, f. lacerum medium, f. ovale), while others that are visible on the skull are less certainly identified (Figs. 15C, 27). The locality is the same as that for PM 1666 (above).

PM 54406B (Fig. 16) consists of part of the skull of an adult, preserving much of the basicranium and occiput, right parietal, and maxillary horns, part of the connecting frontal, and the edentulous left mandible. The associated palate and upper dentition, PM 54406A, was initially taken to be a part of this skull, but the evidence indicates otherwise. It is not the same individual, for its subadult dentition, with M3 fully formed but deep within its crypt, precludes that relationship. Furthermore, the portion, PM 54406B, is preserved within a fine, tan, laminar claystone, while PM 54406A is in a greenish gray sandstone, apparently a part of an adjacent channel that had cut into the clay bank containing PM 54406B. The locality for both PM 54406B and A is FM-1-85-KL/WDT, in NE ¼, NW ¼, Sec. 26, T15N, R95W, Powder Mountain NE Quadrangle, from ~Bed 591 (TWkA1).

The partial skeleton, PM 53921, had only scraps of the skull, including the associated nasal bones (Fig. 17). It is that of a fully adult individual, notable primarily for its complete pelvis (Fig. 49) and major limb bones. It came from a single horizon at a bench high on the bluff. It was disarticulated and spread over a 30 × 6–9 foot (9 × 1.8–2.7 m) area. The ventral side of each elongated nasal is deeply grooved for the entire length, and the grooves extend through the maxillaries and anterior part of the frontals. Dorsally, there is hardly any nasal horn development at all in spite of its adult status. It is from locality FM-8-85-KL/WDT, discovered with Mary Jane and Murray Daniels, in SE ¼, SE ¼, Sec. 27, T16N, R95W, Salazar Butte Quadrangle. It was collected over two field seasons, 1985 and 1988, from ~Bed 573 (TWkA1).

The fragmentary skull specimen, PM 8020, consists of only the nasal bones, pieces of an upper canine, three lower incisors, and a partial lower premolar. Figure 18A shows the low oval nasal horns, little more than buds, which measure 6 cm by 3 cm at their bases and protrude only ~3 cm above the dorsal surface of the main portion of the bone. They are comparable to the nasal horn development seen in the young adult, PM 53933 (the Funderburk skull). The incisors (Fig. 18B–D) are discussed in the section on the lower dentition. The locality is FM-2-59-WDT, located in SW ¼, SE ¼, Sec. 22, and NW ¼, NE ¼, Sec. 27, T16N, R95W, Salazar Butte Quadrangle, from ~Beds 571–575 (TWkA1).

PM 39393 consists of a number of skull scraps, including parietal and maxillary horns. Parts of this same individual, which apparently had at one time been a nearly complete skeleton, consisted of four articulated thoracic vertebrae, pelvic fragments ?, the distal parts of two limbs, front (Fig. 47) and hind (Fig. 53B), and their articulated but incomplete feet. It was discovered by Murray Daniels in 1979 at my locality FM-4-79-WDT, which is located near the center of N ½, SW ¼, Sec. 19, T13N, R96W, Upper Powder Spring Quadrangle, Bed 595 (TWkA1).

The University of Wyoming skull, UW 13644, is that of an aged male with heavily worn teeth (Fig. 57). Originally it was identified as *U. anceps* because it corresponds well in skull length (Figs. 2A, 3; Table 1). However, using the Wheeler (1961) ratios and values, its B/A ratio (1.06) is closer to that of *Eobasileus cornutus* (0.8–0.9) than to that of *U. anceps* (1.5–2.2). The B/C ratio of about 2.2 is just within the top of the range for *Uintatherium* (1.2–2.3), and just within the bottom of that of *Eobasileus* (2.1–3.1). Also it corresponds more closely in its cheek teeth (Fig. 57C; Tables 3 and 6) with *E. cornutus*. Thus, from its intermediate condition, I take this individual to be representative of a transitional stage in the evo-

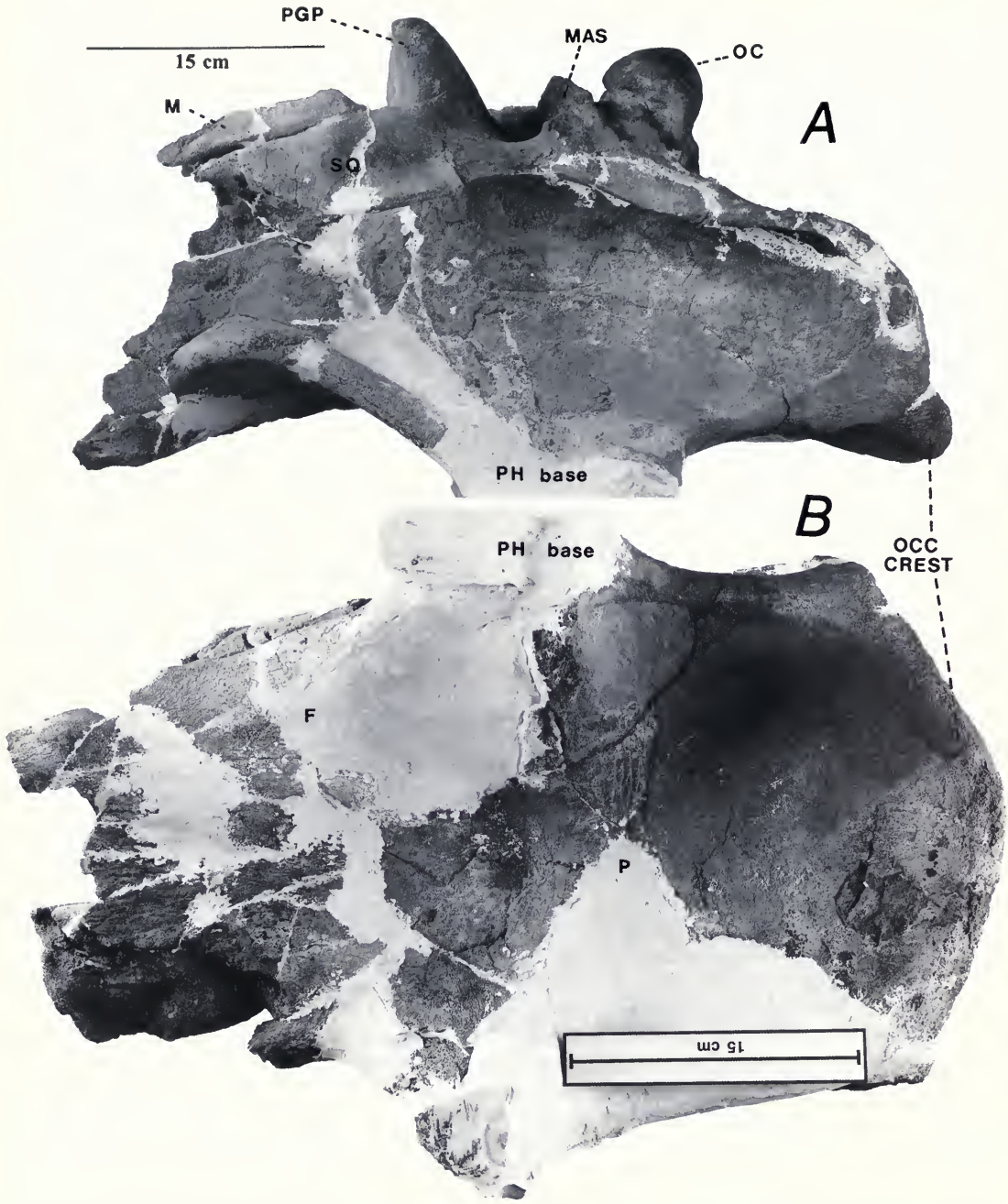

FIG. 15. PM 1667, the second of the vandalized skulls of *Uintatherium anceps,* consists of most of the cranium of a large adult. The anterior part was broken into mostly small fragments, but the more deeply imbedded rear of the skull is in fair condition. Much of the frontals and most of the parietals, right alisphenoid, squamosal, and malar and all of the occipital and basicranium are intact. The ear region is present, but the preservation is inadequate for observing many details (see section devoted to the ear region). The skull is shown in right lateral aspect in **A,** where the ventral side is up and where dorsoventral compression is most apparent; in **B,** dorsal aspect; and in **C,** ventral aspect, in which most features from pterygoid wings (Pt) to occipital condyles (OC) are clear. Other abbreviations: BO = basioccipital, BS = basisphenoid, EAM = external auditory meatus (porus), FM = foramen magnum, FO = foramen ovale, G = glenoid, M = malar, MAS = mastoid process, NB = neuchal boss, P = parietal, PH = parietal horn (broken), POP = paroccipital process, PET = petrosal (anterior tip), PGP = postglenoid process, Pt = pterygoid, SM = superficies meatus, SQ = squamosal, and T ? = tympanic (ant. crux)? (FMNH neg. nos. GEO 85789, 85790, and 85792).

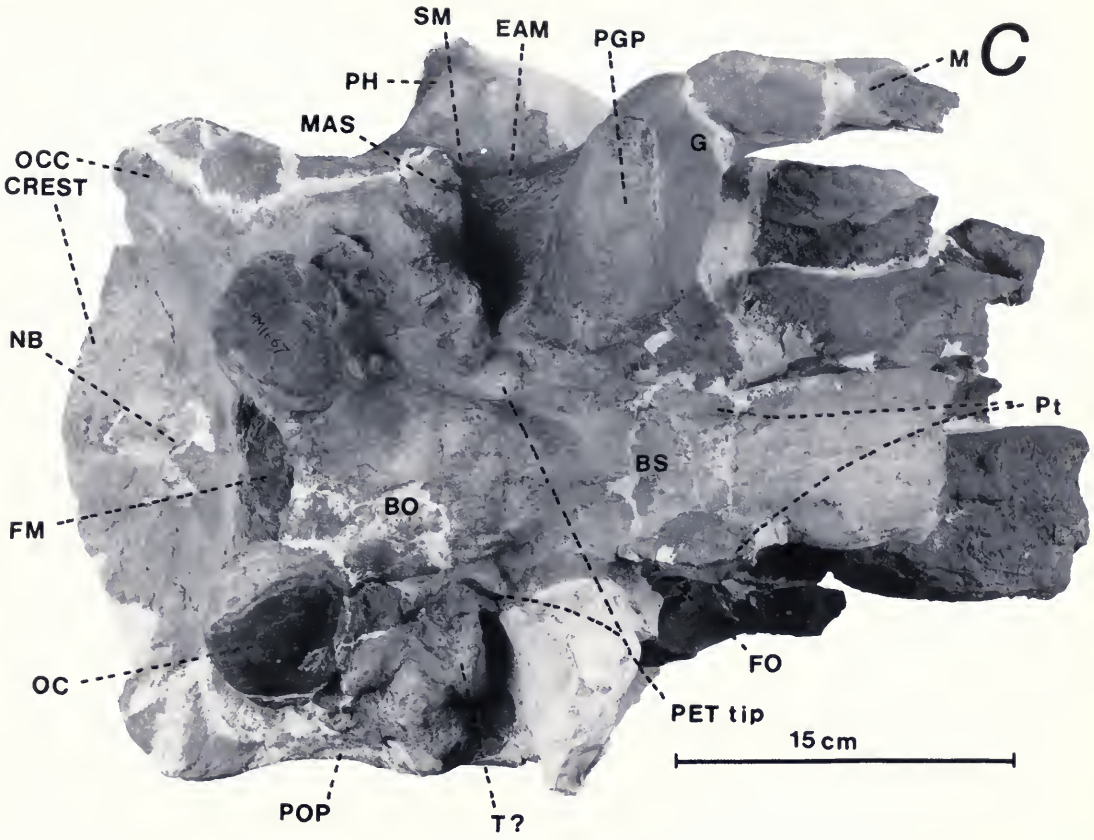

FIGURE 15. *Continued.*

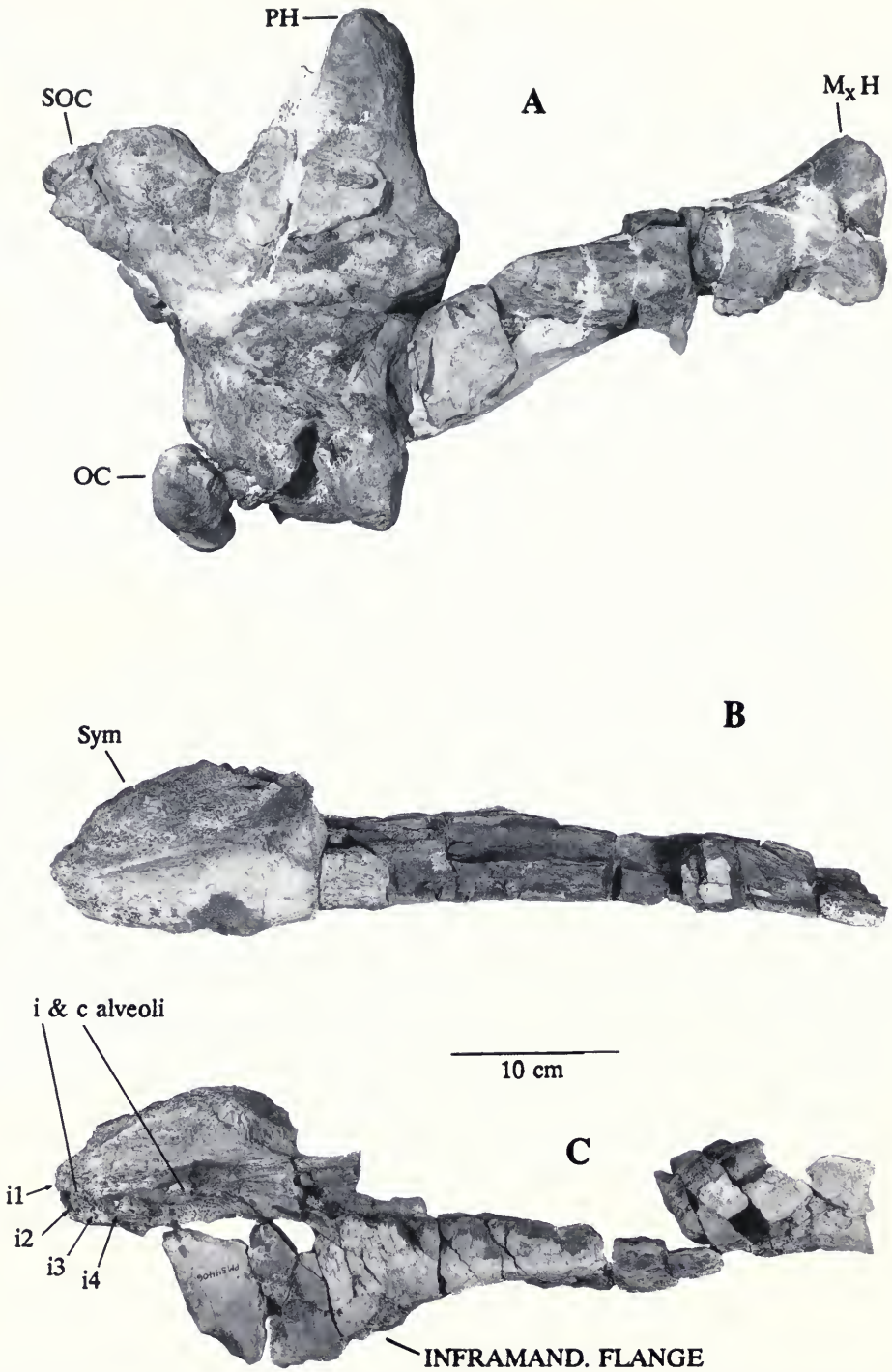

FIG. 16. PM 54406B, partial skull and left jaw ramus found associated with PM 54406A (Fig. 12). It represents an older individual, however, and the entombing coarser matrix of PM 54406A suggests that it came from within an adjacent channel to that with the finer clay matrix embedding PM 54406B. (At least six other uintathere bones came from this same finer-grained sandy clay bed in a linear array about 50 m long.) These edentulous fragments tell us little beyond the fact that they appear to represent a fully adult individual, with a developed inframandibular process. In **A**, the right side of the rear portion of the skull is shown. It extends from the condyle forward through part of

lution of *E. cornutus* from *U. anceps*. Because the teeth show it to be *Eobasileus,* I now so classify it. Not only does this combination of features suggest this, but also its stratigraphic position (low in TWkA2), intermediate between TWkA1 and the greater part of TWkA2, makes the interpretation reasonable. Its short skull length (Fig. 2B) may be accounted for by its transitional status between *U. anceps* and *E. cornutus*.

Its UW locality number is V79013, which is in the center of N-central ½, SW ¼, SE ¼, NW ¼, Sec. 15, T16N, R97W, Manuel Gap Quadrangle. This is within my locality FM-3-57-WDT, low in TWkA2. This is the only member to yield *Eobasileus,* and it is not surprising to find a transition zone within the bottom beds of the unit. Therefore, the remainder of the description and discussion concerning this skull will be found under the *Eobasileus* heading.

P 26925, a right M2 (Fig. 18E), is from a sandstone above the Evacuation Creek Member. The locality is given as "about 8 mi. NNE of Magnolia Petroleum Co. wells, NE of Piceance Creek in the Green River Formation, Piceance Creek, Roan Plateau, Garfield County, Colorado." This is the J. Leroy Kay locality of the Carnegie Museum, which Patterson worked and usually designated as "Kay's" locality. It is the same as the University of Colorado's "Bone-anza" locality (L. 78049), Shooty (Tschuddi) Gulch, Scenery Gulch, or junction of Shooty and Scenery Gulches. The specimen was collected by John M. Schmidt, a member of Patterson's field crew in 1941. A. J. Kihm (1984) provided most of the details, as Secs. 22 and 27, T2N, R96W, Rio Blanco County. The Garfield County designation may have been correct at one time, for Rio Blanco County was cut out of a formerly much larger Garfield County, according to one local rancher. The locality is on the White River City and Indian Valley Quadrangles. I am unsure about its coming from the Green River Fm., although it is the only formation mapped for the area. Perhaps deposition of that formation continued longer in this western Colorado area than in the Green River and Washakie Basins, or perhaps the upper part of the Green River Fm. there is made up of unrecognized transition beds comparable to the Sand Butte, Hardt Cabin, and Kinney Rim Beds in the Washakie and Green River Basins. However that turns out, there is no doubt about the identity of the tooth. It is typical of an M2 of an advanced uintathere such as *U. anceps,* or *E. cornutus* in its dimensions and morphology. Possession of both posterior and anterior interdental wear facets precludes its being an M3, the only tooth with which it might be confused.

The Texas Memorial Museum (University of Texas) has one fragmentary tooth, which West (1982) referred to as c.f. *U. anceps,* TMM-42287-9. He described and illustrated it, and in his discussion West pointed out that the most noteworthy feature of this specimen is the range extension that it documents for the genus and species. It consists of the labial half of a right M1 or M2. The tentative assignment was necessary because there is broad size overlap between the teeth of *U. anceps,* both *Tetheopsis* species, and *E. cornutus.* One could make a more educated guess were it a Washakie specimen, where the species are well correlated with the units of the formation. In this case, it would help to know the exact age of the Whistler Squat l. f. In 1974, Wilson gave 46.2 m.y. as the age of biotite within the bone bearing tuff containing the Whistler Squat l. f. Then later Wilson (1978) reported a 47 m.y. date for a tuff that directly underlies "a very Early Uintan Whistlers Squat l. f. and that is in turn overlain, but not directly, by a biotite rich tuff dated at 42.9 m.y." Although these last dates bracket the locality, it is not a fine enough bracketing to allow an unequivocal choice between *U. anceps* (the Washakie, TWkA1 species) and *E. cornutus* (that from TWkA2). If it is from the latter species, the range extension is the same, and the tooth is probably either P4 or M1. The specimen is from the Pruett Fm., from the Whistler Squat locality, TMM 42287, which is below the Alamo Creek Basalt in the Hen Egg Mountain Quadrangle, UTM grid reference Z 13R FC E 3897.

A University of Michigan specimen, UM 101208, is a left maxillary fragment, probably of *Bathyopsis fissidens.* It is that of a juvenile, about

---

←

the basicranial region and includes the occipital crest and parts of the right parietal and maxillary horns. The left ramus is shown in dorsal (**B**) and left lateral (**C**) views, where roots of four incisors, the canine and inframandibular flange can be seen in the symphyseal region. This jaw is mentioned again on p. 61 in connection with variation of incisor numbers (FMNH neg. nos. GEO 85915 (A), 85916 (B), and 85917 (C)).

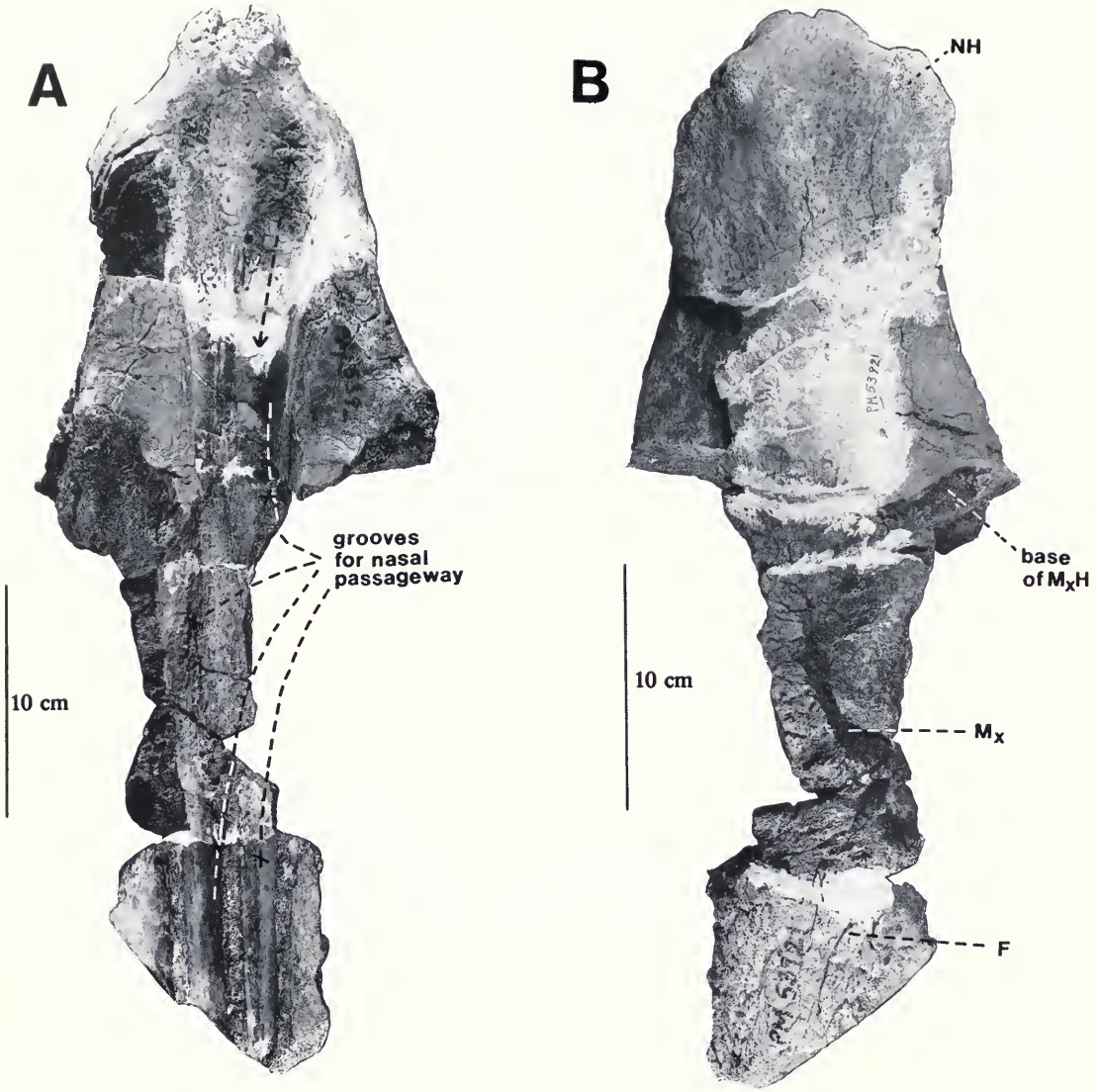

FIG. 17. PM 53921, a portion of a fragmented skull of *Uintatherium anceps* that was found in close association with a disarticulated partial skeleton. This skeleton is noteworthy for its complete pelvis (Fig. 51A) and femur (Fig. 51B–C) and various other elements, all of which show it to be that of a large adult. The largest skull bits consist of nasals and partial maxillaries and the midline region of the frontals. Its nasal horns are small oval projections, and the maxillary horns, although broken, appear to have been small, to judge from the size of their bases. From these features, I judge it to be female. It is shown in ventral aspect in **A,** where the grooves for the nasal passageway are seen, and in dorsal view in **B,** where nasal horn and other features are identified (FMNH neg. nos. GEO 85693 (A) and 85698 (B)).

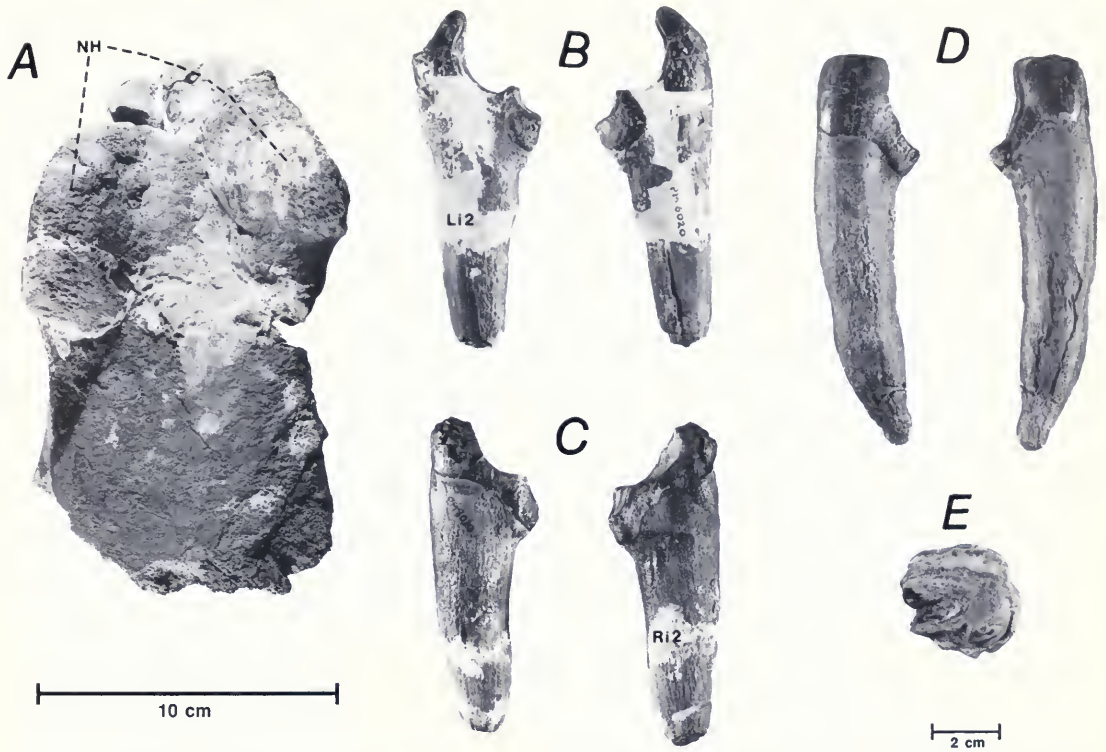

FIG. 18. PM 8020, a very fragmentary *Uintatherium anceps* specimen consisting of the anterior half of a pair of fused nasal bones with small elliptical horns, is shown in **A.** Found associated with it are three lower incisiform teeth. Two of them are a pair of incisors, probably i2s, one shown in lingual (left) and labial views (**B**), the other in labial (left) and lingual views (**C**). The other incisor is the right i1; it is shown in lingual (left) and labial views (**D**). In **E,** the isolated right M2, P26925, from the Piceance Creek Basin, Garfield County, Colorado, is shown in occlusal view (see p. 37) (FMNH neg. nos. GEO 85703 (A), 85712 and 85713 (B–D), and 85714 (E)).

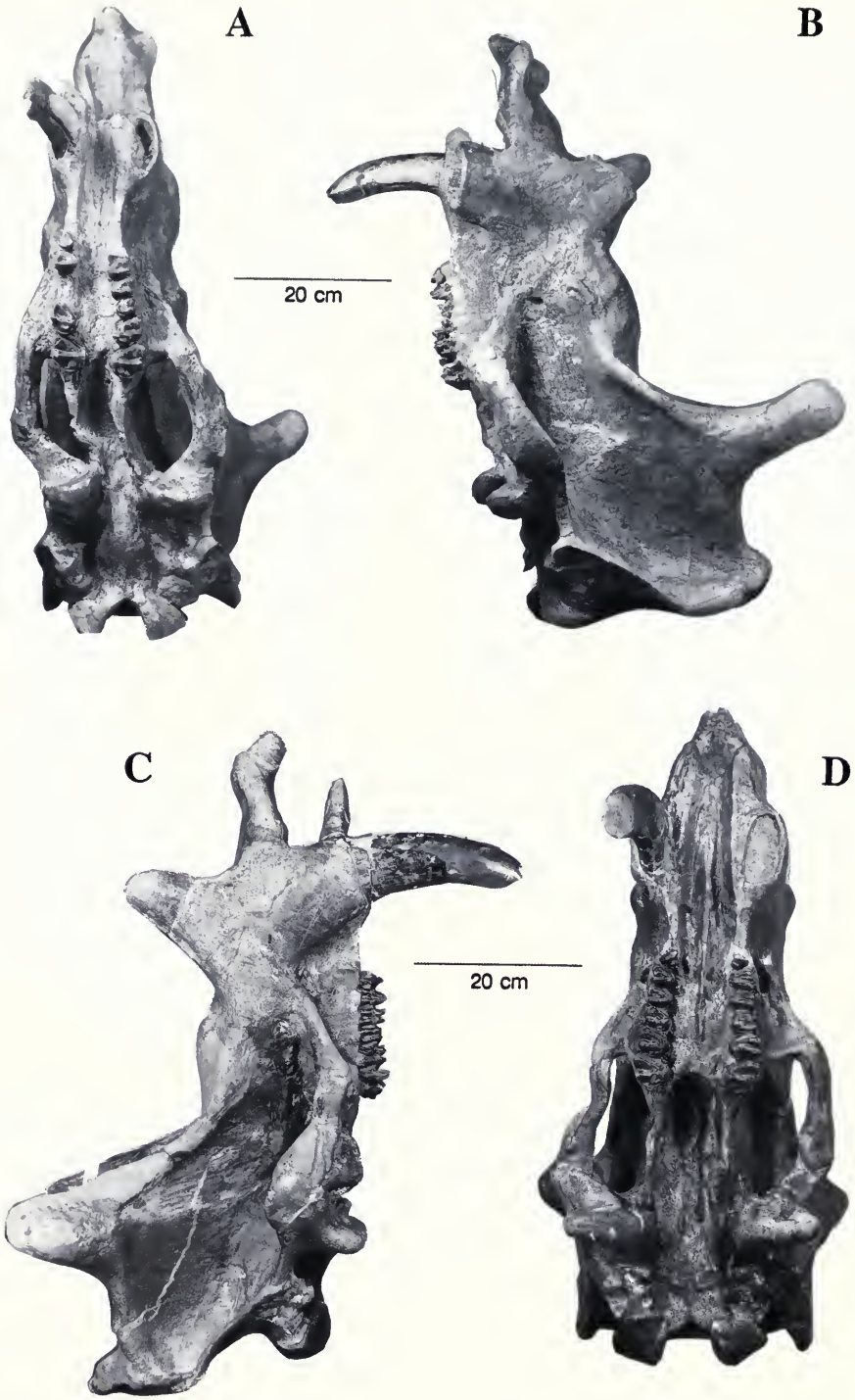

FIG. 19. Skulls of two fine American Museum specimens are shown. Both had been listed as *U. alticeps* Scott (1886), which taxon Wheeler (1961) correctly treated as a synonym of *U. anceps*. In **A** and **B,** AMNH 1664 is shown in ventral and left lateral views. In **C** and **D,** AMNH 1694 is shown in right lateral and ventral views (FMNH neg. nos. GEO 82514 (A), 82515 (B), 82518 (C), and 82519 (D)).

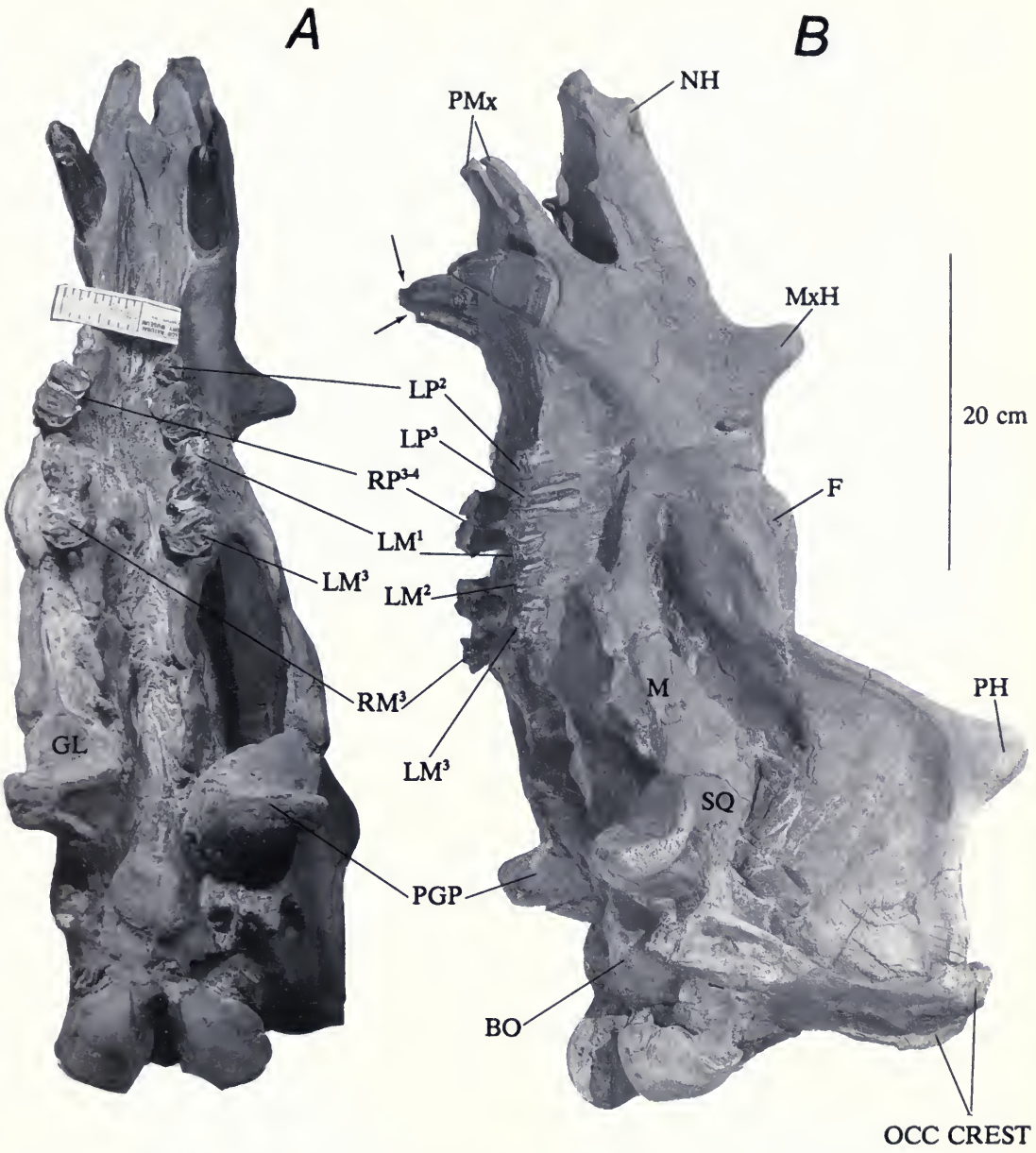

FIG. 20. Ventral (**A**) and left lateral (**B**) views of another American Museum skull of *U. anceps,* AMNH 1671. This is the specimen that Wheeler (1961) commented on, noting its relatively small size and the extremely reduced (worn) canines, he took to be broken, then worn to the state shown, but see text for another interpretation (AMNH neg. no. 322458 (A) and FMNH neg. no. GEO 82444 (B)).

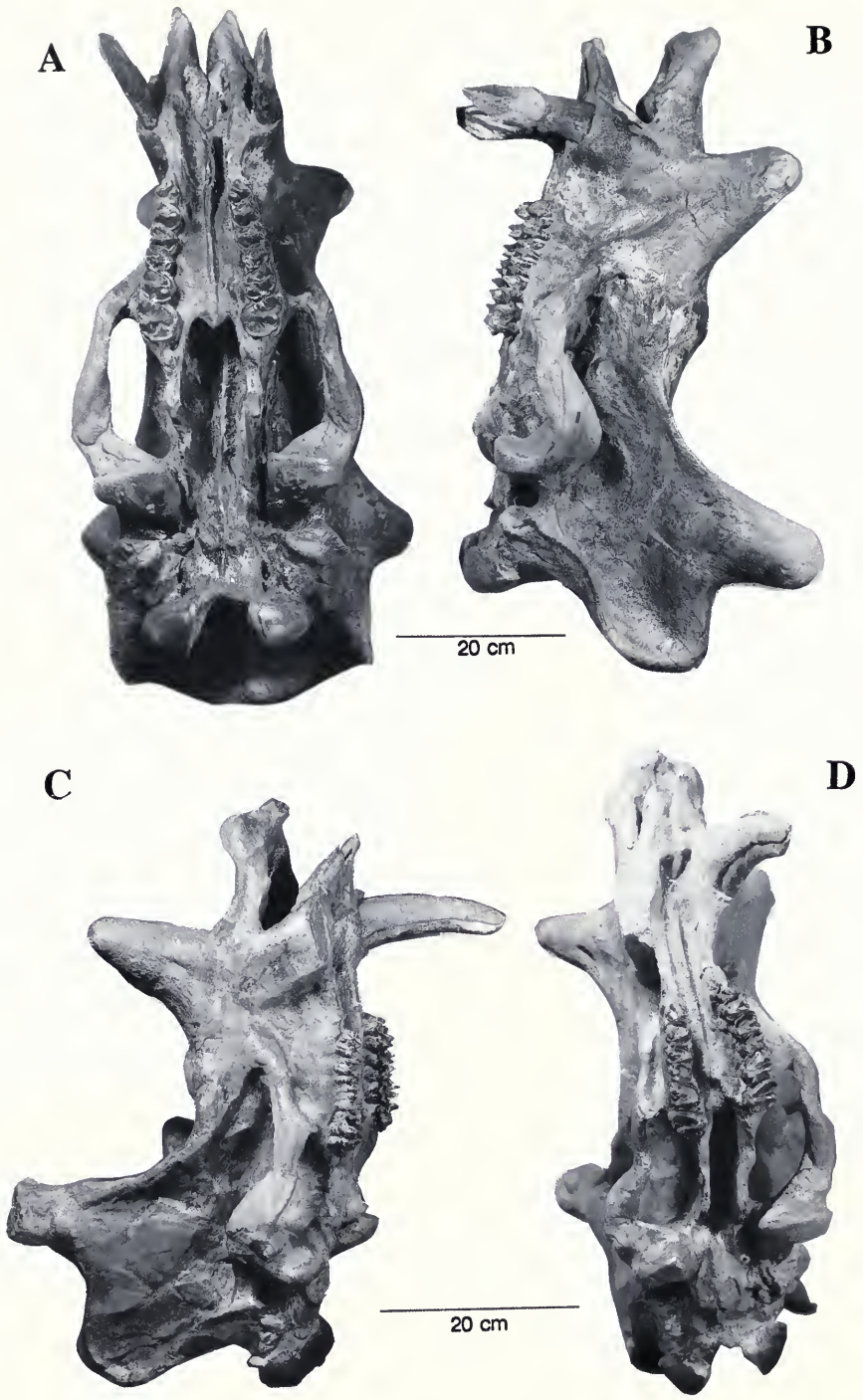

FIG. 21. Two more of the American Museum skulls of adult *U. anceps* are shown: in **A** and **B,** AMNH 2366, with its well-preserved and little worn dentition, and in **C** and **D,** AMNH 1689, another nearly complete skull with cheek teeth (FMNH neg. nos. GEO 82504 (A), 82505 (B), 82510 (C), and 82511 (D)).

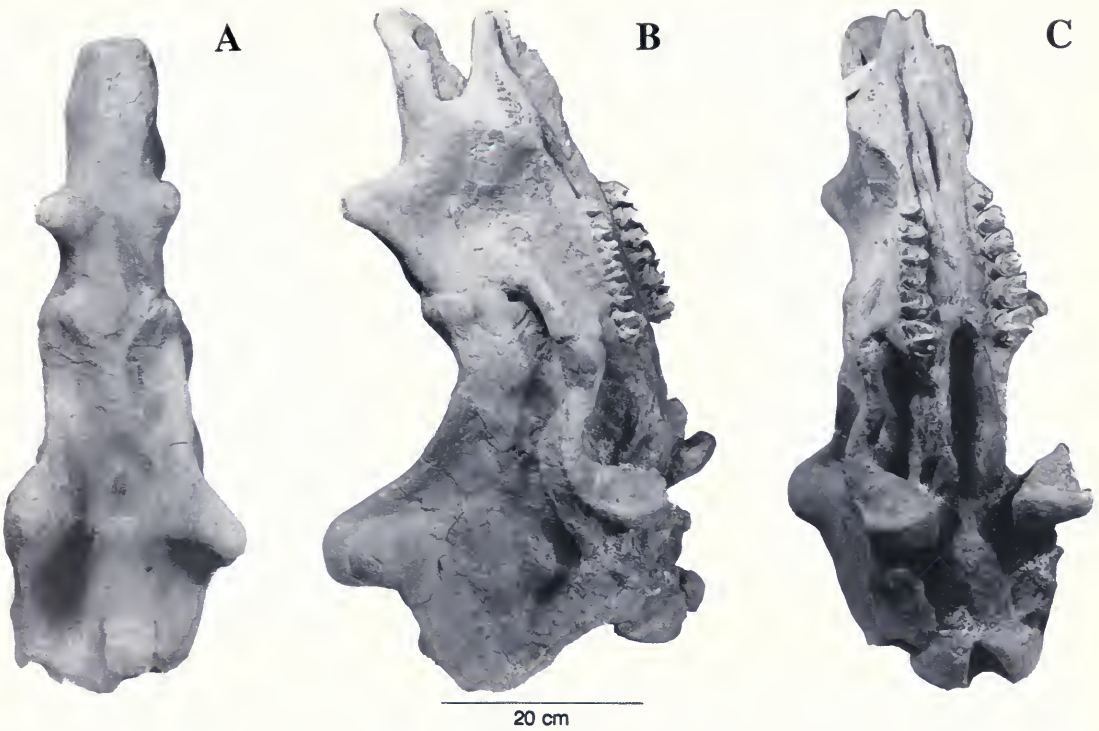

FIG. 22. Three views of another fine American Museum skull of *U. anceps,* AMNH 1693: **A,** dorsal, **B,** right lateral, and **C,** ventral views. It lacks only the canines and shows the bony ridge between parietal horns and the depression just anterior to that ridge. Also, the maxillary–frontal sutural union is markedly bulged (FMNH neg. nos. GEO 82445 (A), 82446 (B), and 82447 (C)).

20% smaller than *U. anceps,* and it has dP2–4 and a partly formed M1. I mention it here for two reasons: because it is a juvenile and because its stratigraphic position, 25 m (82 ft) above the Sage Creek White layer, places it just below the transition zone of the evolution of *B. fissidens* toward *U. anceps.* The latter taxon is also present (represented by a jaw fragment, UM 101209) from 50 m above the Sage Creek White layer. Apparently the transition took place rapidly during that interval (represented by the 25 m of sediments) between them, a relatively fast change, if not an actual punctuation. It is from University of Michigan locality BRW-40 (R.M. West's locality 2187) in NW ¼, SE ¼, Sec. 6, T13N, R113W, Reed Reservoir Quadrangle, Uinta County, Wyoming.

Several fine American Museum specimens that either have not been previously illustrated or are notable for other reasons are thus deserving of mention. AMNH 1664, which includes the skull (Fig. 19A–B), is labeled *U. alticeps,* a synonym of *U. anceps* (Wheeler, 1961, p. 28). Of its upper dentition, the left P3–M3, and the right canine, P2–3, and M2–3 are preserved. Two pairs of jaws also bear this number. The edentulous one (Fig. 38C), now carried as AMNH 1664A, I suspect may belong to the skull AMNH 1694 (the 9 inverted to become 6), because it is a reasonable size match, and I did not find any other jaws with that number. But the catalogue does not list one either, so this must remain as only a suspected association. Note, at some time after I photographed it in 1960 and before the 1996 Society of Vertebrate Paleontology meeting at AMNH, the right cheek teeth and most incisiform teeth had been restored. The other mandible, AMNH 1664B, I believe belongs to the skull. It has most of the right cheek teeth well preserved (Fig. 38A–B) and clearly is from a smaller individual than the other jaws with the number 1664 (AMNH 1664A). Also, it is a better size match for the skull AMNH 1664. An attached wire suggests that it may have at one time been mounted with the skull. To retain the record of this history, R. H. Tedford and I decided to just append the suffix lettering to the catalogue numbers on the two mandibles, which are illustrated in the section on lower jaws and dentition (Fig.

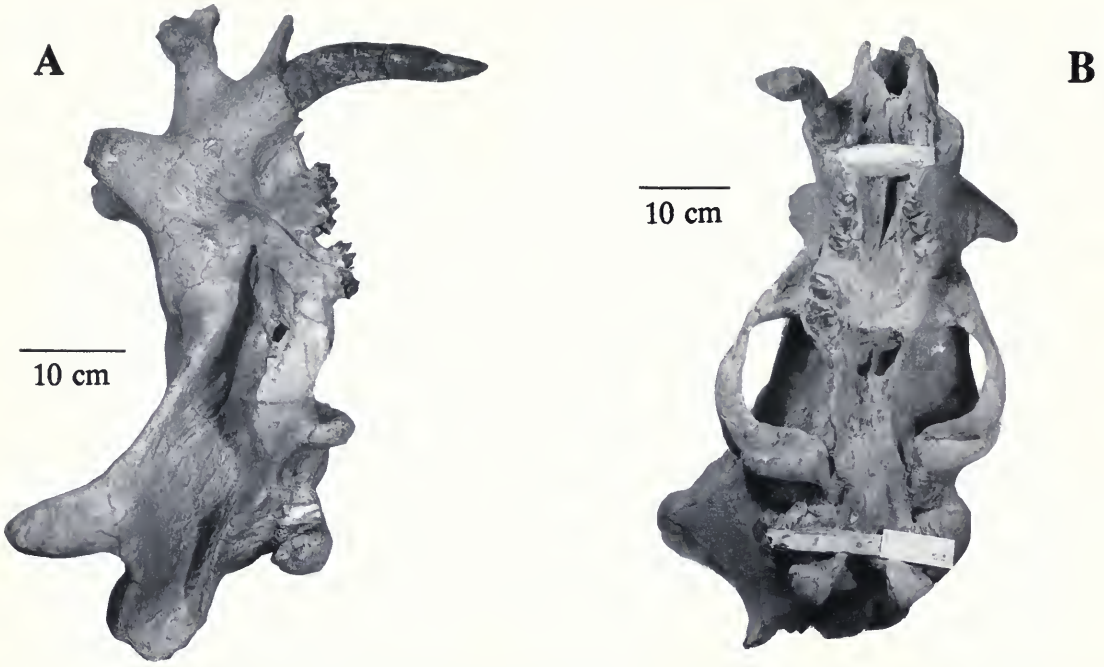

FIG. 23. YPM 11044, right lateral **(A)** and ventral **(B)** views of the skull of *Tinoceras (Laoceras) pugnax* Marsh, 1885, another synonym of *U. anceps*. Here the horns, including the nasal, are well developed. The left canine is missing, and the right appears to be partly out of its alveolus. Several views of the jaws and lower cheek teeth are shown in Figure 39 and discussed on p. 45 (FMNH neg. nos. GEO 82432 (A) and 82433 (B)).

38, p. 70). Specimen AMNH 1664 is from the Washakie Fm., TWkA1.

The large skull with nearly complete dentition, AMNH 1694, to which the jaws AMNH 1664A may possibly belong, is shown in Figure 19C–D. It is well preserved, lacks only the left canine, and is from the Washakie Fm., presumably from TWkA1.

AMNH 1671 (Fig. 20) is the specimen that Wheeler (1961) had determined to be a mature female notable for its small size and for its canines, which were broken and then worn smooth. I reillustrate it here, showing the ventral and left lateral aspects. I agree with the sex determination but am less sure about the canines having been broken. The rest of the dentition is heavily worn, with the molars being deeply scalloped. It appears to me that the tusks may just have been worn from heavy use and need not necessarily have been broken first, because they are very much alike in length. However, while the left is smoothly rounded from wear, the right has an additional peculiarity, a distinct but shallow notch that nearly surrounds the worn stub at its tip (arrows in Fig. 20B). This suggests that something fibrous has been repeatedly dragged around it. This laterally compressed skull is from the Washakie Fm.

Three other good American Museum skulls and upper dentitions of *U. anceps* illustrated here are AMNH 2366 (Figs. 21A–B) from the Washakie Fm., TWkA1, the skull that Wheeler (1961, p. 44) stated to be "without doubt, the finest uintathere skull ever collected." (Both the FMNH Funderburk *U. anceps* and the Denver Museum and FMNH Riggs/Abbott *E. cornutus* skulls now share that distinction.) Wheeler further commented, "The otic region shows much detail," but he did not describe anything of that detail, an omission I attempt to rectify in the next section.

AMNH 1689 (Fig. 21C–D) is from the Washakie Fm. It is about average in size and proportions for *U. anceps* as Wheeler noted. Actually, there are 10 specimens that are larger and 15 smaller in his chart 3, p. 78. It too has a fine set of cheek teeth; they show more wear than those of AMNH 2366, but not enough to have completely destroyed the lophs.

AMNH 1693, a small female (Fig. 22) is from the Washakie Fm., TWkA1 (Wheeler, 1961 p. 44). It has the full series of upper cheek teeth, all in

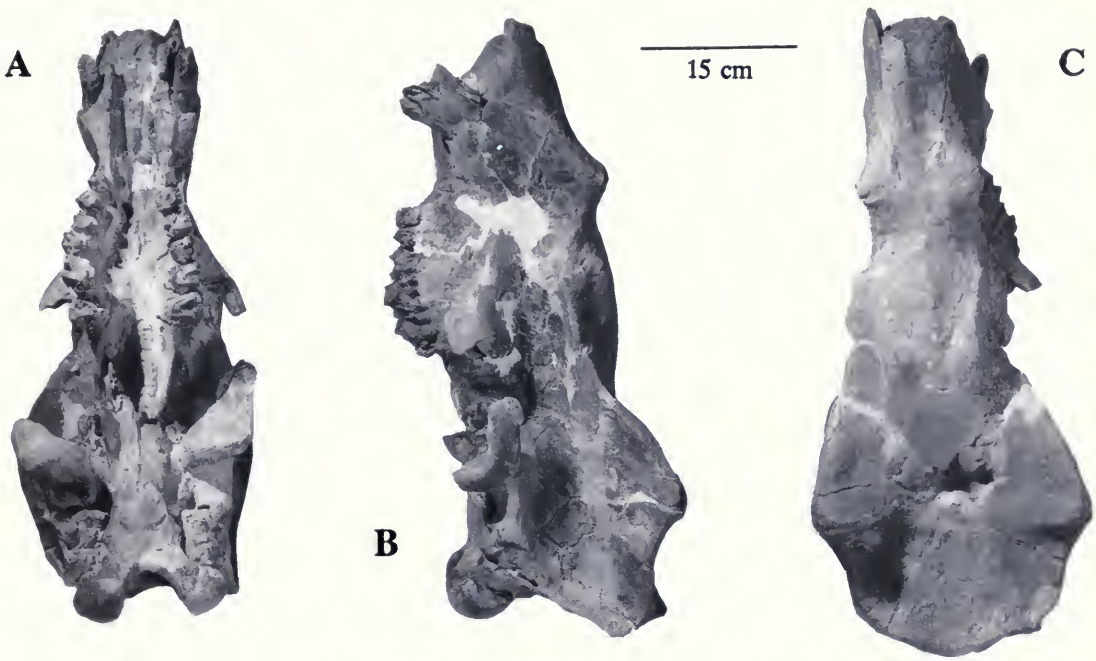

FIG. 24. Three views of the skull of *Elachoceros parvum* Scott, 1886, PUM 10298: **A,** ventral, **B,** left lateral, and **C,** dorsal. Its relatively undeveloped horns suggest a more youthful age stage than a prior assessment did, and I interpret the uneven tooth wear on left and right sides differently (see text) than did Wheeler (1961). *E. parvum* is a synonym of *Uintatherium anceps* (FMNH neg. nos. GEO 82394 (A), 82395 (B), and 82396 (C)).

fine condition, with the M3s just beginning to wear. I show it in dorsal, right lateral, and ventral views.

Wheeler (1961) illustrated two of the best Smithsonian specimens of *U. anceps,* USNM 16663 and 18600 (figs. 1 and 2 of his pl. 10). Both are from the Bridger Fm., from units "C" and "D" respectively. He also showed (his pl. 9, fig. 1) the right-side view of the Yale University specimen, YPM 11036, the type of Marsh's "*Dinoceras mirabile,*" a synonym of *U. anceps.* This skull was superbly illustrated by Marsh in his monograph (1886, pls. 1–5). It came from "Big Bone Buttes," or Sage Creek Mountain in the Bridger Fm., Bridger Basin.

Figure 23 shows Marsh's (1885/86) holotype of *Tinoceras pugnax,* YPM 11044, another junior synonym of *U. anceps,* as I found it in 1960 when I photographed it. The right canine and all the upper premolars and right M2–3 were present as Wheeler (1961) had noted (Fig. 23A–B). He commented further, stating that this is one of the few uintathere skulls with associated jaws, but he said nothing about the lower dentition, noting only that "The restored [jaw] portion is not indicated in Marsh's illustration (1885b [1886, p. 33], pl. 19)." In the section on lower jaws and dentition, I discuss and illustrate these features.

Elachoceras parvum, PUM 10298, was named and briefly described by Scott (1886) based on a skull, and it was discussed by him and later by Wheeler (1961). I can only offer an observation relating to it. There may be a problem with interpreting it to be a full adult. With the right (actually a left; a lapsus on Wheeler's part) cheek teeth "heavily worn," while the left (right) are strikingly different, being only very slightly worn (Fig. 24A), Wheeler concluded that the specimen was a pathologic female *U. anceps.* I think it more likely to have been an abnormal male of that species, for, as Scott observed, the tusk size suggests male, and I think that the extreme differential wear of the teeth could happen quickly in youth if for some reason, perhaps an injury, chewing was always done on the one side. The lack of horn development could be indicative of it not yet having reached sexual maturity. Hence, I consider it probably to be a subadult male. My 1960 photograph shows the specimen to have what appears to be an unusually well-preserved right ear region (Fig. 30A–B). Unfortunately, I did not study the details at that time because I did not then realize

how rare such well-preserved ear regions actually are. The observed features are discussed in the following section.

There is an unpublished specimen of *U. anceps* in the Utah State Field House collection, UFH 54015. It consists of a skull and partial skeleton largely collected by G. E. and B. R. Untermann in 1954 and subsequently by P. Robinson and W. Wheeler. In 1960, the latter lot of material was donated to the Utah Field House by Yale. The skull and jaw (v-85-23-1) are very crushed dorsoventrally, but I was able to get adequate measurements on the dentition (Tables 5 and 6). It came from the base of TWkA1, from within my locality FM-7-58-WDT.

Recently, three more specimens have been recovered, two (a skull and an unrelated pair of jaws) in the Bridger Fm., Bridger Basin, and one essentially complete skeleton in the Uinta Fm. in Colorado. The first two are in private hands, but good casts can be obtained through Jim Madsen (P.O. Box 9415, Salt Lake City, UT 84109-0415). Copies are in the AMNH. The skeleton, which was collected on private land, has been sold to the Gunma Prefecture Museum of Natural History, Gunma Ken, Japan. Casts may be obtained from Mary J. Odano (Valley Anatomical Preparations, 20614 Skouras Drive, Canoga Park, CA 91306). Although the originals of the first of these is not held by a dedicated repository, I include them here for completeness of the record and note that casts are in the collection of the American Museum. Casts of skull and jaws of the Colorado skeleton, Gunma Museum specimen, are available in the Field Museum, PM 60171.

Table 5 gives dental measurements of all Field Museum specimens of upper teeth of *U. anceps* from the Washakie Fm. and includes certain other specimens from there that have not previously been recorded, as well as a few from other places.

Figure 25 is a bivariate graph in which measurements of the permanent upper cheek teeth of *U. anceps* are plotted—tooth length along the *x*-axis, anterior width along the *y*-axis.

BASICRANIUM, EAR REGION, AND ENDOCRANIAL FEATURES, *UINTATHERIUM* AND *EOBASILEUS*—In this section I treat *U. anceps* and *E. cornutus* together because there are only a few specimens of *E. cornutus,* the more abundant *U. anceps* shows much variation in the ear region, and the few adult endocranial casts show variation as well. None of the specimens I have seen, except AMNH 2366, have well-preserved ear regions. With these conditions, the simplest procedure is to treat them as basically alike, and to assume that age stage probably makes the most extreme difference in the form of the endocranium. Neither Marsh nor Wheeler made a serious attempt to describe or illustrate the ear region in any detail, probably because Cope (1884), who had the best specimen, had illustrated his *L. cornutus* (pls. XXXVII–XXXIX), which he described on pp. 570–572 and 575–576. Leidy and Marsh each treated the endocranial features: Leidy (1872) described and figured the endocranial cast of the type of *U. robustum,* and Marsh (1886) devoted his Chapter IV to the brain, illustrating *Dinoceras laticeps* (YPM 11039 and 11202), *Tinoceras ingens* (YPM 11041), Leidy's *U. robustum* type (on p. 219), and *D. mirabile* in plate VI and text figure 63.

Wheeler's plate 10 (1961) is his only one showing ventral views of skulls of *U. anceps.* Cope's (1884, pl. XXXVIII) not very informative one of the basicranium of *E. cornutus* is his only one to show the ear region and basicranium. Wheeler's figures are not at a scale sufficiently large to allow for interpretation of the various structures in the area, nor did he label any. Marsh (1886) did a little better. His text figures 26–29, each at one-eighth natural size, have seven or eight features labeled (foramen magnum, occipital foramen (= hypoglossal foramen), stylomastoid foramen, foramen lacerum posterius, vascular foramen in basisphenoid (?= foramen lacerum medius), posterior opening of alisphenoid canal (? possibly confused with the foramen ovale), and anterior opening of alisphenoid canal. As the above queries suggest, I am not convinced of the correctness of all of these interpretations. His plate V, at one-quarter scale, labels only an occipital condyle and the postglenoid process (squamosal). The specimens shown and identified by Marsh are *Dinoceras laticeps, Tinoceras ingens, Uintatherium robustum, Dinoceras mirabile,* and *Tinoceras pugnax,* all synonyms of *Uintatherium anceps.* Cope (1884), with few materials at hand but perhaps more adequate ones, illustrated the ventral aspect of one skull. He illustrated eight skulls in all, mostly in side views, and did no labeling of features, but he devoted two paragraphs to description of the occipital-basicranial region of *Eobasileus furcatus* and over a page to the ear region of *Loxolophodon* (presumably his three species, *L. cornutus, L. galeatus,* and *L. speirianus,* all = *E. cornutus*). When taken together with a three-page description of the skull, including ear region, within the section on *L. cornutus,* this is the most comprehensive report I have

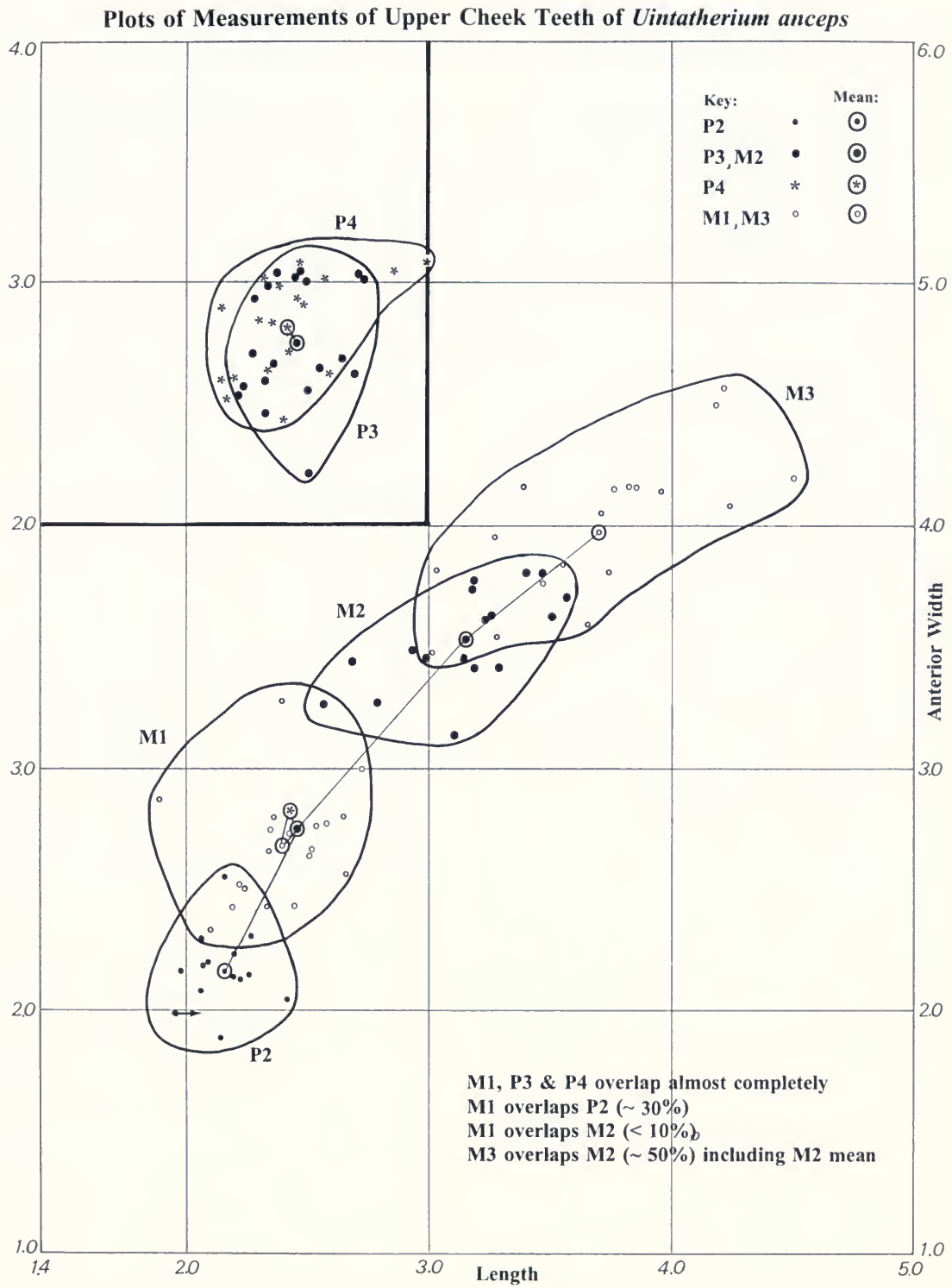

FIG. 25. Bivariate graphs for each cheek-tooth position for length × anterior width in the *U. anceps* upper dentition. Units are cm.

found. His exact words concerning the ear region are,

> The occiput is preserved for four inches above the condyles; it doubtless displayed a posteriorly sloping transverse crest as in *E. furcatus*. The paroccipital and mastoid tuberosities are narrowed and extend obliquely downward and foreward. The lower part of the exoccipital suture runs along a ridge, and there is a tuberosity in front of the mastoid foramen. An irregular [inverted] V-shaped crest extends upward with the apex at the inferior temporal crest, and its anterior limb forms part of the posterior boundary of the *meatus auditorius*. The inferior temporal crest is directed outward below, but foreward above (p. 575).

Cope does not give any hint of what he thinks the inverted V-shaped structure is. Is it tympanic, mastoid, or petrosal? Since he does not say, I can only conclude that he did not know. I suspect it to be tympanic, at least in its more superficial part. Within the immediate ear region, the structures are usually not well preserved and are quite confusing, so it is no wonder that those scholars did so little with it. I may eventually be proved wrong, but I shall make the attempt. I have had an advantage over the others because I have seen more specimens than any of them, including Wheeler. My procedure will be to first label the features that I can be certain of, then give my interpretation of the various more dubious structures. In that way, the reader will at least know my thinking. For my interpretation of the ear region features, I have relied on several of the Field Museum skulls and one each from ANSP, USNM, and UW. Both ANSP and USNM gave me permission to further prepare the specimens as needed to reveal features previously concealed within matrix. Only minor preparation was done on the ANSP specimen and none on the USNM specimen, for fear of doing more damage than good. Final study of AMNH 2366, the fine skull with the well-preserved ear region, was done in 1996.

The Philadelphia Academy of Natural Science specimen ANSP 12607, a part of the type of *Uintatherium robustum* Leidy 1872 (= *U. anceps*), is shown in stereo in Figure 26A–B, with a key to its structures given in Figure 26C–E. It is a partial skull, complete from the glenoid cavities rearward through the occipital condyles and foramen magnum. There is some crushing so that when viewed ventrally, the right ear region is compressed and the basioccipital slightly underlaps it. The specimen has been sectioned parasagittally just to the right of the midline (arrows in C), probably by Leidy. (ANSP 12622 is a plaster endocranial cast, also part of the type, so presumably it was made from ANSP 12607.) It was illustrated by Marsh (1886) on p. 57 of the Dinocerata monograph. Features anterior to the meatus, behind the foramen lacerum posterius, and along the midline pose few difficulties. Within the immediate ear region, the mastoid is clearly identified laterally, but the exposed portions of the apparent petrosals are unusually formed. I am uncertain as to where the mastoid ends and the petrosal begins, but D and E in Figure 26 show an interpretation that I believe to be the most likely one. No ossicles are preserved, nor do I identify any of the usual openings into the petrosal or any sure indication of the tympanic. The left postglenoid process has telescoped enough to obscure the region of the postglenoid foramen; on the right side the surface is damaged in the area, but there does appear to be an opening. Nonetheless, because this is the only specimen to possibly have such a "foramen," I favor an interpretation of damage. I do not detect a stylomastoid foramen. The mastoid foramen is clear on both sides of the skull. Paroccipital processes are only weakly developed, and the hypoglossal foramen is large and may have served more than just cranial nerve XII because it has a very weak constriction. There are bilateral bony protuberances, one on each side of the center of the basioccipital, that probably served for attachment of m. rectus capitus anterior, and m. longus capitus. The specimen came from Dry Creek Canyon (40–50 mi [64–80 km] E of Ft. Bridger), Southern Green River Basin (Bridger Basin), and is part of the type of *U. robustum* (Leidy, 1873), where it is documented in the Hayden Survey, p. 96.

In the Field Museum specimen PM 1667 (*U. anceps*), most of these features are again seen (Fig. 27A–B). Here, between the foramen lacerum posterius and the hypoglossal foramen, there is another foramen to serve the vagus nerve (X). It is nearly as large as that for the 12th. The foramen ovale is evident. The right postglenoid process is well preserved, and the preparation shows no sign of the presence of a postglenoid foramen. The difficult area is much like that in the previous specimen, but I think that I can see a junction where the medial edge of the mastoid abuts the petrosal. There are two openings, either of which could be interpreted as being stylomastoid foramen primitivum, but beyond them, nothing is recognized with certainty.

In the Smithsonian specimen USNM 18599 (Fig.

28A–B), a small, anterolaterally inclined U-shaped structure is the better part of the tympanic, but its poor preservation laterally makes it difficult to be certain of its complete form. The medial crux is slender; the lateral appears to be broader. The tympanic is primitive, but whether it was ring-shaped or horseshoe-shaped, or the extent of its inflation, are all unclear. It is one of the few tympanics preserved. The occipital condyle, paroccipital process, and mastoid are all badly eroded. I had hoped to be able to expose parts of the petrosal but did not do much for fear of damaging the tympanic. The locality is given as between Sage and Cedar Creeks, Southern Green River Basin (Bridger Basin), Wyoming.

The Field Museum specimen, PM 53933, the Funderburk skull (Fig. 28C–D), is for the most part beautifully preserved. Unfortunately, in the ear region there are uncertainties in interpreting the critical features. Even though the preservation is pretty good, I cannot be certain where the mastoid ends and the petrosal begins. The tympanic is missing, but there is a groove in the ?petrosal that may have accommodated its posterior crux. Other landmarks are clear (glenoid and postglenoid process, external auditory meatus, foramen magnum, basioccipital, occipital condyle, basisphenoid). The paroccipital process is recognizable but less distinct, and has a poor surface. On the left side of the skull, the region of the foramen lacerum medium (FLM) and foramen lacerum posterium (FLP), the area between them where the carotid usually occurs, and the hypoglossal foramen are exposed unambiguously. The latter foramen is a large oval opening nearly the size of the FLP, which in turn is nearly as large as the FLM.

In the Field Museum specimen of *E. cornutus,* P 12170 (Fig. 29A–B), on both sides there is a posteroventrolaterally oriented V-shaped structure that I interpret to be the tympanic. It is best seen on the right side, the left being either more telescoped or partially crushed. At the anteromedial end of the medial arm of each V-shaped tympanic a tapered structure descends, lying adjacent to the lateral edge of the basisphenoid. These I take to be the anteromedial tips of the petrosals. The locality given is White River Divide, 2 mi (3.2 km) E of Bonanza Mine, near Vernal, Utah, from Horizon B, Wagonhound Member, Uinta Fm., Late Eocene.

The basicranium of the holotype of *Elachoceras parvum* Scott (= *U. anceps*) is one of the better specimens for study of the ear region (Fig. 30A–B). Nonetheless, although most of the landmark structures within the area can be recognized (postglenoid process, external auditory meatus, mastoid process and foramen, FLP, POP, and basioccipital) interpretation of the tympanic is not satisfying. Most of the arcuate structure (between the mastoid process and the FLP/BO) suggests tympanic, as does its superficial position, but clearly defining its borders is difficult, nor have I been able to see a structure I could with certainty call the petrosal.

In spite of its overall excellent preservation, the ear region of AMNH 2366 is also somewhat disappointing. The ectotympanic fills the area between the lateral edge of the basioccipital and basisphenoid, laterally adjacent the posterior half of the origin attachment scars for the head flexors (m. rectus capitis ventralis major), and the medial side of mastoid (tympanic process) of the squamosal (Fig. 30C–D). The meatal passage turns more posteriorly just ahead of and above this structure. What I interpret to be the anterior tip of the petrosal is seen peeking out from above the anterior border of the tympanic. There is no obvious postglenoid foramen, but the foramen ovale and foramina for most of the posterior cranial nerves can be seen. The mastoid foramen is clear, as is the foramen lacerum medium, which lies anteromedial to and above the tip of the petrosal, and the foramen lacerum posterior, which is near to the anterior edge of the occipital condyle. Occipital and parietal–squamosal crests overlap the basicranium posteriorly and laterally. There is a low midline keel that runs from the anteroventral rim of the foramen magnum forward for the length of basioccipital and basisphenoid bones to the point of its disappearance high above the rear of the palate. Farther forward, the lacrymal foramen is seen to be relatively large, and there is a definite elongate pit that extends from the rear of the infraorbital foramen back for the length and width of the anterior (maxillary) buttress of the zygomatic arch. No exact locality is given in either the catalogue or specimen label, only that it came from the Washakie Fm. However, Wheeler (1961) in his figure caption (pl. 8, fig. 2) gives Washakie A (i.e., = TWkA1).

It appears that Marsh (1886) illustrated the endocranial casts or molds of the braincase of six specimens of *U. anceps,* three quite adequately. His plate VI is that of *Dinoceras mirabile,* and text figures 57–63 and 67 include that species, as well as *D. laticeps, Tinoceras pugnax,* and, most important, those of *Tinoceras ingens* (his figs. 59–

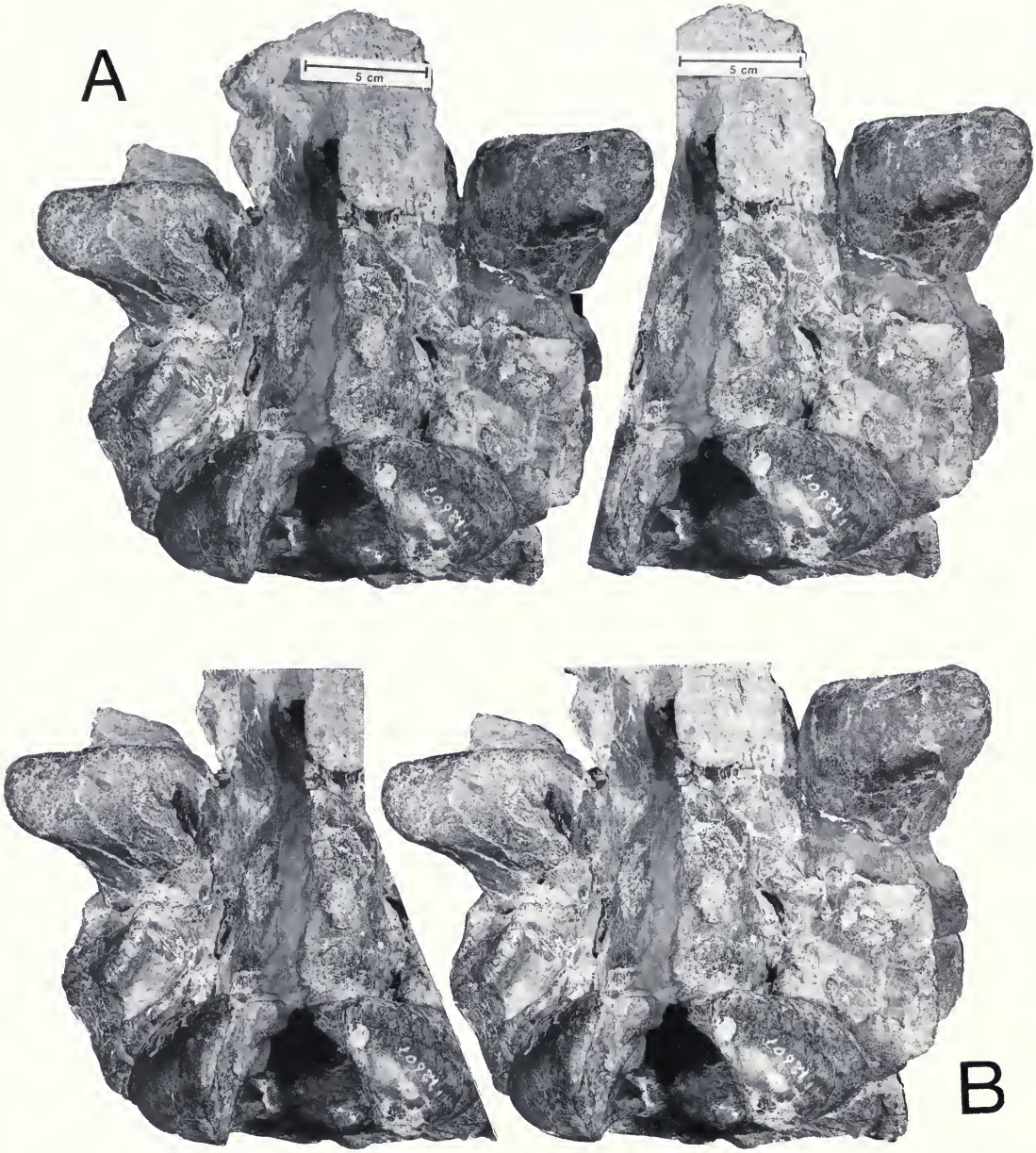

FIG. 26. ANSP 12607, a part of the type of *Uintatherium robustum* Leidy, 1872a = *U. anceps*, the basicranial region of the skull that had been opened in parasagittal section to get at the braincase. **A** and **B** are both the same stereo views. In A, the left side of the basicranium is shown; in B, the right is shown. (*Continued on next page.*)

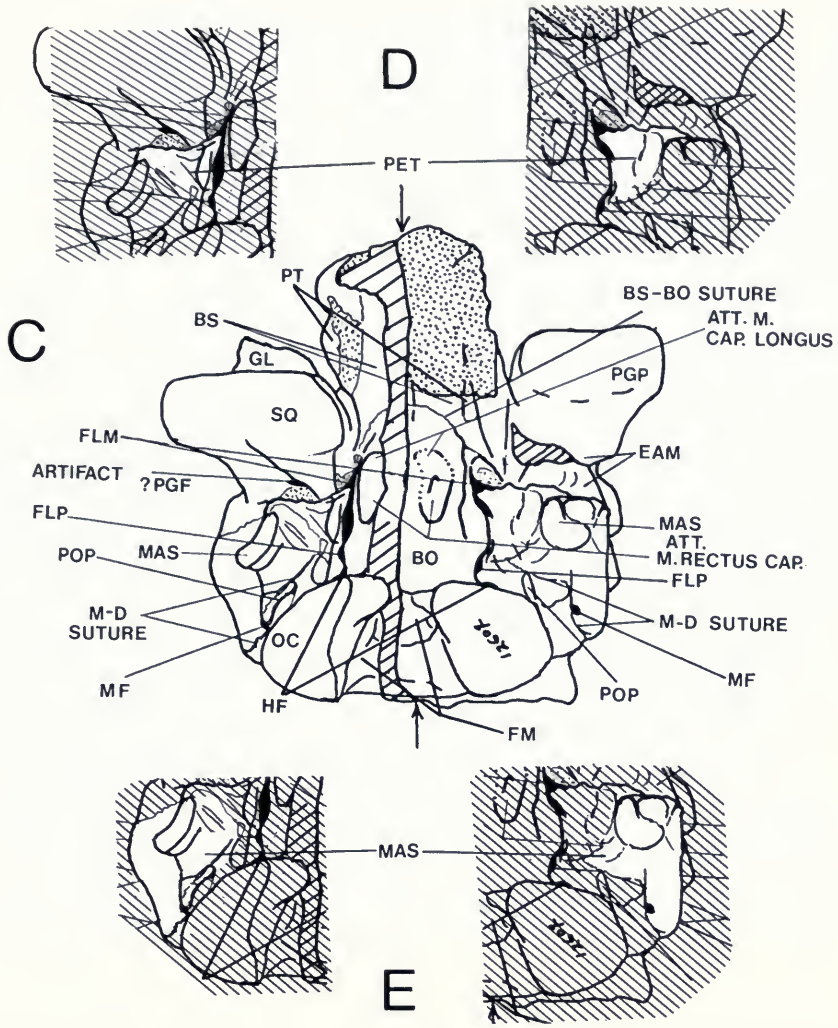

FIG. 26. (*Cont.*) ANSP 12607, part of the type of *U. robustum* Leidy, 1872a. In **C,** a key to the features is given. In **D,** the petrosal is hesitantly identified (some of the more posterior and lateral structures may be parts of the tympanic), and in **E,** the mastoid is marked. I do not see any of the usual petrosal features, other than the anterior tip of the promontorium, but its location and depth argue for that interpretation. It is also possible that it is part of the tympanic (FMNH neg. nos. GEO 85928.2 and 85928.3).

FIG. 27. PM 1667, *Uintatherium anceps*, the basicranial region of the same specimen as in Figure 15 enlarged to show the many features it preserves (**A**) and identified in the key (**B**) (FMNH neg. no. GEO 85912 (A)).

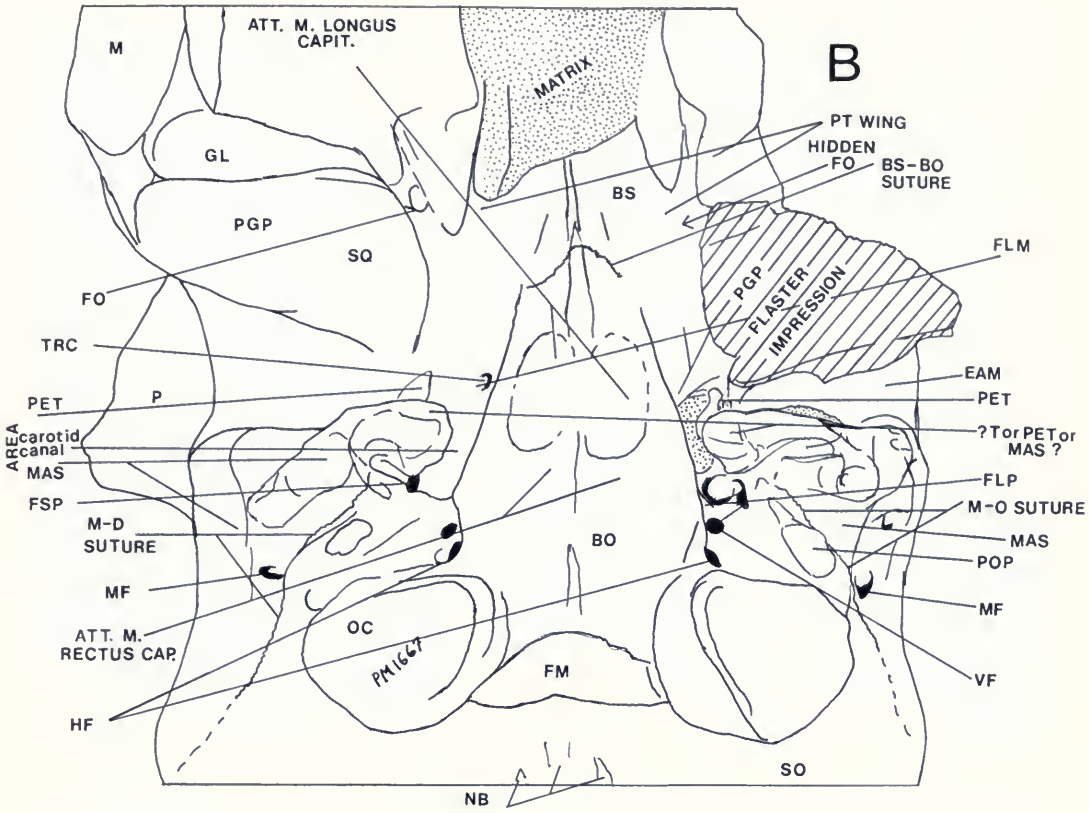

FIG. 27. (*Cont.*) Key to areas shown in part A. FSP = stapedial foramen of petrosal, HF = hypoglossal foramen, MF = mastoid foramen, NB = neuchal boss, VF = vagus foramen. Other abbreviations as defined previously.

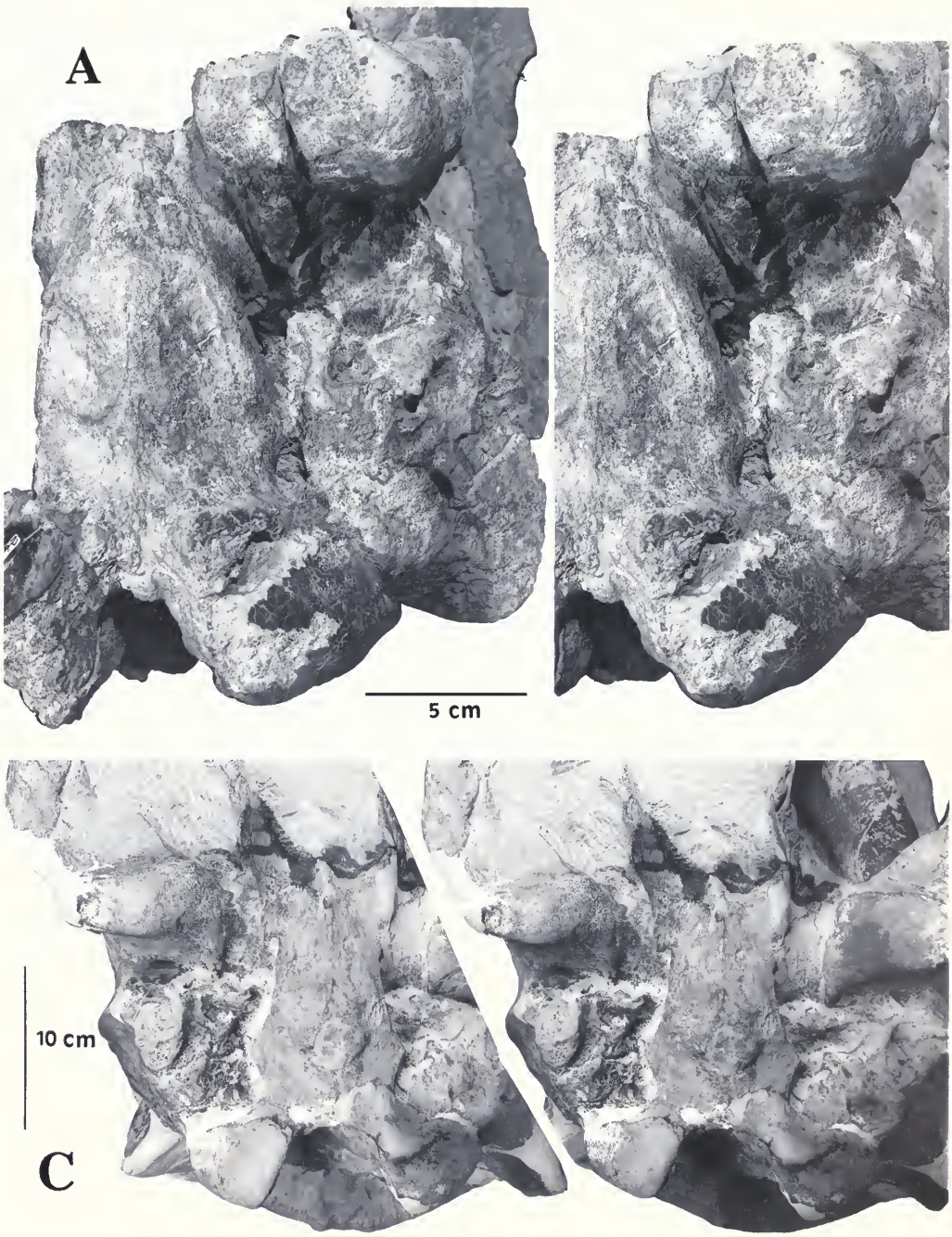

FIG. 28. Stereo views of **A,** USNM 18599, *Uintatherium anceps,* basicranial region of an eroded partial skull that nevertheless preserves several delicate ear region features shown in the key, **B.** This shows one of the best preserved tympanic bones. **C,** PM 53933, basicranial region of the Funderburke skull, *Uintatherium anceps,* shown in stereo. The ventral side of much of its right petrosal is exposed. Key to the identity of its main features is given in **D** (FMNH neg. nos. GEO 85928.2, 85928.3 (A) and 85927.2, 85927.3 (C)).

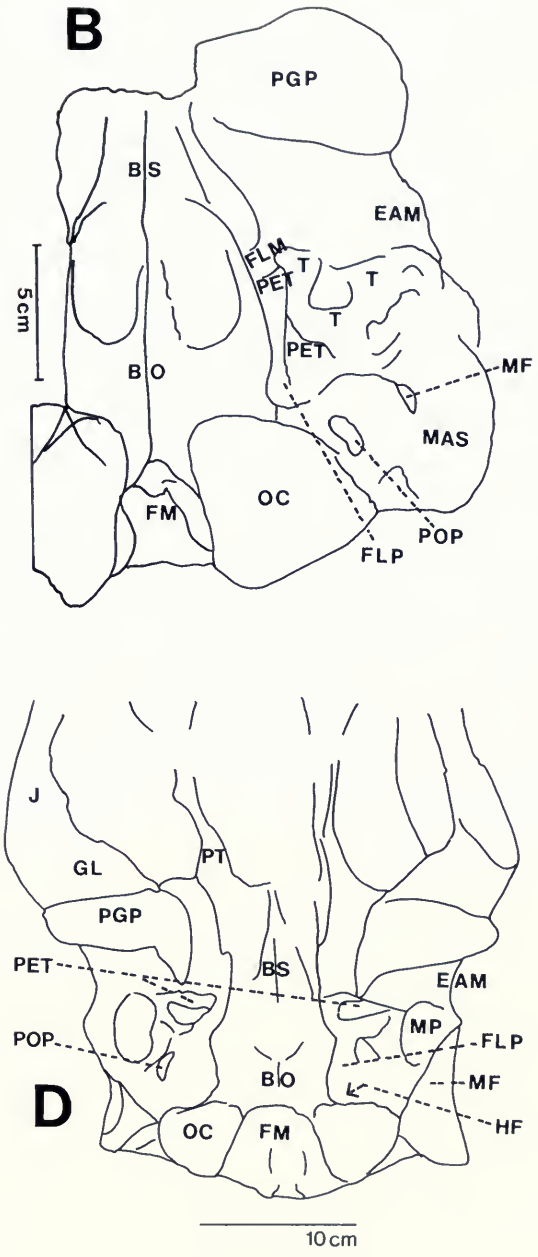

FIG. 28. *Continued.*

FIG. 29. Basicranial region of FMNH P 12170 (= P12212 in error), the Field Museum's fine specimen of *Eobasileus cornutus* (called *E. uintensis* by Osborn in 1929, a nomen nudum) is shown in **A. B** provides the key to its features (FMNH neg. no. GEO 85914).

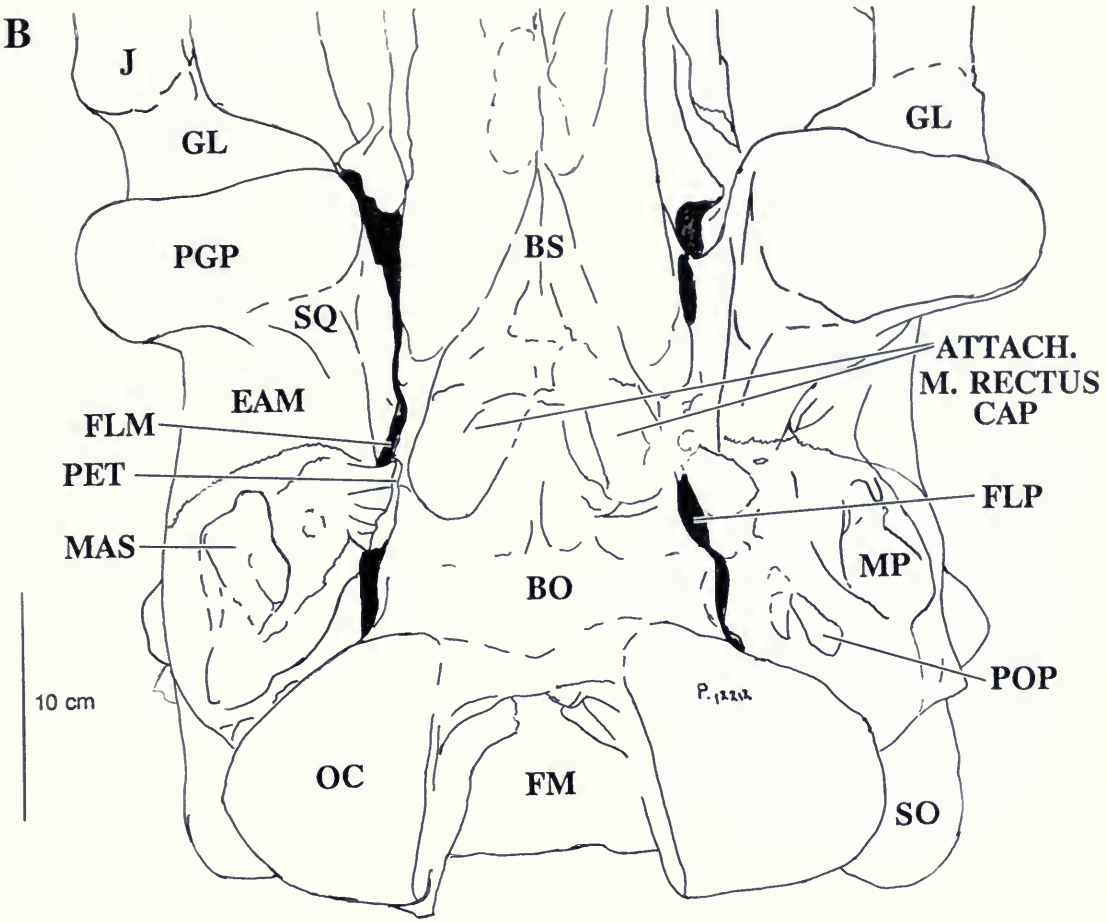

FIG. 29. *Continued.*

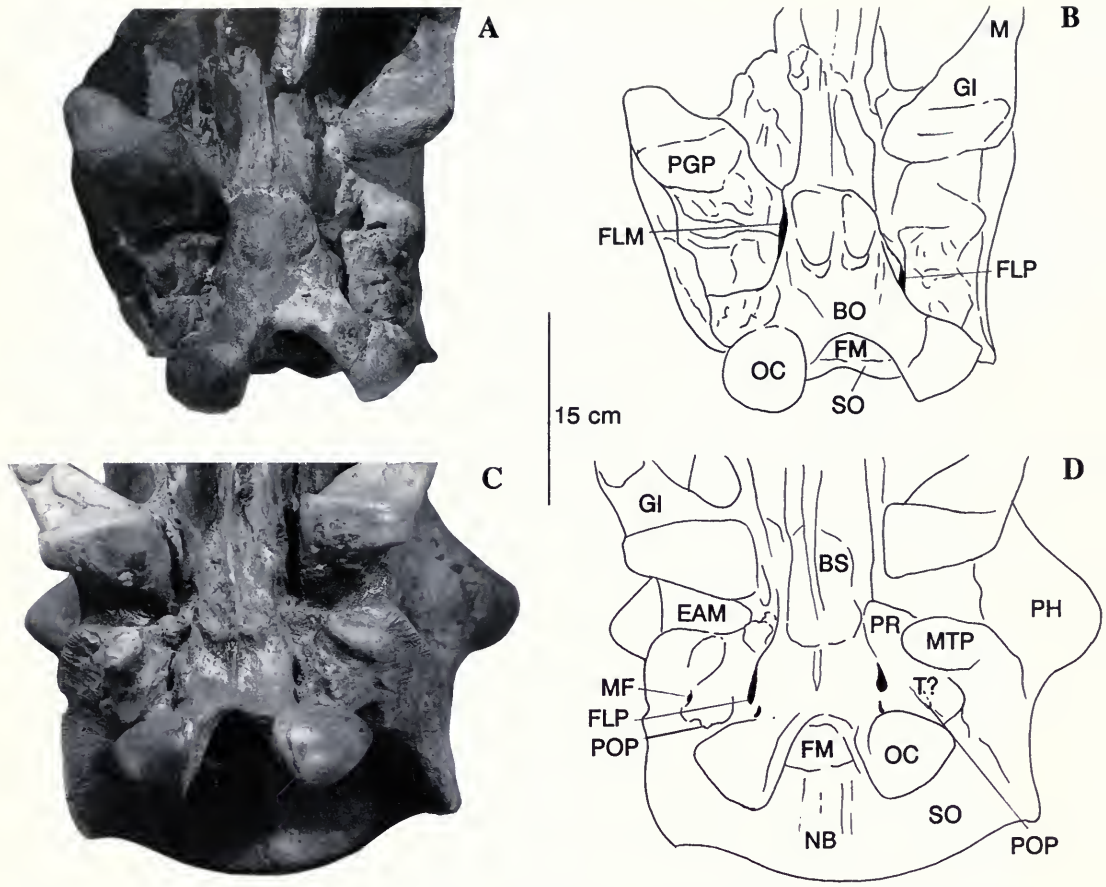

FIG. 30. Two more basicranial regions shown in ventral (surface) views. **A** shows *Elachoceras parvum* Scott (= *U. anceps*), PUM 10298. **B** gives the key to its major features. **C** and **D** do the same for the fine American Museum skull of *U. anceps,* AMNH 2366 (FMNH neg. nos. GEO 82394 and 82504).

60) and *U. robustum* (his figs. 61–62). In plate VI and figures of the last two species, the casts are shown at three-fourths natural size, a scale suitable for seeing most features. He was able to identify the olfactory bulbs, and the following cranial nerves in most: I, olfactory; II, optic; V, trigeminal; VI, abducens; the flocculus (VII+); and XII, hypoglossal, and in his plate VI the sylvian fissure and pituitary. I cannot do much more than to comment on the likelihood that the differences seen in Marsh's many illustrations, which he set forth as specific differences, are, simply, first age, then sex and individual differences. Certainly the small, compact, more spherical (less elongate), barely divided cerebrum seen in the FMNH specimen PM 8019 (Fig. 11C) represents a juvenile developmental stage. In his chapter on the brain, Marsh was struck by two things: its diminutive size and the relatively small size of the cerebral area, which he said was but little larger than the cerebellum (and which in turn is comparable to the diameter of the medulla).

However, Edinger (1961), in her lengthy diatribe, "Anthropocentric Misconceptions in Paleoneurology," faults Marsh for initiating the partly erroneous notions, and dozens of other authors for uncritically following his lead:

> Only through studying in the Peabody Museum . . . did I discover that the actual data on relative brain size in *Uintatherium* are even less satisfactory than a student of the literature had the right to assume. The figures in Marsh's monograph on the uintatheres (1884)[7] give the impression that endocasts had been made of seven or eight skulls. There are complete plaster endocranial casts of only three skulls—one of them, so-to-say, more than complete, as the cast of the olfactory bulb chamber includes the cast of a proximal part of the nasal cavity (fig. 8). (p. 82)

Her main point was that Marsh (1886 and later) was so impressed by the very small size of the brain of *U. anceps* that he next extrapolated this to include all Eocene (and Paleocene) mammals, then soon thereafter jumped to the further conclusion that all Tertiary mammals had small brains. Edinger (1961, p. 83) continued:

> This, then, was the basis for Marsh's repeated assertion that in uintatheres "the brain was proportionately smaller than in any other land mammal" (through 1895, p. 496). When in the monograph he listed 19 chief characteristics of the Order Dinocerata, the first was "Brain small, and smooth" (1884, p. 178). In other words, in words I am quoting from a 20th century textbook of zoology: The most remarkable character of the group is the minute size of the brain which seems to separate this order from all other mammals. . . . Actually, as I cited, Marsh had immediately concluded from the first *Uintatherium* endocranial cast that smallness of brain is a character apparently pertaining to *all Eocene* mammals, and in various contexts he noted that "the Dinocerata were not alone in the diminutive capacity of brain power" (1886, p. 58), or that the brain was diminutive in the early ungulates (e.g., 1897, p. 172). Whatever further endocasts he had prepared from fossil skulls, he described them as first of all, either small or not small. Becoming convinced that "*All Tertiary mammals* had small brains" he conceived what he called "a general law of brain growth". Because I have seen it accepted in too many scientific publications right up to the present year, and never seriously doubted (except by myself: 1929, pp. 85–100, and Tilney 1931, pp. 503–504), I feel called to account, to serve Harvard's motto, *Veritas*. At least as far as they concern mammals, let us try to imagine what Marsh's "laws" would mean if they were true, and realize that they cannot and do not summarize the real record of brain evolution.

Slowly (following Marsh, 1886), with publication of a number of works on various early and later mammals, it became a truism that the early forms were relatively small-brained compared with modern mammals. Of course, Marsh can't be blamed for the uncritical stands taken by those who followed him, and in a loose sense, he was partly right.

Jerison (1961, 1970, 1973) has gone beyond this vague generalization and has documented relative brain size and given us his encephalization quotient (EQ). His 1961 work showed that both relative brain size and EQ values for the archaic forms averaged about one-quarter that of modern mammals; the later mid-Tertiary forms were about one-half that of modern forms. Hence, the EQ values for the three groups are 0.25, 0.5, and 1.0. This supports Marsh's conclusion that early mammals were small-brained, but it refutes the notion that all Tertiary mammals were. I think Tilly Edinger would approve of Jerison's work because of the needed advance he made by documenting brain and body measurement relationships. For Edinger well knew (as does Jerison) what is now well established: cerebral development and complexity, not just brain size, are the hallmarks of advances in intelligence. In fact Jerison (pers. comm.) considers brain size to be highly correlated ($r > 1$) and virtually inseparable from complexity.

[7] Imprint date 1884; author's edition 1885; publication date 1886.

The one Field Museum specimen of importance here, a piece of the braincase (natural endocast) from the juvenile specimen (PM 8019, Fig. 11C) described earlier, shows the youngest developmental stage known until now. Although it represents little more than the dorsum of the cerebrum, its extreme posterior position within the occiput (almost against the supraoccipital) means that at this early age stage, cerebellum and medulla must have been inclined and probably flexed posteroventrally. (Marsh [1886, pp. 31 and 204–205] showed the approximately 45° inclination of the braincase in adult *D. mirabile* and *T. affine*.) As noted earlier, the cerebrum is virtually undivided and short, here interpreted as juvenile features. Lacking are convolutions, also mostly absent in the adults, indications that the brain probably did not fill the cranial cavity, but the dorsal portions of both olfactory bulbs and the pineal pit can be seen.

JAWS AND LOWER DENTITION—Measurements of the jaws and lower teeth of *U. anceps* are given in Tables 2 and 6, and measurements of *E. cornutus* are given in Tables 4 and 14. Methods of measurements, including those of cuspid and lophid, are shown in Figures 6B and 7B, E–F. Some of the best or most interesting adult jaws and lower dentitions are to be found in the AMNH and Yale (including PUM) collections (AMNH 1664B, 1678, 13151; YPM 11043, 11044; PUM 10385).

As with the skull material, the juvenile jaw specimens provide the most new information. AMNH 1678 (Fig. 31A–D) is the most important of these. Although this is not a Washakie specimen (it is from the Bridger Basin), except for several young Washakie skulls and jaws now available and some other subadult specimens that Wheeler thought were adult, it was, as Wheeler (1961, p. 43) indicated, the only juvenile of the genus from North America known to him. I reillustrate it here, more completely and at a larger scale, and expand on Wheeler's descriptions because it is important. The juvenile lower dentition is best seen in this specimen, where, as Wheeler said, the left dp3–m1 are present (and the alveoli of the left m2), and right dp3–m2 are preserved. He remarked on the very worn condition of the dp4s, and I note here the worn condition of all four dps, with the dp3s seen to be more worn than dp4s. Other features not previously stressed are (1) the crypt for the forming left m3 shown in Figure 31C, and (2) the right p3–4, both visible within their opened crypts in Figure 31B–C, the p3 barely so. Radiographs (not shown) further confirm the presence of the p3s (the right with a nearly fully formed crown), as well as the empty crypt for the apparently still unformed left m3. The locality given on the specimen label is Bridger (Fm.), Bridger Basin, Wyoming, 1893.

PM 54801 (Fig. 32A) is a damaged mandible of a juvenile female with most of its symphysis uniting both horizontal rami. Even taking into account the extent of dorsoventral crushing of the region, which has collapsed the mental foramen and its canal, there is no sign of an inframandibular flange (marking it a female). Beneath the collapsed foramen the ventrolateral edge of the jaw appears to be more substantial and less crushed than the rest, but the border is concave—not convex as it would have to be if it were a part of a developed inframandibular flange. The pristine crown of an unerupted left i3 (or i2) lies exposed near the front of the symphysis (arrow in Fig. 32A). It is mitten-shaped and, except for being thinner, matches the i3s of specimen PM 8020 and shows that in that specimen, more than half of the crown has been worn away. This unerupted i3 is cracked between thumb and mitten. Radiographs show that it is a single tooth with a crack, not two teeth. Preserved cheek teeth include left and right m3s (which are deep within their crypts) and the fully erupted right p4. The other preserved cheek teeth are left p3 (unworn) and m1–2 (with only slight wear). There are anterior and posterior alveoli of left p2 and roots of the p4, but an apparent cuspid of yet another tooth can be seen within remnants of the roots of the apparent p4. If this scrap is indeed a tooth, it calls into question the identity of the surrounding roots as p4. Could they be instead roots of the dp4? I think not, because its opposite, the right tooth in the p4 position, has the same size and does not show any significant wear, as surely it would were it the dp4. Also, with the m3s this advanced, it is unlikely that a dp4 would still be functioning. The other right cheek teeth are represented by either roots or alveoli. It was found at locality FM-7-83-KL/WDT (discovered by a BLM crew) in SE ¼, Sec. 12, T15N, R96W, Barrel Springs SW Quadrangle.

PM 55174 (Fig. 32B) is a nearly complete but edentulous mandible, with alveoli, roots, or both of most of the teeth, including the cheek teeth, right incisors, and canine. The alveoli of the left incisors and canine are indistinct, being crushed and partly broken away. Right and left coronoid processes and both condyles are nearly complete and well preserved. The left angular process is missing, but the right one is complete. There are

impressions of parts of the crowns of the left p3–m1, cast in epoxy from the surrounding matrix. To judge from the size of the jaws, and especially from the massive inframandibular flanges, this is undoubtedly the mandible of a large adult male specimen. The mental foramina are small, crushed, and difficult to see. That on the left side is the least obscured, and the indentation on the lateral surface of the flange just anterior the opening flares forward, not downward as in PM 38781. On the right side crushing is more severe, so that the opening cannot be precisely located. Symmetrically placed foramina are present, one high on the anterior edge of each flange near the symphysis. The inframandibular processes measure about 20 cm from the diasternal margin to bottom of each flange. Alveolar measures are given in Table 4. The locality, FM-6-91-WDT, is in SW ¼, SW ¼, Sec. 5, T15N, R94W, Salazar Butte Quadrangle.

A second older juvenile or subadult, PM 54818 (Fig. 33), consisting of the posterior part of a left ramus, including its angular process and two erupted molars (m2–3), provides little new information. It is at a more advanced age stage than the above-mentioned specimen, AMNH 1678. The horizontal ramus is shallow and the masseteric fossa is only weakly developed (both attesting to its young age). Crown features are quite standard: both the metalophid and hypolophid are slightly worn on m2. Those lophids on m3 were just begining to wear. Radiographs confirm that no tooth was forming posterior to the last erupted one, indicating that tooth identifications are correct. The locality is JJF.7.30.90.1, located in NW ¼, Sec. 8, T15N, P94W, Salazar Butte Quadrangle.

A left i1 (or i2) and the pair of 3rd incisors, PM 8020 (Fig. 18B–D), are the only incisiform teeth of any late uintathere in the Field Museum collection other than the one incisor in PM 54801 (Fig. 32A). They show considerable wear, the i3s being deeply scalloped between their anterior and posterior moieties. This wear condition is more extreme than Marsh (1886) showed it to be in his figures 43 and 44, but is more like that shown for his specimen 1490 (YPM 11490) in his figure 45. There is an interdental wear facet that obliquely truncates the main (anterior) cuspid. The largest "occlusal" facet extends in a smooth arc down the posterior face of the main cuspid and up onto the front of the heel, up to its top, where it then turns sharply down along the rear of the heel. The i1 is a stout tooth with a large single main cuspid that is heavily worn (blunt) at its tip and has a low but functional heel. The wear surface is deep, weakly scalloped, and polished, and shows fine transverse striae. The heel of the tooth has a remnant of an interdental wear facet. Clearly, these are the teeth of an adult animal. Locality FM-2-59-WDT is in SW ¼, SE ¼, Sec. 22, and NW ¼, NE ¼, Sec. 27, T16N, R95W, Salazar Butte Quadrangle, near the base of TWkA1.

An American Museum specimen, AMNH 13151, is noteworthy because it preserves four well-developed incisiform teeth on both right and left sides and most of the cheek teeth (Fig. 34A). On the left side, behind the last incisiform tooth, there is a pit that could be the remnant of a small, filled canine alveolus. The i1s are the largest teeth in the series, i2–3s are a little smaller and are about equal, and the last of the incisiform teeth is slightly smaller still, but not as much reduced as the lower canine is in other specimens. The posterior pair of these incisiform teeth Marsh had interpreted to be canines (based on his materials). This is the case in the specimens having three incisors and a small lower canine, but I believe that interpretation may be in error in this case and that they could be i4s. Two arguments suggest this: (1) Canine alveoli in other specimens indicate a canine tooth that is far smaller than any of the incisors, and the tooth crown in the i4 or c position in this specimen is only slightly smaller than that of the other incisors; it also is much more incisiform (mitten-shaped, like the other incisors) than caniniform. (2) Incisor number varies and most commonly is three, but i4s are known to have occurred in a few specimens. In one case, PM 53933, of the four incisors, the i3 is much reduced and staggered (Fig. 34B); in another case, PM 54406B (Fig. 16C), there are alveoli for four subequal incisors followed by a small canine. Here in AMNH 13151, if the pit behind the last incisiform tooth is truly a canine alveolus, then this specimen also has four incisors, and the i3 is neither reduced nor staggered. The locality given for AMNH 13151 is Washakie A, north of Haystack, 100 ft above Brown Sandstone (lower beds). I interpret this to be within TWkA1, but well above the Lower Brown Sandstone.

Our best specimens in which the incisor area is represented are PM 53933 (Fig. 34B) and PM 38781 (Fig. 35). They lack the teeth, but their alveoli show the procumbent orientations of the roots of these single-rooted teeth, and again they show the "canine" to be much smaller than the others. However, PM 38781 has alveoli for only three incisors, not four, so there is variation in this

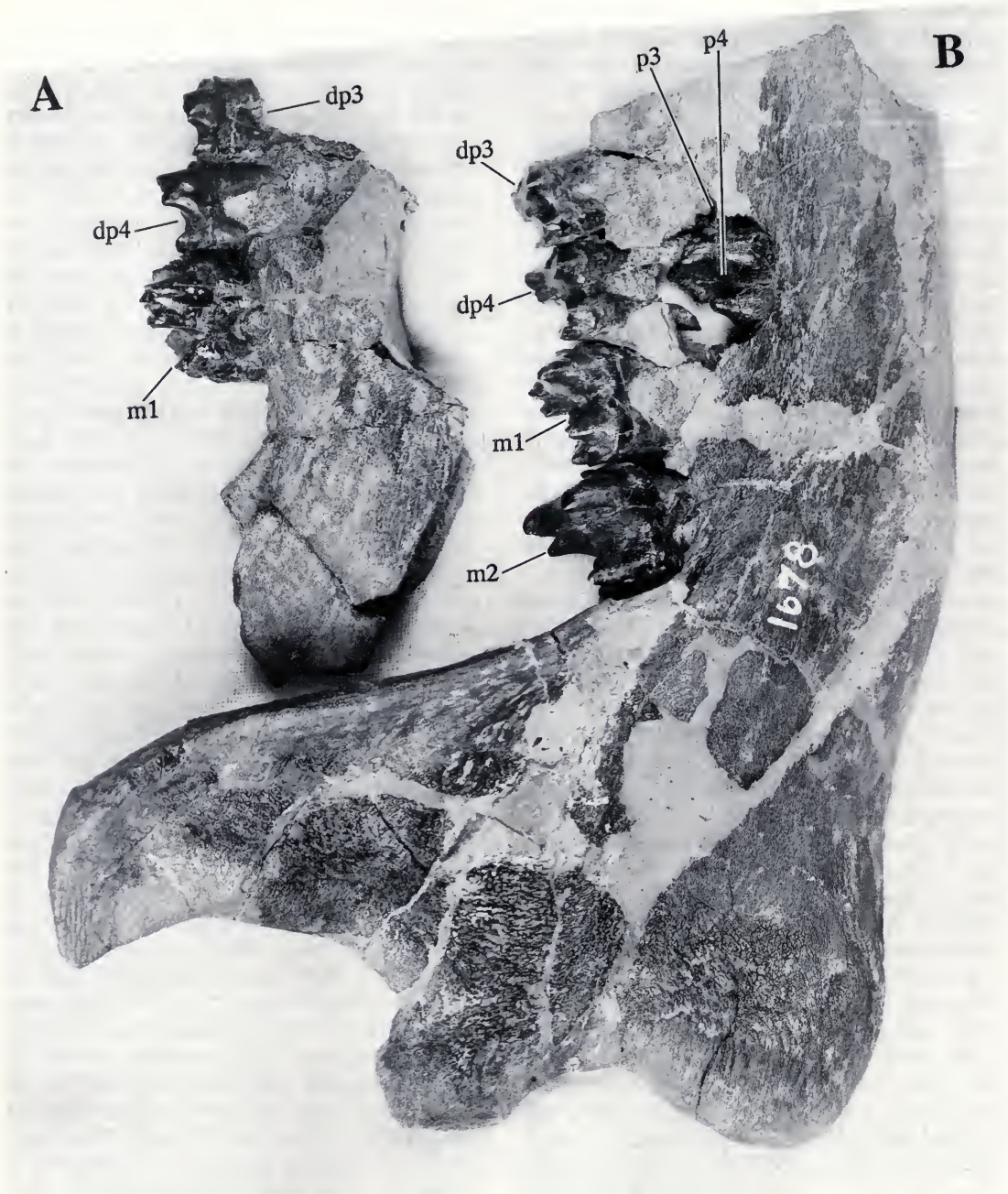

FIG. 31. *U. anceps,* AMNH 1678, a pair of juvenile jaws and dentitions consisting of the posterior two-thirds of the right mandibular ramus (**B** and **C**) including the coronoid, condylar, and angular processes, and (**A** and **D**) a fragment of the left ramus. Preserved teeth are L and R dp3–4, m1; R p3–4, m2. Also present are L m2 alveoli, and a portion of the wall of the crypt for m3. This is the specimen that Wheeler (1961, p. 43 and Pl. 13) referred to as being the only example of a juvenile among the terminal North American uintatheres. I show it at a better scale with more detail (FMNH neg. nos. GEO 82498 (A, B) and 82499 (C, D)).

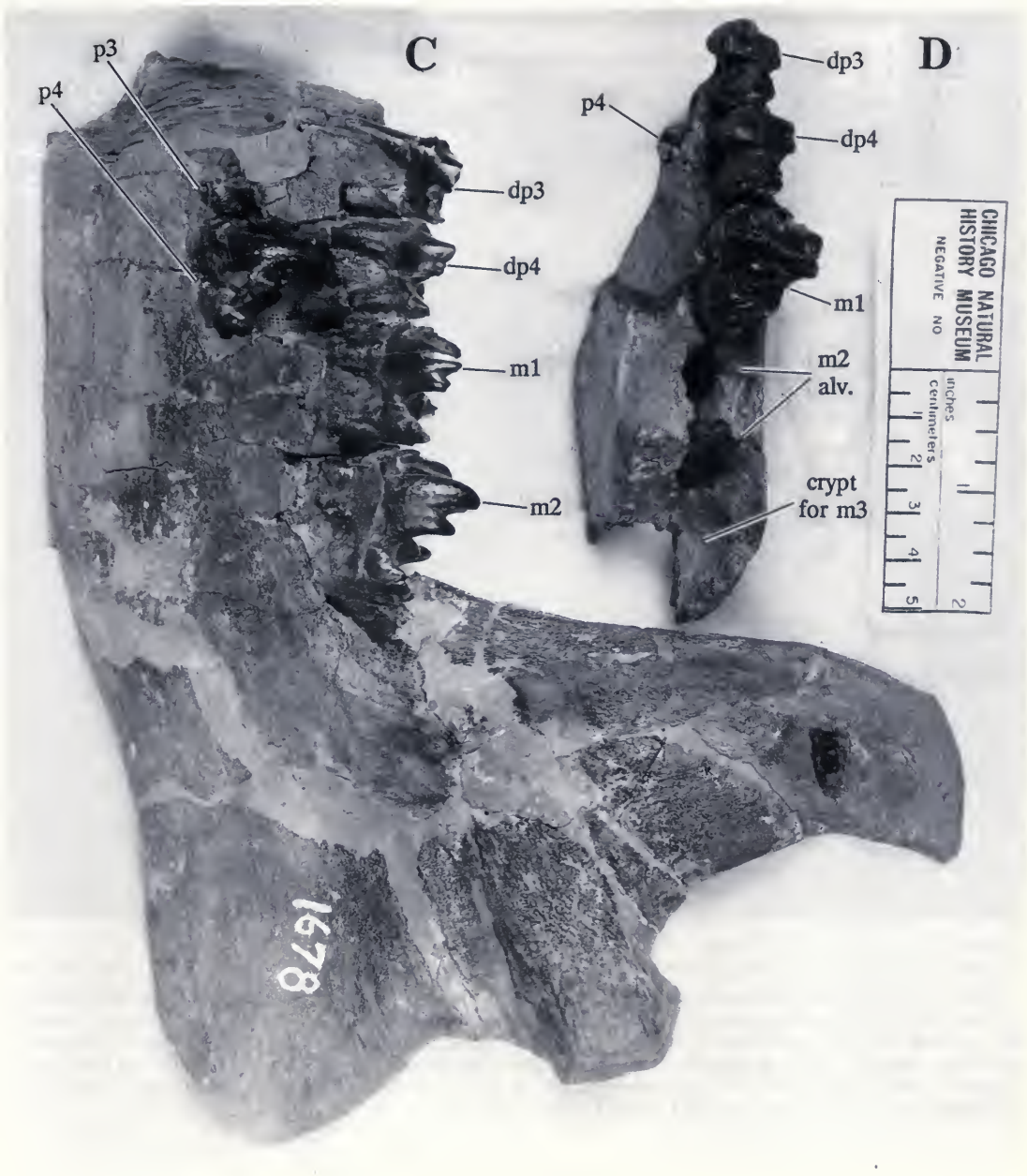

FIG. 31. *Continued.*

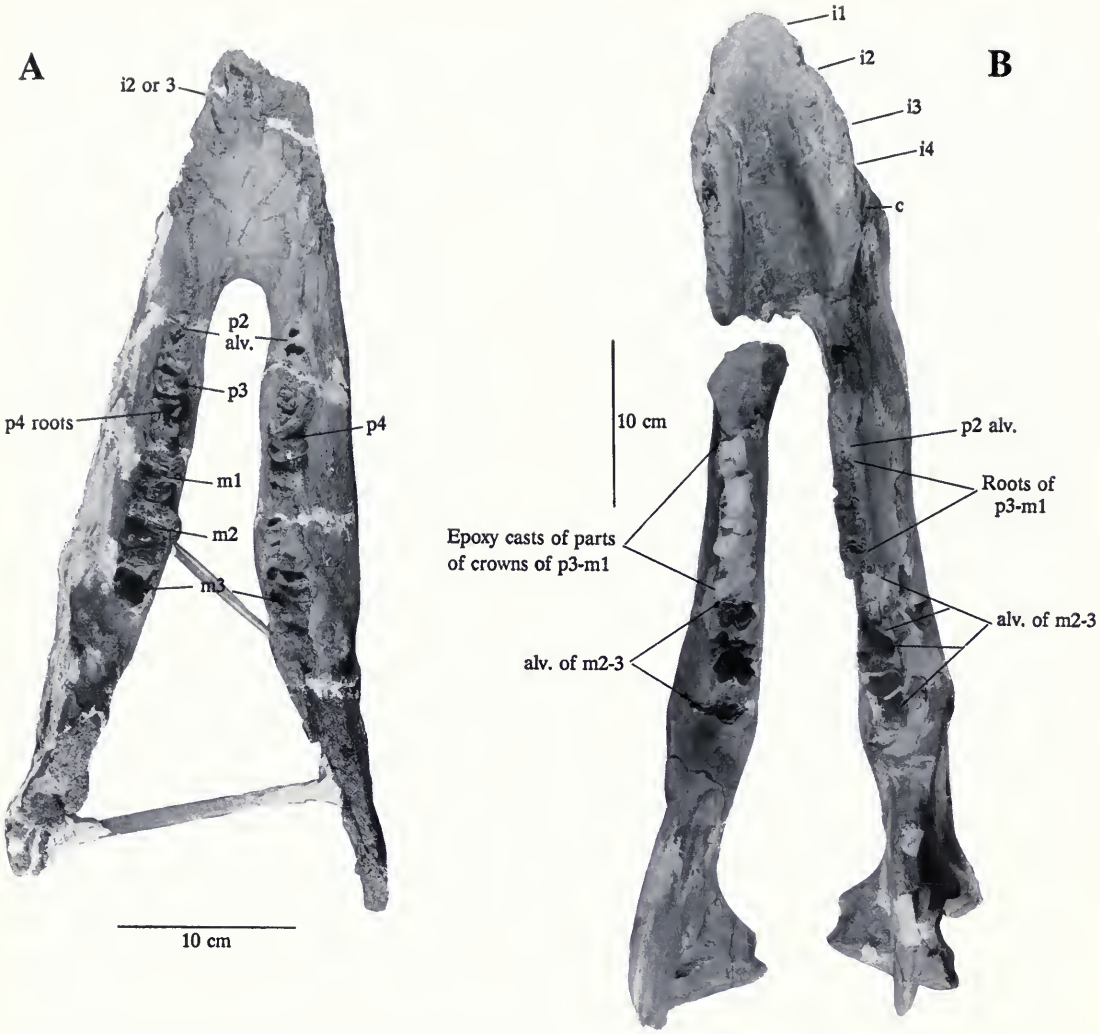

FIG. 32. *Uintatherium anceps,* lower jaws. **A,** PM 54801, a badly crushed and weathered pair of jaws shown in occlusal view. The few teeth present are well preserved: the erupting left i3 (or i2), erupted p2–3, m1–2, and right p4, m2. Both m3s have well-formed crowns that lie deep within their crypts. **B,** PM 55174, a nearly complete but edentulous mandible shown in occlusal view. The symphysis is complete, and there are alveoli for left and right i1–4, right c, and all cheek teeth. The partial impression of the left p4–m1 was made in epoxy from a block of the entombing matrix (FMNH neg. nos. GEO 85704 (A) and 85694 (B)).

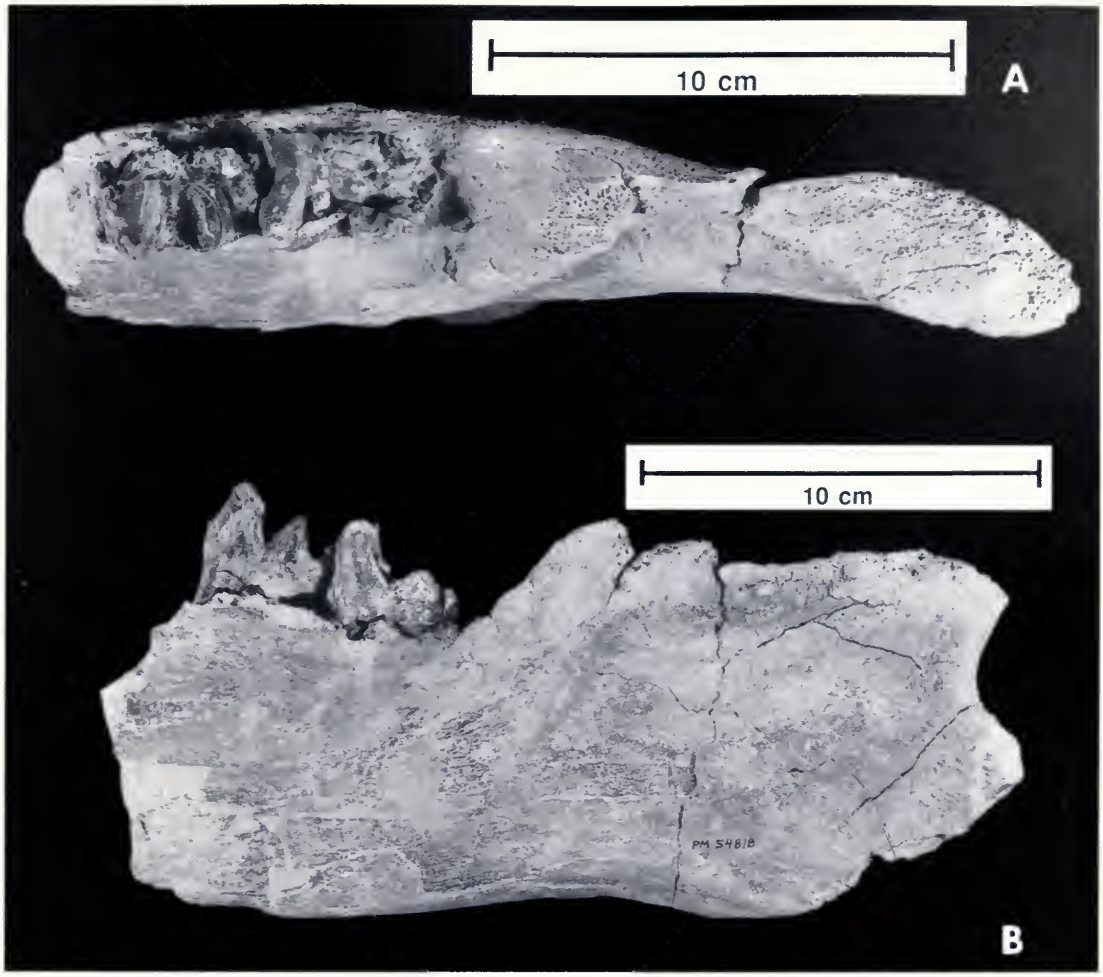

FIG. 33. PM 54818, part of the left jaw of a subadult *Uintatherium anceps* with M2–3 shown in dorsal (occlusal) view (**A**) and left lateral view (**B**). This is one of several subadult and juvenile specimens in the FMNH collection (FMNH neg. nos. GEO 85688 and 85708).

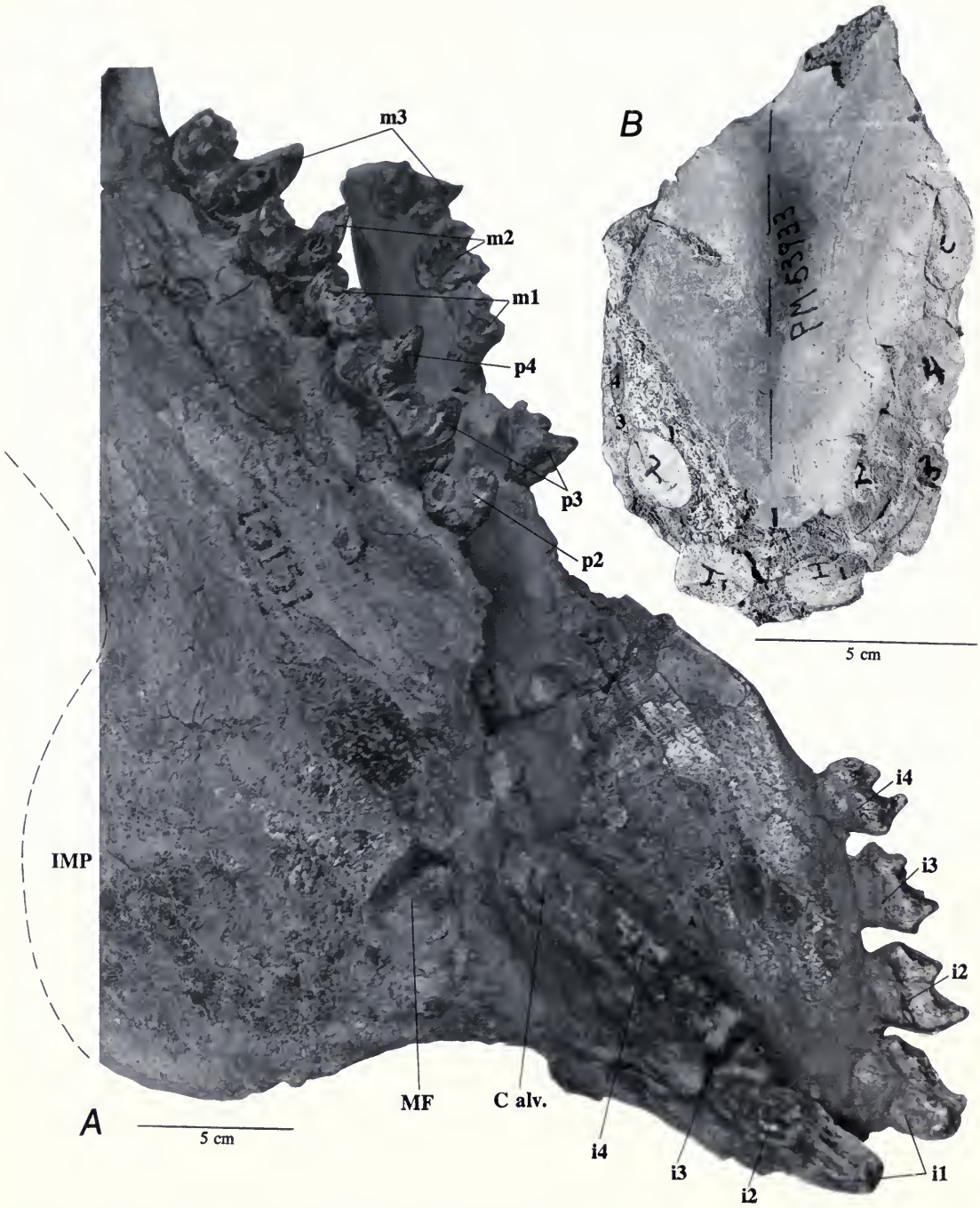

FIG. 34. Two specimens preserving details of the lower incisor–canine area. **A,** AMNH 13151, also showing the cheek teeth; **B,** PM 53933, which lacks teeth, but their matrix-filled alveoli provide information helpful in seeing some of the variation that occurs in the species. Both are variants with i1–4, but they differ in that only the latter has the i3 reduced and staggered (FMNH neg. nos. GEO 82503 (A) and 86052 (B)).

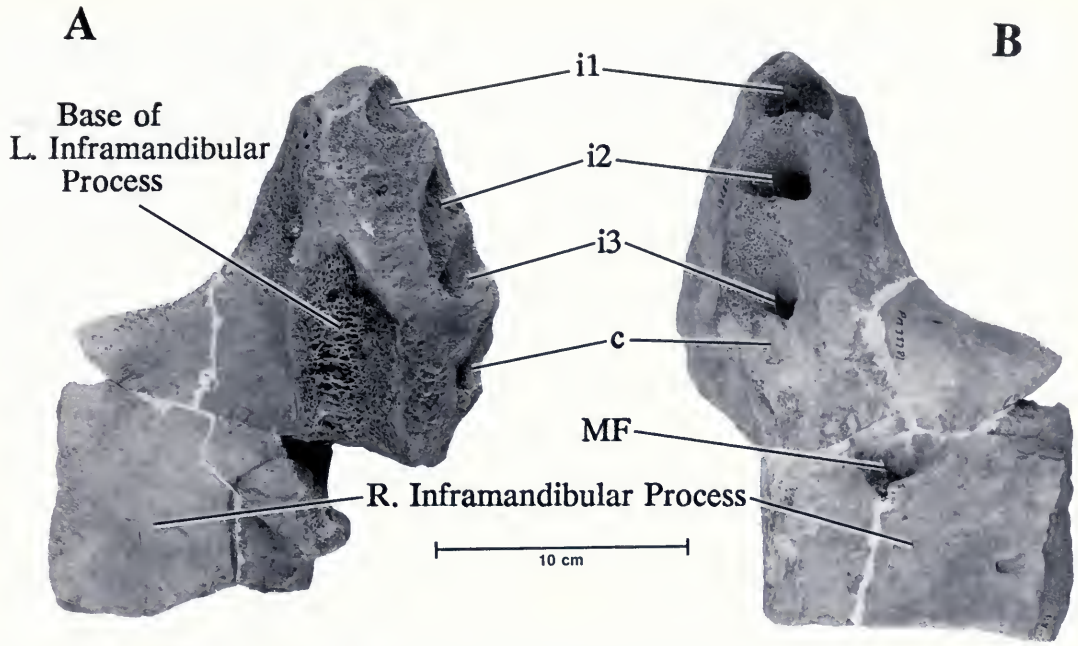

FIG. 35. PM 38781, an edentulous symphyseal mandibular fragment of *U. anceps* in which the more usual incisor formula (i1–3) prevails. Part of the large right inframandibular flange is preserved (FMNH neg. nos. GEO 85696.1 and 85696.2).

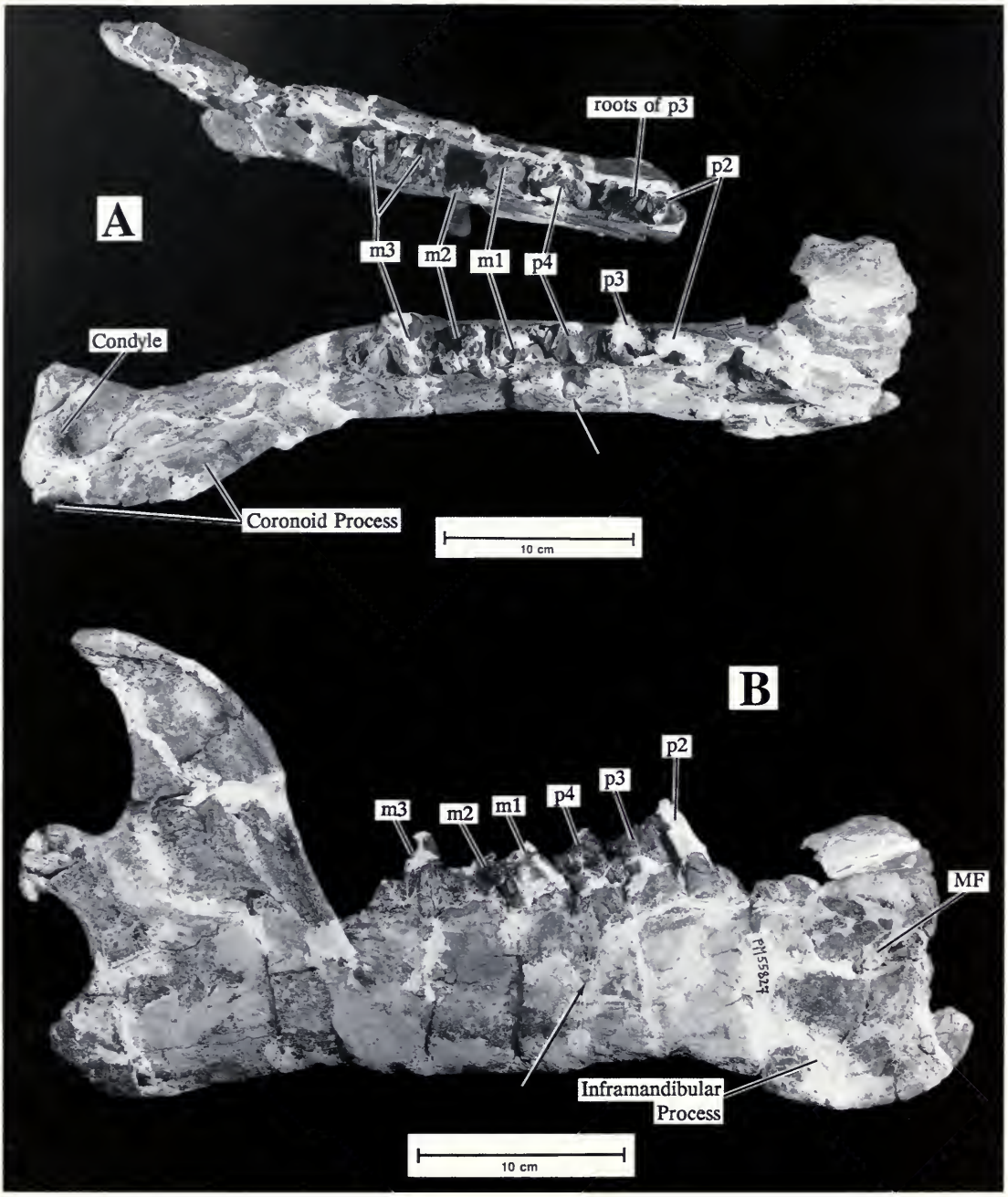

FIG. 36. PM 55827, a pair of fragmented jaws and dentition of a young adult *Uintatherium anceps*. Note the relatively weak inframandibular flange, which has been variously interpreted (1) as a female characteristic of *Tetheopsis* by Marsh (1885, YPM 11256), Osborn and Speir (1879), and Osborn (1881) (for the last two, PUM 10385 and 11611); (2) as probably a female characteristic of *Eobasileus* (Wheeler, 1961, abstract); and (3) not as a female characteristic of *Uintatherium,* in which the process is unreduced, like that of the male, by Wheeler (1961, p. 72). See text for my interpretation.

In **A,** the occlusal views of both rami are shown. In **B,** the lateral aspect of the right ramus is shown. Arrows point to an aberrant pit on the lateral side of the right ramus beneath and between the roots of p4 and m1, a probable pathology (FMNH neg. nos. GEO 85691 and 85707).

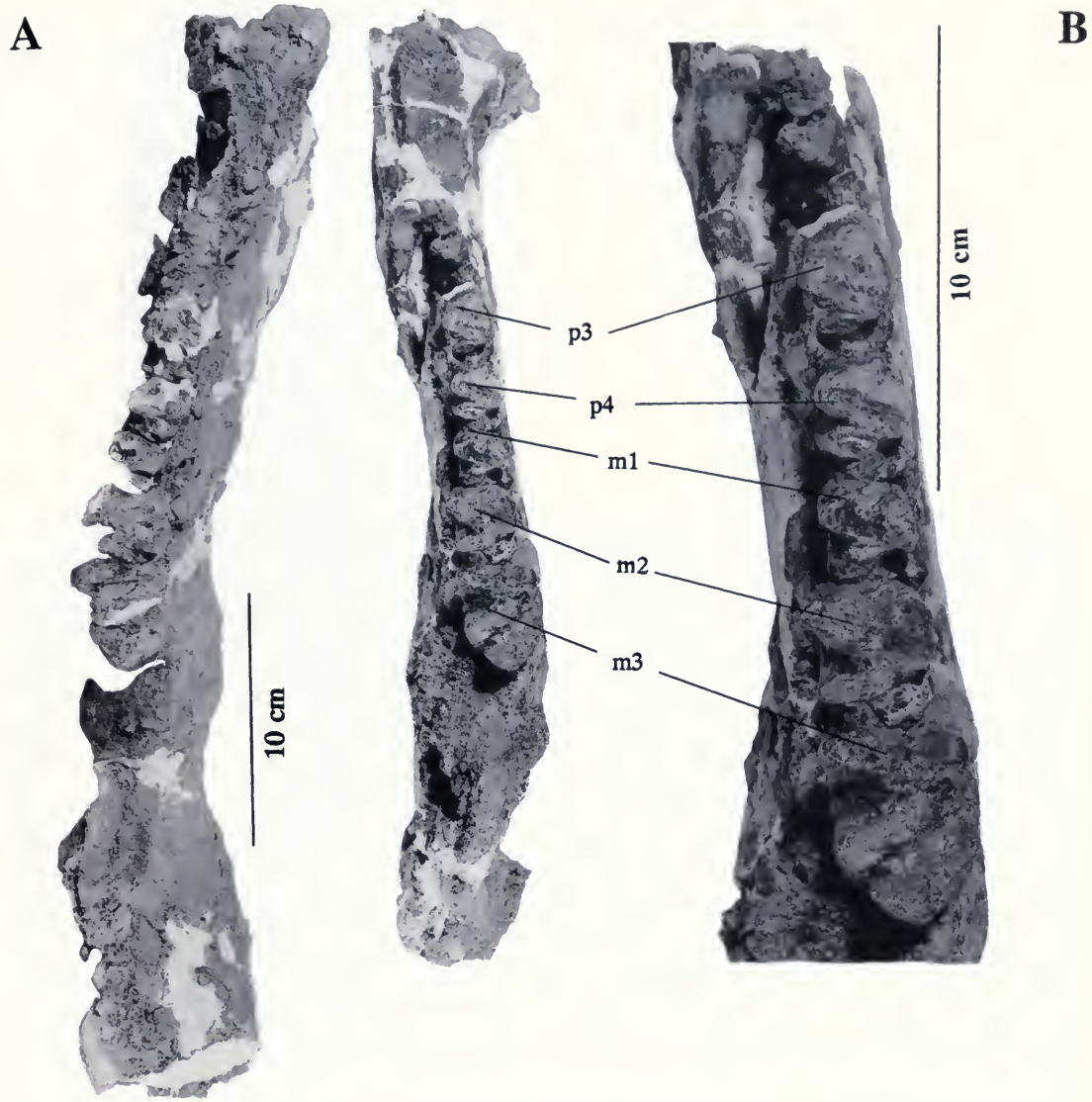

FIG. 37. PM 53932, a pair of fragmented *Uintatherium anceps* jaws shown in occlusal view (**A**) and showing an enlarged view of the right cheek teeth (**B**). In spite of poor preservation, this is the best lower cheek-tooth series of this species in the FMNH collection (FMNH neg. no. GEO 85692).

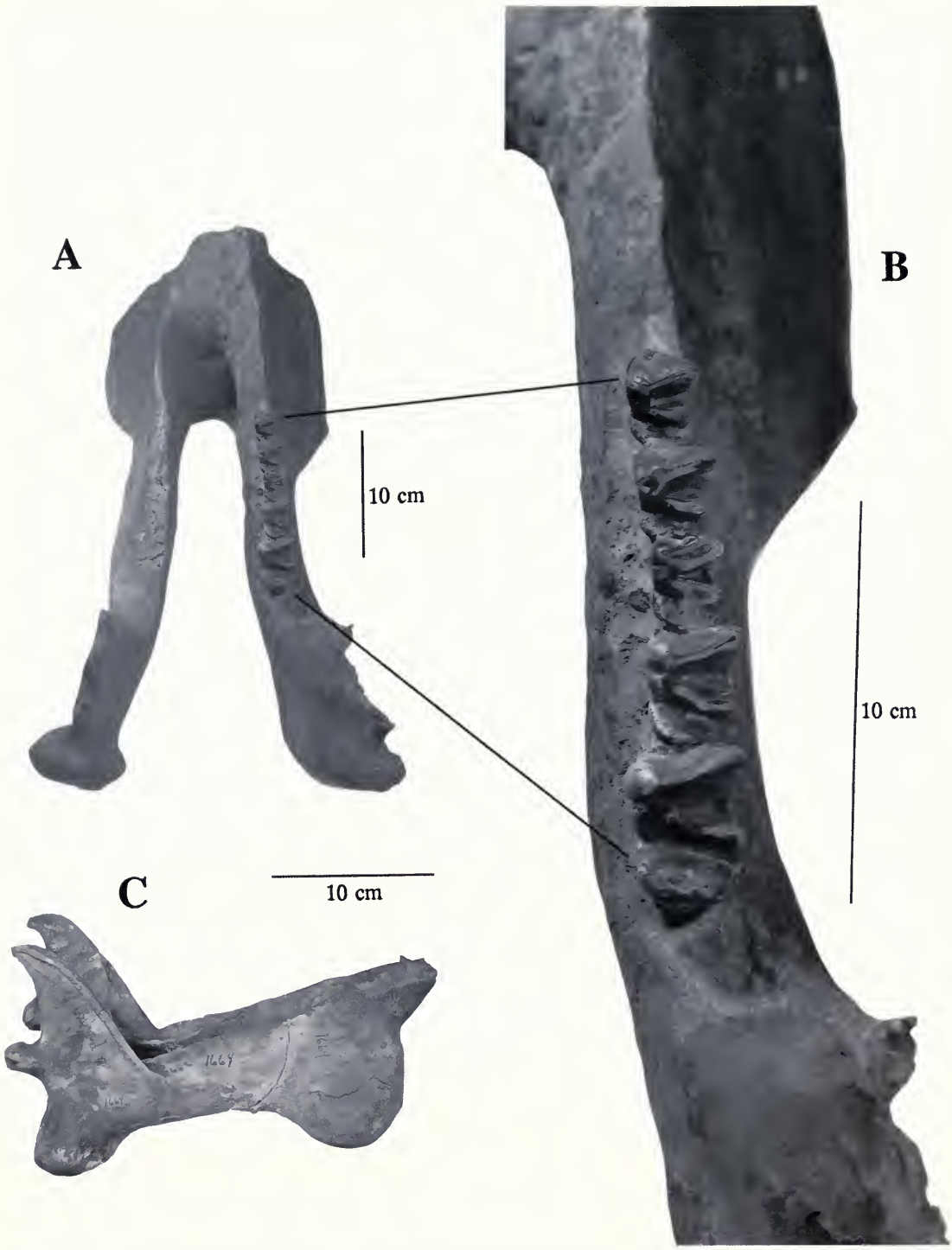

FIG. 38. **A** and **B,** AMNH 1664B, a mandible with its left ramus edentulous and its right with p3–m3. **C,** AMNH 1664A, a completely edentulous mandible. Both are specimens of *U. anceps* that were given the same number. It will probably never be known for certain which belonged to the skull, AMNH 1664 (Fig. 19A–B). Mandible 1664B appears to be the better size fit for the skull 1664. I speculate on the remote possibility that AMNH 1664A may belong to the skull AMNH 1694 (Fig. 19C–D), but there is no proof of that association, and there is no catalogue record of jaws for 1694 (FMNH neg. nos. GEO 82443 and 82509).

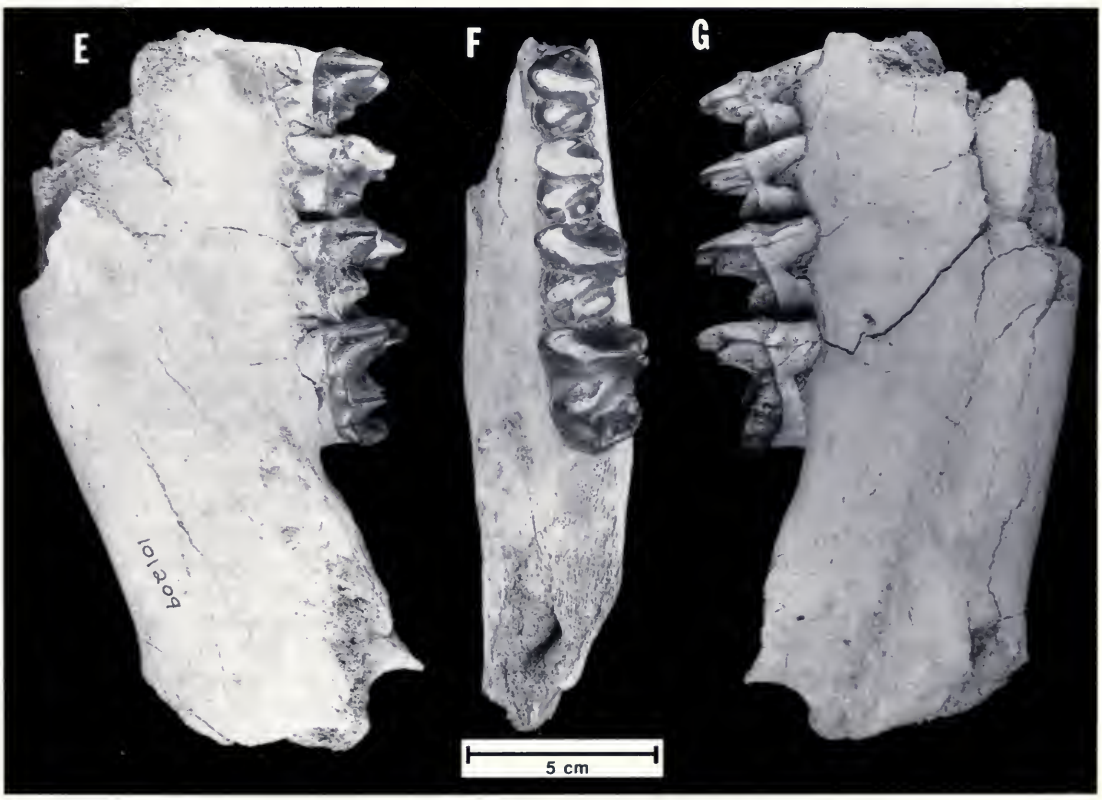

FIG. 39. **A–D,** YPM 11044, views of the mandible, or its separate rami, of *Tinoceras pugnax*, another synonym of *U. anceps*. In **A,** the medial side of the right ramus is shown; in **B,** the lateral side of the left. Dorsal view of the mandible is shown in **C,** and an enlarged occlusal view of its left cheek teeth in **D.**

E–G, UM 101209, a well-preserved University of Michigan left ramus fragment of *U. anceps* shown in left lateral (**E**), occlusal (**F**), and medial (**G**) views (FMNH neg. nos. GEO 82434–5 and 82128).

part of the dentition. All specimens I could locate document not only variation in tooth number, but also in size and placement. The symphyseal fragment of PM 53933 (Fig. 34B), the Funderburk skull specimen, shows the alveoli of i1–2 to be normal (large and procumbent), i3 to be much smaller and crowded (staggered to the outer side of the ramus), i4 to be normal, and c to be small, comparable to the i3 in its root diameter. It appears that when only three incisors are present, the 3rd has dropped out, leaving i1–2, and i4 ahead of the canine.

PM 38781 is a mandibular symphysis with most of the right inframandibular process (Fig. 35). From its massive size it almost certainly was that of an adult male: the inframandibular process is both large and thick (compared with that of PM 55827, which is less massive and not as deep, and which I considered to be either female or young adult male). About 5 cm behind the opening of the mental foramen, at the break surface, the canal can be seen to be expanded, with a triangular cross section that is flat laterally (somewhat dorsolaterally) and rounded medially. A few tiny openings exit within this expanded region, but it seems to be some sort of center, because there is a decided constriction anteriorly as the opening of the foramen is approached. The incisor alveoli are large; that for the canine is of small diameter but elongate. The mental foramen is large and right at the opening shows that the vessels exiting there immediately turned down about 45°, where the lateral edge of the flange is indented for more than 4 cm. The alveoli of i1–3 are inclined for procumbent teeth. The first two measure about 2.5 × 2.5 cm; that for i3 is longer and narrower (~3 cm × 2 cm). That of the canine is much smaller (only the central part of its anterior wall is preserved): on the left side it can be seen that the root was only about 4 cm long from tip to jaw margin and about 1 cm wide. It is from the western edge of locality FM-5-79-WDT and is located in SW ½ Sec. 24, and NW ¼ Sec. 23, T13N, R96W, Upper Powder Spring Quadrangle, and is within TWkA1, Bed 595, which is just below the Middle Red marker bed.

The other Field Museum specimens of jaws (Figs. 36, 37) are all of adult animals, the most complete being PM 55827 (Fig. 36). Its left ramus is missing the diastemal area but has the following teeth: worn p2, roots of p3, worn p4 lacking part of its talonid, m1 heavily worn and badly broken and lacking the posterior half of the talonid, m2 missing except for the rear of its talonid, and fragmented m3 that nevertheless preserves part of each lophid and includes the base of the metaconid (and from the size of the section, it appears that it was a large cuspid). The nearly complete right ramus is lacking only the anterior three-quarters of the symphysis, and it preserves most of the teeth from p2 through m3, as follows. The talonid of p2 is missing, p3 is nearly complete but worn, p4 is lacking only the tip of the metaconid, and its lophids are at a similar wear stage as seen in p3. The m1 is fragmentary; m2 is badly broken, but much of each lophid is present, with a decided wear facet; and m3 is nearly complete. It has a deep, oblique (abnormal?) wear facet on the rear of the metalophid and a more horizontal facet on the hypolophid, and the slightly raised feature in the hypoconulid position is broken away. Coronoid and angular processes are relatively lightly built, and the oval mental foramen is ~2.5 cm long by 1.4 cm high. It is situated in the upper half of the right symphyseal ventral flange (inframandibular process).

This flange for protecting the upper canine is long anteroposteriorly but not deep, all of which suggest that it belongs to a female, or a very young adult male. If a female, then it does not conform to Wheeler's statement (1961, p.72), "probably the female of *Uintatherium* was characterized by short, often tiny horns, slightly smaller average size, canine tusks only slightly smaller than in the male, and *no reduction of the inframandibular process*" (emphasis mine). If however, it is interpreted as a young adult male, then one would have to assume that its upper canine was delayed in its eruption and that the development of the inframandibular process may have been similarly delayed. This might be reasonable if development of the androgenous conditions awaited the achievement of a more advanced general maturation level. Horn development appears to have proceeded in a similarly delayed fashion to that of the dentition. So I conclude that although the specimen could be a young male, dental wear and degree of horn development make that an unlikely alternative. If this specimen is a female, as I believe it to be, both sexes had well-developed but differently proportioned inframandibular processes. Those of the male were more massive and deeper than those of the female (compare Fig. 26B, female, with Fig. 28, male). Only the right ramus preserves the condyle.

A possible pathology can be seen beneath the laterally exposed portions of the roots of the right p4 and m1 where there is a vertical, upward-open-

ing, foramen-like feature (arrows in Fig. 36A–B). It indents the lateral side of the jaw for about half of its height. The opening itself is about 1.5 cm long and nearly as wide. This abnormality may be an unusual vascular or nerve exit, but more probably it may be a drainage pathway of some sort of infection, although no obvious lesser channels are evident within it, as might be expected were that the case. I am uncertain how to interpret it. Marsh (1886) figured several somewhat similar but less prominent features that may or may not have been disease related: His figure 38 of *T. longiceps* (YPM 11256) shows a similar feature beneath p3: his plate XIII, figure 1 of *D. laticeps* (YPM 11039) shows it beneath p2, as does the illustration of *T. pugnax* (pl. XIX, fig. 3). On the other hand, the dorsum of the skull of *D. laticeps* (also YPM 11039) shows a possibly diseased condition within the broken maxillary horn area (pl. XI). Our specimen was found by Susan VandenBosch, then Women's Board Coordinator at the Field Museum, an enthusiastic volunteer member of Flynn's 1992 field crew. The locality is JJF.7.28.92.1, in the center of E ½, Sec. 13. T13N, R96W, Powder Mountain Quadrangle.

The FMNH collection has only two fair specimens of this species that have jaws with cheek teeth: that just described and PM 53932. The Marsh (1886) plate XIX reproduced here (Fig. 7E–F) serves well to illustrate these teeth. PM 53932 (Fig. 37) consists of a poorly preserved pair of jaws which nevertheless have most of the cheek teeth. There is no actual contact between the rami, but they were found together (immediately adjacent to one another), and they correspond well in size and dental wear, so there is no doubt about the association. They are shown in occlusal view in Figure 37A, where the left and right p2–m3 are seen to be nearly complete and little worn. In Figure 37B, the cheek teeth of the right ramus are enlarged to show the one puzzling feature of this specimen. It deserves notice—all of the teeth are worn to the same degree. There is no apparent gradient of wear from p2 through m3. Normally with p2–3 and m3 showing this amount of wear, the other teeth would be more heavily worn, especially m1. I am at a loss to explain this peculiarity. It is not from a missing or broken upper tooth, for the chewing plane is regularly jagged, not disrupted. The locality is FM-4-86-WDT (F.N., T-21-86) at the quarter corner between Secs. 22 and 23, T15N, R98W, Kinney Spring Quadrangle within TWkA1, about Beds 584–588.

PM 56022 consists of many heavily mineralized (ferromagnesian) fragments that make up most of a pair of jaws of *U. anceps*. The only complete tooth is the right m2, but there are more than 100 tooth fragments, including parts of the crowns of a premolar and both m3s. The locality, FM-4-79-WDT is in NW ¼, Sec. 18, T13N, R96W, Upper Powder Spring Quadrangle. The specimen is from ~Beds 596–598 (Middle Red Marker).

There are several jaw fragments of the Funderburk specimen, PM 53933, which apparently were in articulation with the skull before it was toppled from its in situ position (Fig. 13B). The left condylar, angular, and some of the coronoid processes were still in place when we received the specimen, and it is likely that both jaws had been complete but broke away in the fall, because there is a similar portion of the right ramus and the complete but edentulous symphysis among the many scraps. See above (p. 61) for comments on the incisor and canine alveoli. Much effort has been expended in an attempt to recover the missing parts, to no avail.

An American Museum specimen, AMNH 1664B, consists of most of both rami, including the symphysis. The left ramus is lacking teeth, but the right has p3–m3 well preserved (Fig. 38A). The only tooth with appreciable wear is m1 (Fig. 38B). As has been noted, two jaw specimens bore the number 1664 when I saw them in 1960 and 1996. We probably will never know with certainty which pair of jaws belongs with skull 1664 (Fig. 19A–B). From Wheeler's statement (1961, p. 42) it is clear that he associated this pair of jaws with skull 1664. The second jaw specimen with this number, 1664A (Fig. 38C), is edentulous. On the basis of size, 1664A is the better fit for the skull, 1664B being apparently too small. At one time the latter pair of jaws may have been mounted with the skull, probably because it possessed teeth, but no record of this has been located; hence the letters A and B are now appended to these jaws. The locality is the Washakie Basin, and Wheeler, referring to Wortman's letter to Osborn of June 11, 1893, concluded that it (they) was (were) from Washakie A (i.e., TWkA1), from somewhere (in the Lower Brown Sandstone) between LaClede and Barrel Springs.

The fine mandible of Marsh's holotype specimen of *Tinoceras pugnax* (another of the many synonyms of *U. anceps*), YPM 11044, is shown here as I found it in 1960 (Fig. 39A–D). Marsh (1886, pl. XIX) showed the complete left ramus to be lacking only the incisiform teeth. He did not

show the right ramus, which has m1 but lacks p2 and has the coronoid restored. As can be seen in Figure 39B–D, much of the left ascending ramus is now missing, as is m1. Wheeler (1961, p. 33) stated that the coronoid processes had been restored but that the restored portion is not indicated in Marsh's illustration (1886, pl. XIX). Actually, the left ramus has its angular and condylar regions completely restored and its coronoid process partially restored. In the right ramus, the angular and coronoid processes are restored, but the condyle itself looks to be real. Four alveoli, for i1–3 and c, are shown in Marsh's plate, the anterior three being subequal; the last for the canine is much smaller. The inframandibular process is deep and well developed (Fig. 39A–B), as shown in Marsh's plate XIX. Marsh may have restored the missing parts, including the left m1 (the right one is there), neglecting to tell us. It appears that the specimen has been damaged subsequent to Marsh's day, before either Wheeler or I saw it. The right ramus with its p2 missing is shown in medial and occlusal aspects (Fig. 39A–C). Or Marsh may have simply illustrated it as though it were complete, although in actuality, it was as we see it now. I suspect the former to be the case, because the details in Marsh's plate are fine and precise, even showing cracks in the angle and ascending ramus and highlighting the cingular margin of m1. In Figure 39D, the left cheek-tooth series is enlarged to show details of the occlusal surface of the tooth crowns. The locality data, "at Haystack Mountain," is not helpful because both TWkA1 and TWkA2 can be found there. Although Wheeler synonymized *T. pugnax* with *U. anceps,* the skull proportions are more like those of *E. cornutus,* which condition he attributed to dorsoventral crushing of the posterior part. Skull length (see Fig. 2) supports the Wheeler assignment.

The University of Michigan jaw, UM 101209 (Fig. 39E–G), is that of an adult with p4–m3. It is well preserved; the teeth are worn but the wear is not extreme. The specimen is the smallest *U. anceps* that I have encountered; hence its inclusion here, even though it is not from the Washakie. It is a Bridger Basin specimen that, significantly, comes from a unit just 50 m (160 ft) above the Sage Creek White Layer. Interestingly, as noted earlier, from 25 m lower in the section, another uintathere specimen was recovered, this a large ?*Bathyopsis* juvenile with dP2–4. It appears that we are beginning to see the transition from *Bathyopsis* to *Uintatherium* in this basal portion of the Bridger Fm. This and the other Michigan specimen (the upper jaw piece, UM 101208) are the only ones in that collection pertinent to this study, and it is of interest to note that this transition, like that from *Uintatherium* to *Eobasileus,* appears to be a gradational yet relatively fast one that apparently happens within the time represented by the 25 m part of the section between the two horizons. It comes from low in the Bridger Fm. at UM locality BRW-10 (1102, stuck truck), which is in NW ¼, SE ¼, SE ¼, Sec. 2, T13N, R114W, Reed Reservoir Quadrangle, Uinta County, Wyoming. It is from a unit 50 m above the Sage Creek White marker bed in horizon Br3, collected by the R. M. West field party in 1972.

The best of the Denver Museum's uintatheres belong to *E. cornutus,* but there are 10 specimens listed as belonging to Uintatheriidae and another 10 as *Uintatherium* sp. Of these last, which I presume to be *U. anceps,* only three pertain to jaws or lower teeth: EPV 1849, left and right rami for which some jaw and alveolar measurements are taken; EPV 2607, tooth fragments only; and EPV 3200, left m2 and m3 (measurements given in Table 6).

The Utah Field House has three specimens assigned to *Uintatherium.* One is a mounted life-size paper mache model (UFH 50001.5/50501), doubtless a replica of Marsh's "*Dinoceras mirabile.*" This model of the Yale specimen represents one of three mounted skeletons in the United States; the others are at the American Museum and the U.S. National Museum. The Gunma Museum has the recently collected skeleton.

UFH 54015/54515 and UFH 85023 together comprise the best specimen of *U. anceps* in that collection, a skull and partial skeleton. UFH field nos. v-85-23-1 and v-228-1, *U. anceps,* are lower jaws that are thought to belong to 54015. Dental measures for this specimen are given in Tables 3 and 4. They were first collected by G. E. and B. R. Untermann in the late 1940s (catalogue entry dated 9/16/54). The remainder was collected in 1950 by P. Robinson and W. Wheeler and donated to Utah Field House by Yale University on 9/21/60. It came from "Barrel Springs, Haystack Mt. area S of Wamsutter, Wyo." This is the locality known locally as "the bone pile"; it is within locality FM-7-58-WDT, near center of S ½, Sec. 22, T15N, R95W, Salazar Butte Quadrangle, low in TWkA1.

UFH 93002 (*Uintatherium* sp.) is a right ramus with m1–3 that is on exhibit. But it is too small to be a *U. anceps* and is either one or the other

of the two *Bathyopsis* species, probably *B. middleswarti* or a transition form of that species between *B. middleswarti* and *U. anceps*. Dental measurements, in mm, are: length m1–3 = 52; m1 L > 14 (broken), AW = 8.3, PW = 9.6; m2 L = 17.2, AW = 10.1, PW = 11.1; m3 L = 19.5; PW = 12.9. It is on loan to the Utah Field House by its discoverer, Mike Apeztequia of Lyman, Wyoming. It is recorded as coming from Hickey Mountain, near Lonetree, Bridger Basin, Wyoming, from Bridger C or D.

PUM 11611 is a problem. It (they) came from "15 mi, south of LaClede," according to Osborn and Speir (1879, p. 304) in their initial description and illustration, and Osborn (1881) reported and illustrated it (them) again. Part of the problem is to ascertain the contents of PUM 11611. Presumably two jaw specimens are included if everything in the Osborn and Speir (1879) report was given that number. They stated that

> The following description is based upon specimens collected in the South Bitter Creek country. . . . The material comprises two jaws, the first found with a large (upper) canine tusk belongs, without doubt to *L. cornutus*; the second is smaller, possibly of a female of the same species. . . . The accompanying plate figures the former specimen, the incisor-canine series have been placed in position from the latter specimen, in which the alveoli are preserved. (p. 304)

My notes from 1960, when I examined the specimen, make no mention of the incisor-canine series, nor did the catalogue at that time, although Osborn and Speir (1879) and Osborn (1881) showed those teeth, as did Wheeler (1961, p. 51), who referred to them as being PUM 11611. He erred in the locality given in the caption to the illustration (his pl. 13, fig. 2). "Near Haystack Mountain, Washakie fm., Washakie Basin. . . . This is a photograph of Plate 2, Fig. 3 of Osborn's Memoirs of 1881" (actually plate 3, figs. 3 and 4, of Osborn 1881). How Wheeler made this slip is uncertain (probably just a lapsus), because in the text (p. 51) he gives the 15 mi S of LaClede designation, following Osborn and Speir.

A further problem arises from the fact that the incisor-canine series is notably large, much larger than any of those teeth in our *U. anceps* materials. So I accept the assignment to *E.* (*L.*) *cornutus* for them, and presumably the jaw they were associated with.

The jaw shown in Osborn's plate 1 (1881) is supposed to be the same specimen as is shown in Osborn and Speir (1879), but its angle is more complete, the inframandibular process appears to be even less developed, and there are three mental foramina versus two for the Osborn and Speir specimen. It is possible that further preparation and restoration could account for these differences.

Marsh (1886, p. 51) stated that all of the incisors, canines, and premolars were preceded by temporary teeth in *Dinoceras* and *Tinoceras* (both = *Uintatherium*), noting that sometimes the replacement teeth appeared before the temporaries were shed. On p. 38 he illustrated one such specimen, his *D. mirabile* (YPM 11251), where a bit of di2 is present lateral to the alveolus of i2. Although I was unable to locate this specimen, additional supporting evidence, not given by Marsh but clearly shown on his figure, is the comparable ventrolateral wrinkle on the alveolar edge of the i1, the di1 alveolus. On the following page he shows another specimen, which he referred to *Uintatherium segne* (YPM 11194), in which a pair of small alveoli follow immediately behind the much larger alveolus of the last of the lower incisiform teeth,[8] which he labeled the lower canine. The pair of small alveoli he took to be for dp1, an identification Wheeler did not question but that I consider to be wrong. Now that we know the dC to have been double-rooted and situated within the eruption area of the permanent tooth, I interpret these to be the alveoli of a double-rooted dc. (With growth, that area would have expanded, allowing the permanent tooth to erupt in front of its milk predecessor.) Behind this, the Marsh figure also shows a puzzling single alveolus (far forward within the diastema) that he did not label. Possibly it could be for a single-rooted dp1. I say possibly because it seems unlikely that the lower tooth would be so differently positioned when its upper counterpart is more normally located. In the FMNH juvenile maxillary (Figs. 7, 8) the single alveolus of dP1 lies immediately ahead of the alveoli for the dP2, and behind the lengthy diastema (not within it); it also has the small paired alveoli for a double-rooted upper deciduous canine in the usual canine region. Thus, I am confident that the correct identification of these alveoli in the canine region of Marsh's YPM 11194 specimen should be dc, not dp1, for the anterior pair, and that the more

[8] In AMNH 13151, in which four incisiform teeth are in place, there are either four incisors and a small lower canine (if the pit is a canine alveolus), or there are three incisors, and the last incisivorm tooth is much larger than in other specimens.

posterior alveolus, if it really is an alveolus, is for a single-rooted tooth, perhaps a supernumerary or the dp1 or p1. This then gives comparable position assignments to corresponding upper and lower teeth and suggests that much growth subsequent to the juvenile age took place within the expanding diastemal region.

From all of this, the dental formula of the Uintatheriini can now be determined with only one common exception, that of the P/p1s, which are usually missing. The (maximum) dental formula, based on *Uintatherium,* is: dI/i 0/1–3 (or 4?), dC/c 1/1, dP/p 1 or 2–4/1 or 2–4; I/i 0/1–3 or 4, C/c 1/1, P/p 1 or 2–4/1 or 2–4, M/m 1–3/1–3. With the P/p1/1s lost (missing or never formed), P/p 2–4/2–4 is the usual pattern, but it would be no surprise to find an occasional specimen with evidence of one or more of these "absent" teeth. Also, it is just possible that the P1/1s are consistently missing (lost) and that the root or alveolar traces may in fact belong to deciduous teeth. We still know nothing about the deciduous dentition of *Eobasileus* or if it had P/p1/1s. Until more is known, I assume that the two genera probably had the same formula.

Figure 40, a bivariate graph for the lower cheek teeth of *U. anceps,* shows extensive overlap between all of the lower premolars and the m1s, and even some with the m2s. The molars show less extensive overlapping. Measurements for the lower dentition of *U. anceps* are given in Table 6.

Postcranium—Most items in the Field Museum's collection of specimens belonging to the terminal uintathere species are postcranial elements of *Uintatherium anceps.* Here, for simplicity, I treat both *U. a.* and *Eobasileus cornutus* together, but distinguish them in all cases where possible, first on stratigraphic grounds and then by their measurements (Tables 7–12). Only the latter species will be labeled; the more numerous other specimens are all assigned to *U. a.* Since the Marsh monograph (1886), which so beautifully illustrates most elements, is still readily available. I shall not attempt to do more than comment on those FMNH specimens that are informative in one way or another beyond the descriptions Marsh gave, and only some of them will be illustrated. I also do not illustrate many specimens in the collections of other institutions. Further, the text tabulations are not all-inclusive, because minor or very fragmentary specimens are omitted here.

There are no complete skeletons in the FMNH collection; however, the following specimens each consist of a major, or at least a significant, portion of the skeleton: PM 3896, the near-newborn (Figs. 8–10, 41, 42, 46, 51), PM 39393 (Figs. 47A–B, 53A–B), PM 53921 (Figs. 17, 50A–C), and PM 55423 (Figs. 43–45, 52). These will each be treated when they contribute to our knowledge of the following skeletal regions.

Axial Skeleton

The following specimens contain one or more of these bones:

Cervical vertebrae: atlas and axis

PM 2079, atlas and axis.

PM 53921, part of an atlas.

PM 54405, atlas.

PM 55175, axis from locality FM-16-91-WDT, Bed ~590, at corner between Secs. 29, 30, 31, and 32 (mostly in 32), T14N, R95W, Prehistoric Rim Quadrangle (with scrappy partial pelvis, and hind limb).

PM 55423 includes both atlas and axis, and most of the presacral vertebrae and three caudals as well (Fig. 43). There are four atlas fragments that appear to belong to two individuals, and there are two axis vertebrae in the lot, one of which is complete and is considered to be from the partially articulated skeletal specimen. It was recovered weathered out and in a number of pieces. The other is more weathered and consists of little more than the centrum. Three other cervical centra are present in a similar state and are presumed to belong with the weathered axis. That a second specimen (PM 55423A) was present is further indicated by a second (partial right) scapula that was picked from the eroded debris. All are from locality JJF.7.30.90.1 in NW ¼, Sec. 8, T15N, R94W, Salazar Butte Quadrangle, ~Bed 569–570.

PM 55578 includes a partial axis from locality FM-11-91-WDT from just SE of quarter corner between Secs. 24 and 25 (rest of locality is in SE ¼, SW ¼ Sec. 24) T15N, R95W, Salazar Butte Quadrangle.

PM 60173 includes a partial atlas, skull, and pelvis, and nearly complete radius and podial, from TWkA1, about the level of Bed 574.

Cervical vertebrae: posterior cervicals

PM 3896 includes parts of the arches thought to be of C3 and C4 (Fig. 41B). This is the juvenile (newborn), in which all vertebral segments are in unfused condition.

PM 53921, two cervical centra.

PM 55423 includes all five posterior cervicals,

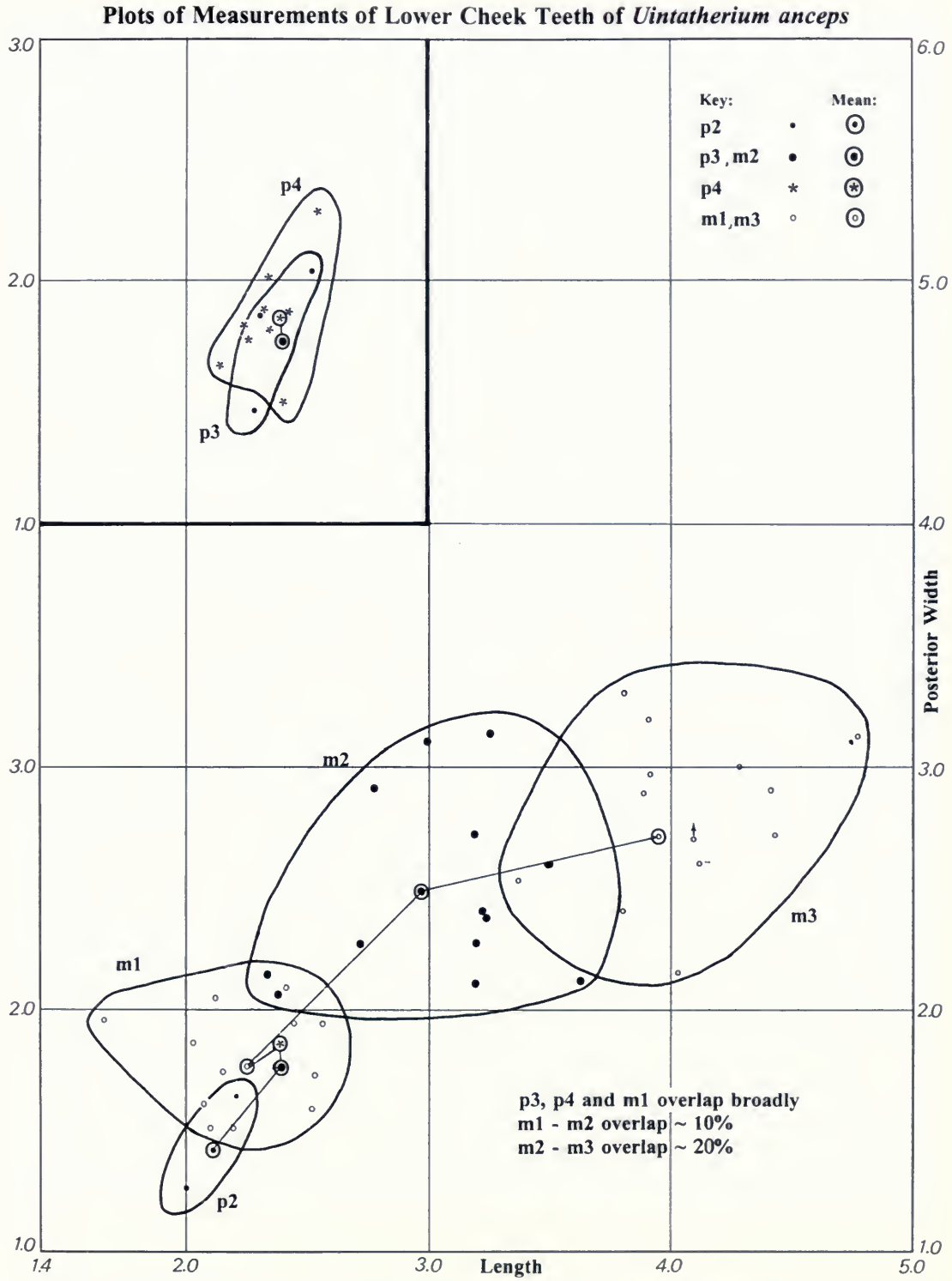

FIG. 40. Bivariate graphs for each cheek-tooth position for length × anterior width in the *U. anceps* lower dentition. Units are cm.

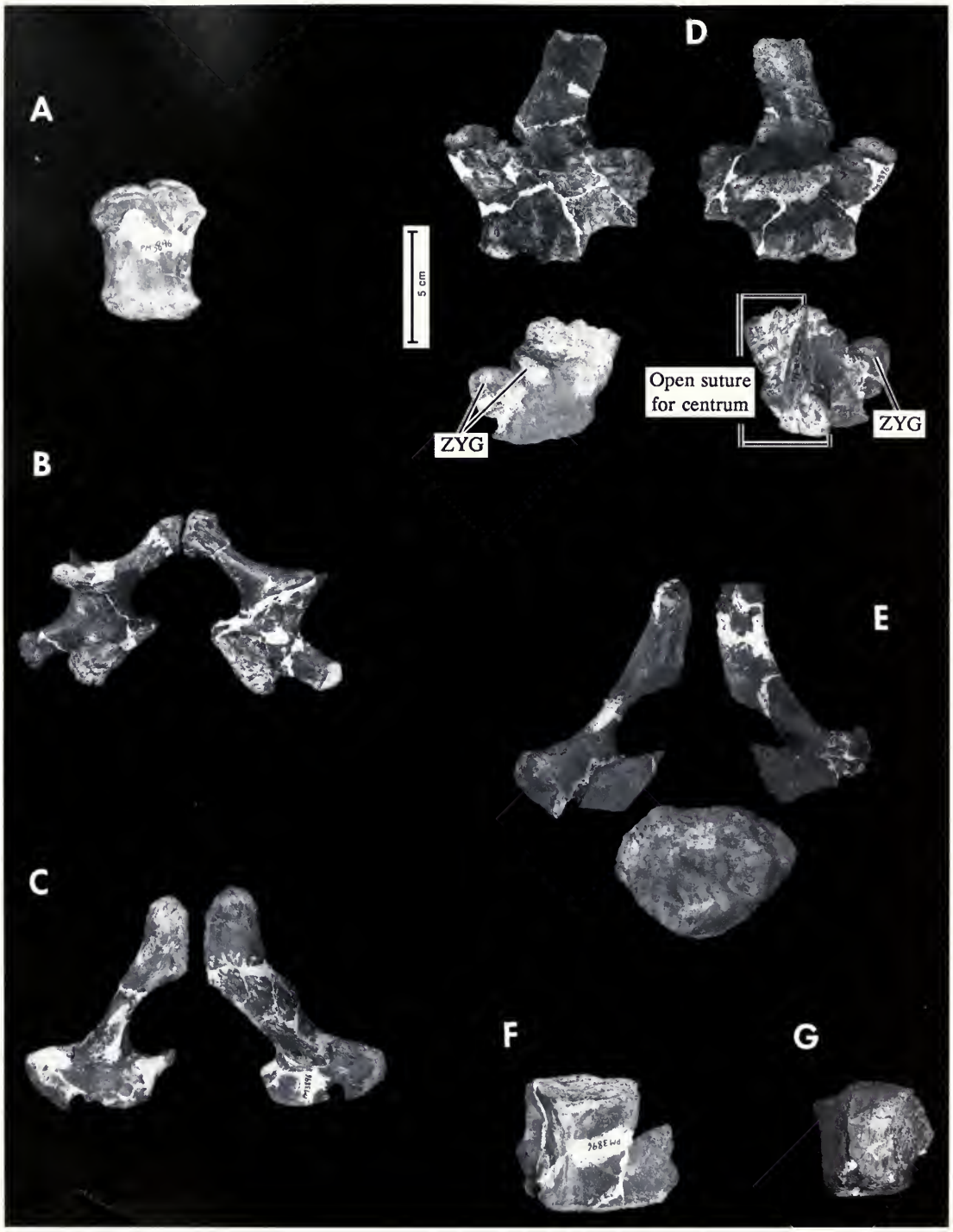

FIG. 41. *Uintatherium anceps* juvenile, probably newborn, PM 3896. **A,** Second sternal element shown in presumed ventral view. **B–G,** A series of the vertebrae exhibiting their early development, before fusion of arch elements and centrum. In most cases the positions indicated are approximate. **B,** Posterior views of arches of the 3rd cervical on left and 4th cervical on right, posed as though belonging to a single vertebra. **C,** Arches of two different anterior thoracic vertebrae seen in anterior view, again posed as a pair. Both have facets for rib articulation that lack epiphyseal caps. **D,** *top left,* dorsolateral view of a left neural arch (anterior end to right), and *top right,* the reverse (ventromedial)

C3–C7, of the partial skeleton, each a nearly complete vertebra having been assembled from dozens of scraps. When restored they are seen to articulate reasonably well (Fig. 43).

P 12170, a complete cervical, about the fifth, of *Eobasileus cornutus,* found with skull, from the Uinta Fm., Uinta Basin.

Thoracic vertebrae

PM 3896 includes five or six unfused separate thoracic arch pieces (one may be that of a lumbar vertebra), and three centra (Figs. 41C–E,G; 42A–B).

PM 8020 and 8022 each contain one thoracic vertebra, the latter from locality FM-4-59-WDT in W ½, NE ¼, Sec. 27, T16N, R95W, Salazar Butte Quadrangle.

PM 39393 contains three posterior thoracic vertebrae and the first lumbar from top of TWkA1 (Bed 595), from below but close to the "transition unit" from *U. anceps* to *E. cornutus.*

PM 53921 contains seven thoracic vertebrae.

PM 53933 is associated with the Funderburk skull. In addition to parts of both jaw rami there are three ribs and other postcranial fragments, including three thoracic vertebral centra.

PM 54866, an anterior thoracic vertebra, c.f. *E. cornutus* from TWkA1-2, at locality FM-4-81-WDT, center W ½, Sec. 18, T13N, R96W, Upper Powder Spring Quadrangle.

PM 55423 contains the first 11 weathered-out thoracics (Fig. 43) plus seven from the rear part of the region that are articulated in two groups (nos. 13–15 and 16–19). These posterior thoracics lie within the large block containing much of the partially articulated rib cage. T12 is also present: it was removed in a separate block from just in front of the main block, where it had been in articulation with no. 13. It is shown in Figure 43 and again in Figure 44A–B, where it is set in an open area on the block, behind T15.

P 12541, *Eobasileus cornutus*, Uinta Fm., Uinta Basin, includes four partial thoracics.

Lumbar vertebrae

PM 3894 includes the last lumbar vertebra in articulation with the first sacral vertebra (Fig. 50A–B).

PM 3896 includes one or two lumbar (or posterior thoracic) vertebrae of the newborn specimen (Fig. 41F and possibly 41D).

PM 39393 includes the first lumbar (associated with last three thoracics).

PM 53921 consists of four, including the penultimate lumbar (Fig. 51A).

PM 54866 is from TWkA2, *E. cornutus.*

PM 54867 includes a posterior lumbar vertebra, c.f. *E. cornutus,* from near the top of TWkA1, ~Bed 615 at locality FM-3-81-WDT, NE ¼, NE ¼, Sec. 27, T15N, R95W, Powder Mountain, NE Quadrangle.

PM 55423 preserves two lumbar vertebrae, one of which is complete (L3); the other (L2 or L1) consists of only the centrum (Fig. 43).

P 12541 includes two lumbar centra of *E. cornutus* from Uinta Fm., Uinta Basin.

Sacral vertebrae

PM 3894 includes all three true sacrals plus the sacralized first caudal, the block in articulation with the pelvis, and the last lumbar and caudals 2 and 3 (Fig. 50A,C).

PM 53921 includes the sacrum and pelvis in articulation and the first two caudals articulated with the sacrum (Fig. 51).

P 12541 includes the first sacral centrum of *E. cornutus,* Uinta Fm., Uinta Basin.

Caudal vertebrae

PM 3894 includes the anterior three caudals in articulation with the pelvic girdle.

PM 53921 includes the first two caudals articulated with the pelvis (Fig. 51A).

PM 54866 includes five anterior caudals, about nos. 3–7, cf. *E. cornutus,* from TWkA1-2.

PM 54867 includes the centra of five anterior caudals of *E. cornutus,* from TWkA2.

←

aspect of the same element, where the fusion attachment area for the centrum can be seen above the lateral edge of the neural canal. In both views the transverse process is at the top and the zygopophyses protrude anteriorly and posteriorly. I believe the neural arch to be from a posterior thoracic or anterior lumbar vertebra. Dorsal (*bottom left*) and ventral (*bottom right*) views of a partial arch with part of its transverse process, an interlocking zygopophysis, and part of the fusion area for the centrum, probably a posterior thoracic, are shown. **E,** thoracic arches, seen in posterior view, that I interpret to be the last (*left*) and penultimate (*right*), posed together with the centrum, which may also belong to the last thoracic. **F,** Ventral view of the centrum of one of the lumbar vertebrae. **G,** Dorsal view of right half of a centrum of one of the last thoracics (FMNH neg. nos. GEO 85913 (A), 85924 (B), 85923 (C), 85925.1 and 2 (D), 85922 (E), and 85913 (F–G)).

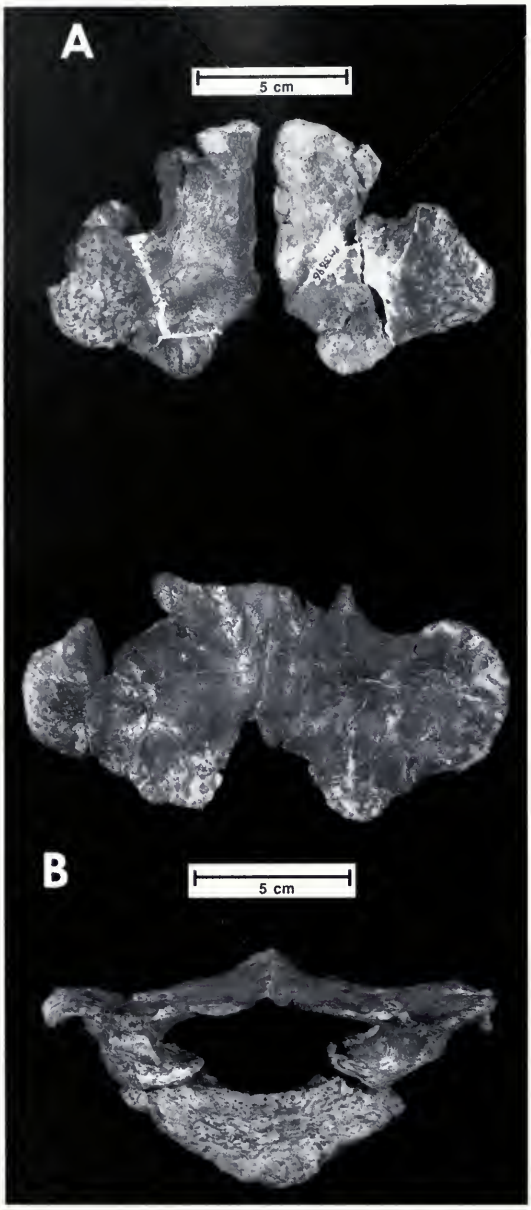

FIG. 42. *Uintatherium anceps* juvenile, more of the "newborn," PM 3896. **A,** Dorsal view (anterior down) of one of the posterior thoracic vertebrae. It may belong with the centrum shown in Figure 41G. In **B,** another of the posterior thoracic vertebrae is shown. The dorsal view of the arches (*above,* anterior down) is posed with a centrum that appears to nearly fit, either as shown or reversed front to back (FMNH neg. nos. GEO 85918, 85920, and 85921).

PM 55423 contains three isolated midregion caudals.

P 12541 includes two partial centra of anterior caudal vertebrae found in association with a partial pelvis (including the first sacral centrum, both ilia and acetabulae) and six other vertebral centra, from Uinta Fm., Uinta Basin.

Rib cage and sternum (Table 7)

PM 3896, the "newborn," preserves the second sternal element (Fig. 41A).

PM 53921 contains a large part of each of eight ribs.

PM 55423 has 11 ribs in partial articulation within the rib cage slab (Fig. 44A–B), and at least 10 more that had weathered out. In the slab, the right ribs 12–15 are together in near articulation with their vertebrae, and right and left ribs 18 are loosely articulated with vertebrae T18 and T19. Just behind them lie the pair of ribs 19, but these ribs are not in contact with vertebra T19. Among those that had eroded out, I have been able to assemble complete left and right first ribs, right 2nd, and part of the left 3rd. Table 7 gives rib measurements, arc, and chord lengths for those ribs that are complete and estimates for others that are nearly so. The rest of the rib cage is incomplete, represented only by many broken bits.

PM 60174, consisting of seven or eight associated ribs, is from a sandstone channel low in TWkA1, ~Bed 575, from locality FM-4-59-WDT in W ½, NE ¼, Sec. 27, T16N, R95W, Salazar Butte Quadrangle.

Appendicular Skeleton

Shoulder girdle and forelimb

ARTICULATED FORELIMB ELEMENTS

PM 55423 includes the articulated right limb of the partial skeleton, complete from scapula through the first phalanges (Fig. 45).

PM 39393 includes the articulated right humerus, radius, and ulna, and most of the manus (Fig. 47A–B), from near the top of TWkA1, about Bed 595, cf. *U. anceps,* in locality FM-4-79-WDT, in center of SW ¼, Sec. 19, T13N, R96W, Upper Powder Spring Quadrangle.

SCAPULA (TABLE 8)

PM 3896 includes the right, well-preserved scapula of the "newborn" (Fig. 46A–B) with a broad base for articulation with the head of the humerus, but at this early stage the glenoid itself

had not yet developed. The distance from glenoid base to tip of the stout spine is no greater than the width from the rounded coracoid border to the pointed suprascapular border. This dimension is considerably lengthened in the adult by the addition of the glenoid epiphyseal and unossified suprascapular portions. The external surface is divided into anterior and posterior parts, the former being about half the area of the posterior. The internal surface is smooth and almost flat.

PM 39915, a left scapula from TWkK or TWkA1, ~Beds 567–570 from locality FM-3-86-WDT, in W ½ Sec. 2 and NW ¼, SW ¼, Sec. 3, T16N, R95W, Barrel Spring Quadrangle.

PM 53921, partial left scapula associated with disarticulated partial skeleton.

PM 53934, scapula and associated partial left humerus, from near the top of TWkA1, or the base of TWkA2, cf. *E. cornutus,* from ~Beds 620–624, locality FM-3-81-WDT in NE ¼, NE ¼, Sec. 27, T15N, R95W, Powder Mountain NE Quadrangle.

PM 55423, right scapula (Fig. 45A–B).

PM 55423B, badly weathered specimen associated with, but not part of, the largely articulated partial skeleton (PM 55423).

Humerus (Table 8)

PM 1457, distal end of humerus, *E. cornutus,* from TWkA2, locality FM-10-56-WDT in W ¼, Sec. 2, T16N, R97W, Fort LaClede NE Quadrangle.

PM 1458, complete left humerus from Beds ~570–576, at locality FM-13-56-WDT in SE ¼, Sec. 11 and SW ¼ Sec. 12, T16N, R98W, Kinney Spring Quadrangle.

PM 1509, complete left humerus from TWkA2, at locality FM-8-56-WDT, Beds about 650–670, *E. cornutus,* in S ½, SW ¼, Sec. 31, T17N, R96W, Fort LaClede NE Quadrangle.

PM 1522, left humerus lacking head and part of distal end, from TWkA2, in locality FM-10-56-WDT, Beds ~650–670, in W ¼, Sec. 2, T16N, R97W, Fort Laclede NE Quadrangle, *E. cornutus.*

PM 2079, right humerus (Fig. 46C–D) associated with atlas, axis, parts of the left humerus and radius (PM2079A), two right tibiae (one of which obviously is from another individual, PM2079B), patellae, rib, and other fragments

PM 3894, partial right humerus associated with complete pelvis, FM-1-58 WDT, ~Beds 600–618, center S ½, Sec. 19, T16N, R97W, Manuel Gap Quadrangle.

PM 38781, partial left humerus associated with an edentulous mandibular symphyseal area from N ½, Sec. 25, T13N, R97W, Upper Powder Spring Quadrangle.

PM 38782, left humerus (shaft only) found in association with a pair of tibiae, from ~Beds 580–620 in NE ¼, Sec. 19, T13N, R96W, Powder Mountain Quadrangle.

PM 39393, right humerus of *U. anceps* in articulation with radius, ulna, and manus (Fig. 47), from below, but near to, the transition zone to the *E. cornutus* level.

PM 53921, part of the disarticulated "Lombardi" skeleton.

PM 53934, distal two-thirds of a left humerus, TWkA1 (top), associated with scapula; Beds 620–622, from transition unit, cf. *E. cornutus.*

PM 53935, humeral head only, from Beds ~569–570 at locality FM-4-58WDT, near top of Lower Brown Sandstone, SW ¼, SE ¼, Sec. 7 and N ⅙ Sec. 18, T17N, R96W, Fort LaClede NE Quadrangle.

PM 54676, complete left humerus from Bed ~590 at Locality FM-1-85-KL/WT in NE ¼, NW ¼, Sec. 26, T15N, R95W, Powder Mountain NE Quadrangle.

PM 55423 (Fig. 45), complete humerus of the articulated right forelimb.

PM 55581, partial humerus head, scraps of skull from Beds ~569–571, at FM-9-91-WDT, in SW ¼, NW ¼, NW ¼, Sec. 8, T15N, R94W, Salazar Butte Quadrangle.

PM 60172, proximal half of a humerus from locality FM-3-58-WDT, Bed 569–570, in NW ¼, Sec. 18, T 17 N, R96W, and E ¼, Sec. 13, T17N, R97W, Fort LaClede NE Quadrangle.

Radius (Table 9)

PM 1452, distal half of a right radius of *E. cornutus,* from TWkA2, ~Beds 650–670, at locality FM-6-56-WDT, in SE ¼, NW ¼, Sec. 36, T17N, R97W, Fort LaClede NE Quadrangle.

PM 2079, left radius, articulated with humerus, ulna, and partial manus.

PM 2079A, very weathered proximal end.

PM 3211, proximal half only, *E. cornutus,* from ~Beds 650–670, TWkA2, at FM-1-57-WDT, SE ¼ and center, Sec. 10, T16N, R97W, Fort LaClede NE and Manuel Gap Quadrangles.

PM 39393, articulated with right humerus, ulna, partial manus (Fig. 47): from horizon at top of TWkA1.

PM 53936, distal end of a left radius from bed 569–570, locality FM-4-58-WDT, in SW ¼, SE

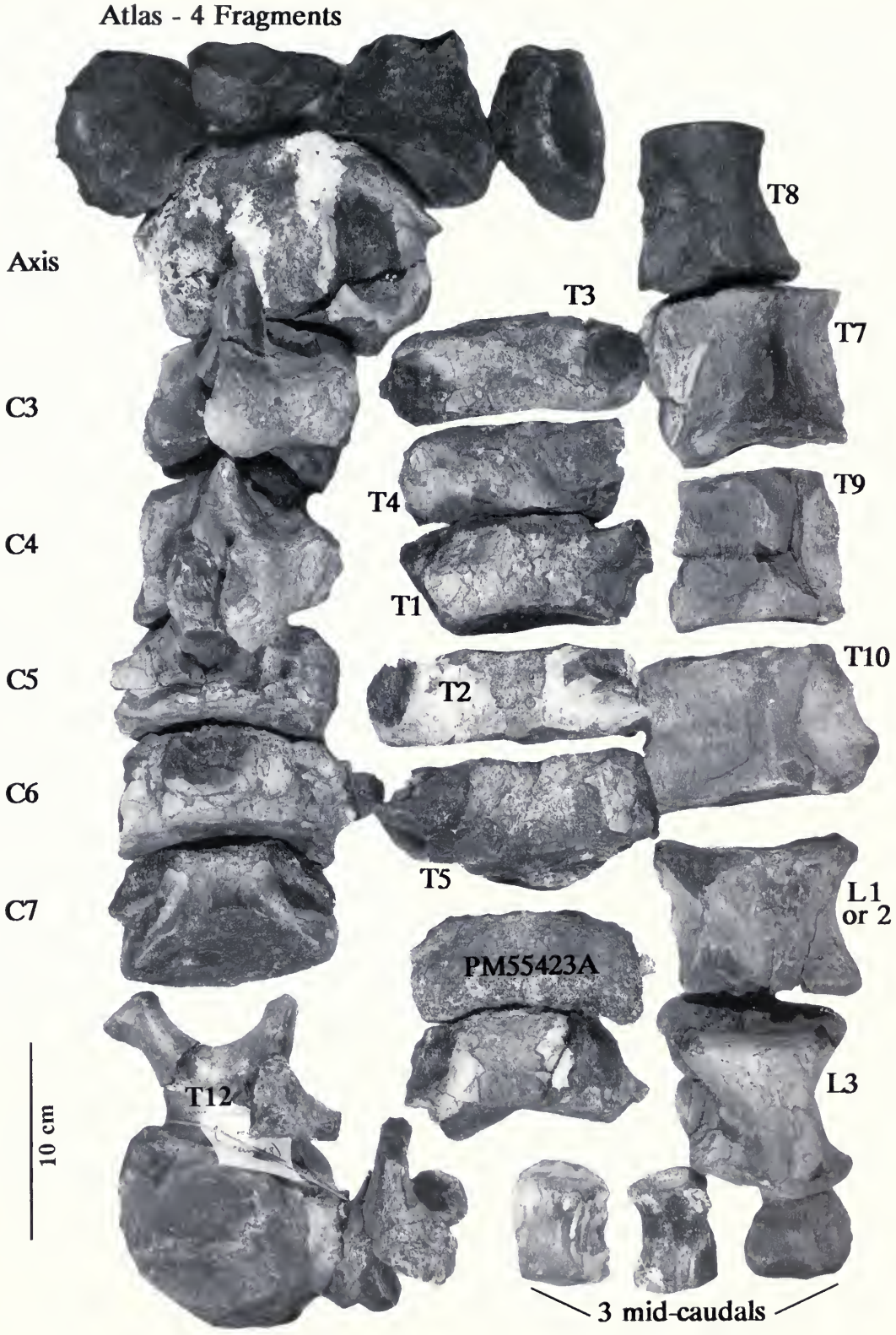
Atlas - 4 Fragments
Axis
C3
C4
C5
C6
C7
T12
10 cm
T8
T3
T7
T4
T9
T1
T10
T2
T5
L1
or 2
PM55423A
L3
3 mid-caudals

¼, Sec. 7 and center N 1/6, Sec. 18, T17N, R96W, Fort LaClede NE Quadrangle.

PM 55423, a part of the articulated right forelimb (Fig. 45).

PM 55540, nearly complete left radius and associated proximal end of an ulna, at locality FM-13-91-WDT in ~Bed 590 (i.e., TWkA1) in extreme SE ¼, NE ¼, Sec. 5, T13N, R95W, ~⅛ mi (0.2 km) W of ¼ corner between Secs. 4 and 5, Powder Mountain NE Quadrangle.

PM 60173, a nearly complete radius and podial associated with partial atlas, skull, and pelvis, from TWkA1, about level of Bed 574.

Ulna (Table 9)

PM 1451, right ulna lacking most of the proximal articulation surfaces, TWkA2, c.f. *E. cornutus*, between Beds 650–670, in FM-6-56-WDT, Manuel Gap Quadrangle.

PM 1455, TWkA2, left ulna complete except for tip of olecranon process; cf. *E. cornutus*. from locality FM-8-56-WDT, Beds ~650–670, in S ½, SW ¼, Sec. 31, T17N, R96W, Fort LaClede NE Quadrangle.

PM 2079, left ulna associated with humerus, radius, and partial manus.

PM 39393, right ulna of one of the articulated forelimbs (Fig. 47).

PM 53931, shaft and proximal end of a right ulna, from ~Beds 603–608, at FM-7-69-WDT in NW ¼, NW ¼, Sec. 20, T13, R98W, Cow Creek Reservoir SW Quadrangle.

PM 55540, proximal end of left ulna and associated radius from just below LBS (i.e., TWkK).

PM 56038, proximal end only, from ~Beds 606–616 at locality JJF-7-23-90-1 in SW ¼, SW ¼, Sec. 20, and NE ¼, NW ¼, NW ¼, Sec. 29, T13N, R98W, Cow Creek Reservoir SW Quadrangle.

Carpus and Manus

PM 3212, articulated partial left carpus and metacarpus (Fig. 48), from TWkA2, *E. cornutus*, at FM-2-57-WDT, from ~Beds 650–670, in SE ¼, and center Sec. 10, T16N, R97W, Fort LaClede NE and Manuel Gap Quadrangles.

PM 36023, an isolated left scaphoid, one of the few extraneous elements recovered in the otherwise monospecific titanothere quarry assemblage reported by me and David Martill in 1988, from ~Beds 641–643, TWkA2, cf. *E. cornutus*, locality FM-12-70-WDT, in NE ¼, SE ¼, Sec. 19, T15N, R96W, Barrel Springs SW Quadrangle.

PM 39393, in right articulated forelimb, from TWkA1 (Fig. 47).

PM 55423, a part of the articulated right forelimb, Flynn specimen (Fig. 45).

Pelvic girdle and hind limb

Pelvis (Table 10)

PM 1454, partial right ilium of *E. cornutus*, from locality FM-8-56-WDT, TWkA2, ~Beds 650–670 in S ½, SW ¼, Sec. 31, T17N, R96W, Fort LaClede NE Quadrangle.

PM 3212, partial right ilium and pubis of a juvenile, from TWkA2, *E. cornutus*.

PM 3894, the most complete adult pelvis (Fig. 50A–C). The sacroiliac fusion is complete and the last lumbar and first three caudals are in articulation. There is an associated humerus.

PM 3896, right ilium of the "newborn" (Fig. 49A–B) with a relatively large open sutural scar for union (and later fusion) with the sacrum, an ill-defined acetabular portion, and open sutural areas for pubis and ischium. The bone is rounder than in the adult, in which it is more stretched out laterally.

PM 37434, left pelvic piece including ilium, and acetabular portions of pubis and ischium, TWkA2, *E. cornutus*.

PM 53921, nearly complete pelvis (Fig. 51A) of one of the partial adult skeletons (Lombardi) and its associated femur (Fig. 51B–C).

PM 54408, right side of pelvis from ~Bed 590 at locality FM-1-85-KL/WT in NE ¼, NW ¼, Sec. 26, T15N, R95W, Powder Mountain NE Quadrangle.

P 12541 (= P 12858), *E. cornutus*, Uinta Fm., Uinta Basin, Utah, a partial pelvis including both

---

←

Fig. 43. *Uintatherium anceps*, PM 55423, shows the weathered-out vertebrae (mostly only their centra) pretty much as found before many of the neural and transverse processes had been fitted on. The four fragments of the atlas could not be fitted together, but the cervicals all articulated with one another reasonably well. The thoracics (shown out of order, but the labeling suggests the probable proper order) occupy most of the right and central rows in the figure. T12 was attached to the front of the large block (Fig. 44) with the rest of the thoracics and ribs. It was blocked out separately. The lower two centra of the central row probably belonged to another individual (PM 55423A). Two lumbar vertebrae and three midcaudals are shown in the lower right corner (FMNH neg. no. GEO 85930.1).

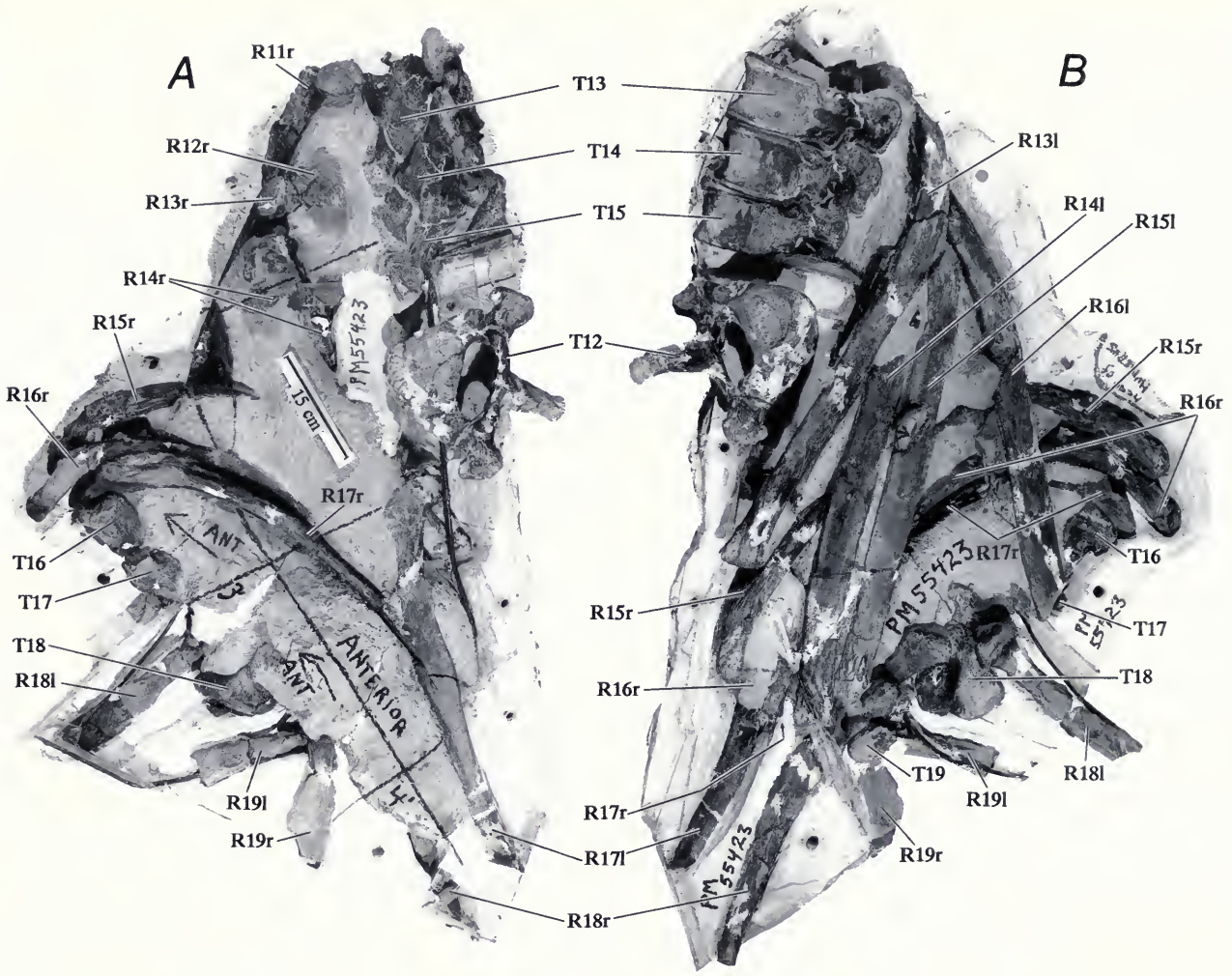

FIG. 44. *Uintatherium anceps,* PM 55423, a large block with thoracic vertebrae 12–19, ribs 12–19, some one side only, but adequate to determine that no. 14 is the longest. In **A,** the weathered "up" side of the block is shown, in **B** the "under" side. All elements are labeled and are exposed but remain within the block except T12, which had been articulated with T13 but was placed in an open space for the photographs (FMNH neg. nos. GEO 85930.2 and 3).

FIG. 45. *Uintatherium anceps,* articulated right forelimb of the partial skeleton, PM 55423, collected by *J. J.* Flynn and his field crew. **A** and **B** show approximately opposite sides of each set of elements laid out separated, except the manus, which is still held in the position in which it was found by a thin layer of matrix (FMNH neg. nos. GEO 85930.5 and 85930.7).

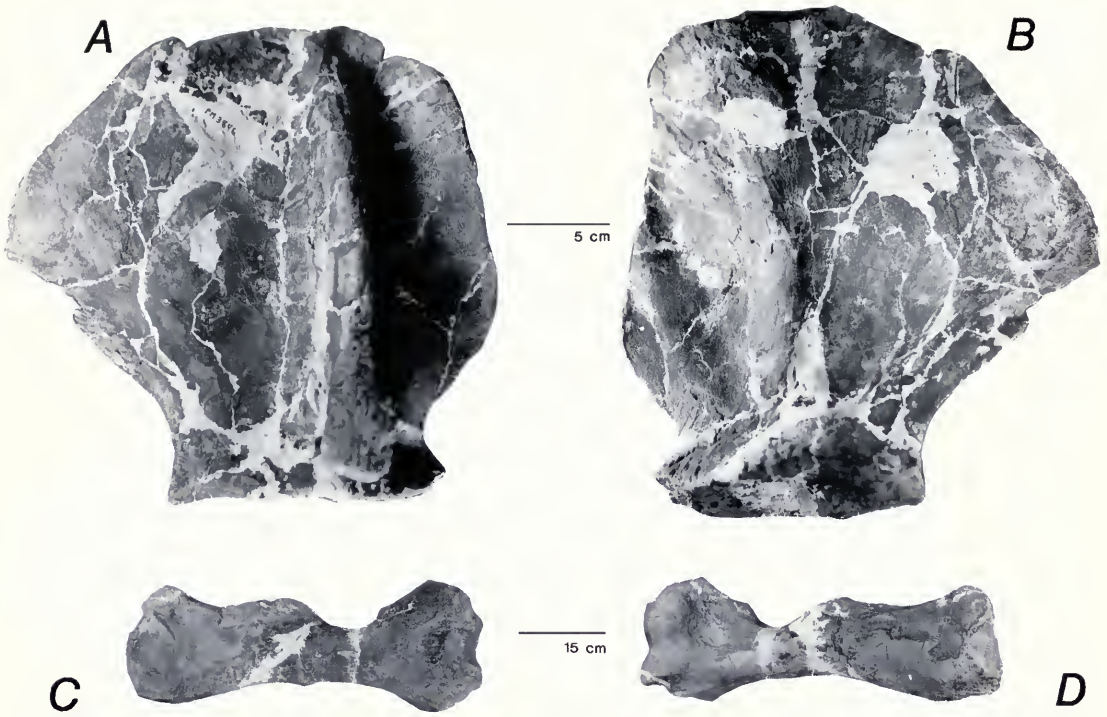

FIG. 46. *Uintatherium anceps.* **A** and **B,** right scapula of the "newborn" specimen, PM 3896, shown in external (A) and internal (B) views. The glenoid epiphyseal end had not yet formed, and there is no suprascapular cartilage, but the spine, seen in A, is well developed and divides the pre- and postscapular areas into unequal fossae proportioned as in the adult at ~1:1.5. The inner surface is even and almost flat. **C** (anterior) and **D** (posterior) are views of the left humerus of an adult, PM 2079 (FMNH neg. nos. GEO 82125–6 and 86079–80).

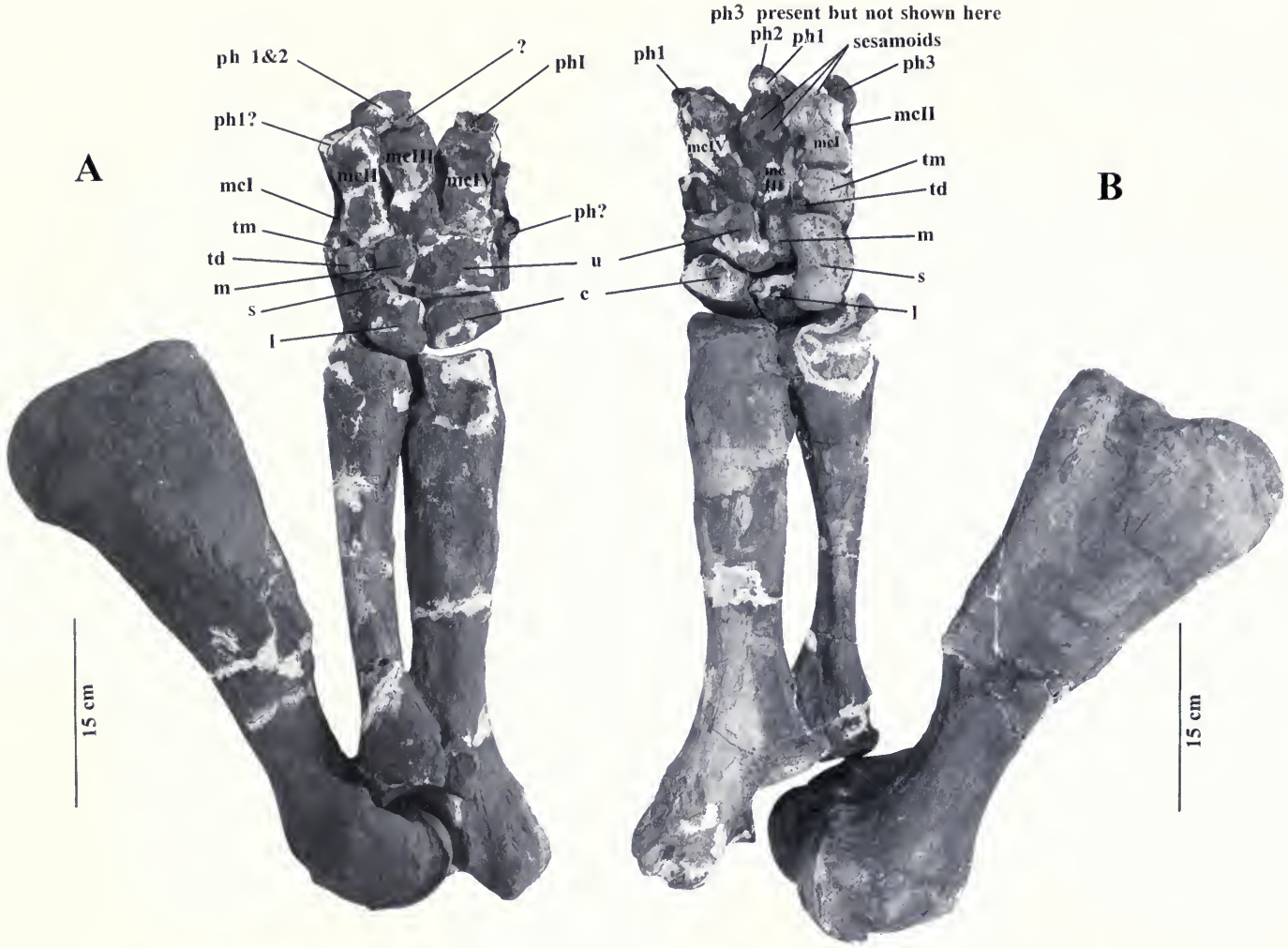

FIG. 47. *Uintatherium anceps*, articulated humerus, radius, ulna, and most of the manus of PM 39393, one of the partial skeletons. **A,** Anterodorsal view of the right forelimb. **B,** The reverse. Abbreviations are: c = cuneiform, l = lunar, m = magnum, mc I, II, III, and IV = metacarpals, ph 1, 2, 3, = phalangeals, s = scaphoid, td = trapezoid, tm = trapezium, u = unciform (FMNH neg. nos. GEO 86099 and 86100).

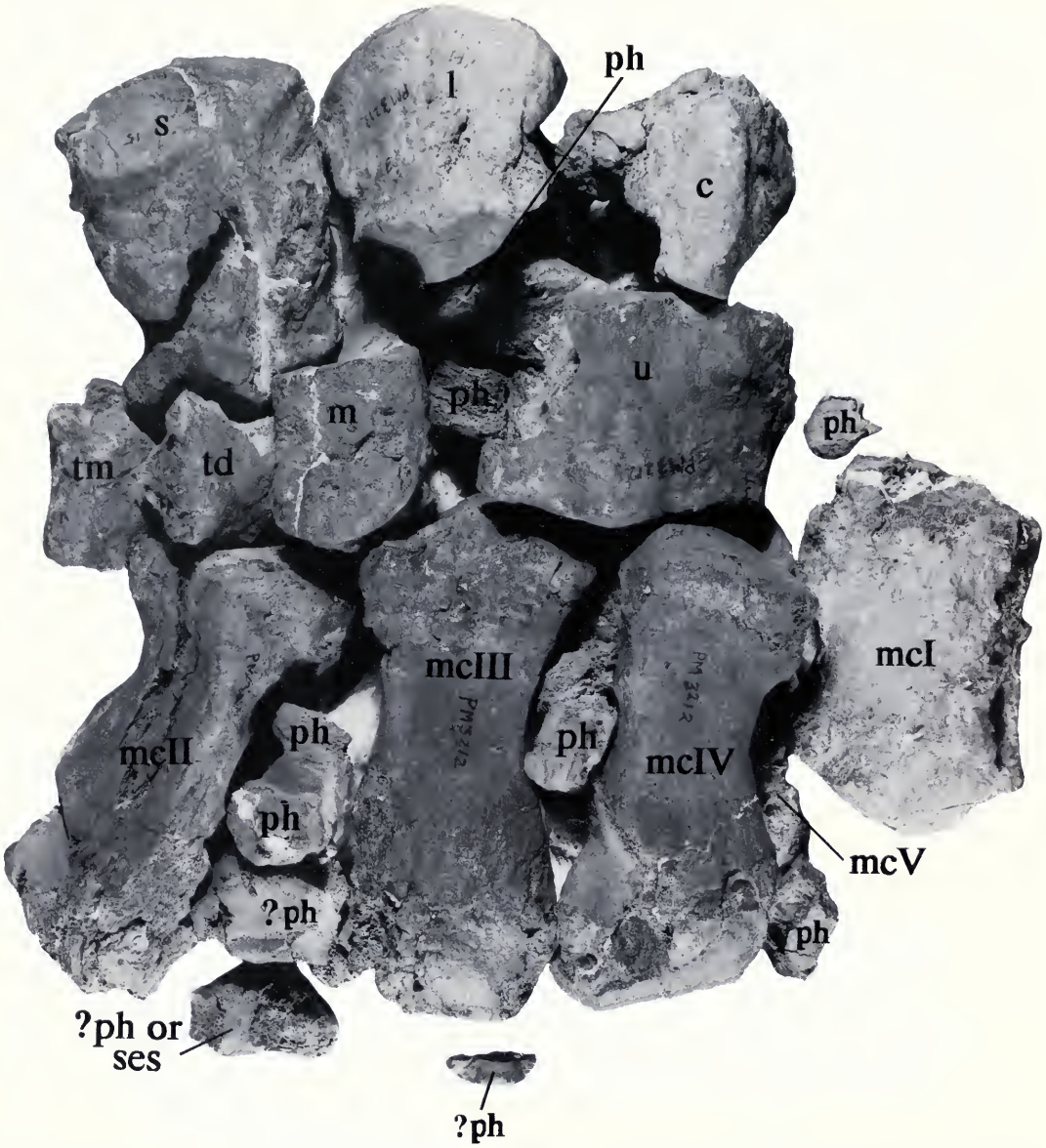

FIG. 48. PM 3212, articulated partial left forefoot of *Eobasileus cornutus* shown in dorsal view. The first metacarpal has been placed next to the fourth and unintentionally inverted side to side, ventral side up. Otherwise the position of each bone is as it was found, before preparation. Abbreviations: ses = sesamoid; others as in Figure 47. Note the apparent borings in the cuneiform and unciform, where large parts of the bone are missing (FMNH neg. no. GEO 85695).

FIG. 49. *Uintatherium anceps,* right ilium of the "newborn" specimen, PM 3896, shown in dorsolateral (**A**) and ventromedial (**B**) views (FMNH neg. nos. GEO 82123–4).

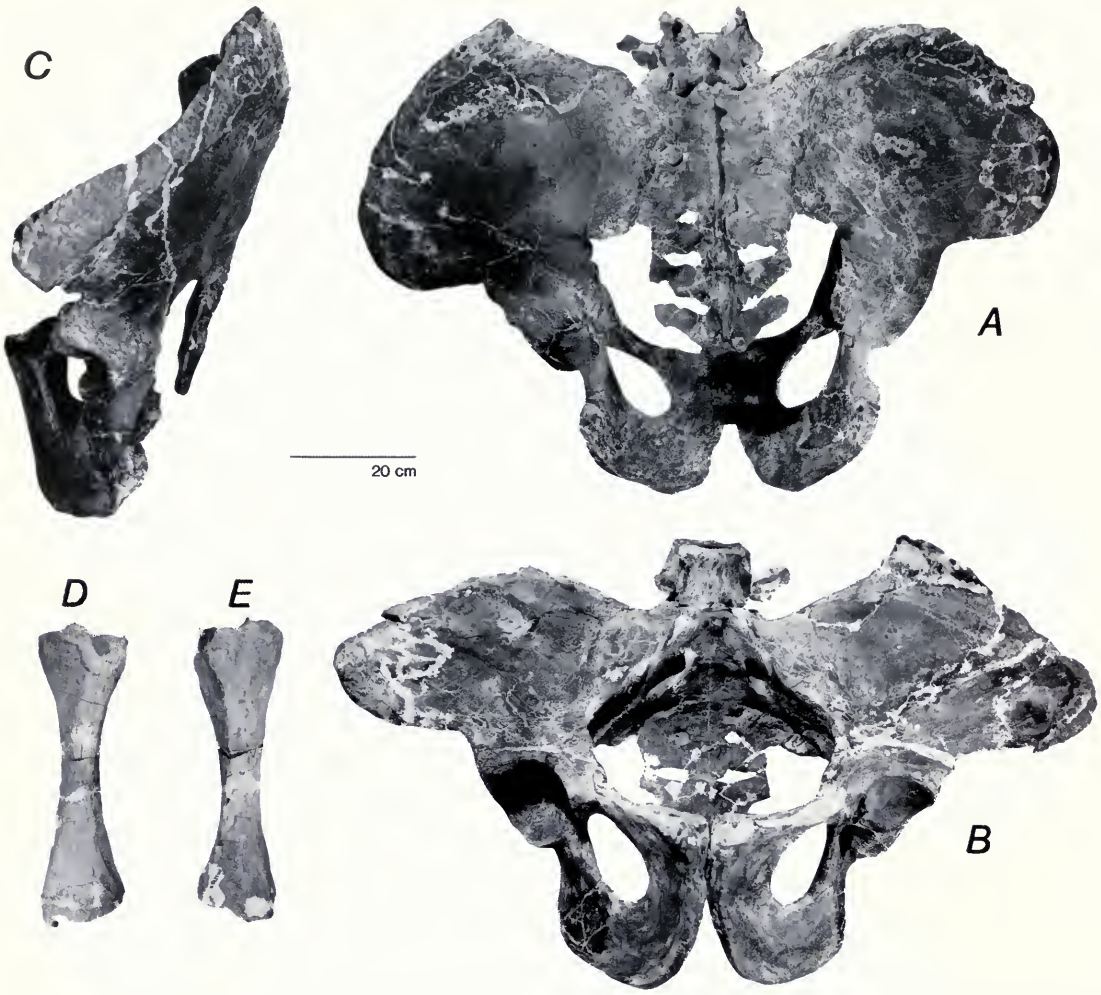

FIG. 50. *Uintatherium anceps,* articulated pelvis with the last lumbar, vertebra, sacrum, and first three caudal vertebrae in place; PM 3894. It is shown in dorsal (**A**), ventral (**B**), and left lateral (**C**) views. In **D** and **E,** anterior and posterior views of a tibia, PM 38782, are shown (FMNH neg. nos. GEO 82120–2 and 86086–7).

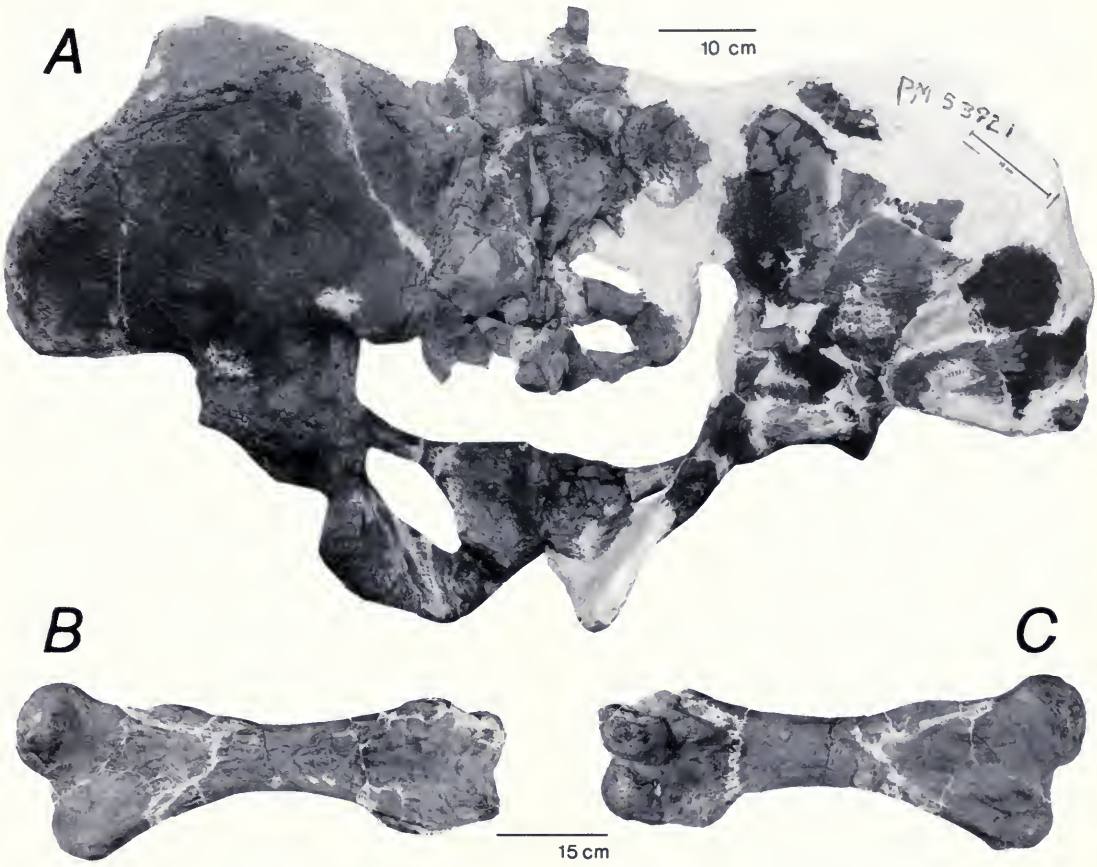

FIG. 51. *Uintatherium anceps*, another articulated pelvis, PM 53921, shown in dorsal view in **A**. In **B** and **C**, anterior and posterior views of the right femur are shown. They both are parts of an associated, disarticulated, partial adult skeleton collected with the help of Mary Jane and Murray Daniels and Kubet Luchterhand in 1985 (FMNH neg. nos. GEO 85686 and 86081–2).

ilia and the acetabular portions of both pubes and ischia, in association with six to eight vertebrae and many scraps.

Partially articulated hind limb

PM 3212 partial left foot (Fig. 53A), from TWkA2, *E. cornutus.*

PM 39393 distal end of a left hind limb (Fig. 53B), top of TWkA1, cf. *E. cornutus.*

PM 55423 partial articulated right hind limb (Fig. 52A–B).

Femur (Table 10)

PM 1453, distal end left femur of *E. cornutus,* from ~Beds 650–670, TWkA2, at locality FM-6-56-WDT, in S ½, SE ¼, Sec. 36, T17N, R97W, Fort LaClede NE Quadrangle.

PM 3212, juvenile left femur, associated with partial pelvis, tibia, fibula, and partial left foot, long bones with unfused epiphyses, *E. cornutus,* TWkA2.

PM 3224, crushed left femur lacking distal end, *E. cornutus,* from TWkA2 about Beds 630–640, locality FM-8-57-WDT, in N ½, SE ¼, and SE ¼, SE ¼, Sec. 13, T15N, R98W, Kinney Spring Quadrangle.

PM 35934, right femur of *E. cornutus,* from Bed ~630–635, TWkA2, at locality FM-6-74-WDT, in SE ¼, Sec. 13, T14N, R99W.

PM 53921, complete right femur (Fig. 51B–C), part of the disarticulated partial skeleton.

PM 53931, complete except for distal epiphysis, juvenile.

PM 54407, right femur, from ~Bed 590 at locality FM-1-85-KL/WT in NE ¼, NE ¼, Sec. 26, T15N, R95W, Powder Mountain NE Quadrangle.

PM 54421, left femur, from ~Bed 590 at locality FM-1-85-KL/WT in NE ¼, NE ¼, Sec. 26, T15N, R95W, Powder Mountain NE Quadrangle.

PM 55175, distal end, from ~Bed 590 at locality FM-16-91-WDT, near corner between sections 29, 30, 31, and 32, T14N, R95W, Prehistoric Rim Quadrangle.

PM 55423, includes the articulated right limb, extending from the distal end of femur, through most of the foot (Fig. 52); part of Flynn's articulated partial skeleton.

PM 55826, a complete right femur and condyles of the left femur.

Patella (Table 11)

PM 2079, complete right and partial left patellae.

PM 3236, left patella from ~Beds 569–570, at locality FM-10-57-WDT, in N ¼, Sec. 24, and NE ¼, Sec. 23, T17N, R97W, Fort LaClede NE Quadrangle.

PM 39393, with partial left hind limb (Fig. 53B).

PM 54401, left patella.

PM 54402, right patella.

PM 54404, patella, ? right or left.

PM 55407, right patella. These last four specimens from TWkA1, ~Beds 591–600, from locality FM-1-85-KLWT, NE ¼, NW ¼, Sec. 26, T15N, R95W, Powder Mountain NE Quadrangle.

PM 55423, right patella (Fig. 52), part of the articulated partial skeleton.

PM 55577, patella, ? right or left, from near center NW ¼, Sec. 8, T15N, R94W, Salazar Butte Quadrangle.

Tibia (Table 11)

PM 3212, tibia in association with left femur, partial pelvis and foot, TWkA2, *E. cornutus* (Fig. 53A).

PM 38782, a pair of tibiae and an associated humerus.

PM 39393, tibia of articulated partial left hind limb (Fig. 53B).

PM 53921, both tibiae of this disarticulated partial skeleton are preserved.

PM 53936, proximal end of a tibia.

PM 54403, nearly complete left tibia from about Beds 591–600, at locality FM-1-85-KL/WT, in NE ¼, NW ¼, Sec. 26, T15N, R95W, Powder Mountain NE Quadrangle.

PM 54825, complete right tibia from locality FM-2-58-WDT, center, S ½, Sec. 19, T16N, R97W, Manuel Gap Quadrangle.

PM 54865, proximal end of a badly eroded tibia, Beds 620–622, TWkA1, cf. *E. cornutus,* from E ½, Sec. 31, and SW ¼, Sec 32, T16N, R95W, Barrel Springs SW Quadrangle.

PM 54866, proximal end of a tibia and the associated fibula, from TWkA2, ~Beds 620–624, *E. cornutus,* from locality FM-4-81-WDT, center W ½, Sec. 18, T13N, R96W, Upper Powder Spring Quadrangle.

PM 55423, right tibia (Fig. 52) of articulated skeleton.

Fibula (Table 11)

PM 53921, both left and right fibulae present; "Lombardi" partial skeleton.

PM 54866, complete but distorted fibula associated with proximal end of tibia, one thoracic and five caudal vertebrae, TWkA2, cf. *E. cornutus.*

PM 55423, a right fibula (Fig. 52), the "Flynn" partial skeleton.

Tarsus and Pes (Table 12)

PM 3212, partial left pes including astragalus, navicular, metatarsals II, III, and IV (Fig. 53A), from TWkA2, *E. cornutus*.

PM 39393, articulated partial left hind limb and foot (Fig. 53B). Pes includes astragalus, calcaneum, navicular, cuboid, metatarsals II, III, and IV, some phalangeals and sesamoids.

PM 53921, incomplete right astragalus and cuboid.

PM 55423, right (Fig. 52); the "Flynn" partial skeleton includes a nearly complete, articulated lower hind limb, pes with tarsals, most metatarsals, some phalangeals, and sesamoids.

Eobasileus cornutus (Cope, 1872)

***Lefalaphodon discornutus* Cope, 1872a**
***Eobasileus cornutus* Cope, 1872b**
***Loxolophodon cornutus* Cope, 1872c**
***Tetheopsis speirianus* (Osborn, 1881)**
***Tetheopsis ingens* (Marsh, 1885)**
***Tinoceras laturn* (in part) Marsh, 1886, p. 214 (often cited as 1884 or 1885)**
***Uintacolotherium blayneyi* Cook, 1926**
***Eobasileus uintensis* Osborn, 1929, p. 3 (*nomen nudum*)**

Holotype—AMNH 5040 (Fig. 54A–B)

Distribution—Upper Eocene of three adjacent intermontane basins: the Washakie Fm., Adobetown Memb., TWkA2 of the Washakie Basin, southwestern Wyoming; the Uinta Fm., Uinta Basin of northeastern Utah; and the Sand Wash Basin of Moffat County, northwestern Colorado.

Diagnosis—The largest of the North American, terminal uintatheres, it is distinguished from *Uintatherium anceps,* its immediate predecessor, by its larger size and very dolichocephalic skull proportions. Skull length of adult specimens is 85–95 cm (fide Wheeler, 1961) and upper cheek-tooth row (P2–M3) 168–188 mm long. Relative horn position ratios, where distance from nasal tip to maxillary horn is called A, that from maxillary horn to parietal horn is called B, and that from parietal horn to rear of occipital crest is called C, are shown in Figure 3. B/A is about 1, B/C about 2–3; by contrast, in *U. anceps,* B/A is between about 1½ and 3, and B/C is between about 1 and 2⅓.

Skull and Upper Dentition—The holotype, AMNH 5040 (Fig. 54A–B) has been described by Cope, briefly first (1873a) then in detail (1884, pp. 569–85, pls. 37–42). In 1961, Wheeler expanded upon and summarized Cope's accounts, so it is only necessary for me to correct an obvious lapsus on Wheeler's part. He stated (p. 53) that "This dolochocephalic skull is the largest known of any uintathere (95 cm)." Yet on his chart 3 he shows it as being about 92 cm long, and notes that two specimens are decidedly longer (PUM 10079 and Col. Mus. Nat. Hist. 475 [now DMNH 495]). He probably had not measured the latter specimens when he wrote that line, and forgot to alter it later on.

The Field Museum's Washakie collection contains only a few specimens of this species. They are from the Upper Washakie Fm., TWkA2. PM 1501, a left M2 (Fig. 56C), was collected by R. Zangerl in 1941. The exact locality is unknown but is most probably the Wild Horse Spring locality of the Mammoth Buttes area or Haystack Mt. PM 1737 is a pair of poorly preserved lower jaws that are broken away at the rear of the symphysis in front and behind the cheek-tooth rows in the rear (Fig. 62). Fortunately, the teeth are well-preserved; they include left p2–m3 and right p3–m3. It is described on page 104, where its features are discussed and its locality reported.

We do have two very important specimens from the Uinta Basin that J. B. Abbott (one of E. S. Riggs's field crew) collected in 1910, which Wheeler (1961) referred to. The first, P 12170, is a beautifully preserved skull that Wheeler illustrated and that I figure again at a larger scale (Fig. 55A–C). Both tusks, left P3–M3, and right P2–M3 are preserved, the m1s being well worn so as to nearly obliterate the lophs, but the P3–4s and the M2s, although worn, still retain much of the body of their lophs. The M3s and the P2 are only slightly worn. The maxillary and parietal horns are high and attenuated, and the nasal horns are as high as they are long (although somewhat hidden in the support base; the photos are oriented with the anterior end up). Both tusks show considerable wear, and the right one has apparently drifted partway out of its socket. Dental measurements are given in Table 8. P 12170 came from the White River Divide, 2 mi (3.2 km) E of Bonanza Mine, Near Vernal, Utah, from Horizon B, Wagonhound Member, Uinta Fm., Late Eocene. This well-preserved skull is one of the three most complete of its species, the others being the type in the American Museum and the Denver Museum specimen. It is currently on exhibit in the Teeth, Tusks, and Tarpits Hall, the last of the Mu-

FIG. 52. *Uintatherium anceps,* articulated partial right hind limb of the (Flynn) partial skeleton, PM 55423, shown in dorsal (anterior) (**A**) and ventral (posterior) (**B**) views (FMNH neg. nos. GEO 85930.4 and .6).

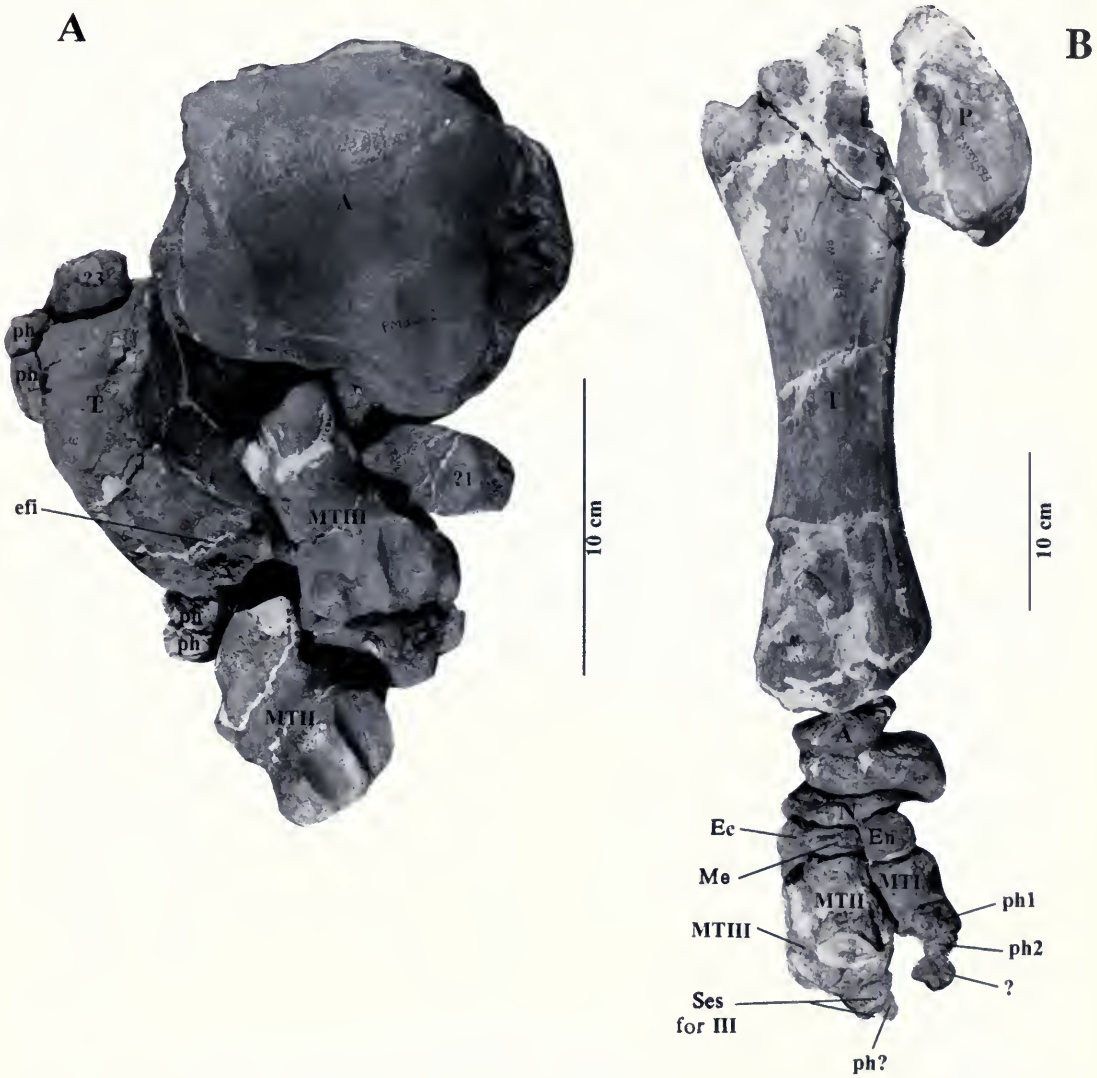

FIG. 53. **A**, *Eobasileus cornutus*, PM 3212, a partially articulated hind foot that includes the distal tibial epiphysis with probable facet for reception of the distal epiphyseal end of fibula (efi); astragalus (A); part of the navicular (N); metatarsals II and III (Mt II and III); 4 phalangeals (ph) and three bones shown with a numbered question mark: tentatively identified: ?1 = possibly another part of the navicular (N), or ectocuneiform (Ec.); ?2 = probably part of the cuboid (Cb); and ?3 = fragment of entocuneiform (En).

FIG. 53. **B**, *Uintatherium anceps*, partial right hind limb in articulation, included are patella (P), tibia (T), and some of the foot, PM 39393. Of the foot bones, the astragalus (A) is present, its tibial articulation surface in contact with the tibia, but the calcaneus and cuboid are missing. Other tarsal elements preserved are the navicular (N), and the three cuneiformes, ectocuneiform (Ec), mesocuneiform (Me) and entocuneiform (En), metatarsals (MT I, MT II, and MT III), with phalanges of digit I and some of the sesamoids (FMNH neg. nos. GEO 85685 and 85697).

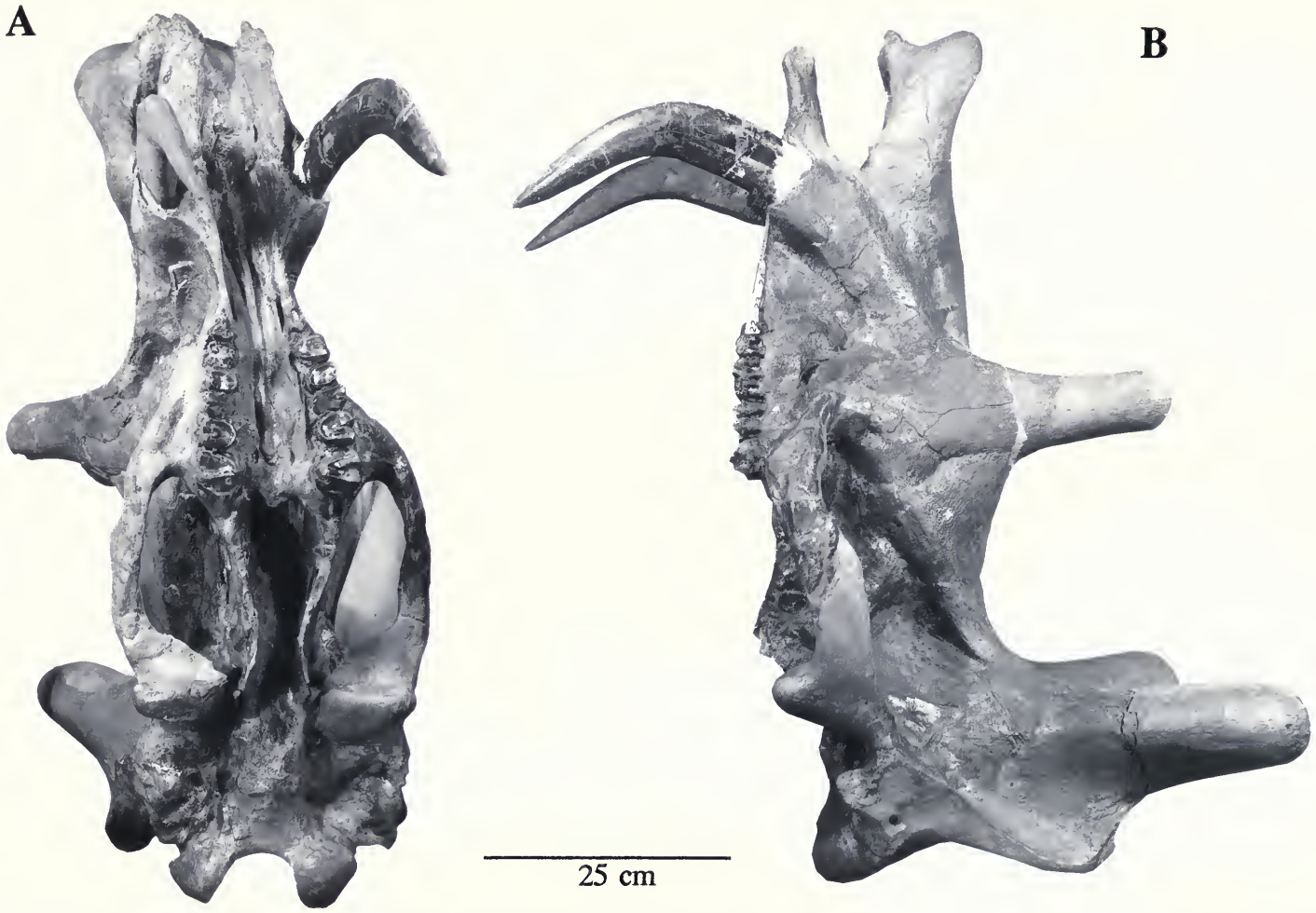

FIG. 54. *Eobasileus cornutus* Cope, AMNH 5040, holotype. Skull shown in ventral (**A**) and left lateral (**B**) views. The canine teeth are partly out of their sockets, but the cheek teeth are less worn than those of the other three skulls of the species (FMNH neg. nos. GEO 82516–7).

seum's three halls devoted primarily to vertebrate evolution.

P 12164, the other Riggs (Abbott-collected) specimen, is the partial skull with a molar dentition that Wheeler said is exceeded in size only by the Denver Museum specimen, DMNH EPV 495, the largest individual specimen known. Further, Wheeler commented on the "surprising feature of the skull," the maxillary and parietal horns, which are merely tiny bumps. He concluded that it was that of a female, and he illustrated it (and P 12170, in his pl. 12, figs. 2 and 3). I agree with that interpretation and would add my opinion that this may be the evidence for an extreme degree of sexual dimorphism in this species. The skull is small but, with its worn molars, cannot be that of a very young adult individual, certainly not that of a juvenile, yet the horns are just small bony bumps, little advanced over those of the Field Museum's two juvenile specimens of *U. anceps* (PM 3896 and PM 8019), both of which evidenced precocious dental states relative to horn development. Preserved are left P3–M3 and right M2–3, much of the laterally crushed basicranium, and most of the left side of the skull. On the left side of the basicranium, the anteroventral tip of the promontorium is distinct and well preserved, but the rest of the petrosal, which appears to be mostly present, is crushed and badly fractured. It is missing many bits, so that I am unable to identify any other structures with certainty. On the right side the damage is, if anything, worse. Certainly the petrosal is present, and possibly some of the tympanic, but the damage is too great to permit anything more than speculation about their features. I provide these additional illustrations to better show the ventral aspect of the skull and especially its dentition (Fig. 56A–B). P 12164 came from Horizon B, Wagonhound Member in Coyote Basin, Uintah Co., Utah, near Vernal.

The University of Wyoming skull appears to represent a transitional stage in the evolution of the genus *Eobasileus* from its ancestor *Uintatherium*. Inasmuch as it shares characteristics of both genera, it has been discussed briefly in the section on *Uintatherium*, where its characteristics and provenience were set forth (pp. 33 and 37). Because an assignment to *Eobasileus* appears to be more fitting, its description and further discussion of it are considered here.

The skull, UW 13644, is not badly distorted, but many cracks and small fractures are visible on its dorsum and both sides (Fig. 57A–B, D). It is very elongate, especially anterior to the maxillary horns, and it is deep for its whole length (Fig. 57B, D, E). It is narrow (Fig. 57A, C, E), and, because neither the arches, the palate, nor the occiput include the condyles, the specimen shows an unusual lateral crushing. I believe it to be essentially in its natural, relatively undistorted condition. There has been a skewing of the basioccipital region such that the right condyle is pushed forward relative to the left one. The cheek teeth occupy about one-quarter the length of the skull. The palatal area anterior to the cheek teeth, the region behind the palate extending to the glenoid, and the basioccipital region are also each roughly one-quarter of the total skull length.

Dental measures are given in Tables 13 and 14 (see also Tables 5 and 6), and the bivariate graph (Fig. 61) provides a tooth-to-tooth visual comparison of size and proportion of these teeth. Table 15 shows how they compare to samples of *U. anceps* and *E. cornutus* but are closer to the latter. The tusks are broken away, but the worn cheek teeth have the usual form seen in both species.

The American Museum specimen (AMNH 13149) was mentioned by Wheeler as *Tetheopsis* or *Eobasileus* (1961, p. 52):

> A specimen collected from the Washakie B on the northwest face of Haystack Mountain by the American Museum Expedition of 1906 (AMNH 13149) is still mostly encased in plaster jackets. It can be seen that the femur, canine and innominate bone are notably bigger than those of any *Uintatherium*. The catalogue records that there is a lower jaw.

When I examined the prepared portion in 1960, I did not note anything unusual. Subsequently I borrowed and prepared the one unprepared block I found (no. 16), which contained the following materials: the tip of the right coronoid process (Fig. 58C) and three teeth, a complete, heavily worn upper left canine (Fig. 58A) of large proportion, the left M3 (Fig. 58B), and a heavily worn right lower incisiform tooth I believe to be the canine (Fig. 58D). It has two blunt coalesced occlusal wear facets, and it and the upper canine are poorly preserved. The latter is boomerang-shaped, except that the crown portion is only about half as long anteroposteriorly as its closed root. The crown is much like that of P 12170, but it has lost most of its enamel from wear, except on its anterolateral surface; the anterior and posterior flanges, although heavily worn, are nevertheless sharp and lack any flairing of the blade, and the tip is still rather pointed.

The M3 (Fig. 58B) is well preserved and nearly

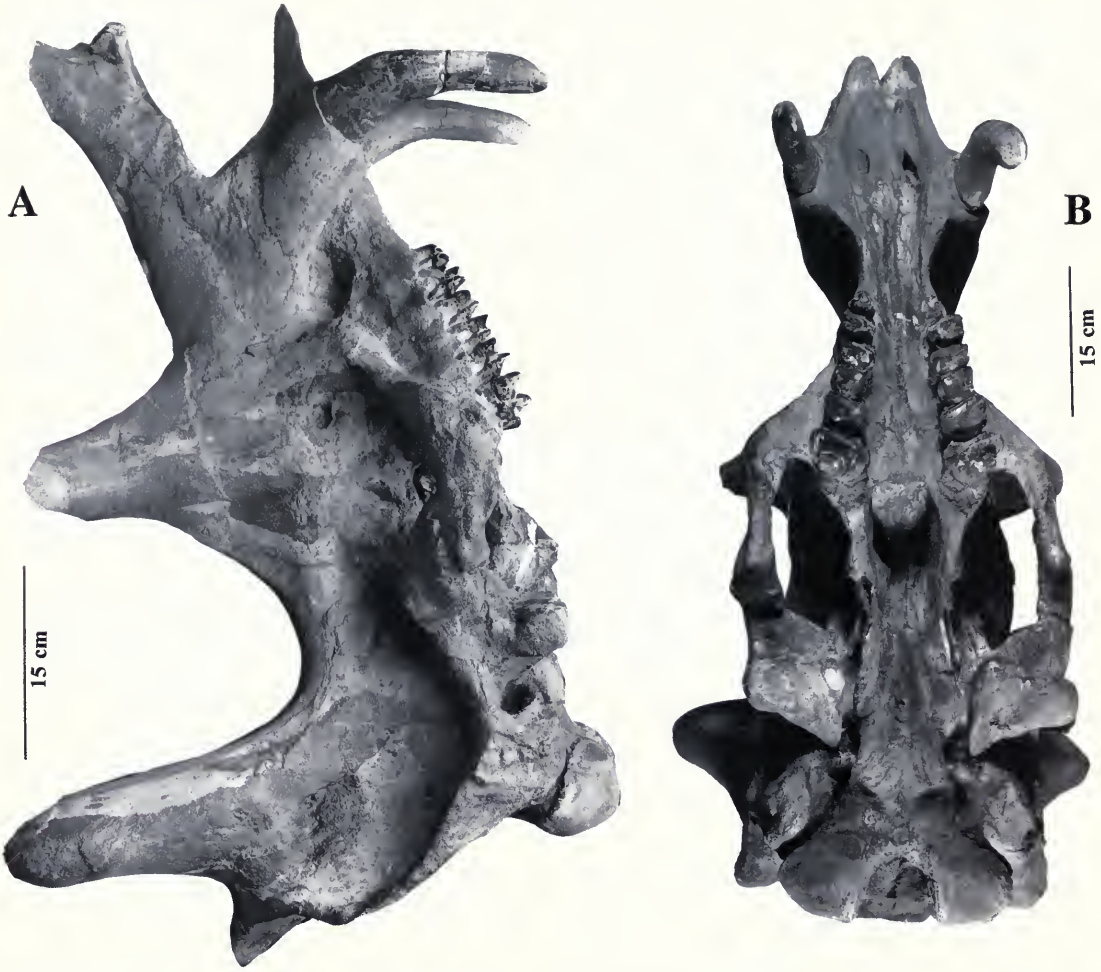

FIG. 55. *Eobasileus cornutus* from the Uinta Basin, P 12710. This is the only complete skull of this taxon in the FMNH collection. It was collected in 1910 by J. B. Abbott, chief assistant to E. S. Riggs, and is the most complete and well-preserved specimen of the species. It is shown in right lateral (**A**) and ventral (**B**) views. In **C,** the palate and cheek teeth are shown enlarged. The specimen has recently been installed in the new hall of fossil vertebrates (FMNH neg. nos. GEO 85710–11).

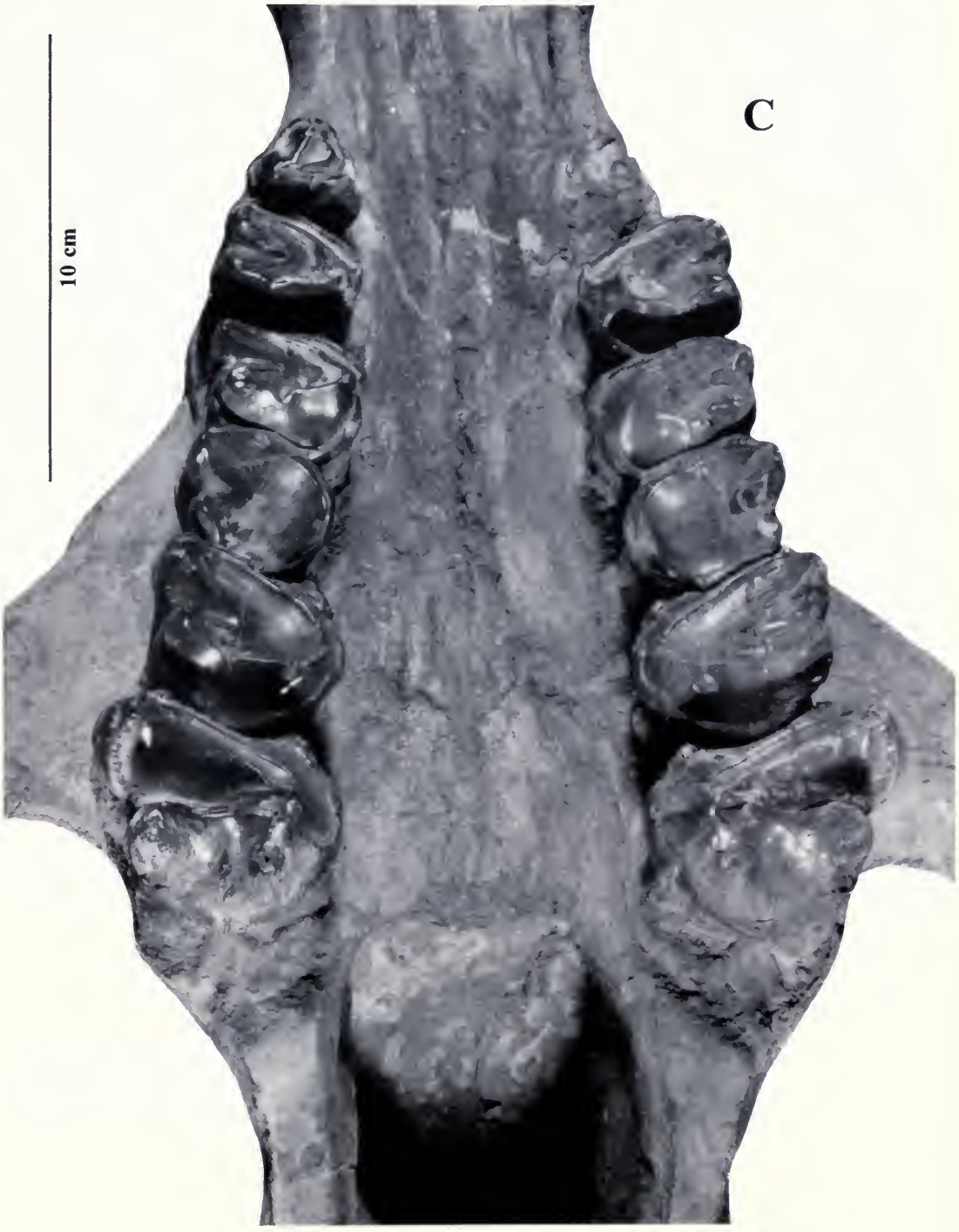

FIG. 55. *Continued.*

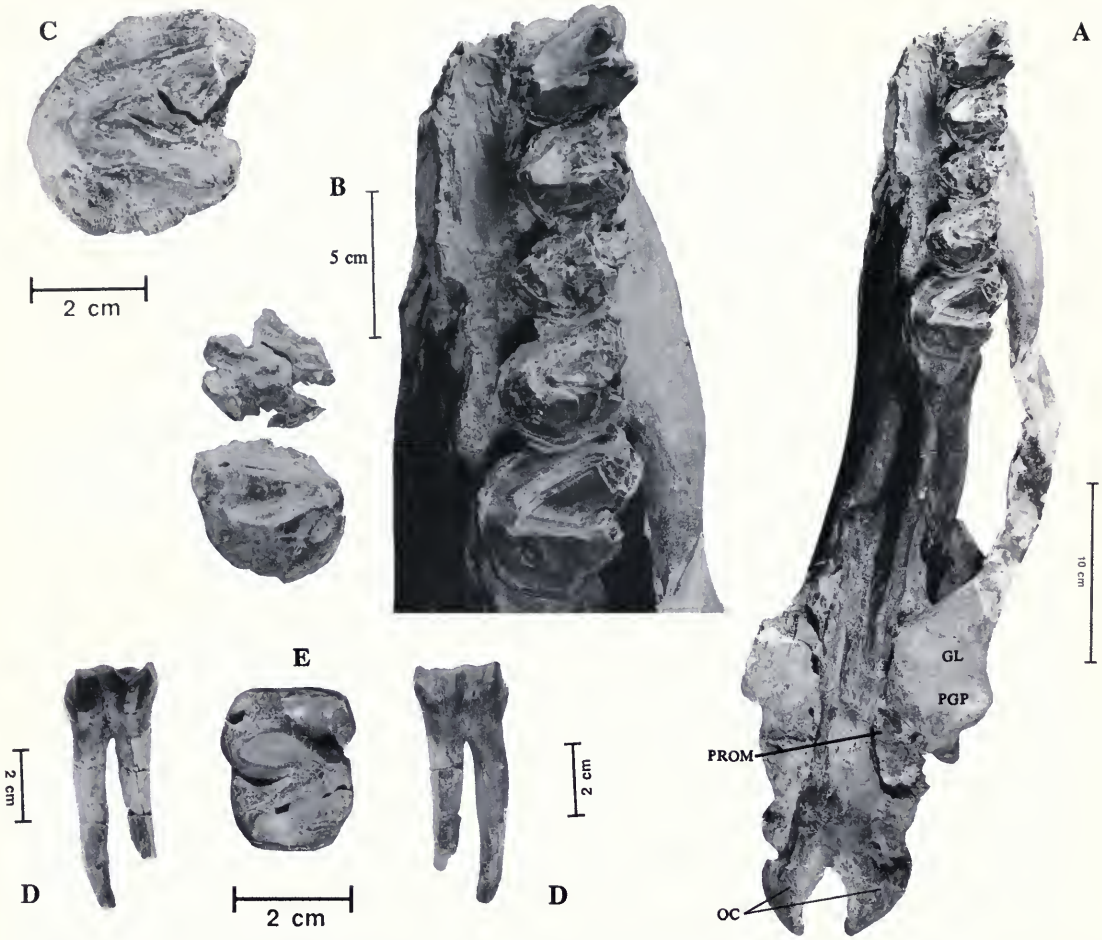

FIG. 56. *E. cornutus,* also from the Uinta Basin, and collected by Riggs, P 12164, the partial skull that Wheeler mentioned as having one of the largest dentitions known for the species, shown in ventral view (**A**) and with the cheek teeth enlarged (**B**). From the Washakie Fm., two isolated teeth are shown: **C,** PM 1501, a left M2 is seen in occlusal view: and in **D–E,** a right m1, or p3 or p4, PM 1674, is shown in labial, crown, and lingual views. In **E,** anterior is down (FMNH neg. nos. GEO 85709, 85699, 85700, and 85797–8).

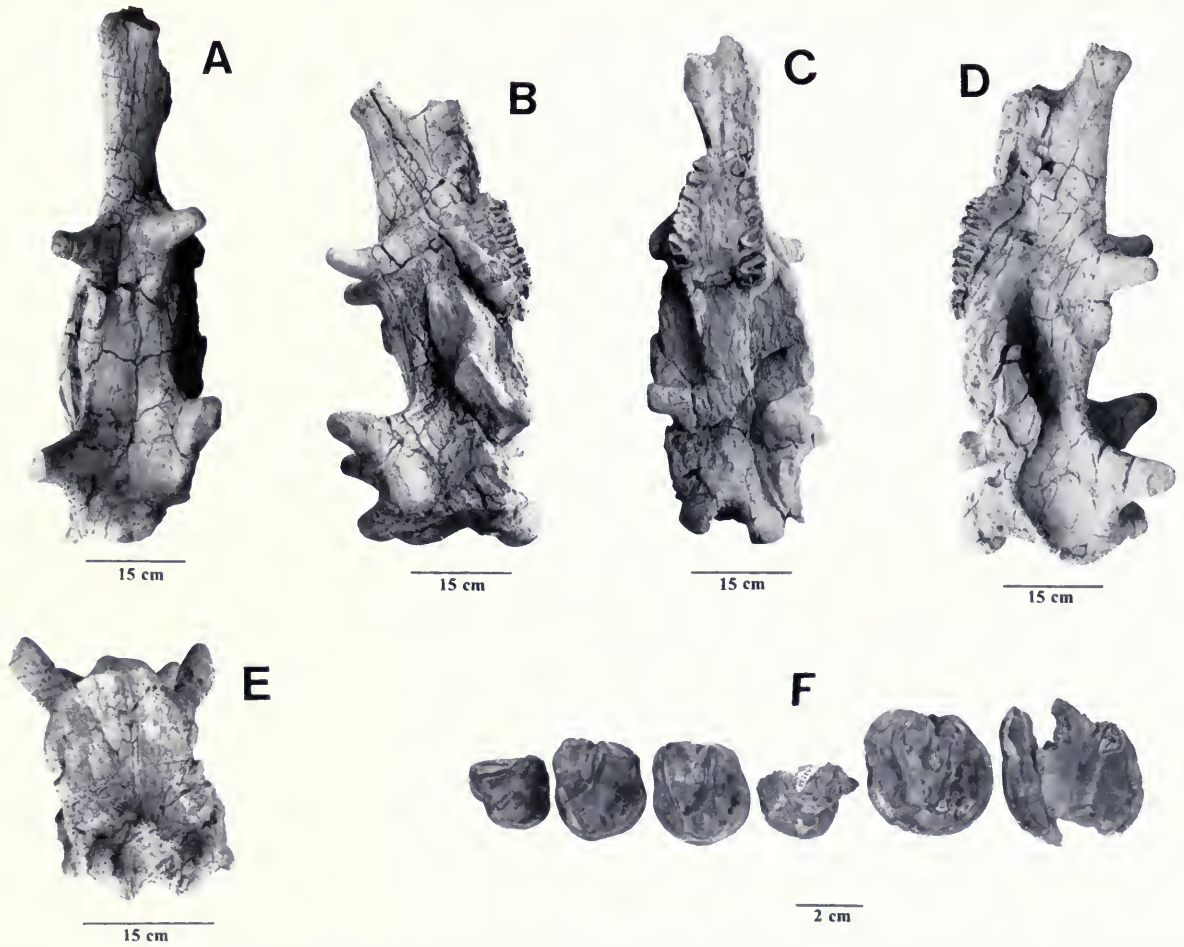

FIG. 57. University of Wyoming specimen UWM 13644, the skull of an aged individual with worn dentition, is shown in dorsal (**A**), right lateral (**B**), ventral (**C**), left lateral (**D**), and posterior (**E**) views. This specimen is unique in that it has the skull length of *Uintatherium,* but its dentition measures with that of *Eobasileus* (where I classify it; see Tables 5, 6, 13, and 15). It came from low within unit TWkA2 and is considered to represent a transitory stage in the evolution of *Eobasileus* from *Uintatherium.* The University of Wyoming locality number is V79013, which is somewhere within my locality FM-3-57-WDT. Photos A–E are by Linda E. Lillegraven, courtesy of J. A. Lillegraven. In **F,** crown views of the isolated teeth, Burke Museum, University of Washington specimen UWBM 59204, are shown placed in approximately correct positions: P2–4, ?eroded M1 (see text), M2–3.

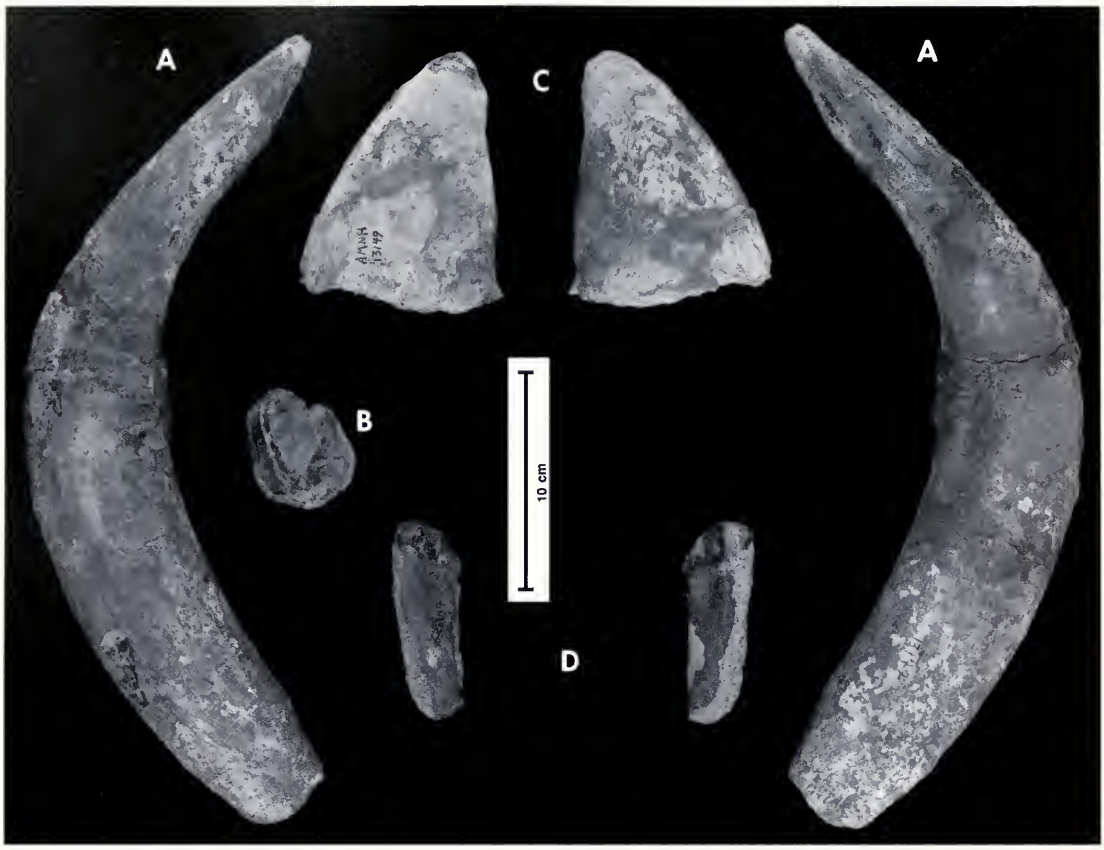

FIG. 58. AMNH 13149, a specimen that Wheeler (1961) found to be mostly still in jackets, but because of the large size of the femur, canine, and innominate, he assigned to *Tetheopsis* or *Eobasileus.* I prepared the one block I was able to find, which contained an upper canine tusk (**A**), left M3 (**B**), tip of the right coronoid process (**C**), and a heavily worn right lower incisiform tooth (**D**). Both size and stratigraphy cause me to assign it to *Eobasileus,* because I do not consider *Tetheopsis* to be valid (FMNH neg. nos. GEO 86043–4).

complete, with both protoloph and metaloph showing some wear. The tip of the paracone is broken off. There is a small but distinct hypocone pressed against the posterior edge of the protocone, and a cingulum surrounds the tooth anteriorly, lingually, and posteriorly, but breakage labial to the paracone leaves its presence in that region unresolved. Since I believe *Tetheopsis* to be a composite of the other two genera, and since these teeth from their size and M3 morphology and dimensions (Table 5) show it to be *Eobasileus*, I so assign it.

The Denver Museum of Natural History exhibits the skull, DMNH EPV 495 (Fig. 59), the holotype of *Uintacolotherium blayneyi* Cook, 1926 (= *E. cornutus*). Cook's paratype specimens, the associated tusk, EPV 529, and jaws, EPV 496, may belong to the same specimen. He illustrated these in left lateral and occlusal views and again in right-side view restored and in articulation. They were collected by H. C. Markman in 1924 from an area between Vermillion Creek and the Little Snake River. Sand Wash Basin, Moffat County, Colorado, DMNH locality no. 233, Spicer Spring—Seep Draw, in NW ¼, SE ¼, Sec. 4, T9N, R99W, G Spring, Colorado Quadrangle. The age is Uintan, a TWkA2 equivalent, Washakie Fm. Cook (1926) had the then recently published map by J. D. Sears (1924) available; it shows Spicer Spring itself to be in NE ¼, NE ¼ of Sec. 13, T9N, R100W. Unfortunately, Spicer Spring is not indicated on the G Spring Quadrangle, and the stream patterns of this area differ on the two maps. Features such as G Spring itself and the Bears Ears correspond well, so I assume the drainage pattern on the Sears map to be sketchy and less accurate than that on the more recent G Spring sheet.

R. Stuckey recently had the older exaggerated, restored portions of the skull and jaws removed and corrected, and the specimen is now on exhibit again. Cook's description will suffice, but I show it again as it is now restored (Fig. 59). It, Cope's holotype (AMNH 5040), the Wyoming skull (UW 13644), and the Abbott-Riggs specimens (FMNH P 12170 and P 12164) are the only complete, or nearly complete, skulls of this species on record. Skull and dental measurements are given in Table 8. (The full listing of the DMNH holdings of the species is available from the author.) If the jaws do belong to the type skull, then the specimen may be female or young adult male, to judge by the weakly developed inframandibular process. However, the skull itself with its enlarged horns looks to be that of a male.

Wheeler (1961, p. 49) commented on the specimen YPM 11043, the holotype of *Tinoceras annectens* (Marsh), which he assigned to *Tetheopsis speirianus* (Osborn). I illustrate it (Fig. 60A–B) to show the condition of the restored top of the skull. From the measurements given by Wheeler for the skull length (91 cm) and cheek-tooth row lengths (upper, 184 mm; lower 192 mm; his charts 5 and 6, pp. 80–81) it is at the large end of the range of these measures for *E. cornutus*, where I therefore assign it. As Wheeler has noted, the collector J. Heisey gave only Haystack Mountain as its locality, and the measurements suggest that it probably came from somewhere high in TWkA2.

The Burke Museum, University of Washington, has one uintathere specimen (UWBM 59204) from the Washakie Fm. (Fig. 57F). It came from above, but near to, the base of Haystack Mountain and therefore is from low in the TWkA2 division of the Adobe Town Member. It consists of five teeth, left P2–4, M2–3 and a confusing piece listed as ? a petrosal fragment. Other than its apparent density, I cannot recognize any petrosal features. The fragment appears to preserve two distinct tissues, a lighter tannish one similar to the roots of the other teeth and a darker one that has a bulbous shape. I think it is a damaged M1, or aberrant tooth (?M1). However, the dark portion is not enamel, so the question remains. The P2 shows only a trace of wear; the others have minor dentine exposure along at least one loph except for M3, which was unworn and apparently unerupted. Both tooth measurements and locality indicate assignment to *Eobasileus cornutus*. The teeth can be viewed on the Internet courtesy of J. Rensberger at the following web address: http://weber.uwashington.edu/~vertp/BurkeVertPage.html.

There are two isolated upper teeth in the Berkeley Washakie collection, both collected by L. Kent for M. C. McKenna in 1954, from locality V78102 (a subdivision of V5429) from the south side of Haystack, from horizon 17 of Granger.

UCMP 81359 is a worn right P4 (or M1) that measures (cm), L = 2.7, AW = 2.82, PW = 2.86.

UCMP 81360 is most of the central region of a left M3. Both protoloph and metaloph are present but incomplete, worn so as to expose dentine for their full length as preserved, because none of the major cusps is complete. Only the labial side of the hypocone is present. Most of the posterior face of both the metacone and posterior cingulum is present, but a small bit of the cingular edge is missing lingual to the angle at the posteriormost corner of the tooth. The cusplet in the center of

the finely crenulate cingular basin is a well-developed small cone. Shape and wear stage are close to those features in our specimen P 12164.

Other Denver Museum specimens (skull, upper dentition) presumably of this taxon are:

DMNH EPV 493, which includes various skeletal parts of an old female. An extremely worn tusk is all that represents the upper dentition. It is polished on all sides from wear, and measures 15.46 cm from tip to base; its mesial-distal length at the alveolar margin is 3.6 cm.

DMNH EPV 498, which consists of two horns.

DMNH EPV 11568, a left P2 in a maxillary fragment.

Note: EPV 493 and 498 also appear under Uintatheriidae, as do EPV 520, a partial incisor tooth, and EPV 530 and 14776 (both listed as tooth fragments that I did not find).

In the Field Museum, an isolated upper tooth tentatively referred to *E. cornutus* is PM 1682, a P3, P4, or M1. It was collected by O. L. Gilpin and me from the NW flank of Haystack ~5 mi NE of the junction of the track along the Rim Below the Adobetown Rim with the track crossing Adobetown, locality FM-6-56-WDT. This locality is mainly in SE ¼, Sec. 36, T17N, R97W, and it extends into W ¼, SW ¼, Sec. 31, T17N, R96W, Fort LaClede NE Quadrangle.

Jaws and Lower Dentition—The best FMNH Washakie specimen is PM 1737, a pair of lower jaws (horizontal rami only) with left p2–m3 and right p3–m3 (Fig. 62). It is the only good jaw specimen of this taxon we have. Although the jaw bones themselves are poorly preserved, there is enough of the ventral edge to show that an inframandibular flange was present, but not enough is left to estimate its size. The teeth are in good shape, and only the m1s show much wear. The premolars increase in size from front to rear. The trigonid of p2 is laterally compressed, and it is slightly smaller than, and does not stand quite as high as, that of p3. Its talonid is wide, more like that of p3. In all lower teeth the metalophid dominates the crown, followed by the hypolophid and a weak "protolophid," which is a lesser structure than the posterior cingulid. The molars, too, increase from M1 to M3, but by a greater increment than is seen in the premolars. Metastylids are present on all of the cheek teeth, but they are not greatly enlarged except on M3, where that cuspid is a distinct entity separate from the metaconid. The specimen is from locality FM-15-56-WDT, SW ¼, SW ¼, Sec. 2, T16N, R97W, Fort LaClede NE Quadrangle, the area that I called "NW Flank of Haystack."

PM 1674, is a right lower p3, or p4 or m1 (Fig. 56D–E). Both of its major lophids are well worn but are not obliterated. The talonid shows no occlusal wear, but it has a notable interdental wear facet that has breached the enamel in a small oval area lingual to the midline (and mid- or postlink). It is from the NW flank of Haystack Mountain from locality FM-6-56-WDT, which is in S ½, SE ¼, Sec. 36, T17N, R97W, Fort LaClede NE Quadrangle.

The Berkeley jaw, UCMP 81356 (Fig. 63), is an essentially complete left ramus. It lacks the anterior half of the symphyseal region, the posterior margin of which is situated about halfway between the mental foramen and the alveolus of the missing p2. The inframandibular flange is very small, the mental foramen large and collapsed from crushing. The entire jaw is slightly crushed. The ascending ramus is complete, the angular process nearly so. It belonged to an older individual with heavily worn teeth (p3–m3). The m1 has all crown features worn off, p4 and m2 nearly so, and only remnants of the bases of the lophids remain on p3 and m3. The jaw lacks any trace of incisors or their alveoli, the part that would contain them being broken off. The posteroventral border of the angular process is also missing.

The cheek teeth are within the range of those of *E. cornutus,* with the exception of m3, which is decidedly small, much more like that of *U. anceps* (Table 9). This difference, which does not appear to have resulted from wear, could be due to sexual dimorphism, as could the reduced inframandibular process. Both features suggest that it was a female. It was collected by L. Kent and M. C. McKenna in 1954 from locality V83216, which is a subdivided portion of V5429 and is located on the south side of Haystack, in the lower third of horizon 17 of Granger.

The Yale University specimen of *Eobasileus cornutus* is shown in right lateral and dorsal views (Fig. 60C–F). It is YPM 11043, the holotype of Marsh's *Tinoceras annectens,* which Wheeler (1961) placed in synonymy with *Tetheopsis speirianus* and which I consider to belong within *Eobasileus,* based on its large size and probable stratigraphic position (Haystack Mt., TWkA2?). I show both rami: Marsh had shown drawings of the left ramus (1886, p. 36, figs. 36 and 37) and Wheeler (1961, pl. 14, fig. 2) a photograph of the left side of the same ramus. If the Marsh inter-

FIG. 59. Denver Museum's *Uintacolotherium blayneyi* Cook, a synonym of *Eobasileus cornutus*. Skull of holotype, DMNH 495, and the almost certainly associated mandible, DMNH 496, are shown in right anterolateral oblique view. This specimen, the type (AMNH 5040), the University of Wyoming skull (UWM 13644), and the FMNH skull (P 12170) are by far the best cranial representatives of the genus, and this is the only good skull with associated jaws. (The following figure shows a partial skull with its associated pair of jaws.) (Photograph by Rick Wicker, courtesy of R. Stucky and DMNH.)

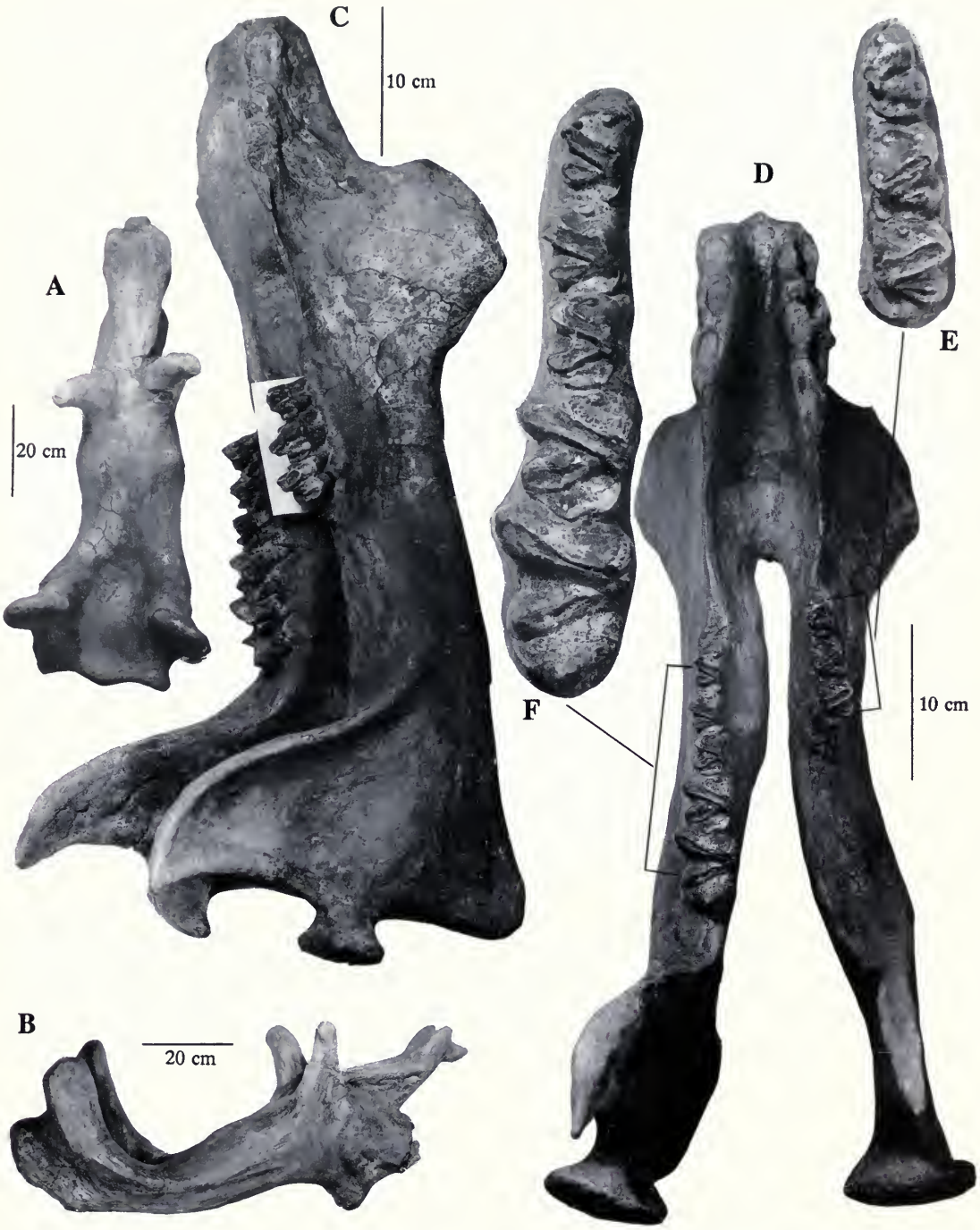

FIG. 60. Partial skull (**A** and **B,** dorsal and right lateral views) and mandible (**C** and **D,** right lateral and occlusal views) of *Tinoceras annectens* Marsh (= *Tetheopsis speirianus* (Osborn) = *E. cornutus*), in the Yale University collection, YPM VP 11043. The skull is considerably restored, but its dorsal surface is largely preserved. In the mandible there are three incisor alveoli on each side of the symphysis, and the inframandibular processes are prominent. The left cheek-tooth series, which preserves p3–m3, and the right series with p2–p4, are shown in occlusal views in **E** and **F** (FMNH neg. nos. GEO 82428–31).

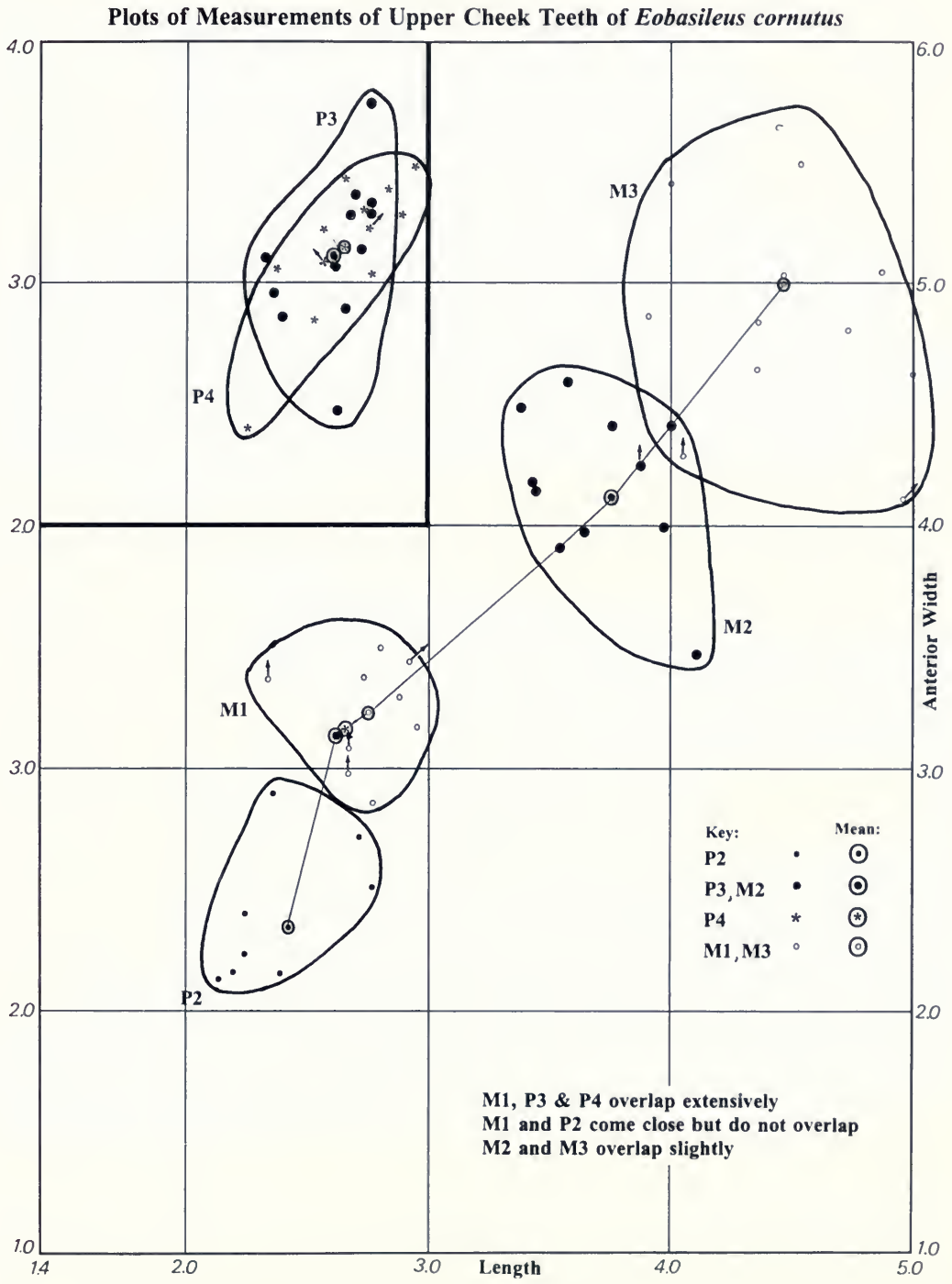

FIG. 61. Graph showing bivariate plots, length × anterior width, for the upper cheek teeth of *Eobasileus cornutus*. Measurements are in cm.

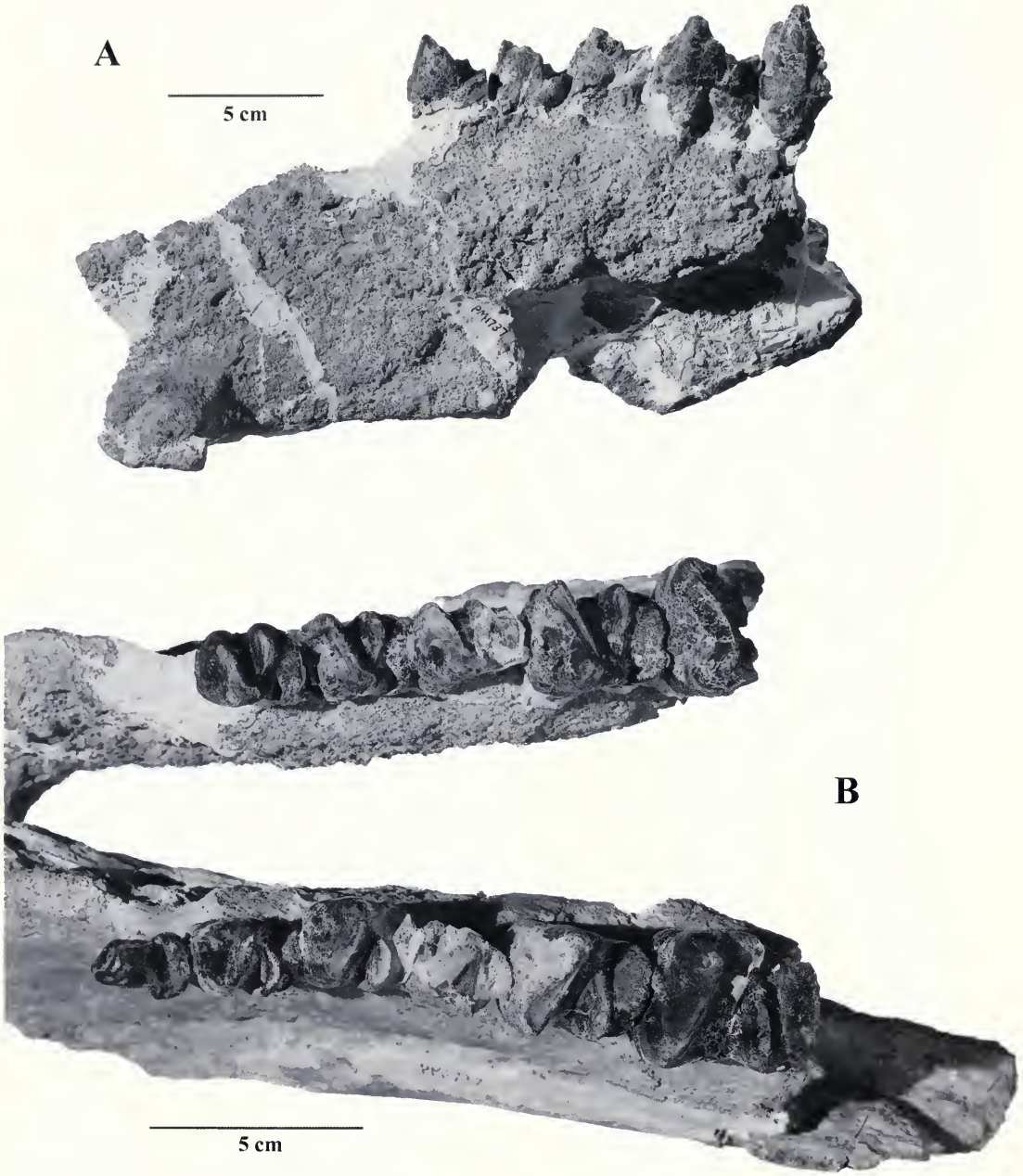

FIG. 62. The best FMNH specimen of the lower jaws and dentition of *E. cornutus* from the Washakie Fm. is PM 1737. The right ramus is shown in its lingual aspect (**A**), and the occlusal view of both rami is shown in **B.** These are followed by labial (**C**) and lingual (**D**) views of the left ramus (FMNH neg. nos. GEO 82000–82002 and 82003).

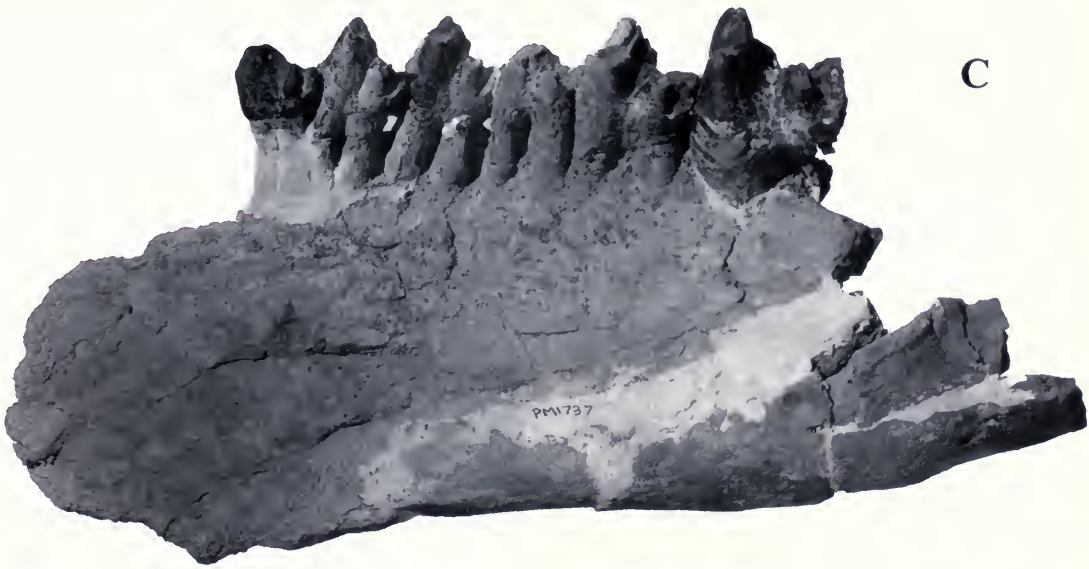

5 cm

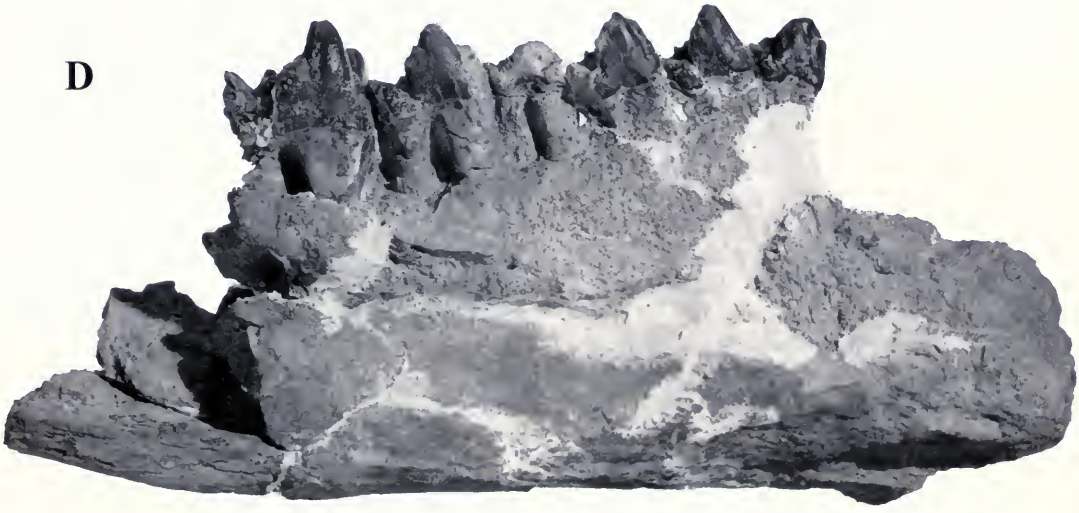

FIG. 62. *Continued.*

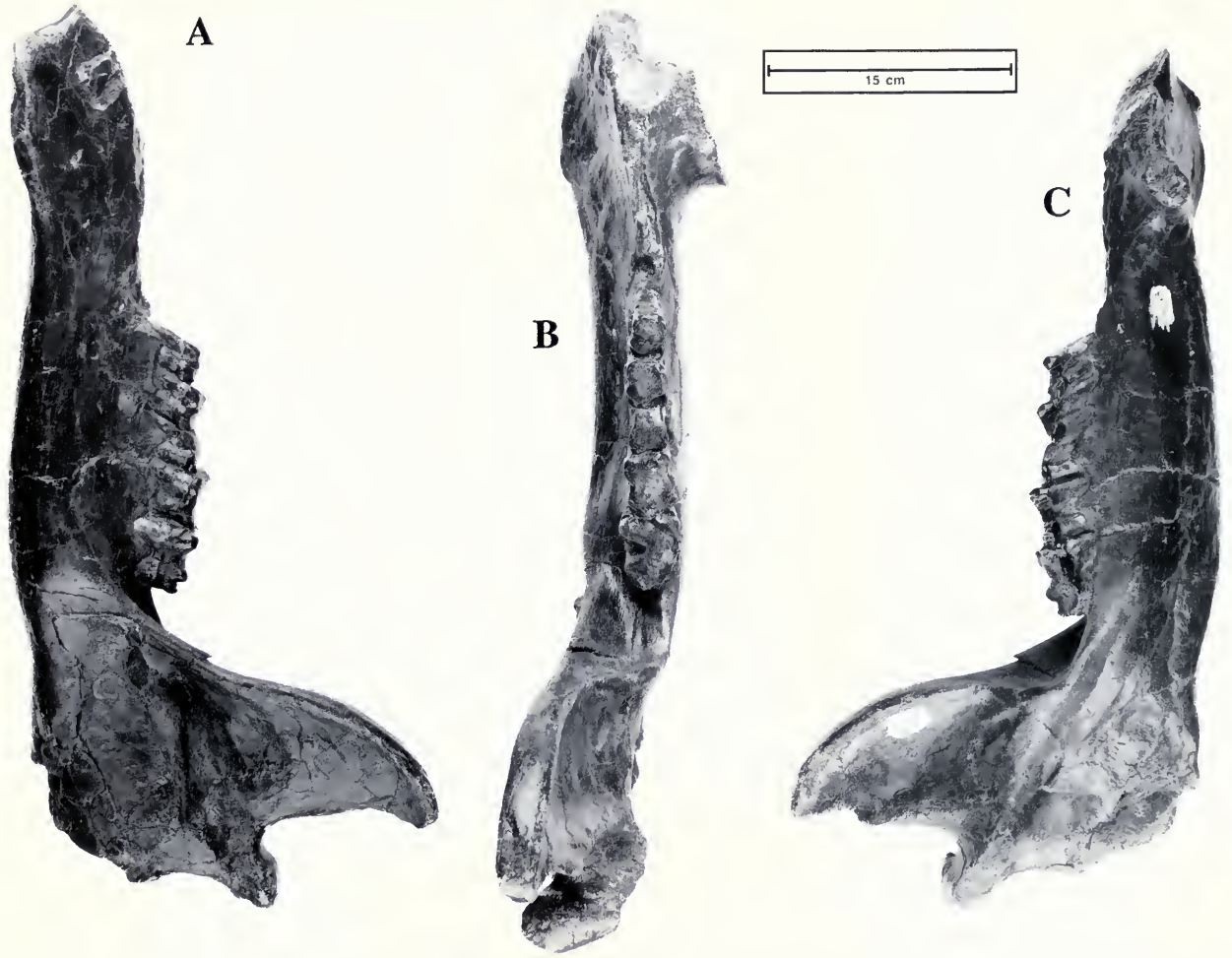

FIG. 63. UCMP 81356, a left mandibular ramus with alveoli of the incisiform teeth and preserving most cheek teeth (p3–m3). This previously unreported specimen was initially recorded as *Uintatherium anceps* but is here considered to be a female of *E. cornutus*. The ramus itself is slender and has only a weakly developed inframandibular process; the coronoid, condylar, and angular processes are also delicately built. The teeth are quite worn. It is shown in left lateral (**A**), occlusal (**B**), and medial (**C**) views. It is from Berkeley locality V83216, which is in Granger's Horizon 17, which puts it low in TWkA2 (FMNH neg. nos. GEO 85793, 85795, and 85796).

FIG. 64. Carnegie Museum mandible, CMNH 29493, here assigned to *E. cornutus* mainly on stratigraphic grounds. It is that of a female, judging by its weakly developed inframandibular process. The teeth are all worn (FMNH neg. no. GEO 82128).

pretation of the incisor-canine alveoli is correct, then this is an instance of a larger than usual lower canine tooth, one comparable to the incisors, to judge from the diameter of the alveolus. Considering the variation seen in this area in *U. anceps*, it is unclear whether this condition can be considered typical for *E. cornutus*. Although there is no suggestion of the presence of a staggered incisor, there is a possible remnant of a smaller alveolus (? canine) behind the last of the four large ones in the right ramus. An X-ray might clarify this question.

Wheeler commented on the great length of the jaw and lower cheek teeth (1961, p. 49), giving 192 mm (chart 6, p. 81) as the second largest cheek-teeth measurement of all specimens. There is a considerable inframandibular flange, but it is not extremely massive. These features, along with size of the skull and the upper dentition, including the missing canine that Marsh figured, combine to suggest that it was probably a male of *E. cornutus*.

The Denver Museum collection contains the jaws of two specimens mentioned in the section on the skull and upper dentition: DMNH EPV 496, which probably belongs to the holotype skull EPV 495, and DMNH EPV 493, a heavily worn, upper canine tusk that seems to be the only skull piece belonging to this specimen. The latter has a scapula, humerus, radius and ulna, and a tibia, as well as the mandible, which is what concerns us here.

EPV 496 (Fig. 59) is seen to have long, relatively slender rami with distinct but modest inframandibular flanges and a prominent angular process (see also my earlier comments on p. 103). The few dental measures I was able to take are given in Table 9. The catalogue lists an incisor, but those in the jaws in the mount with the skull all appear to be restored. Perhaps DMNH EPV 529 formed the basis for the restoration. It is an isolated incisor with an anteroposterior crown length of 3.91 cm. AW = 1.43 cm, and PW = 1.21 cm. Crown and root length = 9.66 cm. Measurements for the few premolars belonging to this specimen are given in Table 14. Cook (1926) relates that the lower cheek teeth were weathering out and badly broken up, but that m2, m3, and part of m1 were fitted back together, and he gave some measurements for them, which I include in Table 9.

The mandible that bears the number EPV 493 has left p2–m3 and right p3–4 and m2–3 (m1 had been shed). The left m1 and m2 are heavily worn, as are the right p4 and m2. Individual tooth measurements are given in Table 14. The length of

the symphysis is 16 cm, and the inframandibular flange depths are left, 9.7 cm, and right, 9.77 cm.

The Carnegie Museum jaw, CMNH 29493, appears on stratigraphic grounds to be that of *Eobasileus cornutus* (Fig. 64), which is how I tentatively assign it, but the morphologic evidence is slim. It surprised me to learn that this is the only Washakie uintathere in the Carnegie collection, since J. Leroy Kay made several field trips into the Washakie Basin and collected many other specimens (rodents, primates, condylarths, perissodactyls, artiodactyls, etc.). Collected in 1942, this specimen (FN 21/1942) appears to be the jaws of a female, united by the rear part of the symphysis. It possesses small inframandibular processes; the left ramus preserves p3–m3, the right p4–m3, and both m1s are very worn. Only the right ramus extends back into the angular region. The locality is given as the SW end of Haystack Mtn., near the top. Here we have an ambiguous designation, because Kay did not define what he meant by "Haystack Mtn." If he meant Haystack Mountain proper (i.e., in NW ¼, Sec. 6, T16N, R96W), then it came from high in TWkA2, and the *E. cornutus* assignment is assured. If from Haystack Mountain in the broad, more usual sense, then it probably came from low (or higher) in TWkA2, but it could have come from within the area I have called the NW flank of Haystack, near to Sec. 23, T17N, R96W, which includes beds high in TWkA1 and others near the base of TwkA2, as well as higher ones. In that case, depending on the exact horizon, it is either *E. cornutus* if from high in that part of the section, or if from the lower part it could be another transitional specimen between *U. anceps* and *E. cornutus,* best assigned to the latter taxon. (The University of Wyoming specimen came from those lower units of TWkA2 in that same area, and it has features that mark it as transitional and caused me to assign it to *E. cornutus.*)

The Berkeley collection, in addition to UCMP 81356 (jaw, above), contains three isolated lower cheek teeth collected in 1954 by L. Kent and M. C. McKenna, from locality V78 102 (a subdivision of V5429) from the south side of Haystack (Mammoth Buttes), from horizon 17 of Granger.

UCMP 81357 is a right p4 or m1 with protoconid tip broken and its lophids worn, exposing the dentine. Its measurements (in cm) are: L = 2.51, AW = 2.04, PW = 2.24.

The unworn posterior half of a left m3, UCMP 81358, consists of the posterior face of its metaconid and about one-fourth of the metalophid. There is a small metastylid behind the metaconid. The hypolophid extends to the base of the metastylid. A stout posterior cingular "lophid" is undivided, but its "hypoconulid" portion is missing.

UCMP 81406 is a complete left p3, p4, or m1 that has its lophids deeply worn to their bases. The posterior cingulid has suffered enough interdental wear for about one-third of it to be worn away. Tooth measurements (in cm) are: L = 2.49, AW = 1.87, PW = 2.11.

The Denver Museum specimens of lower teeth of *E. cornutus* other than DMNH EPV 496, the paratype, are:

DMNH EPV 483, an isolated left premolar of uncertain position. Its length is 2.52 cm, AW = 1.91 cm, PW = 1.82 cm or 1.86 cm (minimum or lophid lengths respectively).

DMNH EPV 2604, a right m2 whose measurements are given in Table 14.

Dental measures of the lower teeth of *E. cornutus* are given in Table 14, and Figure 65 shows graphs of the lower cheek teeth.

Figures 66 and 67 are provided for the easiest direct visual comparisons of the sizes and size ranges of the cheek teeth of *U. anceps* (solid lines) and *E. cornutus* (broken lines). The values of the means for each tooth, and the limits of the point clouds, are shown. Note that for both upper (Fig. 66), and lower (Fig. 67) teeth, there is extensive overlap of the point clouds within and between taxa. Tooth for tooth, *U. anceps* teeth tend to be smaller than their counterparts in *E. cornutus* in both dimensions, except for the 3rd and 4th premolars, where the overlap is almost total.

Feces: Possibly Belonging to *Eobasileus cornutus*—PM 59510 (Fig. 68) comes from an area that has produced several similarly appearing fecal masses, this being the largest and the least broken down. Internally, they all have an even green color, to judge from the numerous break surfaces. No inclusions such as tooth or bone chips were seen. Assignment of such a specimen as being produced by *E. cornutus,* or even by a uintathere, is highly speculative. But from its size, only *Dolichorhinus,* the largest titanothere in the fauna, or the smaller, more common *Metarhinus/Mesatirhinus,* or the rare *Achaenodon* or *Stylinodon* are the other most likely contributors. (Scraps of uintathere and titanothere bones occur at the locality.) As the two views show, it is dorsoventrally flattened and probably was more or less cylindrical, at least for the preserved portion. It is

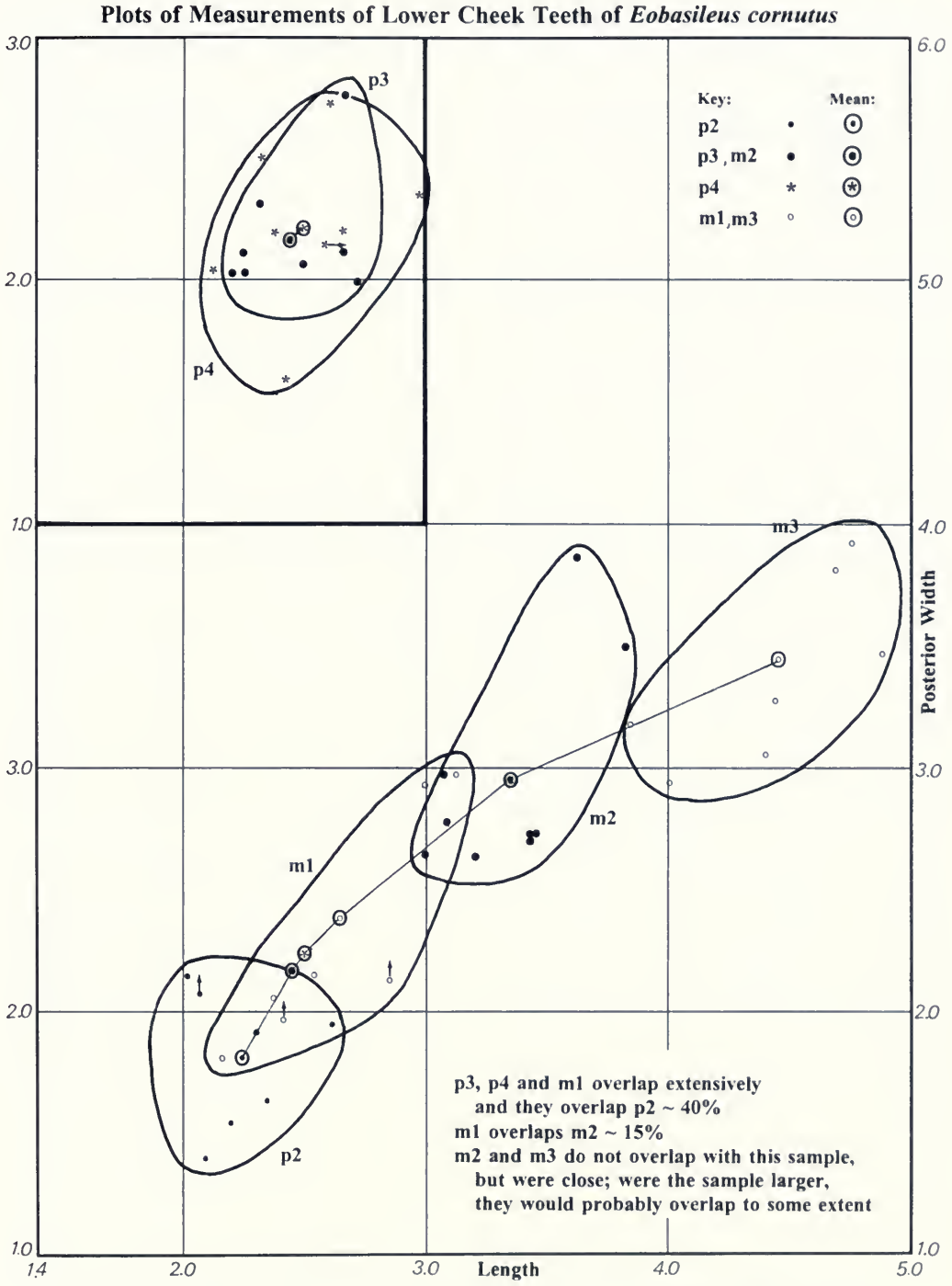

FIG. 65. Bivariate graph of lower cheek teeth of *E. cornutus*. Measurements are in cm.

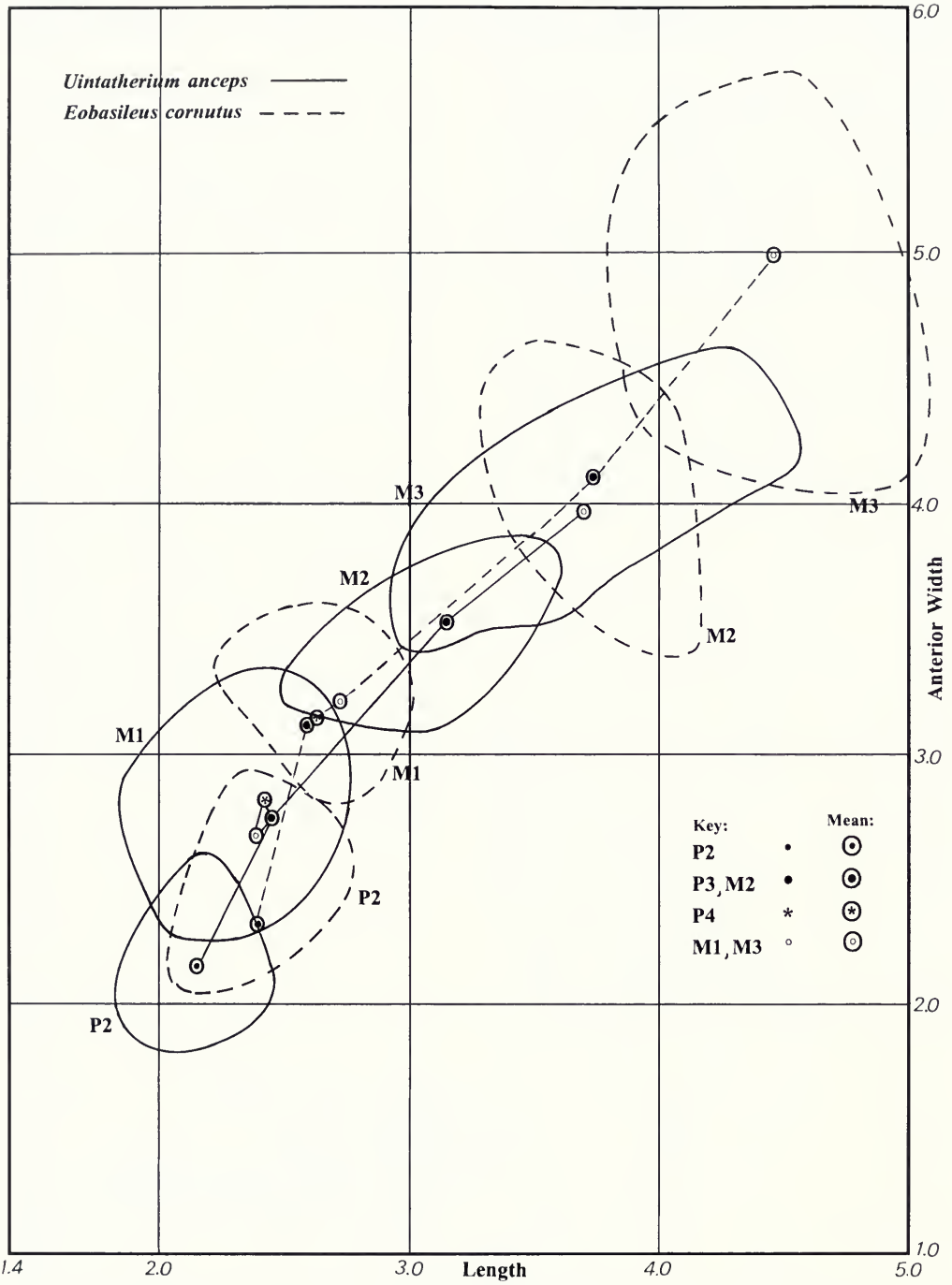

FIG. 66. Plots of upper cheek teeth of *E. cornutus* (dashed line) overlain by those of *U. anceps* (solid line) to give a visual comparison of the relative sizes, tooth for tooth and of the two series. Units are cm.

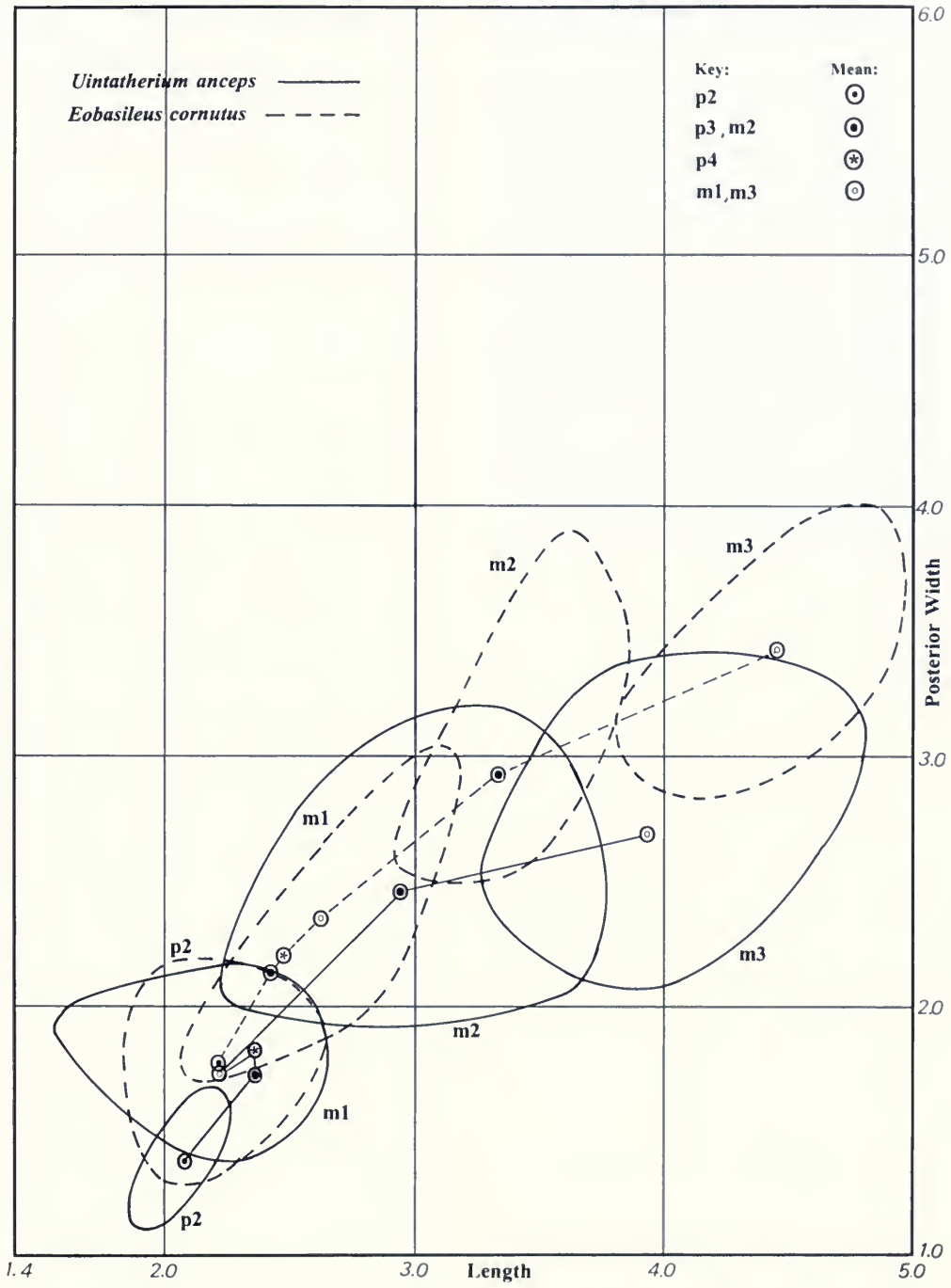

FIG. 67. Plots of the lower cheek teeth of *E. cornutus* (dashed line) overlain by those of *U. anceps* (solid line) to give a visual comparison of the relative sizes, tooth for tooth and of the two series. Units are cm.

FIG. 68. Two views of a fecal mass, PM 59510, in the position that it lay in when exposed on the bedding surface (**A**), and showing its form vertical to the bedding, presumed to be due to compression (**B**). It is considered likely, from its size, to be a coprolite of *E. cornutus,* but it could be from one of the titanotheres or from *Achaenodon,* all large members of the fauna (FMNH neg. nos. GEO 86026–7).

weakly lobate, and other similar fragments suggest that the ends were tapered. In spite of its cylindrical form and tapered ends, and mainly because of its amorphous interior, I think it is from a herbivore. It came from locality FM-2-93-WDT, which is at Moonstone Reservoir in W ½, NW ¼, Sec. 3, and E ½, NE ¼, Sec 4, T13N, R98W, Cow Creek Reservoir Quadrangle, high (near top) in TWkA2.

The Status of *Tetheopsis*

As was shown in the Preface, the skull size of the larger of the *Tetheopsis* specimens corresponded with those of *Eobasileus cornutus,* while the smaller corresponded with those of *Uintatherium anceps.* These facts caused me to question the validity of the genus *Tetheopsis.*

Dental measures tend to support the notion (Tables 5, 6, 13, 14) that *Tetheopsis ingens* (Marsh), which is known only from this one specimen (YPM 11041), is a synonym of *Eobasileus cornutus.* It is longer than all other uintathere skulls except DMNH EPV 495, *E. cornutus,* and two skulls that Wheeler (1961) considered to belong to *T. speirianus* (PUM 10079 and YPM 11043) and that, because of their size, I now assign to *E. cornutus.* All of the other skull or jaw specimens that Wheeler (1961, pp. 48–51) assigned to *Tetheopsis speirianus,* I assign either to *E. cornutus* or to *U. anceps,* as follows:

PUM 10079 (PM 8088 cast), the holotype of *Loxolophodon speirianum* (Osborn), I classify as *E. cornutus* in spite of its being found in a unit where only *U. anceps* is expected, mainly because of its extreme skull length and also because the dental measures lend some support. Its 16.25 cm cheek-tooth row length, although 0.5 cm shorter than the smallest of the specimens Wheeler assigned to *E. cornutus,* is longer than most (14 of 17) specimens he assigned to *U. anceps.* Wheeler (1961) noted that this is the only specimen of *Tetheopsis* for which the stratigraphic level is known exactly. It was collected from Bed 9 of Granger (~ = Roehier's Bed 614), high, near top, in TWkA1 (i.e., it is from a lower bed than any other specimen of the species), coming from somewhere about 86 feet (~28 m) below Granger's Bed 11. So it appears that the transition zone extended at least that far downsection.

According to Wheeler, the lower jaw that Marsh illustrated with PUM 10079 is a different specimen, from a different horizon and locality. The caption to Wheeler's plate 11 identifies that jaw as PUM 10385 and gives LaClede Meadows as its locality in Washakie A. That appears to be correct, but since only the bluffs to the east, immediately adjacent the meadows, are at all likely to have been identified with the LaClede name, it must have come from the Lower Brown Sandstone unit at the base of TWkA1 (Bed 569), which has yielded several *U. anceps* specimens. I assign it to *U. anceps* based on its size, most probable stratigraphic position, and short cheek-tooth row, which is close to, but less than, the mean for that species. It is decidedly shorter in that respect than any other specimen that has been referred to *Tetheopsis* and is much shorter than any specimen of *E. cornutus.* Wheeler noted the "small size" of the inframandibular process—an understatement, for the process is nearly nonexistent. It seems that at least some of the females of both *U. anceps* and *E. cornutus* have only minor development of the process, and probably that condition is correlated with possession of relatively small upper canines.

YPM 11043, the holotype of *Tinoceras annectens* Marsh, is one of the longest of the skulls of

any uintathere. As noted, I assign it to *E. cornutus* on that basis as well as on its very long cheek-tooth row lengths. Originally assigned to *Tetheopsis speirianus,* it came from somewhere in the Haystack Mountain area, most probably from TWkA2.

YPM 11256, the holotype of *Tinoceras longiceps* Marsh, I also assign to *E. cornutus* because of the upper cheek-tooth row length. Wheeler (1961, p. 49) had assigned it to *Tetheopsis speirianus.* The locality is "Red Dog Buttes," or the eastern end of Haystack Mountain, but no more precise position of the locality or its stratigraphic position are given. Wheeler suggested that it is probably from Washakie A (i.e., TWkA1). I think it more likely to have come from TWkA2.

The following specimens are less certainly assigned. YPM 11567 and PUM 11611 are both tentatively considered to be *E. cornutus,* the first based on skull length and proportion, the other based on similar lower toothrow length to that of YPM 11567. PUM 10385 and AMNH 1687 are tentatively assigned to *U. anceps* based on skull length and proportion. However assigned, they are transitional between the two taxa.

Biological considerations also strongly argue against the simultaneous presence of more than one species of such closely related large animals competing for food and territory in so limited a region. Both *U. anceps* and *E. cornutus* are known from other basins, whereas the two named species of *Tetheopsis* are known only from the Washakie Basin, the only place where all three genera are known to co-occur. Were *Tetheopsis* to be considered valid, each of its two species would have had to have lived side by side, partitioning the resources and competing not only with its sister species but also with a species of a closely related genus. Hence, I consider *Tetheopsis* to be invalid, and that *U. anceps* evolved directly into *E. cornutus.*

Regarding the transition of *U. anceps* into *E. cornutus,* two skulls are of interest, one at the University of Wyoming, the other in the Princeton Museum. Length measurements for UWM 13644 fall nicely within those of *U. anceps* (Fig. 2B, Table 1), where it had been classified, but its dental measurements fit best with those of *E. cornutus* (Tables 5 and 13). Table 15 gives the statistics for the two species and includes two of the new intermediate specimens. Furthermore, the locality from which it came is low down within TWkA2 (within my locality FM-3-57-WDT), which includes beds from about 630 to 650—just where one might expect to find the transition. Therefore, I consider it to be an early representative of *E. cornutus,* coming as it does from slightly above the uppermost of the units that are known to contain *U. anceps,* and that it probably represents an initial transition stage in the evolution of *Uintatherium* into *Eobasileus.* PUM 10079 is in a similar situation (but near the end of the transition), coming as it does from slightly below the lowermost units known to contain *E. cornutus,* and hence it, too, is in the transition zone, which now appears to be from about Bed 614 to as high as Beds 630–650.

Taken together, these interpretations are, I believe, much more compelling biologically and ecologically, without considering there to be a competing sympatric genus, *Tetheopsis,* living only in this one intermontane basin, where it first would have had to compete with *Uintatherium,* then finally with *Eobasileus.* Accordingly, as noted above, I place both species of the genus *Tetheopsis* into synonymy with *E. cornutus.*

Paleobiology

It has long been realized that many anatomical, physiological, ecological, and behavioral aspects of living animals—mammals in particular—are directly related to body size. The past three decades have brought refinements to that general understanding (Eisenberg, 1981; Peters, 1983; Calder, 1984; Schmidt-Nielsen, 1984; Janis, 1990; Maiorana, 1990; Janis & Carrano, 1992), and today precise scaling formulas for characterizing these relationships are known (Damuth & MacFadden, 1990, and authors within that work). It is reasonable to assume that size in fossils should be similarly related to their biology, yet a troublesome practical problem is always encountered in attempting to arrive at the body size or mass of a fossil animal. We cannot directly measure or weigh it, as can be done with a living form (as difficult as even that can be when dealing with the largest ones). Hence, we are forced to resort to estimates derived from proxies, such as teeth, limbs, and head–body length. Such estimates can vary widely, often so widely as to be nearly useless for application within these modern scaling formulas, although they might give a range that is useful.

Therefore, to gain as accurate an assessment of the size of a fossil organism as possible so that

we can best understand, and more confidently speculate about, its biology, it is always important to choose the most appropriate ways of making the estimates. I have reviewed some of them, checking works of Gingerich (1974, 1977), Gingerich et al. (1982), Anderson et al. (1985), Damuth (1990), Fortelius (1990), and many others, including Jerison (1971, 1973). Some are far better than others, but limitations of the fossils available often render even the poorest of them useful. Several poor estimates together may give a range that may be helpful (Roth, 1990). Damuth (1990, pp. 236–237), following Van-Valkenburgh (1990), showed that for all extant ungulates, head–body length correlates highest with body mass (r = .975) and that it also had the lowest percent prediction error (%PE = 31.42) and lowest percent standard error of the estimate (%SEE = 45.54), followed closely by a variety of measures of the lower dentition, and finally by others of both upper and lower dentitions. Some workers have used limb-bone dimensions with considerable success for a broad range of forms (Alexander, 1980, 1985), others within limited groups (Ruff, 1990, for anthropoid primates; Roth, 1990, for dwarf elephants). Jerison (pers. comm.) told me he found this to be the most reliable method from an extensive series of tests.

For the terminal uintatheres, the big question is to determine, with the greatest possible accuracy, just how large they really were. Interestingly, early on both Cope (1873) and Marsh (1886) spoke of elephants when making size comparisons to these uintatheres, and later on they and others also made comparisons with living rhinoceroses and hippopotamuses, thereby suggesting the "traditional" size range usually considered for these last genera of the uintathere line. Damuth (1990), using modern scaling formulas, has arrived at notably smaller size estimates, about half of those deduced by the earlier workers. It is my opinion that none of these latest formulas, which are good predictors for most extant forms, and for probably most fossils, works really well for the uintatheres. So we are faced with an additional question: Why is this so?

Clearly the terminal uintatheres rank with the largest of living terrestrial mammals in body size. Hence, those forms will be the source in our search for other biological analogues. These uintatheres were the first land mammals to grow so large, back in the Middle and Late Eocene, but they belong to a long extinct order, one with no living relative to serve even as a good partial analogue, so the situation is made difficult. With no living biological true analogue, we must rely on several partial analogues, each of which has some drawbacks that hamper the study. Nevertheless, they are our working base, and from each we may learn something applicable to the uintatheres.

I begin by assessing the species of living large mammals, for which live body weights (given in kilograms) are known, as listed by Eisenberg (1981). He gives the following values: *Loxodon africanus* and *Elephas maximus* (2,766 kg and 2,730 kg respectively),[9] *Diceros bicornis* (1,081 kg), *Hippopotamus amphibius* (1,277 kg), *Giraffa camelopardis* (1,017 kg), *Bos gaurus* (702 kg), *Camelus dromedarius* (570 kg), *C. bactrianus* (450 kg), *Syncerus cafer* (447 kg), *Bubalus bubalis* (425 kg), *Tapirus indicus* (380 kg), and *Taurotragus oryx, Ovibos moschatus,* and *Ursus arctos mindendorfi* (each 300 kg).

The most recent sophisticated attempts to estimate size for various fossils, not surprisingly, have come from MacFadden and Hulbert (1990) in their faunal study and from Damuth (1990) for a more general survey, as follows. *Amebelodon* cf. *A. barbourensis* (3,440 kg), *Tapirus simpsoni* (381 kg), *Aphelops malacorhinus* (889 kg), *Teleoceras proterum* (635 kg), *Aepycamelus major* (1,026 kg) and *Procamelus grandis* (498 kg) all by MacFadden and Hulbert. The rest by Damuth, *Coryphodon testis* (440 kg), *Uintatherium anceps* (807 kg),[10] *Paleosyops leidyi* (286 kg), *P. palu-*

[9] Walker (1975), cited by MacFadden and Hulbert (1990), gave 5,000 kg for *Elephas maximus* and 5,000–7,500 kg for *Loxodon africanus*; Roth (1990), drawing on others, gave weights of more than 5,000 kg for *L. africanus* and 6,500 kg for *E. maximus*. Most recently Silva and Downing (1995) published an extensive compilation that gave 6,100 kg for the mass of the largest *L. africanus*. For rhinosceroses they gave *Ceratotherium simum* 1,400–2,300 kg, *Dicerorhinus sumatrensis* 900–1,000 kg, *Diceros bicornis* 816–1,300 kg, *Rhinoceros sondaicus* 1,500–2,000 kg, *R. unicornis* 1,410–2,000 kg; and for *Hippopotamus amphibius,* they gave 568–2,000 kg.

[10] Damuth calculated the bulk of *U. anceps* using three regression formulas: (1) that based on multiple regressions using head and body length (HBL) and length of m1–3 for all ungulates, which gave the lowest value, 690 kg; (2) that for HBL alone, which gave 867 kg; and (3) that which he termed his "best" estimate, based on multiple regressions for nonselenodonts or selenodonts, as appropriate, which gave 807 kg. Except for the second of these, some sort of dental measurement was involved, and this may partially account for the spread. As the following pages show, I think that Damuth's estimates are all far too low and that 1,500–2,000 or even 2,500 would be closer to the mark. His HBL values were

dosus (276 kg), *Dolichorhinus longiceps* (421 kg), *Menodus giganteus* (1,339 kg), *Brontotherium gigas* (2,073 kg), *Trigonius osborni* (334 kg), *Metamynodon planifrons* (887 kg), *Subhyracodon tridactylus* (517 kg), *Moropus elatus* (1,179 kg), *Teleoceras fossiger* (1,016 kg), *Equus simplicidens* (476 kg), and *Procamelus occidentalis* (579 kg).

From these lists, two biological attributes immediately stand out. First, all except the bear are ungulates (*sensu lato*), and as herbivores, in spite of their very large size, they fit relatively near the base of the Eltonian pyramid for the mammals. Second, from their very large size, all are clearly K-selected (Pianka, 1970; Maiorana, 1990), with all that this implies.

The highlighted taxa in each of the lists, mostly animals of over 1,000 kg body weight, are those of most concern to us here. In the Eisenberg list, the three largest are the most comparable in size to the terminal uintatheres, but for reasons given below, none of them are true analogues. It would be great if, as in the MacFadden and Hulbert (1990) study, we were dealing with animals that have a living relative, because that would increase our confidence that we had a reliable analogue to consider. But uintatheres, because they have no living relative, force the use of less certain comparisons.

Estimating Uintathere Body Size

Damuth and MacFadden (1990) and their collaborators have nicely drawn together much of what is known about the various means of estimating body size, and they incorporated this information into a valuable synthesis for paleobiology. Now I would like to apply relevant parts of this to the uintatheres. But first I would like to review where things stood before the developments of the past decade or so.

An overlooked true pioneer in this school is Jerison (1971, 1973). In the 1973 work, he gave estimates of body weights for a number of archaic and evolutionarily intermediate fossil mammals based on his considerations of relative brain size to body size in modern mammals. Among the archaic orders, he included estimates for the two species of the terminal members of the Dinocerata, *Uintatherium anceps* (1,400 kg, two estimates averaged) and *Tetheopsis ingens* (= *Eobasileus cornutus,* 2,500 kg). Additionally, he had the estimates made by Marsh (1886) of 1,400 kg and 2,750 kg, respectively. Further, his own scale models gave values of 1,300 kg and 2,300 kg. These three different sorts of estimates are close enough to one another to add a degree of confidence that they are well within reason.

The method Jerison used to arrive at these values deserves renewed attention. First, he realized the need for a means of measuring body length of a fossil mammal with consistency (Jerison, 1971). For this he used a mounted skeleton of *Poebrotherium labiatum.* Then, by applying the resultant head–body length (HBL) measure within a formula that he also developed, he arrived at the estimated value. The formula represents the relationship of HBL to weight in modern mammals. In Jerison's (1971) own words, reiterated in 1973 (pp. 52–53),

> The formula was developed for this and related applications by a least squares fit to all the usable carnivore and ungulate data in Walker (1964), which include data on living camelids. My procedure was actually to determine lines that connected the extremes of the ranges of the reported lengths and weights and then to fit an "average" line to those lines.

The formula is, P (wt. in grams) = 0.021 $L^{3.03}$, where L is HBL in cm. This formula is applicable for animals of light habitus, and for empirical applications he simplified it to P = 0.025 L^3. Comparable formulas for animals of heavy habitus, such as rhinoceroses, hippopotamuses, and elephants [and uintatheres] the equations are P = 0.043 $L^{3.03}$ and, simplified, P = 0.05 L^3 respectively.

With the Jerison (and other older) estimations differing from the Damuth ones by roughly 2:1, it has become apparent to me that two factors are the primary causes. First is the extreme dental size differences between uintatheres (with their small, relatively simple, bunolophodont cheek teeth) and each of the living large mammals (with their larger, more complex, and more hypsodont teeth).

---

based on his measures of mounted composite skeletons at USNM and AMNH, and following my inquiry, he stated (pers. comm.) that, of all his data, this set he considered to be the least reliable. His revised estimate is, "as a guess perhaps 1,200 kg to 1,500 kg tops." With uintatheres, I am sure that any calculation involving dental measures is bound to fail, for uintathere teeth are so very different (far smaller) than those of the other large ungulates—too different for such formulas to work. Body proportion differences also contribute.

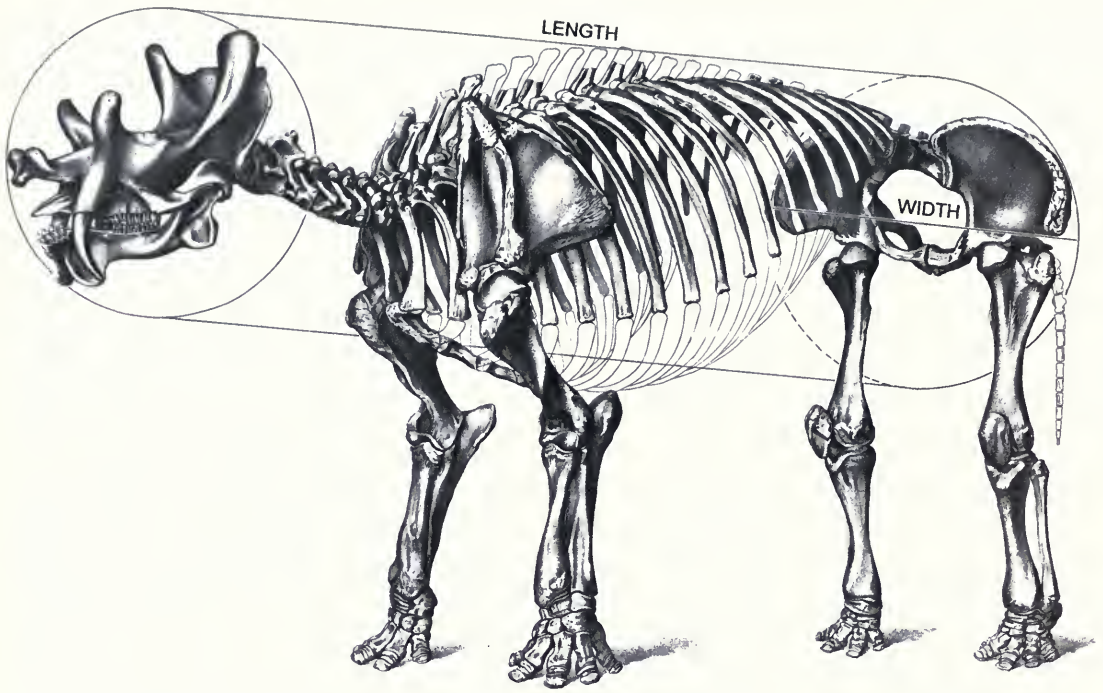

FIG. 69. Illustration of the concept of the "body cylinder" of Damuth (1990). Here I borrow Marsh's illustration of *Tinoceras ingens* (Pl. LVI) to show the "body cylinder" and its defining parameters.

Without this confounding factor, a better analogue might be found among them. As things stand, this renders totally useless any scheme based on dental measurements of uintatheres and the largest living ungulates. (I will return to this topic in a moment.) The second factor is "body cylinder" differences. In this connection, Damuth (1990) has commented astutely.

> The relatively high level of precision for body length estimates is not surprising, because body length measures the length of a "cylinder" that encompasses the majority of a mammal's mass—that comprising the head, neck, viscera, and proximal limb musculature.[11]

This, although true enough, neglects the equally important second dimension of a cylinder: its diameter or radius. Differences in the diameter of the "body cylinder" normally are not a problem with most ungulates because the length and width of that cylinder are in a more or less constant relationship. This may even be true of most mammals, for Jerison (pers. comm.) found variation in body shape to be surprisingly low. But such differences become a significant problem with animals that have a very large diameter "body cylinder" (or very short cylinder length, or both) that departs from the usual body proportions, or, even worse, if the cylinder is more like a truncated cone. For them, even the HBL measure fails. I believe these to be the two major factors that together account for Damuth's low values.

We must add the diameter measurement to the length measurement to define the "body cylinder" properly. The surest means to do this is to use the measurement of greatest width across the pelvis, taken from one outer ilium margin to its opposite. It is our best (osteological) means of determining the diameter of that "cylinder" (Fig. 69). It is more accurate and less subject to distortion than any other single measure (such as rib cage size) because it utilizes prominent fixed points that are frequently preserved. Table 16 provides data relating to these useful measurements. With elephants and uintatheres however, the pelves indicate that the body cylinder has an exceptionally large diameter, and when this is accom-

[11] Here I believe he meant to include the entire proximal limb. In any case, I think it may be best to exclude all parts of the proximal limb elements, for they are involved functionally in locomotion and are not primarily part of the "body cylinder" that Damuth mentioned.

panied by a short HBL (and short limbs), as is the case with the uintatheres, the result is a serious underestimate of body size. Figure 69 illustrates Damuth's point and adds my modification.

When I try to apply the volumetric formula for a cylinder, in this case head–body volume (HBV = HBL × πr^2), I find that something is still amiss. Using Damuth's HBL values in this formula together with my measurements of the two complete adult pelves in the FMNH collection gives 3,286.7 kg (or 3,515.5 kg) and 3,387.1 kg (or 3,622.9 kg). These values certainly are far larger than the 867 kg he arrived at, and I am sure they are much too high. Some sort of constant multiplier factor is needed (perhaps about 0.5)[12] because the notion of a body cylinder or cone really is too symplistic. The body is not a true cylinder because it is somewhat bulging in its middle, truncated in front, and in that region the neck and head cause the "cylinder" to become conically tapered. Perhaps it would work best to average values of volumes of a cylinder and a cone, or use the fructum of a cone. For my purpose, it is unnecessary to pursue this.

Damuth's way of estimating bulk, which involves both HBL and dental measures, is doubly in error for uintatheres, and it shows the lowest value of the three he gave, 690 kg. His "best" means (807 kg), based on multiple regressions for selenodonts suffers from the same flaw where the uintatheres are involved (use of dental measurements). His largest value (867 kg) resulted from calculations based on HBL alone and probably would have been more reasonable had it taken into consideration body cylinder diameter (i.e., pelvic radius or diameter) and distortion of the "body cylinder."

Others have used different criteria as required by the nature of their materials. For example, MacFadden and Hulbert (1990) used two characters to estimate body mass: first lower molar length (LM1APL) and first lower molar area (FLMA) = LM1APL times first lower molar trigonid width (LM1TRW), because these measures offered the best samplings for the fauna they report. (In the case of their *Amebelodon*, in spite of the reasonable appearing value, I doubt that dental measures would have been the most appropriate ones to use, had other choices been available.) In any case, these are inappropriate here. Roth (1990) found shoulder height and femur and humeral lengths and circumferences to be useful for her study of dwarf elephants. She concluded as follows:

> In sum, estimates of mass can be obtained for dwarf elephants from lengths and circumferences of humeri and femora, and these estimates are consistent with masses based on shoulder heights. Although 95% confidence intervals for single estimates are too broad to be informative, use of more than one mass estimation technique allows one to define a range that is likely to encompass the actual mass of the animal.[13] For small elephants (less than approximately 2000 kg), bone lengths appear to yield the most accurate mass estimates, whereas larger masses are better approximated by using mass estimation equations based on bone circumferences.

Earlier in her paper, she had observed:

> Comparisons of mass estimates based on skeletal dimensions with known body masses for the same individuals (of *E. maxumus* and *L. africanus*) revealed the following: (a) for the three specimens smaller than 2000 kg, bone lengths consistently provided the best mass estimates; estimates based on shoulder height either embraced or slightly overestimated, and circumferences consistently overestimated, the actual body mass of these animals. (b) For the three specimens larger than 2500 kg, con-

[12] I attempted to use the formula for the volume of a cylinder, V (in kg) = πr^2. HBL, substituting Damuth's HBL values, as well as my measure of the Vernal specimen (3,110, 3,205, and 3,530 mm), along with the radius values from the two FMNH pelves (580 and 625 mm). When I use only the lowest radius value in combination with each of the three different HBL values, the results are obviously much too large: 3,287, 3,387, and 3,731 kg. These are worse than the results using Damuth's regression equations for all ungulates: 1,431, 1,447, and 1,494 kg! Still unsatisfied, although these last values seemed about right, I reasoned that the "body cylinder" is actually too crude a model. A truncated "body cone" in which the largest radius is in the region of the hips and the smallest is taken to be the widest part of the head region (maximum width across the zygomatic arches) appears to be a somewhat better model. So again I repeated the procedure using the volume formula of the frustum of a cone, with r_1 being the pelvic radius, and estimating r_2 to be 175 mm (radius of cross section of the head plus flesh allowance), V = π − HBL/ $3(r_1^2 + [r_1 \cdot r_2] + r_2^2)$. The results are 1,526 kg, 1,573 kg, and 1,732 kg with an average of 1,610 kg. If the largest values are used in combination, the added values are 1,728 kg, 1,781 kg, and 1,962 kg, and the overall average is 1,717 kg. That these are better values is considered likely because they match the weights of the larger living rhinoceroses and the several early estimates.

[13] In this regard Roth (1990) has provided a very illuminating graph that shows the extreme range of variation found in both *E. maximus* and *L. africana* (her fig. 9.2) where "Some individuals of the same shoulder height (e.g. 280 cm) differ in mass by nearly a factor of 3."

versely, shoulder heights and bone circumferences yielded accurate and similar estimates, whereas bone lengths underestimated actual body mass.

From the pelvic dimensions of uintatheres (Table 16), it is clear that in this regard they are closer in size to living and Pleistocene elephants than to either modern rhinoceroses or hippopotamuses, as was noted early on by Marsh (1886, pp. 135–137). Cope (1873) also was impressed by this comparison, as his comments and first restoration show. Nevertheless, for skull length, as can be seen (Table 17), they are much closer to rhinos, being only slightly larger, and they all are considerably smaller than elephants (× about 0.75). Furthermore, as noted earlier, a single elephant molar tooth is longer than the length of the entire cheek tooth dentition of a uintathere and is many times more massive because it is both wider and higher and hypsodont (Fig. 70A,D, Table 17). So, as shown earlier, the teeth are not at all comparable between the two groups. Uintathere cheek teeth, as noted above, are bunolophodont, much more comparable to those of rhinos and hippos (Fig. 71A–D). All of the latter, compared to elephants, are relatively much lower crowned and smaller, but uintathere teeth are at most only between one-half to two-thirds the size of those of rhinos and hippos, and for this reason useful comparisons even with them are not possible.

In terms of long bone proportions (Table 18), uintatheres lie between elephants, on the one hand, and rhinos and hippos on the other. They are closer in size to the larger of the rhinos long bones than to those of elephants or hippos. For proximal limb bone dimensions Roth (1990) has shown a most convincing estimator in her conclusion no. 6. She expanded her earlier statement, in which she compared mass estimates based on skeletal dimensions with known body masses for the same individuals of *Elephas maximus* and *Loxodon africanus,* to reveal the following:

(a) for the three specimens smaller than 2000 kg, bone lengths consistently provided the best mass estimates . . . (b) for the three specimens larger than 2500 kg, conversely . . . bone circumferences yielded accurate and similar estimates, whereas bone lengths underestimated body mass.

Although uintatheres and elephants are not the same, a test using the four equations of Roth (1990) might be revealing.[14] *Uintatherium* limb-bone measures all fall close to the breakpoint she found between smaller and larger elephants, so I substituted the values of a specimen from near the middle of the range in my sample. Her four equations and the derived mass estimates are:

1. Mass (kg) = $2.767 \times 10^{-5} \times$ humerus length $(\text{mm})^{2.675}$ = 660.8 kg using the 573 mm length value (Table 18).
2. Mass (kg) = $1.774 \times 10^{-5} \times$ femur length $(\text{mm})^{2.654}$ = 595.5 kg using the 685 mm length value (Table 18).
3. Mass (kg) = $9.448 \times 10^{-4} \times$ humerus circumference $(\text{mm})^{2.611}$ = 2493.5 kg using the 288 mm circumference value (Table 18).
4. Mass (kg) = $3.790 \times 10^{-4} \times$ femur circumference $(\text{mm})^{2.827}$ = 2715.1 kg using the 266 mm circumference value (Table 18).

Here the circumference values appear to give masses that are too large and the length values appear to give mass estimates that are far too small. Because uintathere body proportions are more like those of living hippos and fossil river rhinos, all characterized by having short limbs, it would be expected that formulas based on lengths would give exceptionally small mass estimates. Circumference values therefore appear to be much closer to the mark than the length values.

To judge just from direct comparisons of lengths and circumferences of each of the proximal limb bones (Table 18), and without using any formulas, it is clear that those elements of *U. anceps* are a bit larger than those of any living hippo or rhino, except possibly *Ceratotherium* (i.e., body weight probably > 1,277 kg). Skull comparisons (Table 17) of the same suite indicate that its skull is about equal in size to skulls of *Ceratotherium, Rhinoceros,* and *Hippopotamus,* and slightly larger than our *Diceros* specimens (again suggesting a body weight ± 1,277 kg). HBL measures (Table 19) are shorter than those of most rhinos and hippos (the short body cylinder), suggesting a body weight slightly less than 1,277 kg. Pelvic widths are comparable to those of elephants and suggest a much greater body weight (~2,730 kg or more). Drawing on all of this, it

[14] I did not use the sum of humerus and femur circumferences, which Damuth and MacFadden (1990, appendix table 16.1) found to be the most accurate of estimators for all mammals, giving the highest correlation coefficient and the least %SEE (standard error of the estimate) and mean %PE (predictive error) because no equation was given.

would appear that my earlier guesses of 1,500–2,000 kg could be reasonable for *U. anceps* and that the larger *E. cornutus* could be at ~2,500 kg.

Damuth has kindly sent me his skeletal measurement data for *Uintatherium anceps,* which, when used with the Jerison formula, give the following results: His HBL measure for the AMNH mounted composite specimen is 3,110 cm, giving a weight estimate of 1,504 kg; that for the Smithsonian skeleton (USNM 16662), 3,205 cm, gives 1,646 kg. An average of the estimates made by Marsh, Jerison, and these based on Damuth's measurements used with the Jerison formula gives 1,400, 1,400 and 1,300, and 1,504 and 1,646 kg = average of 1,450 kg.

I recently compared uintatheres with elephants, rhinos, and hippos in a related work that evolved out of this study (Turnbull, 1995). There I made these body-size proportion comparisons, as well as dental comparisons, which I repeat here. Elephants are absolutely larger than uintatheres and all the other largest living terrestrial mammals (Tables 16–19). The most important differences that preclude elephants from being good partial analogues are the dentitions and body size. Uintathere cheek teeth (Figs. 68D and 69D) are small bunolophodont structures (low-crowned, with relatively simple lophs). In contrast, elephant teeth (Fig. 68A) are greatly enlarged, hypsodont structures with multiple lophs. Beyond this, tooth replacement mechanisms are drastically different, in that elephants have evolved in a way that adapts mesial drift to such a highly specialized degree that the cheek teeth in each jaw quadrant erupt and function sequentially so as to follow one another forward as if on a conveyor belt. These differences preclude the application of any scaling formula that depends on dental measurements when comparing uintatheres with elephants (or actually, elephants with anything else).

Living rhinos and hippos are about as large as the terminal uintatheres (Tables 16–19) and they provide somewhat better, but still poor, dental comparisons. Their cheek teeth too are larger (Table 17, Figs. 68B, C and 69A–C), more hypsodont, with stronger and more complex lophs than the teeth of these uintatheres. But, as in rhinos and hippos, mesial drift is not the primary means of tooth replacement, nor are tooth size differences as extreme as with the proboscideans. The hypsilophodont cheek teeth of rhinos and hippos, although less divergently specialized than the massive teeth of proboscideans, are still too different and too large to permit either of them to serve as truly good analogues for uintatheres. So once again, we see that use of dental measures in scaling formulas will not work when dentitions are as divergent as those of uintatheres from any of the very large living mammals.

Pachyostosis: Another Partial Analogue?

Russell and Russell (1993), with their mammal–dinosaur convergence study, have spurred me to search further for some less obvious partial analogue appropriate to the uintatheres. I am convinced that these terminal uintatheres were semiaquatic (i.e., they had found the hippopotamus niche). Body proportions, relatively short legs and large "barrel" rib cage point toward this conclusion. Most significantly, the femora and other major long bones are pachyostotic (Fig. 72). Years ago, Zangerl (1935) showed that for reptiles that have become secondarily adapted to an aquatic life, there are various stages of pachyostotic bone alteration associated with the degree of that adaptation. As can be seen in Figure 72, the compacta is dense to the point that it is difficult to find a haversian system, and the medullary area is occluded, with cancellous bone totally filling the opening at midshaft. This is a condition typical of early-stage pachyostosis associated with the return to an aquatic life by a reptile that has had a long prior nonaquatic terrestrial life. Since Zangerl's work, others have documented similar conditions in birds and mammals (Fawcet, 1942; Wall, 1983; Ricqles, 1989), but this example is not a wholly satisfactory analogue, because hippos today are foregut fermenters that live almost entirely on grass (Kingdon, 1979; Estes, 1991). Owen-Smith (1992) reported that:

> Hippos are area selective grazers with a preference for short green grass. Grasses and sedges form 95–99% of the food eaten by hippos in different regions, the remainder being made up by forbs, which increases in representation during the dry season.

In the Eocene, however, even C3 grasses had not yet experienced their great adaptive radiation, and C4 grasses (hippo food) only became dominant about 8 million years ago (Cerling et al., 1998). So these uintatheres browsed on something else, and furthermore their dentitions were not equipped for grazing. Still, in both body size and aquatic adaptation, hippos appear to be the best of the partial analogues from among the largest living land mammals.

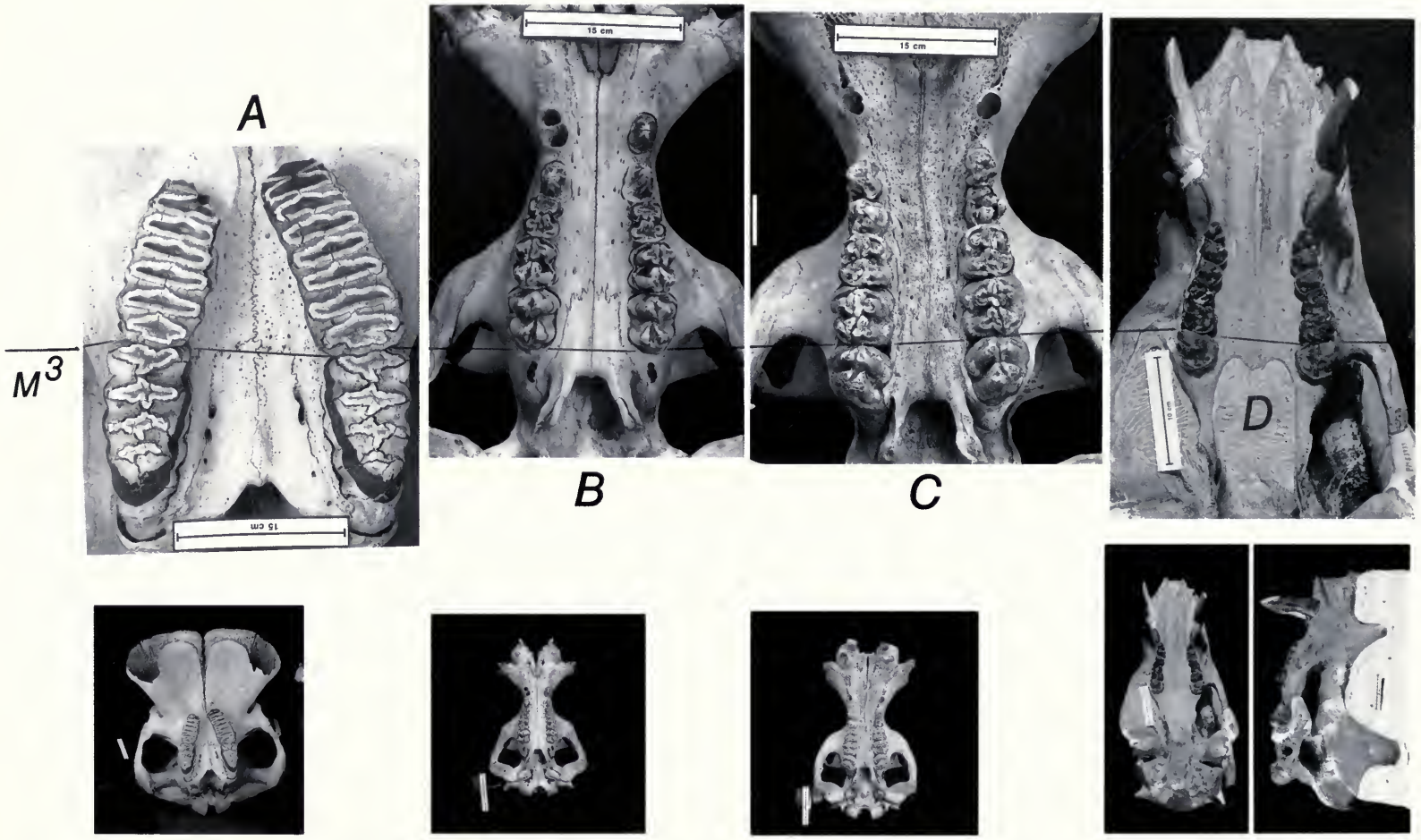

FIG. 70. Comparisons of upper cheek teeth of (**A**) *Loxodonta africana,* FMNH 34364 and (**B–C**) subadult and adult *Hippopotamus amphibius,* FMNH 105018 and 22367, with (**D**) those of *U. anceps,* PM 53933. Full skull vignettes are shown below (FMNH neg. nos. GEO 85972.2–.6 (A); 85970.5–.6 (B); 85971.10–.11 (C); 85689–85690 (D)).

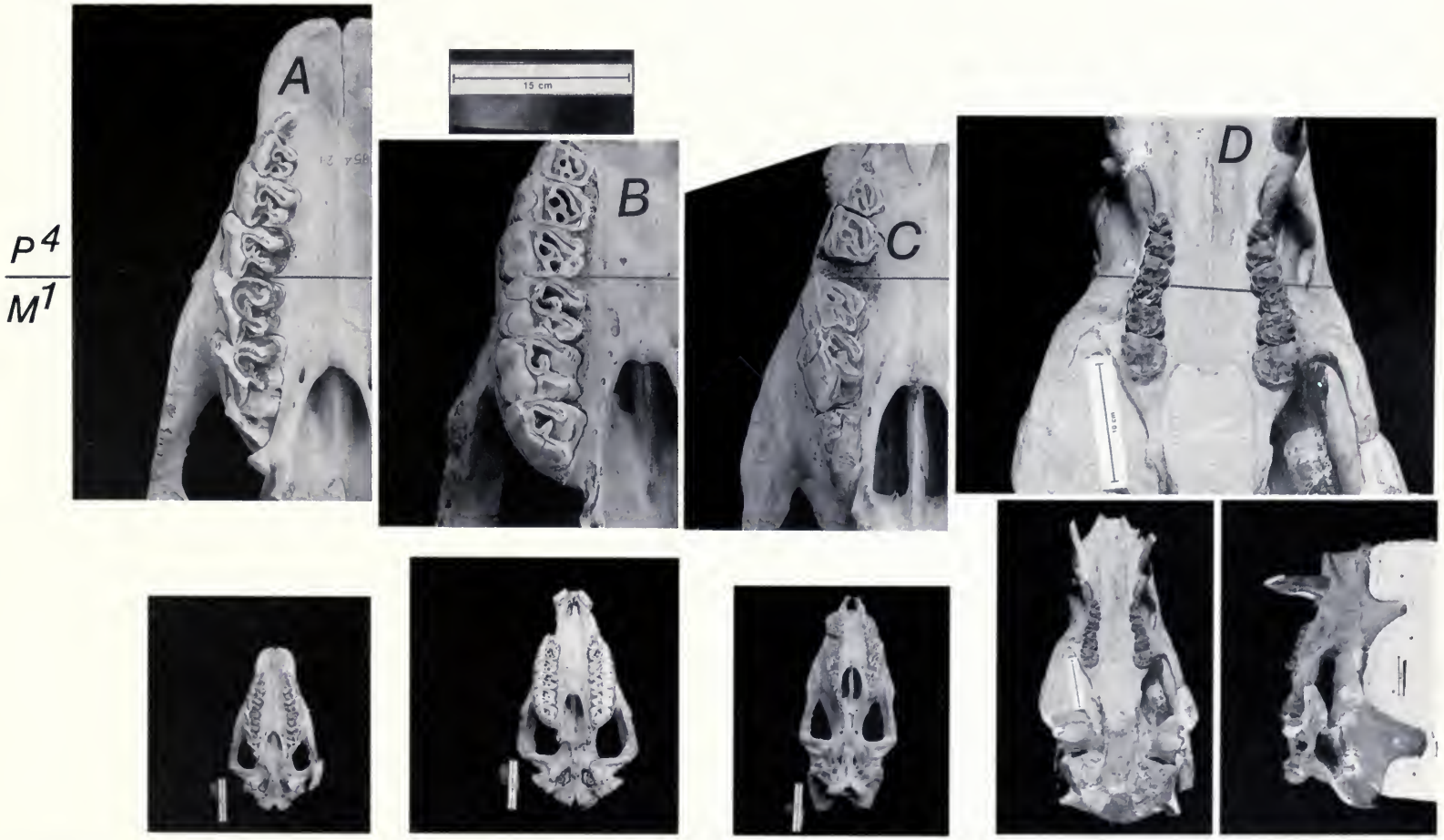

FIG. 71. Comparisons of upper cheek teeth of rhinoceroses (**A–C**) with those of *U. anceps* (**D**). **A,** *Diceros bicornis,* FMNH 85429; **B,** *Ceratotherium simum cottoni,* FMNH 29174; **C** *Rhinoceros unicornis,* FMNH 57639 (FMNH neg. nos. GEO 85970.1 and .3 (A); 85971.3 and .?? (B); 85970.8 and .?? (C); 85689 and 85?? (D)).

FIG. 72. Cross-sectional cut of the midshaft region of a uintathere femur, PM 39393 (?), showing an early stage of pachyostosis. The compacta is so dense that it is difficult to see any lamination or to find a haversian system within it. The medullary portion is filled with bony struts and trabeculae, so that no open area remains.

The great similarity of uintathere pelves to those of elephants suggests that these immense spreading ilia are there to support a very large hindgut. The fact that these uintathere ilia approximate those of elephants (Table 16), whereas the rest of their body is decidedly smaller, greatly reinforces that notion. A majority of modern ungulates are foregut fermenters, with efficient digestion taking place in about 2–3 days in that region (Owen-Smith, 1988). Perissodactyls, on the other hand, use hindgut fermentation, and those that keep their digesta for only a short time (e.g., horses) derive relatively little nutrition (Foose, 1982; Owen-Smith, 1988) but compensate by eating more and being more selective in the quality of the food. Those with extended retention times for processing their food (e.g., rhinos) can tolerate higher fiber and lower nutritional quality than the faster (i.e., shorter retention time) ruminants or other foregut fermenters. Large body size allows greater retention times, which is the pathway taken by rhinos and hippos. Of the living large ungulates, hippos have the longest retention time, about 4 days, which Owen-Smith equated with low digestive efficiency. However, I think that digestive efficiency has to be judged more on a case-by-case basis, considering not just time of passage but also the quality of the food (fiber/protein ratio) and quantity of intake. Janis (1976 pp. 765–766) has shown this most convincingly in her comparison of ruminant and equid feeding strategies. Following a discussion of several means of conserving nitrogenous breakdown products, she was able to conclude:

> Ruminants will also be at an advantage where the quantity, not the quality, of food is limiting, since they need to take in smaller amounts per unit body weight than perissodactyls. However, the cecal digestion of horses, coupled with their food selection strategy, opens for them food resources inaccessible to similar sized ruminants.

In fact, Janis (1976) made the most thorough comparative assessment of digestive structures and physiology of artiodactyls and perissodactyls and the evolution of the herbivorous digestive systems up to that date. Identifying fundamental differences in the feeding strategies of ruminants (foregut fermenters) and equids (hindgut fermenters) sets the stage for a better understanding of artiodactyl–perissodactyl differences. Janis qualified the notion that foregut fermentation ranks superior to hindgut fermentation by showing the case in which the only food available has a high fiber/protein ratio. When that occurs, perissodactyls are more efficient than artiodactyls (able to retain cellulose digestion), whereas that ability decreases for artiodactyls. Many new data have been added since her 1976 review. Most notable for this work is the recent documenting of the very long passage times in sirenians.

Clemens and Maloiy (1982), in their study of digestive physiology of the largest living land mammals, compared gut proportions in relation to body length for *Loxodon* (~ × 5), *Diceros* (~ × 7.5), and *Hippopotamus* (~ × 17), confirming the tremendously increased hindgut for the hippo. In this case, however, hindgut fermentation does not appear to be the cause of the hindgut enlargement, because although the hindgut is shown to be a very elongate, simple tube lacking sacculation, chemical analysis indicates that not much fermentation takes place there. Instead, the greater part of the fermentation takes place in the forestomach. So why the tremendous increase in length of the hippo hindgut? Perhaps absorption of prefermented digesta is what is happening.

Could the pachyostotic condition in the uintathere long bones be a clue? Recalling the work of Hartman (1979) on *Trichechus,* I determined to further investigate the Sirenia, which I knew to be large[15] and to have both pachyostotic ribs and long retention times for their digesta. Returning to that work, I learned that they retain their digesta for nearly a week, and that they use hindgut fermentation. Further search was frustratingly slow until, by a timely serendipity, I opened my just-arrived copy of the *Australian Journal of Zoology* to find the Lanyon and Marsh (1995) study, "Digesta Passage Times in the Dugong." This confirmed the weeklong (or longer) digesta passage period and went further to determine the completeness of the process. Here was another hindgut fermenter par excellence. It gets out 80%–90% of all the nutrient value of its food, so in this regard is as efficient as the best foregut fermenters. Earlier, Best (1981) had cited comparably high digestibilities found by Lomolino (1977), which he found difficult to reconcile with lower values reported by others, and he decided that "[a]t present it would probably be better to accept the more conservative values of 50–60%."

[15] *Trichechus* commonly are up to 4.5 m long and weigh about 400 kg, occasionally up to 1,600 kg; *Dugong* commonly are 3.2 m long, and ~300 kg (some larger); *Hydrodamalis* was 15–30 m long and was estimated to have weighed 6,000 kg or more.

Intriguingly, the one other modern sirenian, Steller's Sea Cow, *Hydrodamalis gigas,* which is now extinct (made so within less than 40 years after its scientific discovery[16]) and never studied other than osteologically and for its behavior, until Steller (1751, 1899), who was so impressed by the size of the digestive tract, had one removed intact. It was over 20 times the length of the animal. The conclusion seems abundantly clear: Here was another more efficient hindgut fermenter. (For a concise account of the animal, see Forsten and Youngman, 1982.)

It is most interesting that all modern members of the Order Sirenia show a common pattern of size reduction of the dentition. This reduction has occurred subsequent to, and in spite of, very different earlier dental evolutionary specializations within the two suborders.

In trichechids, mesial drift had earlier developed to such a high degree that they are unique in exceeding the usual mammalian number of adult cheek teeth.[17] The teeth do have complex but low crowns (Fig. 73A). They form in the rear of each maxillary and jaw quadrant, drift forward, and are shed anteriorly. The process is similar to that in elephants, but unlike the elephants, which have but one or two teeth per quadrant functioning at a time, manatees have a continuous series, with six, eight, or more teeth functioning simultaneously. The teeth are used, and they do show wear, but like the teeth of uintatheres, they appear to be inadequate for processing the food for such a large animal.

Dugongs, although hypsodont, have a more standard, reduced cheek tooth number. They too have reduced the size of their teeth. In the past, the line had developed hypsodonty to a high degree, a feature the living dugongs retain (Fig. 73E; arrows indicate the right M2 and the alveolus from which it was removed to show its advanced hypsodonty). Again, the teeth are relatively small, and in spite of the hypsodont condition, they also appear to be inadequate.

Steller's Sea Cow, the largest of the modern dugongids, had done away with its teeth entirely. Instead, it had horny plates and did little food processing with them (Fig. 73F). So within this one order, we see animals with such highly efficient hindgut digestion that the teeth largely became unnecessary. This superfluous condition seems to be what happened with the terminal uintatheres.

The genetics for the teeth are deeply rooted and because of this, I suspect run counter to Dollo's law. Obviously, it is there for the first two lineages, in which the teeth had become so highly specialized, either for extreme mesial drift, on the one hand, or for hypsodonty, on the other, that the teeth—even though not critically needed—persist in miniature in two of the lines. In the third line, in which no teeth are retained, it is likely that the genetic basis for tooth formation is also (at least partially, if not largely) still present, masked by some mutation with a stronger selective advantage that could not succeed were the teeth still highly selected.

From all of this, especially from their massive pelves, I conclude that the terminal uintatheres had a digestive system similar to that of the sirenian. Surely they had a very large hindgut, and almost certainly they had hindgut fermentation and long residence times for the digesta, resulting in nearly complete digestion. As with the sirenians, demands placed on the teeth were greatly reduced. That this was achieved accounts for their anomalously "inadequate appearing" (Wood, 1932) small cheek teeth.

Summary and Conclusions

The Field Museum's collection of uintatheres from the Washakie Formation is here described and illustrated for the first time. It is compared with other uintathere materials of about the same age in our collection and in other collections from various locations in western North America. The collection consists of more than 80 specimens col-

[16] From Yakovlev's account, translated by G.N. Shkurkin and published by Domning, 1978, we learn that the meat of Steller's Sea Cow was the primary protein source of the inhabitants of Commander (= Bering) and Mednyy (= Copper) Islands, whose coastal shallows were its home. Consumed extensively not only by the people living in the area it inhabited, but also taken to provision ships stranded in those northern waters, it was sluggish and relatively easy to catch. Apparently many were fatally wounded quite unnecessarily. Domning (1978), in his major study of sirenian evolution, has provided the most thorough work on the order. In addition to osteology, paleontology, and systematics, he presents further evidence to that of Steller (1751, 1899) relating to the demise of this large inoffensive beast. Stejneger (1883, 1893, 1925) and Golder (1922), with translation by Stejneger.

[17] In addition to the comparable situation in elephants, many macropodids also have an extensively developed condition of mesial drift. Most notable among them is *Peradorcas* (Sanson, 1983). Here, too, normal tooth numbers are exceeded, but probably not to the extent that occurs in *Trichechus.*

lected over the past 46 years by my field parties and for the past decade by John Flynn's crews. It includes one of the very best adult skulls of *Uintatherium anceps* in existence (PM 53933, the Funderburk skull) and, more important, the skull of a young juvenile (PM 8019). There are several partial skeletons; one is that of a young adult with most of its rib cage and right fore- and hindlimbs in partial articulation (PM 55423). Another, that of a newborn animal (PM 3896), is at an ontogenetic stage never before reported. It consists of a left maxillary, the unfused ossifications of 8–10 vertebrae, a scapula, an ilium, some ribs, and other scraps. Three other partial skeletons are in the collection: one that had been articulated but was badly weathered out; and two others that were disarticulated and spread out, one of them over an area of about 6 × 30 ft (1.8 × 9 m), and the other was strung out along a shallow stream channel for about 300 ft (91 m). Finally, several specimens of lower teeth and jaws preserve the incisor–canine area adequate to begin to give a glimpse of the sort of variation that occurs in that part of the jaw. Additionally, many of the better specimens in the collections of the American Museum, Denver Museum, Princeton and Yale Museums, and the U.S. National Museum are illustrated and discussed, including the type specimens.

For *Eobasileus cornutus,* there is much less material. Our best pair of lower jaws (PM 1737) is incomplete, but fortunately its cheek teeth are nearly all present and fairly well preserved. We are extremely fortunate in having the well-preserved complete skull of this species that E.S. Riggs collected in the Uinta Basin early in the century. Presently on exhibit in the last of the Life Over Time halls, it is as fine a skull of the species as exists, being more complete than the type and Denver Museum specimens. As with *U. anceps,* the types for *E. cornutus* and its junior synonym (*Uintacolotherium blayneyi*) are illustrated.

Measurements (skull, jaw, dental, and postcranial) for these two taxa (*U. anceps* and *E. cornutus*) are presented in a series of 19 tables. Bivariate plots, measurements of each of the cheek teeth, are shown in four figures (Figs. 25, 40, 61, and 65). Included in these tables and graphs are the type specimens and many of the specimens in collections at other institutions.

The genus *Tetheopsis* is eliminated: the genus, its type species *T. speirianus,* and the other named species *T. ingens* are in synonymy with *Eobasileus cornutus. Tetheopsis* was known only from the Washakie Formation; a few came from the top of TWkA1, most from more or less throughout TwkA2. I now recognize a transition zone within the formation, from the top 86 ft (~28 m; about Bed 615 of Unit TWkA1, Old Lower Washakie, and the bottom ~70 ft (21 m; up to about Bed 625 of TWkA2, Old Upper Washakie. Previously for the Washakie Basin, Wheeler (1961) had considered *U. anceps* to be restricted to TWkA1 and *E. cornutus* to TWkA2. I now modify that view so as to extend the latter species downsection slightly into the transition zone at the top of TWkA1 and keep its upper limit at the top of TWkA2. Those *Tetheopsis* specimens that are in some way "aberrant" *U. anceps* all come from the transition zone, and they show a departure from that species in the direction of *E. cornutus,* where I therefore assign them. The few specimens from this zone that remain are of uncertain assignment. Elimination of *Tetheopsis* makes sense not only from a systematic perspective, but also on ecologic and geographic grounds.

Following the descriptions is a section on the paleobiology of these unique terminal members of the Order Dinocerata, Family Uintatheridae. Modern partial homologues for these two monotypic genera were looked for and considered, and the appropriateness of each was evaluated. In spite of the successful use of teeth as estimators of body size for most mammals, it does not work for all of the truly gigantic terrestrial mammals, and it works even less well for these terminal uintatheres; it therefore is inappropriate. Either the teeth are disproportionately large, as is the case in the modern large ungulates, or they are, disproportionately small in the uintatheres compared with teeth of most mammals. They simply do not scale with teeth of the majority of mammals, so that size estimators based on dental measures fail to give reasonable results.

The longstanding puzzle about the supposedly inadequately small dentitions of these uintatheres (Wood, 1932) is reevaluated and explained. That these uintatheres were giant mammals—about the size of hippos and large rhinos, to judge from limb bone proportions and head and body lengths—has long been accepted. A recent assessment based on regression equations incorrectly gave estimates of about half that size. That assessment failed, I am convinced, because it was based mostly on regression formulas that involved the teeth, which, as shown, is inappropriate in this case. One other terrestrial partial homologue exists: the elephants. Elephants are so much larger than rhinos, hippos, and uintatheres that one is apt

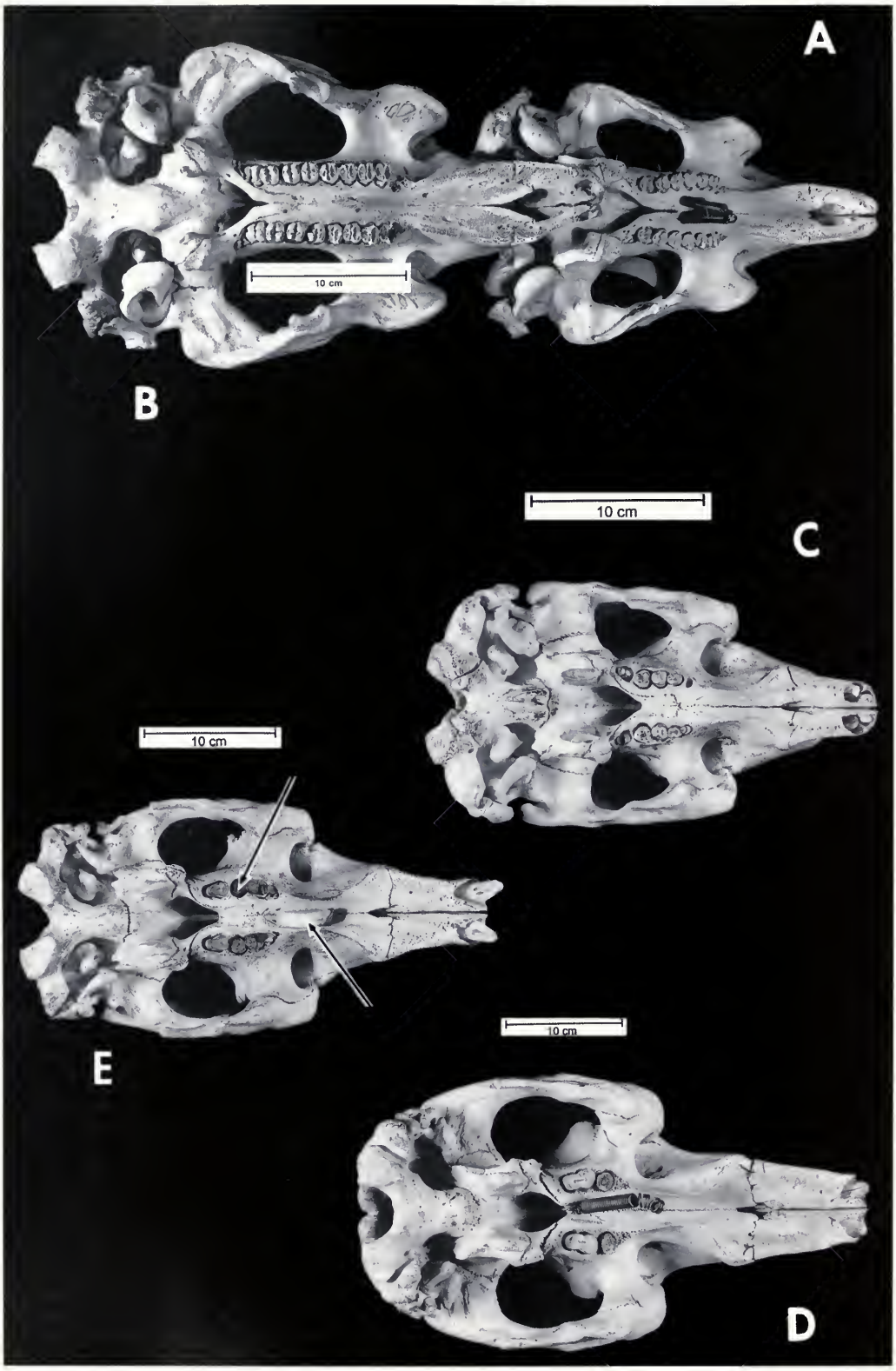

FIGURE 73.

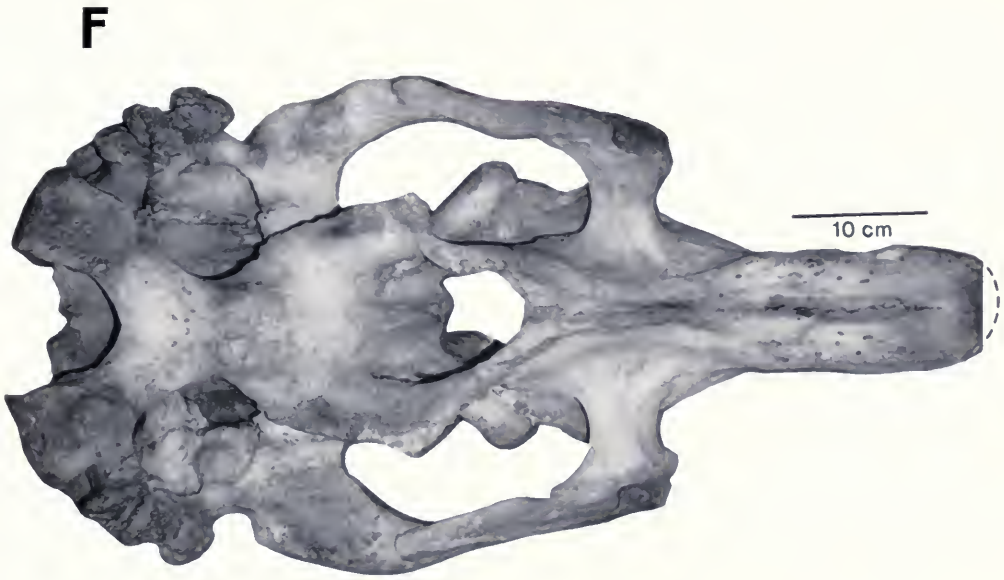

←

FIGURE 73.

Palatal views of sirenian skulls to illustrate variations of cheek-tooth conditions in the modern representatives. In this Order, tooth size reduction has been the dominant trend during the Neogene, regardless of whatever earlier dental specialization occurred or what method of tooth replacement was used. All are herbivores, with highly developed hindgut fermentation.

I contend that because of their extremely large hindgut with its highly efficient hindgut fermentation, the teeth of modern sirenians have become nearly, if not entirely, superfluous and that this development of efficient fermentation happened long after the earlier dental specializations were fixed. Because of the deep-seated genetics for their earlier differing dental specializations, however, a size-reduced dentition is usually retained, although it may even be lost.

Trichechus inunguis, FMNH 13888, is shown in **A**; *T. manatus,* FMNH 34911, is shown in **B.** *Dugong dugon,* FMNH 15561, 65744, and 68781, is shown in **C–E.** These modern forms retain relatively small, functional teeth, but they each have a very large hindgut and hindgut fermentation. In **E,** arrows point to one of the miniaturized hypsodont molars and its alveolus, typifying size reduction in *Dugong* with its previously numerically reduced dentition. In **F,** I show *Hydrodamatis rhytina,* BMNH 1947.10.21.2 (a race of *Hydrodamalis gigas*), an animal that has done away with teeth entirely. It had a tremendous hindgut, proportionately larger than the others.

This order demonstrates the probable developments in the terminal uintatheres. They had a long dental development that was rendered nearly superfluous when they "discovered" efficient hindgut fermentation, which explains the size reduction of their dentition (FMNH neg. nos. GEO 86025 (A–B), 86085 (C), 86083 (D), and 86084 (E)).

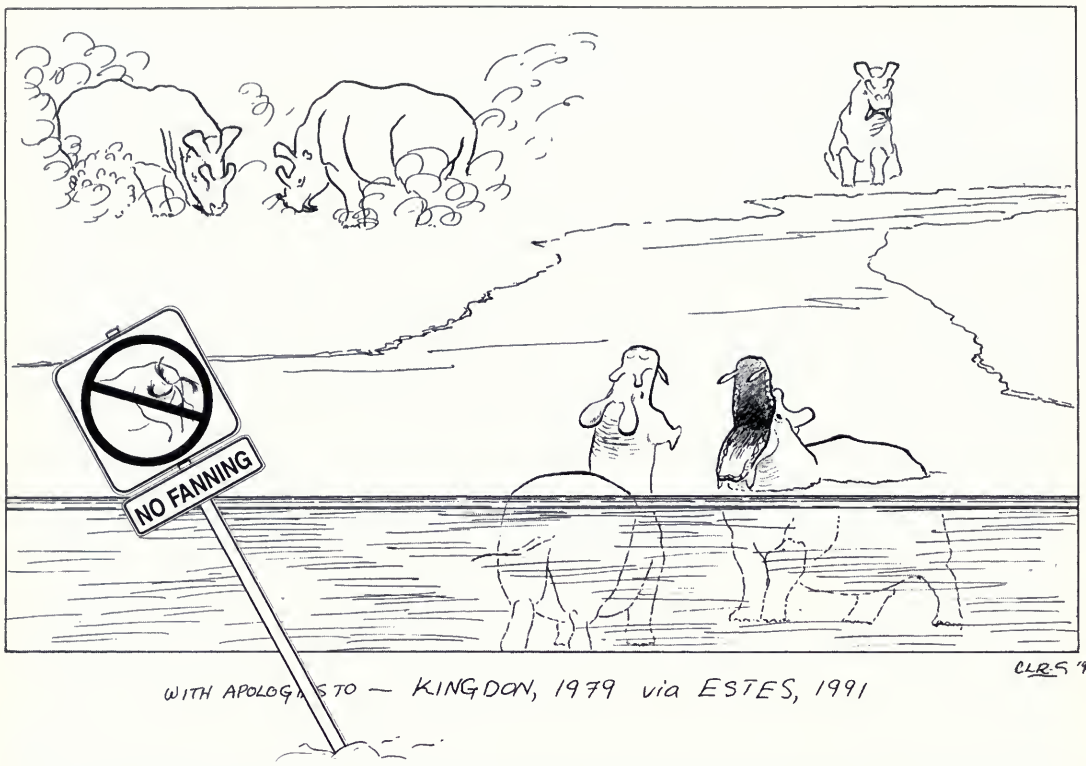

FIG. 74. Whimsical view of uintathere habit and habitat. Cartoon drawn by Clara Richardson Simpson, borrowing from Kingdon's charming hippo sketches.

to dismiss them until the focus turns to their pelves. Uintathere hips are nearly as large as elephant hips, but otherwise their hindquarters are much smaller, far more comparable to the limbs of hippos and rhinos. Such outsized hips must exist in order to support a tremendous gut, especially a large hindgut. This suggested to me the possibility that uintatheres could have been hindgut fermenters, which led in turn to a brief foray into digestive physiology (an area in which I have no background training). I did know that foregut fermentation was considered to be the most efficient digestive route, and that hindgut fermentation was not only less efficient but also tended to be of longer duration.

Hartman's (1979) study of *Trichechus* suggested the Sirenia as yet another possible partial homologue. Living members are all large, and they are hindgut fermenters with an exceptionally large hindgut. The fact that the living sirenians and the terminal uintatheres both share the pachyostotic condition (which all secondarily aquatic vertebrates have in some parts of their skeleton) also encouraged me. That the sirenians lack large hips results from hips being unnecessary in the water to give support for body and gut. Not only is sirenian digestion by hindgut fermentation a lengthy process, it turns out to be equally as (highly) efficient as that of the best foregut fermenters. So I conclude that the best explanation for the very minimum-sized teeth in the terminal uintatheres is that they too somehow discovered hindgut fermentation. Not only that, but, as in the uintatheres, the living modern sirenians also show similarly reduced, but nevertheless still specialized, dentitions (Domning, 1978).

Also, it is clear that the size reductions seen in the teeth of sirenians came about long after the two main lines had already evolved in divergent, highly specialized ways: trichechids with elephant-like, extreme mesial drift, and with supernumerary molars: dugongids with a more standard tooth number, but with a high degree of hypsodonty. It appears that when the digestive specializations evolved, the previously highly selected dental features were no longer needed but remained in reduced form, doubtless because of a very deep-seated genetic underpinning. Finally, in

one dugongid line, that represented by Steller's Sea Cow, the teeth were finally eliminated altogether. The uintatheres, too, had a dental evolution from simple bunodonty to bunolophodonty that must have occurred before the reduction in tooth size because even with their small size, the teeth retain the bunolophodont speciality.

Thus, the partial analogues for interpreting the uintathere conditions are found to be: (1) large body size and general proportions of the large rhinos; (2) semiaquatic specialization of the hippos (but not necessarily all of their peculiar, unique behavioral features) (Fig. 74); (3) gigantic pelves of elephants: (4) pachyostotic condition of the sirenians; (5) hindgut enlargement of hippos and sirenians; and (6) the efficient hindgut fermentation of the sirenians.

No partial analogue alone can explain the uintathere condition, but taken together, each tells us something that helps explain how the terminal uintatheres managed to function with such small cheek teeth. Because the Sirenia, the only modern lineage with such a highly efficient hindgut fermentation physiology, have tooth reduction, it seems reasonable to infer that the uintatheres took that route as well.

Acknowledgments

As with almost any protracted project of over 40 years' gestation, many people have offered assistance with this work. The Field Museum has supported the greatest part of the field work, without which none of these Washakie studies could have been done, and I am grateful for that. I am indebted to my colleagues in the Department of Geology, who have been supportive and encouraging (even though several have had doubts and misgivings, not altogether unjustified, about whether the job would ever be completed). Study of the geology and fauna of the Washakie Formation in its various ramifications has been a serious commitment of mine since 1956, and this uintathere portion of that project has been both fascinating and time-consuming.

First and foremost, I am deeply indebted to both of my wives for their unstinting help and encouragement at home, at work, in the field, with specimen preparation, and with manuscript preparation. Priscilla assisted on all but two of the field seasons between 1956 and 1985; Hedy has done the same from 1986 to the present. Without their help, encouragement, and management, I could not have come this far with the work, nor could it have been nearly as comprehensive. My debt to them both is immeasurable.

I am very grateful for the help of the three generations of the Eversole family who have welcomed us as "neighbors" (we usually camped at the nearby Kinney Spring) and friends, giving much appreciated neighborly assistance. Roy and Emma Eversole helped us to find our way around and helped me make my first map. They also helped locate survey posts (some of which Roy had helped install when he worked for the surveyors early in the century). Since that time, John and Eva (Eversole) Corson, Elza and Lois Eversole, and, for the past two decades, John and Debbie Eversole have also offered assistance. It was during the late 1950s and early 1960s, when Roy and Emma had left the ranch, and before Elza and Lois could take over full time, that first the Corsons and then two hired manager famlies, the Gardner (Wise) Potters, and Sam and Bea Dusenbery, ran the Eversole ranch for several years. All these individuals also became our friendly, helpful "neighbors."

Very special thanks go to Mary Jane Daniels, the late Murray Daniels, and their family, not only for help in the field, including finding many new localities, but also for opening their home to us, offering assistance, and keeping us going when breakdowns (mostly broken springs) required repair that otherwise would have been very time-consuming and expensive.

Other helpers in the field include Orville L. Gilpin, then chief preparator in the Department of Geology; David Collier; the late Pete Lambert, preparator; and my son Jonathan; John W. Wilson III and Ann Wilson; Alan and Gwen Turnbull and family, especially Elizabeth (Turnbull) Green and Alan III; Andrzej and Jane (Turnbull) Przedpelski, and their sons Karl and Thomas Przedpelski, John Joyce, Dr. Edgar Allin and his wife Drucilla Allin; Earl Hoffman, Richard Axtell, Betsy Mayer, Sue (Hutchins) Heimer; the late Mark Dudnikov; Thomas Brooks; Charles Henry; Walter Mockler; Robert Hicks; Dan McCann; the late Jim and Ruby Poydack; Ethan Beasley; Geoffrey Gable; Jean (Seiler) Luchterhand, Dr. Kubet Luchterhand, and his students, Bill Ponte, Andy Moyad, Robert Emblade, Jim Sadlowski, Charles Wisniewski, Kathy Bergman, and Robert Costello; John Flynn, the late Steve McCarroll, and their field crews, including Robin Watley, Susan Vandenbosch, Greg Buckley, Bob Masek, and Paul

Brinkman; and several Bureau of Land Management crews that have found and reported specimens for us to investigate and collect.

Two sets of friends of mine (and of the Museum) each spent a week helping in the field: Richard and China Oughton, and Lincoln and June Douglas and their son David. I believe that we all benefited, for in addition to help with prospecting and collecting, I got on-the-spot opportunities to explain the fossils and geology to avid listeners and enthusiastic helpers.

Preparation was by Orville Gilpin, Stanley Kuczak, John Harris, Sue (Hutchins) Heimer, David Techter, Walter Mockler, Robert Hicks, Katherine Krueger, William Simpson, Hedy Turnbull, the late Steven McCarroll, Robert Masek, and me.

I would also express my gratitude to friends and colleagues who have helped in various other ways with suggestions and discussions relating to the work: Rainer Zangerl for all of that, for introducing me to the Washakie Basin in 1948, and for his constant help and encouragement ever since then; Malcolm McKenna for allowing me to photocopy his personal copy of the air photo coverage of the basin so that I could make the montaged map for my locality and stratigraphic designations (until the USGS topographic sheets became available, mostly in 1970s); Henry Roehler for sharing his vast knowledge of the basin; Kubet Luchterhand for keeping up the field work in 1983 and again in 1985, when Priscilla's illness prevented my full-time participation; John Flynn for his paleomagnetic studies and subsequent collecting and assuming continuation of the project with the help of the late Steve McCarroll; Paul Predecki and his students for the X-ray diffraction work; Ernest Lundelius for many repeated discussions and suggestions; and Everett Olson,† Bryan Patterson,† Dwight Davis,† Paul McGrew,† Mac West, Mary Dawson, Peter Robinson, Jack Wilson, Wann Langston, and Craig Black† for less frequent, but nevertheless meaningful suggestions or assistance.

In 1960, the late Morris and Marie Skinner generously loaned their New York apartment for the month I spent studying the American Museum collections, and Ned Colbert loaned me his office while he was in the field. Without that help, I could not have done the work in New York. Donald Baird and Glenn Jepsen led me through the Princeton materials, and J. Leroy Kay arranged for my study at the Carnegie Museum, as did Karl Waage and Elwin Simons at Yale. More recently, I have been helped by Jason Lillegraven and Brent Breithaupt at Laramie, by Richard Stucky in Denver, and by Sue Ann Bilbey and Alden Hamblin in Vernal.

Many of the photographs were taken by John Baylis and Homer Holdren or Ferdinand Huysmans in the 1960s, when they were the Museum's photographers. More recently, Ronald Testa, then Nina Cummings, John Weinstein, Diane Alexander White, James Balodimos, and Kim Mazanek have all contributed to that effort, and I am thankful for their fine work. Linda E. Lillegraven took the photographs of the Wyoming skull, and Dick Wicker took the photograph of the Denver skull (DMNH Photo Archives copyright ©1995). Jeremy Hooker took measurements for me so that I could scale my photograph of the BMNH *Hydrodamalis* skull. To all of them go my sincere thanks.

Three museum artists have aided with every step in the preparation of the figures; montaging the photos, labeling them and dropping out the background clutter, and advising with the layouts: Zbigniew Jastrzebski† and Lori Grove have done the greater part, and Clara Simpson and Marlene (Hill Werner) Donnaly were consulted from time to time.

Finally, my thanks go to a good friend and benefactor who has given much encouragement, especially since my retirement. He wishes to remain anonymous. He knows who he is, and I take this opportunity to thank him again for his continued friendship and support.

If I have forgotten anyone, please excuse the lapsus; it has been a long time in the works, and I have no other excuse.

Three reviewers—Jason Lillegraven, Spencer Lucas, and one anonymous person—all gave constructive criticisms. I appreciate their efforts, and have complied with most suggestions, with improved results. However, I could not bring myself to divide the work into two papers, as one reviewer advised.

Literature Cited

ALEXANDER, R. MCN. 1980. Forces in animal joints. Engineering in Medicine, **9:** 93–97.

———. 1985. Mechanics of posture and gait of some large dinosaurs. Zoological Journal of the Linnean Society, **83:** 1–25.

ANDERSON, J. F., A. HALL-MARTIN, AND D. A. RUSSELL. 1985. Long-bone circumference and weight in mammals, birds and dinosaurs. Journal of Zoology, London, **207:** 53–61.

BERING, V. (see Golder, F. A. 1922. Bering's Voyages, Vol. 1: The Log Books).

BEST, R. C. 1981. Foods and feeding habits of wild and captive Sirenia. Mammalian Review, **11:** 3–29.

BRADLEY, W. H. 1945. Geology of the Washakie Basin, Sweetwater and Carbon Counties, Wyoming, and Moffat County, Colorado. Oil and Gas Investigations, Preliminary Map 32 United States Geological Survey.

———. 1964. Geology of the Green River Formation and associated Eocene rocks in southwestern Wyoming and adjacent parts of Colorado and Utah. United States Geological Survey, Professional Papers, no. **496-A:** i–iv, A1–A86.

CALDER, W. A. III. 1984. Size, Function, and Life History. Harvard University Press, Cambridge.

CERLING, T. E., J. R. EHLERINGER, AND J. N. HARRIS. 1998. Carbon dioxide starvation, the development of C4 ecosystems and mammalian evolution. Philosophical Transactions of the Royal Society, Biological Science, **353:** 159–171.

CLEMENS, E. T., AND G. M. O. MALOIY. 1982. The digestive physiology of three East African herbivores: The elephant, rhinoceros and hippopotamus. Journal of Zoology, London, **198:** 141–156.

COMBS, M. C. 1983. Large mammalian clawed herbivores: A comparative study. American Philosophical Society, Transactions, **73**(7): 1–96.

———. 1989. Interrelationships and diversity in the Chalicotheriidae. In Prothero, D. R., and R. Schoch, eds., The Evolution of Perissodactyls. Oxford University Press, Oxford, 537 pp.

COOK, H. J. 1926. A new genus of uintatheres from Colorado. Colorado Museum of Natural History, Proceedings, **6:** 7–11.

COPE, E. D. 1872a. The famous telegram describing extinct proboscideans from Wyoming. Palaeontological Bulletin, **5.**

———. 1872b. Notices of new vertebrata from the upper waters of Bitter Creek, Wyoming Territory. Palaeontological Bulletin, **6:** 1–4, and American Philosophical Society, Proceedings, **12:** 483–486.

———. 1872c. Second notice of extinct vertebrates from Bitter Creek, Wyoming. Palaeontological Bulletin, **7:** 1–2, and American Philosophical Society, Proceedings, **12:** 487–488.

———. 1872d. Notice of proboscideans from the Eocene of southern Wyoming. American Philosophical Society, Proceedings, **12:** 580.

———. 1872e. The Proboscideans of the American Eocene. American Naturalist, **6:** 773–774.

———. 1873a. Geology and Paleontology. *In* Hayden, F. V., Sixth Annual Report of the United States Geological Survey of the Territories (see Hayden 1873).

———. 1873b. The Monster of Mammoth Buttes. The Penn Monthly, *August, 1873,* pp. 521–534.

———. 1874. Eocene Period. *In* Hayden, F. V. Annual Report of the United States Geological Survey of the Territories (see Hayden 1874).

———. 1881. On the Vertebrata of the Wind River Eocene Beds of Wyoming. Bulleton, United States Geological and Geographic Survey of the Territories, **6**(1): 132–202.

———. 1884 (1885). The vertebrata of the Tertiary Formations of the West. Book 1. Report, United States Geological Survey of the Territories, no. 3, 1009 pp.

———. 1885. The genera of Dinocerata. American Naturalist, **19:** 594.

COVEY, D. S. G., AND S. M. MCCARROLL. 1996. The Artiodactyl fauna of the Washakie Formation, Eocene age, of southwestern Wyoming. Abstracts, Journal of Vertebrate Paleontology, **16** (Suppl. 3): 29A.

DAMUTH, J. 1990. Problems in estimating body masses of archaic ungulates using dental measurements, pp. 229–253. *In* Damuth, J., and B. J. MacFadden, eds., Body Size in Mammalian Paleobiology: Estimation and Biological Implications. Cambridge University Press, Cambridge, 397 pp.

DAMUTH, J., AND B. J. MACFADDEN (eds.). 1990. Body Size in Mammalian Paleobiology: Estimation and Biological Implications. Cambridge University Press, Cambridge, 397 pp.

DOMNING, D. P. 1978. Sirenian evolution in the North Pacific Ocean. University of California Publications in Geological Sciences, **118:** 1–176.

EDINGER, T. 1929. Die fossilen Gehirne: Ergebnisse Anatomie und Entwicklungsgeschichte, **28:** 1–249.

———. 1961. Anthropocentric misconceptions in paleoneurology. Proceedings of the Rudolf Virchow Medical Society, New York, XIX (1960), pp. 56–107. S. Karger, Basel and New York.

EISENBERG, J. F. 1981. The Mammalian Radiations: An Analysis of Trends in Evolution, Adaptation, and Behavior. University of Chicago Press, Chicago, 610 pp.

ESTES, R. D. 1991. Behavior Guide to African Mammals. University of California Press, Berkeley, 611 pp.

FAWCETT, D. W. 1942. The amedullary bones of the Florida manatee (*Trichechus latirostris*). American Journal of Anatomy, **71:** 271–309.

FLEROV, K. K. 1952. New Dinocerata from Mongolia (in Russian). [Prodinoceratidae; Gobiatheriinae]. Doklady Akademiya Nauk SSSR, **86:** 1029–1032.

———. 1957 (1967 transl. from Russian). Dinocerata of Mongolia. Akademiya Nauk SSSR, Trudy Paleontologicheskovo Instituta, **67:** 1–84.

FLOWER, W. H. 1876 (1873). Professor Flower's Hunterian lectures on the relation of extinct to existing Mammalia. Part IV. Nature, **13:** 387–388.

FLYNN, J. J. 1983. Correlation and geochronology of middle Eocene strata from the western United States. Ph.D. diss., Columbia University, New York.

———. 1986. Correlation and geochronology of middle Eocene strata from the western United States. Palaeogeography, Palaeoclimatology, Palaeoecology, **55:** 335–406.

FOOSE, T. J. 1982. Trophic strategies of ruminant vs nonruminant ungulates. Ph.D. diss., University of Chicago, Chicago.

FORSTEN, A., AND P. M. YOUNGMAN. 1982. *Hydrodamalis gigas.* Mammalian Species, no. 165, pp. 1–3.

FORTELIUS, M. 1990. Problems with using fossil teeth to estimate body sizes of extinct mammals, pp. 207–228. *In* Damuth, J., and B. J. MacFadden, eds., Body Size in Mammalian Paleobiology: Estimation and Biolog-

ical Implications. Cambridge University Press, Cambridge, U.K., 397 pp.

Foss, S. E., W. D. Turnbull, and L. Barber. 2001. Observations on a new specimen of *Archaeonodon* (Mammalia, Artiodactyla) from the Eocene Washakie Fm. of southern Wyoming. Journal of Vertebrate Paleontology, Abstracts, **21**(3): 51.

Gingerich, P. D. 1974. Size variability of the teeth in living mammals and the diagnosis of closely related sympatric fossil species. Journal of Paleontology, **48:** 895–903.

———. 1977. Correlation of tooth size and body size in living hominoid primates, with a note on relative brain size in *Aegyptopithecus* and *Proconsul.* American Journal of Physical Anthropology, **49:** 517–532.

Gingerich, P. D., B. H. Smith, and K. Rosenberg. 1982. Allometric scaling in the dentition of primates and prediction of body weight from tooth size in fossils. American Journal of Physical Anthropology, **58:** 89–100.

Golder, F. A. 1922. Bering's Voyages. Vol. 1, The Log Books. American Geographical Society, Research Series, 371 pp. (See also Steller, G. W., 1925 for Vol. 2: Steller's Journal, ibid, 290 pp.)

Granger, W. 1909. Faunal horizons of the Washakie formation of southern Wyoming. American Museum of Natural History, Bulletin, **26:** 13–23.

Hartman, D. S. 1979. Ecology and behavior of the Manatee (*Trichechus manatus*) in Florida. American Mammal Society, Special Publication, **5:** 1–153.

Hayden, F. V. 1873. Sixth annual report of the United States Geological Survey of the territories embracing portions of Montana, Idaho, Wyoming and Utah,: 1872: Part II. Special Reports—Geology and paleontology; E. D. Cope, "On extinct vertebrates of Eocene of Wyoming," pp. 545–649.

———. 1874. Annual Report of the U.S. Geological Survey of the territories embracing Colorado: 1873 (Seventh); E. D. Cope, Chapter III, "Eocene Period," pp. 456–458.

Hutchison, J. H. 1971. CF. Uintatherium (Dinocerata, Mammalia) from the Uintan (Middle to Late Eocene) of Southern California. PaleoBios, **12:** 1–8.

Janis, C. M. 1976. The evolutionary strategy of the Equidae and the origin of rumen and cecal digestion. Evolution, **30:** 757–774.

———. 1990. Correlation of cranial and dental variables with body size in ungulates and macropodoids, pp. 255–299. *In* Damuth, J., and B. J. MacFadden, eds., Body Size in Mammalian Paleobiology: Estimation and Biological Implications. Cambridge University Press, Cambridge, U.K., 397 pp.

Janis, C. M., and M. Carrano. 1992. Scaling of reproductive turnover in archosaurs and mammals: Why are large terrestrial mammals so rare? Annales Zoologici Fennici, **28:** 201–216.

Jerison, H. J. 1961. Quantitative analysis of evolution of the brain in mammals. Science, **133:** 1012–1014.

———. 1970. Brain evolution: New light on old principles. Science, **170:** 1224–1225.

———. 1971. Quantitative analysis of the evolution of the camelid brain. American Naturalist, **105:** 227–239.

———. 1973. Evolution of the Brain and Intelligence. Academic Press, New York, 482 pp.

Johannson, A. 1914. Petrographic analysis of Bridger, Washakie, and other Eocene formations of the Rocky Mountains. Bulletin of the American Museum of Natural History, **33:** 209–222.

Kihm, A. J. 1984. Early Eocene mammalian faunas of the Piceance Creek Basin, Northwestern Colorado. Ph.D. diss., University of Colorado, Boulder.

King, C. 1878. Report of the geological exploration of the 40th parallel. Vol. 1, Systematics. Professional Papers, Engineering Dept., United States Army, No. 18.

Kingdon, J. 1979. East African Mammals. Part IIIB, Large Mammals. University of Chicago Press, Chicago.

Krishtalka, L., R. K. Stucky, R. M. West, M. C. McKenna, C. C. Black, T. M. Bown, M. R. Dawson, D. J. Golz, J. J. Flynn, J. A. Lillegraven, and W. D. Turnbull. 1987. Eocene (Wasatchian through Duchesnean) biochronology of North America, pp. 77–117. *In* Woodburne, M. O., ed., Cenozoic Mammals of North America: Geochronology and Biostratigraphy. University of California Press, Berkeley.

Lanyon, J. M., and H. Marsh. 1995. Digesta passage times in the dugong. Australian Journal of Zoology, **43:** 119–128.

Leidy, J. 1872a. On some new species of fossil mammalia from Wyoming. Academy of Natural Science, Philadelphia, Proceedings, **1872:** 169.

———. 1872b. The above reprinted in September 1872, American Journal of Science.

———. 1872c. Remarks on fossil mammals from Wyoming. Academy of Natural Science, Philadelphia, Proceedings, **1872:** 240–242.

———. 1873. Contributions to the Extinct Vertebrate Fauna of the Western Territories: United States Geological (Hayden) Survey Territories Report, Part 1: 1–358, Pls. 1–37. For uintatheres pp. 93–109; 331–334; Pls. XXV, XXVI (1–8), XXVII (30–34), XXVIII (1–2).

Lomolino, M. V. 1977. The ecological role of the Florida manatee (*Trichechus manatus latirostris*) in water hyacinth dominated ecosystems. M.S. thesis, University of Florida, Gainesville.

Love, J. D. 1961. Definition of Green River, Great Divide and Washakie Basins, southwestern Wyoming. Bulletin of the American Association of Petroleum Geologists, **45:** 1749–1755.

MacFadden, B. J. 1990. Dental character variation in paleopopulations and morphospecies of fossil horses and extinct analogues, pp. 128–141. *In* Prothero, R. D., and R. M. Shoch, eds., The Evolution of Perissodactyls. Oxford University Press, Oxford, U.K.

MacFadden, B. J., and R. C. Hulbert, Jr. 1990. Body size estimates and size distribution of ungulate mammals from the Late Miocene Love Bone Bed of Florida, pp. 337–363. *In* Damuth, J., and B. J. MacFadden, eds., Body Size in Mammalian Paleobiology: Estimation and Biological Implications. Cambridge University Press, Cambridge, U.K., 397 pp.

Majorana, V. 1990. Evolutionary strategies and body size in a guild of mammals, pp. 69–102. *In* Damuth, J., and B. J. MacFadden, eds., Body Size in Mam-

malian Paleobiology: Estimation and Biological Implications. Cambridge University Press, Cambridge, U.K., 397 pp.

MARSH, O. C. 1871. Notice of some new fossil mammals from the Tertiary formation. American Journal of Science, **2:** 35–44.

———. 1872a. Preliminary description of new Tertiary mammals. Part I. American Journal of Science, **4:** 122–128.

———. 1872b. Note on *Tinoceras anceps.* American Journal of Science, **4:** 322.

———. 1872c. Notice of a new species of *Tinoceras.* American Journal of Science, **4:** 323.

———. 1873. On the gigantic fossil mammals of the order Dinocerata. American Journal of Science, **5:** 117–122.

———. 1885. The gigantic mammals of the Order Dinocerata. Fifth Annual Report of the Director of the United States Geological Survey, Washington, D.C.

———. 1886. Dinocerata, a monograph of an extinct order of gigantic mammals. United States Geological Survey Monograph, **10:** 1–237. (Preprinted in 1884 and 1885.)

———. 1897. Vertebrate fossils from the Denver Basin. United States Geological Survey Monograph, **27:** 473–551.

MATTHEW, W. D. 1909. Faunal lists of the Tertiary Mammalia of the West. *In* Osborn, H. F., ed., Cenozoic mammal horizons of western North America. United States Geological Survey, Bulletin, **361:** 91–138.

MATTHEW, W. D., W. GRANGER, AND G. G. SIMPSON. 1929. Additions to the fauna of the Gashato Formation of Mongolia. American Museum Novitates, **376:** 1–12.

MAUGHER, R. I. 1977. K-ar ages of biotites from tuffs in Eocene rocks of the Green River, Washakie, and Uinta Basins, Utah, Wyoming, and Colorado. University of Wyoming, Contributions to Geology, **15:** 17–41.

MCCARROLL, S. M. 1994. Perissodactyls from the Washakie Formation (Middle-Late Eocene), Washakie Formation, Wyoming. Journal of Vertebrate Paleontology, **14**(Suppl. 3, abstract): 37A.

———. 1995. An Early Uintan fauna from the upper unit of the Adobe-town Member, Washakie Formation, Washakie Basin, Wyoming. Journal of Vertebrate Paleontology, **15**(Suppl. 3, abstract): 42A.

MCCARROLL, S. M., J. J. FLYNN, AND W. D. TURNBULL 1993. Biostratigraphic and magnetic polarity correlations of the Washakie Formation, Washakie Basin, Wyoming. Journal of Vertebrate Paleontology, **13** (Suppl. 3, abstract): 49A.

———. 1996a. Biostratigraphy and magnetostratigraphy of the Bridgerian-Uintan, Washakie Formation, Washakie Basin, Wyoming, pp. 25–39. *In* Prothero, D. R., and R. J. Emry, eds., The Terrestrial Eocene-Oligocene Transition in North America. Cambridge University Press, Cambridge, U.K., 688 pp.

———. 1996b. The mammalian faunas of the Washakie Formation, Eocene age, southern Wyoming. Part III. The Perissodactyls. Fieldiana: Geology, n.s., **33:** 1–37.

———. 1996c. A Late Bridgerian fauna from the Kinney Rim Member of the Washakie Formation, Washakie Basin, Wyoming. Journal of Vertebrate Paleontology, **16**(Suppl. 3, abstract): 51A–52A.

OSBORN, H. F. 1881. A memoir upon *Loxolophodon* and *Uintatherium,* two genera of the sub-order Dinocerata. E. M. Museum of Geology and Archaeology, College of New Jersey, Contribution, **1:** 5–44.

———. 1898. Evolution of the Amblypoda. Part I. Taligrada and Pantodonta. Bulletin of the American Museum of Natural History, **10:** 169–218.

———. 1907. Tertiary mammal horizons of North America. Bulletin of the American Museum of Natural History, **23:** 237–253.

———. 1909. Cenozoic mammal horizons of western North America. United States Geological Survey, Bulletin, **361:** 1–90.

OSBORN, H. F., AND W. GRANGER. 1932. Coryphodonts and uintatheres from the Mongolian expedition of 1930. American Museum Novitates, **552:** 1–16.

OSBORN, H. F., AND J. B. MCMASTER. 1881. A memoir upon *Loxolophodon* and *Uintatherium,* two genera of the suborder Dinocerata. Contributions, E. M. Museum of Geology and Archaeology, Princeton College, **1:** 1–54 (McMaster part, pp. 46–54).

OSBORN, H. F., AND F. SPIER, JR. 1879. The lower jaw of *Loxolophodon.* American Journal of Science, **17,** ser. 3: 304–309.

OSBORN, H. F., W. B. SCOTT, AND F. SPEIR. 1887. Paleontological report of the Princeton Scientific Expedition of 1877. Contributions, E. M. Museum of Geology and Archaeology, Princeton College, **1:** 1–107.

OWEN-SMITH, R. N. 1988. Megaherbivores: The Influence of Very Large Body Size on Ecology (Cambridge Studies in Ecology). Cambridge University Press, Cambridge, U.K., 369 pp.

PAULA COUTO, C. DE. 1952. Fossil mammals from the beginning of the Cenozoic in Brazil. Condylarthra, Litopterna, Xenungulata and Astrapotheria. Bulletin, American Museum of Natural History, **99:** 355–394.

PETERS, R. H. 1983. The Ecological Implications of Body Size. Cambridge University Press, Cambridge, U.K.

PIANCA, E. R. 1970. On r and K selection. American Naturalist, **106:** 581–588.

RICQLES, A. 1989. Les mechanismes heterochroniques dans le retour des tetrapodes au milieu aquatique, pp. 171–178. *In* Colloque International du CNSR: Ontogenese et Evolution. Dijon, 1986.

ROEHLER, H. 1969. Stratigraphy and oil shale deposits of Eocene rocks in the Washakie Basin, Wyoming, pp. 197–206. *In* 21st Field Conference, Tertiary Rocks of Wyoming, Wyoming Geology Association Guidebook.

———. 1972. A review of Eocene stratigraphy in the Washakie Basin, pp. 3–19. *In* West, R. M., ed., Field Conference on Tertiary Biostratigraphy, Southern and Western Wyoming. Garden City, New York.

———. 1973. Stratigraphy of the Washakie Formation in the Washakie Basin, Wyoming. United States Geological Survey, Bulletin, **1369:** 1–40.

———. 1985. Geologic Map of Kinney Rim 30 × 60 Minute Quadrangle, Wyoming and Colorado. Miscel-

laneous Investigations Series. United States Geological Survey.

———. 1992a. Eocene Rocks in Green River and Washakie Basins, Southwest Wyoming. *In* Geology of the Eocene Wasatch, Green River, and Bridger (Washakie) Formations, Greater Green River Basin, Wyoming, Utah, and Colorado. United States Geological Survey, Professional Papers (1506-D. I–IV, D1-D83).

———. 1992b. Correlation, composition, areal distribution, and thickness of Eocene stratigraphic units, Greater Green River Basin. *In* Geology of the Eocene Wasatch, Green River, and Bridger (Washakie) Formations, Grester Green River Basin, Wyoming, Utah, and Colorado. United States Geological Survey, Professional Papers (1506-E. I–IV, E1-E49).

ROMER, A. S. 1964. Cope versus Marsh. Systematic Zoology, **13:** 201–307.

ROTH, V. L. 1990. Insular dwarf elephants: A case study in body mass estimation and ecological inference, pp. 151–179. *In* Damuth, J., and B. J. MacFadden, eds., Body Size in Mammalian Paleobiology: Estimation and Biological Implications. Cambridge University Press, Cambridge, U.K., 397 pp.

RUFF, C. 1990. Body mass and hindlimb bone cross-sectional and articular dimensions in anthropoid primates, pp. 119–149. *In* Damuth, J., and B. J. MacFadden, eds., Body Size in Mammalian Paleobiology: Estimation and Biological Implications. Cambridge University Press, Cambridge, U.K., 397 pp.

RUSSELL, D. A., AND D. E. RUSSELL. 1993. Mammal-dinosaur convergence. National Geographic Research and Exploration, **91:** 70–79.

SANSON, G. D. 1983. Evolution of feeding adaptations in fossil and Recent macropodids, pp. 489–506. *In* Rich, P. V., and E. M. Thompson, eds., The Fossil Vertebrate Record of Australia. Monash University Offset Printing Unit, Clayton, Victoria, Australia, 759 pp.

SCHMIDT-NIELSEN, K. 1984. Scaling: Why Is Animal Size So Important? Cambridge University Press, Cambridge, U.K.

SCHOCH, R., AND S. LUCAS. 1985. The phylogeny and classification of the Dinocerata (Mammalia, Eutheria). Bulletin Geological Institutions, University of Uppsala, n.s., **11:** 31–50.

SCOTT, W. B. 1886. On some new forms of the Dinocerata. American Journal of Science, **31:** 303–307.

———. 1937. A History of Land Mammals in the Western Hemisphere. Macmillan, New York, 786 pp.

SHKURBIN, G. V. 1978. Translation of Russian texts (Petr Yakovlev and Stepan Cherepanov). *In* Accounts of the Sea Cow, Appendix II of Domning (1978).

SILVA, M., AND J. A. DOWNING. 1995. CRC Handbook of Mammalian Body Masses. CRC Press, Boca Raton, Fla., 359 pp.

SIMPSON, G. G. 1935. Descriptions of the oldest known South American mammals, from the Rio Chico Formation. American Museum Novitates, **793:** 1–25.

SIMPSON, G. G., AND A. ROE. 1939. Quantitative Zoology. McGraw-Hill, New York.

SINCLAIR, W. J. 1909. The Washakie, a volcanic ash formation. Bulletin, American Museum of Natural History, **26:** 25–28.

STEINEGER, L. 1883. Contributions to the history of the Commander Islands. No. 1: Notes on the natural history, including descriptions of new Cetaceans. Proceedings, United States National Museum, **6:** 58–89.

———. 1893. Skeletons of Steller's sea cow preserved in the various museums. Science, **21:** 81.

STELLER, G. W. 1751. De bestiis marinis. Nov. Comm. Acad. Sci. Petropolitanae, **2:** 289–398, Pls. 14–16 (fide Domning).

———. 1899. The beasts of the Sea. *In* Jordan, D. S., ed., The Fur Seals and Fur-Seal Islands of the North Pacific Ocean. U.S. Government Printing Office, Washington, D.C., Part 3, Art. 8: 179–218 (abridged translation of Steller 1751 by W. Miller and J. E. Miller).

SULLIVAN, R. 1980. A stratigraphic evaluation of the Eocene rocks of southwestern Wyoming. Geological Survey of Wyoming Report of Investigations, no. 2.

TILNEY, F. 1931. Fossil brains of some early Tertiary mammals of North America. Bulletin of the Neurological Institute, New York, **1:** 430–505.

TURNBULL, W. D. 1972. The Washakie Formation of Bridgerian-Uintan Ages, and the related faunas. *In* West, R. M., ed., Field Conference, Tertiary Biostratigraphy of Southern and Western Wyoming, pp. 20–31. Garden City, New York.

———. 1978. The mammalian faunas of the Washakie Formation, Eocene age, of southern Wyoming. Part I. Introduction: The geology, history and setting. Fieldiana: Geology, n.s., **33:** 569–601.

———. 1991. *Protoptychus hatcheri* Scott, 1895. The mammalian faunas of the Washakie Formation, Eocene age, of southern Wyoming. Part II. The Adobetown member, middle division (= Washakie B), TWKa/2 (In Part). Fieldiana: Geology, n.s., **21:** 1–33.

———. 1993. Additions to knowledge of the Uintatheres of the Washakie Formation and aspects of their biology. Journal of Vertebrate Paleontology, **13** (suppl. 3, abstract): 60A.

———. 1995. The problem of the Uintatherium molars (once more), pp 261–265. *In* Radlanski, R. J., and H. Renz, eds., Proceedings of the 10th International Symposium on Dental Morphology. C & M Brünne Gbr., Berlin.

TURNBULL, W. D., AND D. M. MARTILL. 1988. Taphonomy and preservation of a monospecific titanothere assemblage from the Washakie Formation (Late Eocene), southern Wyoming: An ecological accident in the fossil record. Palaeogeography, Palaeoclimatology, Palaeoecology, **63:** 91–108.

VANVALKENBURGH, B. 1990. Skeletal and dental predictors of body mass in carnivores, pp. 181–205. *In* Damuth, J., and B. J. MacFadden, eds., Body Size in Mammalian Paleobiology: Estimation and Biological Implications. Cambridge University Press, Cambridge, U.K., 397 pp.

WALKER, E. P. 1968. Mammals of the World, 2nd ed. J. L. Paradiso, ed. Johns Hopkins University Press, Baltimore; pp. 1332, 1334–1335.

WALL, W. P. 1983. The correlation between high limb-bone density and aquatic habits in Recent mammals. Journal of Paleontology, **57:** 197–207.

WEST, R. M. 1982. Fossil mammals from the Lower

Buck Hill Group, Eocene of Trans-Pecos Texas: Marsupicarnivora, Primates, Taeniodonta, Condylarthra, bunodont Artiodactyla and Dinocerata. The Pearce-Sellards Series, no. 35 (Texas Memorial Museum, University of Texas, Austin).

WHEELER, W. H. 1955. Taxonomy of the larger American uintatheres. Geological Society of America, Bulletin, **66:** 1699.

———. 1960. The uintatheres and the Cope-Marsh war. Science, **131:** 1171–1176.

———. 1961. Revision of the Uintatheres. Peabody Museum of Natural History Bulletin, **14.**

WILSON, J. A. 1974. Early Tertiary vertebrate faunas, Vieja Group and Buck Hill Group, Trans-Pecos, Texas: Protoceratidae, Camelidae, Hypertragulidae. Texas Memorial Museum Bulletin, **23.**

———. 1978. Stratigraphic occurrence and correlation of Early Tertiary Vertebrate faunas, Trans-Pecos Texas. Part I. Vieja Area. Texas Memorial Museum Bulletin, **25:** 1–42.

WOOD, H. E. 1932. The problem of *Uintatherium* molars. Bulletin of the American Museum of Natural History, **48:** 599–604.

WORTMAN, J. L. 1901. Studies of Eocene Mammalia in the Marsh collection, Peabody Museum. American Journal of Science, 4th ser., **11:** 333–450.

ZANGERL, R. 1935. *Pachypleurosaurus edwardsi,* Cornalia sp. Osteologie—Variationsbreite—Biologie, pp. 1–80. *In* Peyer, B., ed., Die Triasfauna der Tessiner Kalkalpen. Abh. der Schweiz. Palaeont. Gesellschaft, **56.**

———. 1994. *Brachyuranochampsa eversoldi,* gen. et spec. nov., a new crocodilian from the Washakie Eocene of Wyoming. Annals of the Carnegie Museum, **30:** 77–84.

Tables 1 through 19 appear on the following pages.

TABLE 1. Skull measurements for *Uintatherium anceps* (in m).

Description of measurement†	Marsh's 1886 data		Cast PM 59828 (*El. parvum*, PUM 10298)	Cast P 26977 (holotype, *U. robustum*, ANSP 12607)
	D. mirabile, YPM 11036	*T. pugnax*, YPM 1104		
(M) Total length of skull from nasals to occipital crest	0.76	0.77	≥0.675	—
(Wheeler's length measurements for above are:	0.74	0.77	0.68)‡	
(M) Total length from premaxillaries to occipital condyles	0.66	0.665	≫0.53	—
Total length from nasals to occipital condyles	0.64[c]	—	≥0.59	—
Skull height from top of occipital crest to bottom of condyles	0.28[c]	—	~0.26	≫0.168
(M) Greatest transverse diameter through parietal condyles	0.385	0.425	0.265	—
(M) Greatest transverse diameter through occipital crest	0.26	0.305	0.212	—
(M) Greatest transverse diameter through postglenoid processes	0.25	0.28	0.225	0.246
(M) Length of palate from end of premaxillaries to posterior nares	0.35	0.33	≫0.23	—
(M) Length of palatine bone on median line	0.030	—	?0.05	—
(M) Length of maxillary bone on median line	0.185	—	?0.15	—
(M) Width of palate between last molars	0.050	0.084	0.049	—
(M) Width of palate between first molars	0.065	0.084	0.069	—
(M) Width of palate between first premolars	0.050	0.056	0.053	—
(M) Width of palate across diastema	0.07	0.096	~0.054	—
(M) Width of palate between canines	0.105	0.132	0.071	—
(M) AP diameter of zygomatic fossa	0.165	0.12	0.124	—
(M) Transverse diameter of zygomatic fossa	0.08	0.096	0.066	—
(M) Distance from top of parietal protruberance to end of postglenoid process	0.37	0.37	0.22	—
(M) Distance from top of maxillary protruberance to end of canine	0.415	0.48	—	—
(M) Vertical diameter of foramen magnum	0.051	0.05	0.058	0.046
(M) Transverse diameter of foramen magnum	0.055	0.075	0.058	0.053
Diastemal length	0.059[c]	—	0.08	—
Maximum distance across condyles	0.146[c]	—	0.15	0.148
Length of canine from alveolar border to tip	>0.18[c]	—	—	—
	[c]Measured on cast FMNH P 26232.		Measured on cast AMNH 14367, now PM 59828. ? = Not included in statistics.	

Statistics for all of Wheeler's specimens plus PM 53933 and 60171:

Notes: [c]Measured on cast, [e]estimated, [k]crushed, [r]as restored.

* See notes in respective columns.

† Marsh's (1886, p. 32) measurements are indicated by (M). The other parameters measured I have interpolated in between Marsh's parameters in this listing.

‡ Wheeler's other values for *U. anceps* are (his chart 3): 2 skulls at 0.081 (AMNH 2367, 1683); 4 at 0.80 (AMNH 1694, USNM 5919, 16663, YPM 11222); 5 at 0.77 (AMNH 1689, PUM 10297, YPM 11039, 11042, 11231); 2 at 0.75 (YPM 11235, 11499); 3 at 0.74 (AMNH 1665, 2366, YPM 11241); 1 at 0.73 (YPM 11202); 1 at 0.72 (YPM 11236); 2 at 0.71 (AMNH 1664, 1671); 1 each at 0.69, 0.68, 0.67, and 0.64 (respectively AMNH 1693, PUM 10298, AMNH 1691, and USNM 4212). One of the specimens Wheeler included in *Tethiopsis* (AMNH 1687) I include in *U. anceps*.

§ This specimen is transitional anatomically and stratigraphically and is not included in the statistics.

TABLE 1. *Extended.*

FMNH specimens				Measured on cast PM 60171 (of specimen in Gunma prefecture Museum of Natural History)		USNM specimen on exhibit	UW 13644§	N*	Range*	Mean*	s*
PM 53933	PM 8019 (juv.)	PM 55406B	PM 55406A (juv.)	L	R						
0.75	0.55[r]	≫0.63	—	0.703		—	0.765*	5	0.675–0.770	0.732	
0.66	0.495[r]	≫0.56	—	0.614		0.67	—	5	0.614–0.670	0.654	
0.72	~0.51[r]	≫0.58	—	0.66		—	≥0.73*	4	0.59–0.72	0.653	
0.272	~0.175	>0.272	—	0.245		—	—	4	0.245–0.280	0.264	
0.36	0.25[r]	—	—	0.302		—	—	5	0.265–0.425	0.347	
0.3	~0.196[r]	—	—	0.253		—	—	5	0.212–0.305	0.266	
0.285	0.23[r]	—	—	0.245		—	—	6	0.225–0.285	0.255	
0.36	>0.17[e]	—	?~0.2	0.315		—	—	4	0.315–0.360	0.339	
0.027	—	—	?0.055	?0.04		—	—	2	0.027–0.030	0.029	
0.285	~0.125[e]	—	~0.14	—		—	—	2	0.185–0.285	0.235	
0.071	~0.05[e]	—	—	0.035[k]		—	—	4	0.049–0.084	0.064	
0.081	0.057[e]	—	0.035[k]	0.038[k]		—	—	4	0.065–0.084	0.075	
0.063	0.036[e]	—	0.038[k]	0.030[k]		—	—	4	0.050–0.063	0.056	
0.086	0.041[e]	—	0.030[k]	0.065[k]		—	—	4	0.054–0.096	0.077	
0.15	0.075[e]	—	0.065[k]	0.088		—	—	5	0.071–0.150	0.109	
0.153	~0.12	—	0.08	0.135	0.14	—	—	7	0.120–0.165	0.141	
0.089	—	—	—	0.076	0.078	—	—	7	0.066–0.096	0.081	
0.374	0.19	0.375	—	0.36	0.30	—	—	8	0.220–0.375	0.343	0.55
0.395	—	—	—	0.322	0.295	—	—	6	0.295–0.480	0.382	
0.045	0.041	~0.048	—	0.045		—	—	7	0.045–0.058	0.049	
0.055	0.066	~0.055	—	0.05		—	—	7	0.050–0.075	0.057	
0.076	dc-p: 0.053	—	≫0.093*	0.045	0.054	—	—	7	0.045–0.083	0.065	
0.161	>0.141	0.128	—	0.144		~0.180	~0.16*	7	0.128–0.180	0.151	
0.182[r]	alv. ~0.155	—	0.06*	0.149	0.154	—	—	4	0.149–0.182	0.163	
			*Canine exposed but unerupted. ?Not included in statistics.	Both crushed ([k]) and ? not included in statistics.			*Not included in statistics.	* Juveniles excluded; only adults and subadults are included in these statistics.			
								29	0.640–0.810	0.748	

TABLE 2. Jaw measurements of *Uintatherium anceps* (in m).

Description of measurement†	Marsh's 1886 data: *D. laticeps*, YPM 11039 L	*D. laticeps*, YPM 11039 R	*U. segne*, YPM 11194 R	Cast of Leidy's *U. robustum*, holotype, P 26977 (ANSP 12610–13)	FMNH Specimens: PM 38781 L	PM 38781 R	PM 53921 R	PM 53932 L	PM 53932 R	PM 53933 L	PM 53933 R
(M) Greatest length of ramus	0.54		0.49	—	—	—	—	—	—	—	—
(M) Height of coronoid process from bottom of ramus	0.235		0.19	—	—	—	—	—	—	—	—
Greatest length from condyles to inferior mandibular process	0.453[c]	0.472[c]	—	—	—	—	—	—	>0.40	—	—
Length from condyles to midpoint of mental foramen	0.420[c]	0.448[c]	—	—	—	—	—	—	~0.355	—	—
(M) Depth of ramus at last molar	0.09		0.075	0.08	—	—	—	>0.072	≫0.05	—	—
(M) Depth of ramus at tusk (IMP) process	0.185		0.17	—	—	≫0.128	—	—	>0.097	—	—
(M) Extent of symphysis	0.18		0.165	—	~0.2		—		—	≫0.155	
(M) Extent of diastema	0.11[c]	0.10	—	—	—	—	—	—	0.078*		
(M) Extent of molar series	0.116[c]	0.124	0.145	—	—	—	—	0.086	0.088	—	—
(M) Greatest width across condyles	0.295		—	—	—		—		—	—	—
(M) Transverse diameter of condyle	0.087	0.093[c]	0.076	>0.061	—	—	0.086	—	—	.079	.079
Distance from anterior of IMP to anterior of symphysis (parallel to dentition)	~0.07[c]	~0.075	—	—	—	>0.103	—	—	—	—	≫0.06
Alveolar length, i1–c	≥0.111[c]	0.107	—	—	−0.108	~0.106	—	—	—	—	—
Height from tip of coronoid to top of condyle	~0.098[c]	~0.100[c]	—	>0.074	—	—	—	—	—	—	—
Distance from bottom of angle to bottom of condyle	~0.108[c]	~0.104[c]	—	≫0.075	—	—	—	—	—	0.12	—
(M) Vertical diameter of condyle	~0.048	0.041[c]	0.040	0.031	—	—	0.046	—	—	0.039	0.040

[c] Measured on FMNH cast P 26233. Marsh's values are used in statistics.

* alv. c-p2

TABLE 2. *Extended.*

FMNH Specimens (*cont.*)								Utah Field House, UFH 54515		American Museum, AMNH 1678 (juv.)		PM 60171 (Cast of specimen from Gunma Prefecture Museum)		Denver Museum, EPV 1849					
PM 54801 (juv.)		PM 55174		PM 55827		PM 56022													
L	R	L	R	L	R	L	R	L	R	L	R	L	R	L	R	N	Range	Mean	s
>0.46	>0.46	—	0.559	—	≫0.43	—	—	—	—	—	—	0.46 alv.	0.48*	0.435	0.472	6	0.46–0.57	0.517	
—	—	≫0.23	0.268	—	0.223	—	—	—	—	—	~0.178[c]	0.212	0.217	—	—	6	0.190–0.268	0.024	
—	—	0.498	0.475	—	≥0.432	—	—	—	—	—	—	0.38	0.377	—	—	5	0.377–0.498	0.432	
—	—	0.442	~0.425	—	0.390	—	—	—	—	—	—	0.344	0.343	—	—	6	0.343–0.442	0.383	
0.068	0.065	0.091	0.090	0.080	0.074	~0.102	~0.103	—	—	—	—	0.066	0.066	—	—	11	0.066–0.103	0.083	0.013
~0.050	0.051	0.211	0.195	—	0.107	—	>0.136	0.195	0.200	—	—	>0.12	0.108	0.150	0.148	10	0.107–0.211	0.167	0.038
>0.124		0.174		—		—		—		—		0.15		0.16		6	0.150–0.200	0.176	
~0.071	~0.066	—	~0.15	—	—	—	—	—	—	—	—	0.086	0.116**	—	—	6	0.066–0.150	0.087	
~0.092	~0.089	~0.17 alv.	~0.16 alv.	0.096	0.100	—	—	~0.089	~0.090	m3's not formed		0.078	0.072	—	—	13	0.072–0.195	0.098	0.021
—		0.184		—		—		—		—		0.245		—	—	3	0.184–0.295	0.241	
—	—	≥0.078	~0.08	—	>0.059	>0.053	≥0.062	—	—	>0.042	≫0.032	0.059	0.058	—	—	11	0.058–0.093	0.076	0.012
No IMP		~0.12	~0.14[e]	—	—	—	—	—	—	—	—	0.075	0.078	—	—	4	0.075–0.14	0.103	
~0.087	—	—	~0.104	—	—	—	—	—	—	—	—	0.104	0.075***	—	—	6	0.104–0.111	0.107	
—	—	0.096	0.088	—	0.087	—	—	—	—	—	0.064[c]	0.099	>0.098	—	—	6	0.087–0.100	0.095	
—	—	—	0.123	—	0.096	—	—	—	—	0.071	0.072	0.104	0.105	—	—	7	0.071–0.123	0.099	
—	—	0.047	0.047	—	≥0.038	0.038	0.038	—	—	0.032	0.032	0.031	0.031	—	—	16	0.031–0.048	0.039	0.006
None of these are included in statistics.		Alveolar measures not included in statistics.										* From tip of i1. ** i3–p2. *** i1–i3.							

Notes: [c]Measured on cast, [e]estimated, [f]as restored.

*, **, *** See notes in respective columns.

† Marsh's (1886, p. 40) measurements are indicated by (M). The other parameters I have interpolated in between Marsh's parameters in this listing.

TABLE 3. Skull measurements of *Eobasileus cornutus* (in m).

Description of measurement†	*Lefalophodon discornutus*, holotype AMNH 5040	Marsh's 1886 measurements, *T. ingens* YPM 11041	Cast PM 8088 (of holotype of *T. speirianus*, PUM 10079)	*Tetheopsis speirianus*, YPM 11043
(M) Total length of skull from nasals to occipital crest	0.915 (W)	0.92 (W) 0.87[c]	0.977 (W) 0.973[c]	0.92 (W)
(M) Total length from premaxillaries to occipital condyles	0.867*	0.815	≫0.75	—
Total length from nasals to occipital condyles	0.844*	0.867[c]	0.85	—
Skull height from top of occipital crest to bottom of condyles	0.303*	0.372[c]	0.34	—
(M) Greatest transverse diameter through parietal protuberances	0.403*	0.47	0.485	—
(M) Greatest transverse diameter through occipital crest	0.291*	0.33	0.265	—
(M) Greatest transverse diameter through postglenoid processes	0.284*	0.30	0.295	—
(M) Length of palate from end of premaxillaries to posterior of nares	0.418*	0.40	—	—
Length of palatine bone on median line	—	—	?0.106	—
Length of maxillary bone on median line	—	—	?0.104	—
(M) Width of palate between last molars	0.078*	0.064	0.063	—
(M) Width of palate between first molars	0.075*	0.065	>~0.074	—
(M) Width of palate between first premolars (P2)	0.050*	0.056	0.065	—
(M) Width of palate across diastema	0.051*	0.09	0.059	—
(M) Width of palate between canines	0.108*	0.10	0.102	—
(M) AP diameter of zygomatic fossa	0.181*	0.19	0.173	—
(M) Transverse diameter of zygomatic fossa	0.083*	0.08	0.092	—
(M) Distance from top of parietal protuberance to end of postglenoid process	0.539*	0.52	0.406	—
Distance from top of maxillary protuberance to end of canine	0.686**	—	—	—
(M) Vertical diameter of foramen magnum	—	0.075	0.04	—
(M) Transverse diameter of foramen magnum	—	0.045	0.053	—
Diastemal length	0.112*	0.088[c]	~0.091 ~0.085	—
Maximum distance across condyles	0.190*	0.18[c]	0.171	—
Length of canine from alveolar border to tip	0.258–0.275**	—	—	—
	* Measured on scaled photograph. Not included in statistics. ** Canine is partly out of its alveolus. Not in statistics.	[c] Measured on cast FMNH P 26234.	[c]Measured on cast FMNH PM 8088. Questionable values (?) not included in statistics.	

Notes: [c]Measured on cast, [e]estimated, [k]crushed, [r]as restored.

*. ** See notes in respective columns.

† Marsh's (1886, p. 33) measurements for *Tinoceras ingens* are indicated by (M). The other parameters measured I have interpolated in between Marsh's parameters. Wheeler's measurements are indicated by (W). For the first measurement, total length of skull from nasals to occipital crest, only Wheeler's data are used in the statistics.

‡ This specimen is included in this table for comparison, and because the individual tooth measurements and stratigraphy suggest it. The data are not included in the statistics. If they are included, N = 9, range = 0.765–0.977, mean = 0.876, and s = 0.08.

TABLE 3. *Extended.*

Uintacolotherium blayneyi, holotype DMNH EPV 495	*Eobasileus uintensis* (nom. nud.) Holotype, P 12170	P 12164*	P 12198	Transition specimen, Univ. of Wyoming Museum, UW 13644‡	N	Range	Mean	s
0.94 (W)	0.85 (W)	—	—	0.765	8*	0.780–0.977*	0.890*	0.07*
—	0.79	≫0.515	—	—	2	0.790–0.815	0.803	—
—	0.84	≫0.52	—	≥0.73	3	0.840–0.867	0.852	—
—	0.375	0.255	~0.22[k,e]	—	4	0.255–0.375	0.336	—
—	0.46	—	0.28[k]	—	3	0.460–0.485	0.472	—
—	0.28	—	0.215[k]	—	3	0.267–0.330	0.292	—
—	0.278	≫0.13	~0.25[k,e]	—	3	0.278–0.300	0.291	—
—	0.418	—	—	—	2	0.400–0.418	0.409	—
—	—	—	—	—	0	0.106?		—
—	—	—	—	—	0	0.104?		—
0.078	0.069	—	—	—	4	0.063–0.078	0.069	—
—	0.067	—	—	—	3	0.065–0.074	0.069	—
(0.081 at P2)	0.048	—	—	—	4	0.048–0.081	0.063	—
—	0.051	—	—	—	3	0.051–0.090	0.067	—
0.087	~0.12	—	—	—	4	0.087–0.120	0.102	—
—	0.152 0.151	~0.18	~0.12[k,e]	—	5	0.151–0.190	0.169	—
—	0.076 0.058	>0.045	~0.08	—	5	0.058–0.092	0.077	—
—	0.503 0.490	0.269	0.303[e]	—	5	0.269–0.520	0.438	—
—	0.566 0.575	—	—	—	2	0.566–0.575	0.571	—
—	—	0.058	—	—	2	0.040–0.075	0.058	—
—	~0.05	—	—	—	3	0.045–0.053	0.049	—
0.062	0.101 0.097	—	—	—	6	0.062–0.101	0.087	—
—	0.197	—	—	~0.16	4	0.160–0.197	0.177	—
—	— 0.186	—	—	—	1	0.186		—

* Laterally very crushed.

[k] Crushed; not included in statistics.

Not included in statistics.

* Includes Wheeler's values for YPM 11567 (0.820) and AMNH 1687 (0.780).

TABLE 4. Jaw measurements of *Eobasileus cornutus* (in m).

Description of measurement†	PM 1737		UCMP 81356 (♀)	*Tinoceras annectens* CMNH 29493	
	L	R	L	L	R
(M) Greatest length of ramus	~0.642	~0.646	≥0.527	>0.52	—
(M) Height of coronoid process from bottom of ramus	—	~0.25	≈0.236	≥0.245	—
Greatest length from condyles to inferior mandibular process	~0.521	~0.54	0.52	0.485	—
Length from condyles to midpoint of mental foramen	—	~0.525	0.443	0.443	—
(M) Depth of ramus at last molar	0.141	—	0.089	0.075	—
(M) Depth of ramus at tusk (IMP) process	—	~0.15	>0.088	—	—
(M) Extent of symphysis	~0.228		>0.121	>0.15	
(M) Extent of diastema	~0.135	~0.135	—	?0.088	—
(M) Extent of molar series	~0.105	—	0.100	0.102	0.098
Greatest width across condyles	~0.272		—	—	
(M) Transverse diameter of condyle	~0.081	~0.084	0.051	—	—
Distance from anterior of IMP to anterior of symphysis (parallel to dentition)	—	—	—	—	—
Alveolar length, i1-c	>0.093	>0.093	—	—	—
Height from tip of coronoid to top of condyle	—	—	0.085	—	—
Distance from bottom of angle to bottom of condyle	—	—	~0.125	—	—
(M) Vertical diameter of condyle	—	—	0.035	—	—

? Not included in statistics.

Notes: [c]Measured on cast.

* See notes in respective columns.

† Marsh's (1886, p. 40) measurements are indicated by (M). The other features I have interpolated in between Marsh's features in this listing.

‡ All measures are scaled from Wheeler's plate 14, fig. 2.

TABLE 4. *Extended.*

Uintacolotherium blayneyi				*Tinoceras longiceps*, holotype YPM 11256	*Tinoceras annectens*, holotype YPM 11043‡	*Tetheopsis stenops*, holotype YPM 11567				
DMNH EPV 493		Holotype, DMNH EPV 496								
L	R	L	R	R	L	L	N	Range	Mean	s
—	—	—	—	0.57	~68.4	—	5	0.527–0.684	0.614	
—	—	—	—	0.26	~0.3	—	5	0.236–0.300	0.258	
—	—	—	—	—	~0.6	—	5	0.485–0.600	0.533	
—	—	—	—	—	~0.56	—	4	0.443–0.560	0.493	
—	—	—	—	0.084	~0.09	—	5	0.075–0.141	0.096	
0.097	0.098	—	—	0.10	—	—	4	0.097–0.150	0.111	
0.160		—	—	0.185	—	—	3	0.160–0.228	0.191	
—	—	—	—	0.145	—	—	3	0.135–0.145	0.138	
~0.093	—	0.110	0.115	—	~1.20	0.098[c]	9	0.093–0.120	0.105	0.009
—		—		—	—	—	1	~0.272		
—	—	—	—	0.070	—	—	4	0.051–0.084	0.072	
—	—	—	—	—	—	—	0			
—	—	—	—	—	—	—	2	both 0.093	0.093	
—	—	—	—	—	~0.12	—	1	0.085		
—	—	—	—	—	~0.14	—	1	~0.125		
—	—	—	—	0.045	~0.048	—	2	0.035–0.045	0.04	

FMNH cast P 26235.

[c]Measured on cast PM 3944.

TABLE 5. *Uintatherium anceps,* upper dentition (in cm).

	Uintatherium anceps								
	Washakie Basin, Washakie Fm., TWkA1								
	PM 53933		Juvenile PM 3896	Juvenile PM 8019		Juvenile PM 54406A		Utah Field House UFH 54015	
Item	L	R	L	L	R	L	R	L	R
L P2-M3	16.12	16.08	—	>14.83	15.48	—	<16.08	—	—
L P3-M3	12.86	12.85	—	11.84*	12.35*	—	<13.77	—	—
L P4-M3	10.82	10.76	—	9.85*	10.22*	—	<11.52	—	—
L P2-P4	6.56	6.62	—	~6.85b	6.83	6.79	7.17	—	—
L P2-P3	4.31	4.28	—	~4.71b	4.51	4.88	4.94	—	—
L P2-M1	8.66	8.7	—	~8.89b	~8.82	~9.75	9.58	—	—
L P2-M2	11.51	11.54	—	>11.25b	11.5	—	12.66	—	—
L P3-P4	4.56	4.55	—	4.73	4.74	4.84	4.88	—	—
L P3-M2	9.67	9.75	—	>9.11	9.75	—	10.4	—	—
L P3-M1	6.74	6.75	—	6.72	6.66	~7.8	7.34	—	—
L P4-M1	5.46	5.47	—	4.43	4.46	~5.6	5.01	—	—
L P4-M2	7.51	7.46	—	>6.87	7.32	—	8.01	—	—
L M1-M3	8.75	8.74	—	~7.8*	8.20*	—	<9.94	—	—
L M1-M2	5.45	5.46	—	>4.84	5.04	—	5.75	—	—
L M2-M3	6.62	6.62	—	>5.83*	6.31*	—	<7.73	—	—
C									
L (at alv.)	5.67	5.87	—	—	—	≫2.11	···	—	5.3
W	2.78	2.53	—	—	—	—	···	—	3.7
L tip → alv.	>17.38 (~18.75)	>11.8	—	—	—	≫6	···	—	—
P2/									
L	1.98	2.07	···	~2.0	2.2	2.06	2.2	—	—
AW	2.16	2.18	···	···	2.14	2.08	2.23	—	—
PW	2.11	2.15	···	2.07	1.96	2.04	2.11	—	—
P3/									
L	2.28	2.19	···	2.37	2.33	2.64	2.5	—	—
AW	2.93	2.71	···	2.66	2.59	≧2.68	3	—	—
PW	2.72	2.72	···	2.57	2.47	2.87	≧2.61	2.8	—
P4/									
L	2.46	2.34	>1.85	2.43	2.36	2.6	2.58	>2.3	—
AW	2.94	≧2.64	>2.56	2.72	2.83	—	2.63	—	—
PW	2.63	2.73	>2.48	2.66	2.64	—	2.52	—	—
M1/									
L	2.51	2.52	1.89	~2.1	~2.2	—	2.66	2.3w	—
AW	2.64	2.67	2.87	2.33	2.43	—	2.57	—	—
PW	2.47	2.47	2.61	2.21	2.36	—	2.57	—	—
M2/									
L	3.22	3.18	>2.08	>2.65	3.11	—	3.29	3.4	—
AW	3.62	3.74	>2.57	>3.0	3.14	—	3.41	3.8	—
PW	3.38	3.38	>2.0	>3.0	2.85	—	3.16	>3.3[b]	—
M3/									
L	3.76	3.85	—	—	3.28	—	—	~4.5	—
AW	4.15	4.16	—	>3.15	3.54	—	—	4.2	—
PW	3.83	3.64	—	>2.8	3.05	—	≧3.73	—	—

*M3 deep in its crypt; not included in statistics.

Notes: [b]Broken, [e]estimated, [w]worn.
*See notes in respective columns.

TABLE 5. *Continued.*

	Uintatherium anceps								
	Washakie Basin, Washakie Fm., TWkA1								
	PM 53933		Juvenile PM 3896	Juvenile PM 8019		Juvenile PM 54406A		Utah Field House UFH 54015	
Item	L	R	L	L	R	L	R	L	R
dC (alv.)									
L			2.23						
W (2 roots)			0.54						
dP1 (alv.)									
L			0.38						
AW (1 root)			0.63						
dP2 (alv.)									
L			1.31						
AW			1.18						
PW			1.32						
dP3 (alv.)									
L			1.66 (root)						
AW			1.89 (root)						
PW			1.84 (root)						
dP4 (alv.)									
L			1.49						
AW			1.9						
PW			1.81						

(This page continues reading vertically from previous page.)

TABLE 5. *Extended.*

	Uintatherium anceps								
	Cast PM 60171 (of specimen in Gunma Prefecture Mus. of Nat. Hist.)†		Green River Fm. PM 26925	Bridger Basin and Fm. D Cast P 26232 (YPM 11036)		*E. parvum*, D-1 Cast PM 59828 (PUM 10298)*		Leidy's holotype (another specimen of *U. robustum*)††	
Item	L	R		L	R	L	R	L	R
L P2-M3	13.76	13.26	—	15.2	14.9	14.7	14.6[b]		
L P3-M3	11.61	11.49	—	13.25	13.08	12.3	12.72[b]		
L P4-M3	9.71	10.13	—	11.02	11.02	10.62	10.08[b]		
L P2-P4	6.61	5.79	—	6.79	6.8	6.33	6.82	ANSP 12607, 12609–13, and 12619–22 compose the holotype.	
L P2-P3	4.4	3.77	—	4.68	4.56	4.35	4.51		
L P2-M1	9.07	8.04	—	9.03	9.01	8.64	9.03		
L P2-M2	11.02	10.56	–	11.79	11.67	11.32	≧11.30		
L P3-P4	4.29	4	—	4.63	4.63	4.53	4.65		
L P3-M2	9	8.72	—	9.76	9.76	9.51	≧9.30		
L P3-M1	6.93	6.21	—	7.01	7.01	~6.64	6.82		
L P4-M1	4.88	4.65	—	4.69	4.75	4.58	4.51		
L P4-M2	7.11	7.01	—	7.54	7.56	7.41	>6.94[e]		
L M1-M3	7.34	7.75	—	8.83	8.88	8.64	~8.25		
L M1-M2	4.65	4.88	—	5.38	5.42	5.75	>5.12		
L M2-M3	5.28	5.51	—	6.8	6.56	6.39	···		
C								ANSP 12608	
L (at alv.)	4.46	4.88	—	6.6	6.76	4.4	4.3	~5	—
W	2.29	2.27	—	2.52	2.73	2.3	2.1	~3.1	—
L tip → alv.	15.5	15.1	—	>18.0[e]	—	—	—	≧17.5	—
P2/								(*Uintamastix*)	
L	2.27	1.9	—	2.27	2.26	2.33	2.26		
AW	1.95	1.93	—	2.3	2.15	~1.36	>0.95		
PW	2.06	2.36	—	2.27	2.29	~1.51	1.63		
P3/									
L	2.28	1.9	—	2.38	2.34	2.51	2.7		
AW	2.39	2.54	—	3.03	2.99	2.21	~2.61		
PW	2.46	2.6	—	2.91	2.85	2.44	2.51		
P4/									
L	2.25	2.38	—	2.33	2.3	2.4	2.19		
AW	2.63	3.01	—	3.0	2.85	≧2.43	≧2.61		
PW	2.6	3.09	—	2.84	2.75	3.16	>2.52		
M1/									
L	2.36	2.4	—	2.43	2.58	—	2.45		
AW	2.8	3.28	—	2.74	2.77	—	2.43		
PW	2.96	3.35	—	2.64	2.45	—	2.27		
M2/									
L	2.57	2.69	3.47	3.14	3.19	2.79	—		
AW	3.26	3.44	3.79	3.44	3.41	3.27	—		
PW	3.55	3.27	3.48	3.06	2.94	2.99	~2.94		
M3/									
L	3.03	3.01	—	4.24	3.55	3.27	—	3.71	3.95
AW	3.81	3.48	—	4.08	3.84	≧3.95	~3.5	4.05	4.14
PW	3.52	3.15	—	3.61	3.41	~3.06	~3.44	3.41	3.64
						*AMNH 14367.		[Above measures apply to left M3 of ANSP 12609, part of the holotype]#	

†New Colorado specimen.

††*U. robustum* and *Uintamastix* are synonyms of *Uintatherium anceps*. *Tetheopsis speirianus* is a synonym of *Tetheopsis stenus*. All four listed are also synonyms of *Eobasileus cornutus* (surviving generic name).

#P 26979 is a cast of ANSP 12609; P 26978 is a cast of ANSP 12608.

TABLE 5. *Extended.*

	Uintatherium anceps									
	USNM 2666 (old 1603)	USNM 2670	USNM W 5919 (old 1651)		USNM ____ (P2–M3 of skull); USNM B 16663		USNM B 18599		USNM B 18600	
Item			L	R	L	R	L	R	L	R
L P2-M3	—	—	17.78	15.98	—	14.5			—	16.16
L P3-M3	—	—	—	—	—	—			—	14.2
L P4-M3	—	12.26	—	—	—	—			—	11.62
L P2-P4										
L P2-P3										
L P2-M1										
L P2-M2	12	—	—	—	—	—			—	10.23
L P3-P4										
L P3-M2	—	—	—	—	—	—			—	>7.67
L P3-M1										
L P-4M1										
L P4-M2										
L M1-M3										
L M1-M2										
L M2-M3										
C					USNM B 16663					
L (at alv.)	—	—	—	—	—	—				
W	—	—	—	—	—	—				
L tip → alv.	—	—	—	—	—	—				
P2/										
L	2.06	—	2.16	—	2.19	2.1	>1.96	2.15	2.23	2.42
AW	2.27	—	2.55	—	—	2.2	1.99	1.89	2.11	2.05
PW	2.03	—	2.36	—	2.14	2.09	2.14	2.11	—	1.92
P3/										
L	2.33	—	2.74	2.72	2.25	2.22	2.56	2.51	2.47	2.46
AW	2.46	—	3.01	3.03	2.56	2.51	2.64	2.55	3.04	3.02
PW	2.2	—	2.80	2.87	2.42	2.52	>2.28	2.44	2.7	2.68
P4/										
L	2.48	2.57	2.86	2.47	2.15	2.17	—	2.16	2.38	3
AW	2.92	3.01	3.05	3.08	2.6	2.52	—	2.9	2.99	>3.08
PW	2.72	2.93	3.03	—	2.43	2.42	—	2.6	2.82	2.89
M1/										
L	2.73	2.34	2.65	—	2.24	2.34	—	2.23	2.36	2.55
AW	3	2.44	2.80	—	2.51	2.65	—	2.52	2.74	2.76
PW	2.76	2.29	2.57	—	—	2.32	—	2.25	2.4	2.41
M2/										
L	3.5	3.57	—	—	2.99	2.94	—	—	3.19	3.23
AW	3.62	3.7	—	—	3.45	3.48	—	—	3.76	3.61
PW	3.21	3.32	—	—	3.1	3.1	—	—	3.19	3.14
M3/										
L	—	4.18	4.21	—	3.46	3.65	—	3.74	3.39	3.83
AW	—	4.5	4.57	—	3.77	3.59	—	3.81	4.16	4.16
PW	—	3.84	4.16	—	3.3	3.29	—	3.34	3.44	3.62

TABLE 5. *Extended.*

				Washakie specimens considered to be *Eobasileus cornutus*				In comparison to *U.a.*, values of the preceding specimens (probable *E.c.*) are above:					
				Cast PM (BMUW 592041, left P2-M3)	Cast M 3944 (YPM 11567, *Tetheopsis stenops*, *type*)	Washakie Basin and Fm., TWkA1		Mean of *U. anceps*			Range of *U. anceps*		
						Cast P 26235 (*U. longiceps*, YPM 11256)	Cast PM 8088 (*T. speirianus*, PUM 10079) L						
N	Range	Mean	s					1	2	4	1	2	4
14	13.26–17.78	15.51	1.21	~17.88	15.96	17.9	16.35	+	+	+	+		
9	11.49–14.20	12.71	0.83	~15.61	13.93	[from Wheeler]	13.59	+	+	+			
10	9.71–12.26	10.8	0.75	~13.13	11.64		11.43	+	+	+			
11	5.79–7.17	6.66	0.31	~7.61	6.70		~7.55	+	≅	+	+		+
11	3.77–4.94	4.47	0.32	~4.84	4.74		~5.08	+	+	+			+
11	8.04–9.75	8.94	0.46	—	9.33		~9.53		+	+			
11	10.23–12.66	11.37	0.64	~14.12	12.46		~13.01	+	+	+	+		+
11	4.00–4.88	4.59	0.24	~5.24	4.63		4.80	+	≅	+	+		
10	8.72–10.40	9.56	0.47	~11.77	10.49		~10.42	+	+	+	+	+	+
12	6.00–7.80	6.83	0.47	—	7.31		~6.98		+	≅			
12	4.43–5.60	4.87	0.42	—	4.92		~4.87		≅	=			
9	7.01–8.01	7.44	0.29	~9.22	—		7.85	+		+	+		
8	7.34–8.88	8.4	0.57	—	9.53		~9.05		+	+		+	+
9	4.65–5.75	5.31	0.38	—	6.04		6.16		+	+		+	+
7	5.28–6.80	6.25	0.60	~7.49	7.18		~6.41	+	+	+	+	+	
10	4.30–6.76	5.34	0.87	—	—		—						
10	2.10–3.70	2.63	0.48	—	—		—						
4	15.10–17.50	16.37		—	—		—						
18	1.96–2.42	2.16	0.13	2.23	2.13		—	≅	–				
14	1.89–2.55	2.16	0.16	2.21	2.11		—	≅	≅				
15	1.92–2.36	2.12	0.12	2.18	2.18		—	≅	≅				
21	1.90–2.74	2.42	0.20	2.66	2.40		—	+	≅				
21	2.21–3.04	2.72	0.25	2.88	2.85		—	+	+				
21	2.20–2.91	2.63	0.19	2.89	2.89		—	+	+				
21	2.15–3.00	2.42	0.22	2.77	2.53		—	+	≅				
19	2.43–3.08	2.81	0.20	3.03	2.84		—	+	≅				
18	2.42–3.16	2.72	0.21	2.88	2.76		—	≅	≅				
20	1.89–2.73	2.39	0.20	—	2.77		≧2.91		+	+		+	+
19	2.33–3.28	2.68	0.23	—	2.84		—		+				
18	2.21–3.35	2.52	0.28	—	2.67		—		+				
17	2.57–3.57	3.15	0.28	3.55	3.65		≧3.53	+	+	+		+	
17	3.14–3.80	3.53	0.20	3.89	3.96		≧3.51	+	+	≅	+	+	
17	2.85–3.55	3.18	0.20	3.49	3.55		>3.37	+	+	+			
18	3.01–4.50	3.7	0.42	4.05	3.91		≳3.22 (alv. 4.0)	+	+	–			
19	3.48–4.57	3.97	0.31	>4.27	4.85		>3.71 (alv. 4.6)	+	+	?		+	
19	3.05–4.16	3.5	0.28	~3.84	4.28		>3.65 (alv. 3.5)	+	+	+		+	

Note: L P2-M3 measures for DMNH EPV 1849, not shown in the table, are included in the statistics: 16.7 cm (left) and 16.5 cm (right).

TABLE 5. *Continued.*

N	Range	Mean	s	Washakie specimens considered to be *Eobasileus cornutus*: Cast PM (BMUW 592041, left P2-M3)	Cast M 3944 (YPM 11567, *Tetheopsis stenops*, *type*)	Washakie Basin and Fm., TWkA1: Cast P 26235 (*U. longiceps*, YPM 11256)	Cast PM 8088 (*T. speirianus*, PUM 10079) L	In comparison to *U.a.*, values of the preceding specimens (probable *E.c.*) are above: Mean of *U. anceps* 1	2	4	Range of *U. anceps* 1	2	4
1	2.23												
1	0.54												
1	0.38												
1	0.63												
1	1.31												
1	1.18												
1	1.32												
1	1.66												
1	1.89												
1	1.84												
1	1.49												
1	1.9												
1	1.81												

(This page continues reading vertically from previous page.)

TABLE 6. *Uintatherium anceps,* lower dentition (in cm).

	Washakie Basin, Washakie Formation, TWkA1					
	PM 8020		Cast PM 8089†		PM 53932	
Item	L	R	L	R	L	R
L p2-m3	—	—	W15.5 16.2	W16	≥15.00	≥15.50
L p3-m3	—	—	14	14	13.04	13.43
L p4-m3	—	—	11.8	11.7	10.75	10.69
L m1-m3	—	—	9.4	9.6	8.52	8.69
L m1-m2	—	—	5.8	5.6	~4.70	4.63
L m2-m3	—	—	6.9	7	6.55	6.7
L p2-m2	—	—	12.4	12	≥11.00	≥11.75
L p2-m1	—	—	9.6	9.2	≥8.00	≥9.00
L p2-p4	—	—	7	6.8	≥6.00	≥7.20
L p2-p3	—	—	4.8	4.6	>3.75	~5.00
L p3-m2	—	—	10.4	10	9.24	9.4
L p3-m1	—	—	7.5	7.2	~6.50	~7.00
L p3-p4	—	—	5	4.8	4.53	5.01
L p4-m2	—	—	7.8	7.8	6.85	6.76
L p4-m1	—	—	5.1	5	~4.30	4.33
i/1						
Root/alv. L	2.18	—	~2.1	~2.2	—	—
Mesial-distal L	2.82	—	—	—	—	—
W	1.74	—	—	—	—	—
Root/alv. W	1.75	—	~1.7 (alv.)	~1.5 (alv.)	—	—
i/2						
Root/alv. L	2.13	2.34	~2.1 (alv.)	~1.9 (alv.)	—	—
Mesial-distal L	2.98	3.13	—	—	—	—
W	≥1.61	1.62	—	—	—	—
Roots/alv. W	1.70	1.64	~2.1 (alv.)	—	—	—
i/3						
Root/alv. L	—	—	~2.1 (alv.)	~2.0 (alv.)	—	—
Mesial-distal L	—	—	—	—	—	—
W	—	—	—	—	—	—
Root/alv. W	—	—	~1.7 (alv.)	~1.3 (alv.)	—	—
c						
Root/alv. L	—	—	~1.9 (alv.)	~2.5 (alv.)	—	—
Mesial-distal L	—	—	—	—	—	—
W	—	—	—	—	—	—
Root/alv. W	—	—	~1.1 (alv.)	~1.2 (alv.)	—	—
p2						
L			1.77 (alv.)	1.8 (alv.)	—	—
AW			0.91 (alv.)	0.9 (alv.)	—	—
PW			1.07 (alv.)	>1.23 1.2 (alv.)	—	—
p3						
L			1.97 (alv.)	>2.17 ~1.8 (alv.)	2.26	2.5
AW			1.34 (alv.)	>1.43	1.69	1.61
PW			>1.51 1.39 (alv.)	>1.55 ~1.4 (alv.)	~1.48	—
p4						
L			2.54 ~1.96 (alv.)	2.25 ~2.04 (alv.)	2.32	2.24
AW			>2.12 ~1.5 (alv.)	1.77 ~1.6 (alv.)	1.78	2.01
PW			2.30 1.17 (alv.)	1.76 ~1.6 (alv.)	1.88	~1.83

Notes: [b]Broken; [e]estimated; [u]unerupted; L, left (for items) or length; W, width (W is also used for Wheeler's measurements of PM 8069). For the incisors and canine, where a root was available, I measured that; otherwise, I took the alveolar measure.

*See notes in respective columns.

†Cast of PUM 10385, a jaw that Osborn placed with the *Loxolophodon speirianus* holotype.

Osborn called the skull Marsh associated with this jaw with *Loxolophodon.* Wheeler assigned them both to *Tetheopis speirianus,* but the jaw's small size bothered him. In spite of its coming from the base of TWkA1 at Laclede Meadows, much lower in the section than the skull, he did not separate them. Wheeler's value (W) is used for L p2-m3; my values are used for the rest of the statistics.

TABLE 6. *Continued.*

	Washakie Basin, Washakie Formation, TWkA1					
	PM 8020		Cast PM 8089†		PM 53932	
Item	L	R	L	R	L	R
m1						
L			~2.45 2.10 (alv.)	≥2.33 ~2.18 (alv.)	2.03*	2.07*
AW			>1.96 >1.72 (alv.)	>1.8 ~1.55 (alv.)	1.86*	≥1.84
PW			>1.94 ~1.9 (alv.)	~1.60 (alv.)	1.85*	—
m2						
L			3.0 ~2.83 (alv.)	3.20 ~2.9 (alv.)	2.72*	2.78
AW			2.87 ~2.78 (alv.)	>2.6 ~2.6 (alv.)	2.51*	~2.65
PW			3.1	>2.72	2.26*	~2.9
m3						
L			3.81	3.91	3.89	4.12
AW			3.20 ~3.07 (alv.)	~3.1	2.76	3.05
PW			3.3 ~2.85 (alv.)	~3.20	2.89	<3.60
dp2						
L			—	—	—	—
AW			—	—	—	—
PW			—	—	—	—
dp3						
L			—	—	—	—
AW			—	—	—	—
PW			—	—	—	—
dp4						
L			—	—	—	—
AW			—	—	—	—
PW			—	—	—	—

(This page continues reading vertically from previous page.)

TABLE 6. *Extended.*

	Washakie Basin, Washakie Formation, TWkA1					
	PM 38781††		PM 54801		PM 55174	
Item	L	R	L	R	L	R
L p2-m3	—	—	≫15.22 (alv.)	≥16.0 (alv.)	~17.03 (alv.)	17.98 (alv.)
L p3-m3	—	—	≫13.30 (alv.)	~13.62	~15.5 (alv.)	15.82 (alv.)
L p4-m3	—	—	≫11.00 (alv.)	11.36	~13.00 (alv.)	13.30 (alv.)
L m1-m3	—	—	≫8.27 (alv.)	~8.90	10.5 (alv.)	10.75 (alv.)
L m1-m2	—	—	5.9	≥5.55	~5.85 (alv.)	~6.5 (alv.)
L m2-m3	—	—	≫5.65	~6.95	7.9 (alv.)	8.2 (alv.)
L p2-m2	—	—	~12.59	~12.59	~13.03 (alv.)	13.62 (alv.)
L p2-m1	—	—	~9.52	≥9.20	~9.4 (alv.)	9.82 (alv.)
L p2-p4	—	—	~7.00e	~7.26	~7.05 (alv.)	7.26 (alv.)
L p2-p3	—	—	≥4.00	>4.44 (alv.)	~4.60 (alv.)	4.85 (alv.)
L p3-m2	—	—	10.94	>10.28 (alv.)	~10.90 (alv.)	~11.36 (alv.)
L p3-m1	—	—	7.73	>6.75 (alv.)	~7.28 (alv.)	7.52 (alv.)
L p3-p4	—	—	~4.58 (alv.)	~4.95	4.90 (alv.)	5.02 (alv.)
L p4-m2	—	—	~8.64	≫7.95	8.40 (alv.)	~8.87 (alv.)
L p4-m1	—	—	~5.49	≫5.20	~4.72 (alv.)	4.96 (alv.)
i/1						
Root/alv. L	2.08 (alv.)	1.64 (alv.)	—	—	PB1§	
Mesial-distal L	—	—	2.20[u]	—		
W	—	—	1.1	—		
Root/alv. W	2.75 (alv.)	2.50 (alv.)	—	—		
i/2						
Root/alv.L	2.4 (alv.)	2.03 (alv.)	—	—		
Mesial-distal L	—	—	—	—		
W	—	—	—	—		
Roots/alv. W	1.65 (alv.)	2.35 (alv.)	—	—		
i/3						
Root/alv. L	1.8 (alv.)	~1.8 (alv.)	—	—		
Mesial-distal L	—	—	—	—		
W	—	—	—	—		
Root/alv. W	~1.5 (alv.)	1.78 (alv.)	—	—		
c						
Root/alv. L	~1.2 (alv.)	—	—	—	—	—
Mesial-distal L	—	—	—	—	—	—
W	—	—	—	—	—	—
Root/alv. W	~1.1 (alv.)	~1.0 (alv.)	—	—	—	—
p2						
L	—	—	~1.75 (alv.)*	~1.80 (alv.)	~2.00	~2.16 (alv.)
AW	—	—	~0.60 (alv.)*	~0.90 (alv.)	~1.22	~0.75 (alv.)
PW	—	—	~0.70 (alv.)*	~1.10 (alv.)	~1.25	~0.80 (alv.)
p3						
L	—	—	2.4**	2.25 (rt.)	2.31	2.44 (alv.)
AW	—	—	≥1.88**	1.12 (rt.)	~1.82	1.31 (alv.)
PW	—	—	≥1.98**	1.22 (rt.)	~1.87	1.32 (alv.)
p4						
L	—	—	root 2.15†	≥2.50	2.39 (alv.)	2.33 (alv.)
AW	—	—	root 1.61†	1.96	≤1.87 (alv.)	1.60 (alv.)
PW	—	—	root 1.36†	2.38	≤1.73 (alv.)	1.54 (alv.)

Notes: [b]Broken; [e]estimated; [u]unerupted; L, left (for items) or length; W, width. For the incisors and canine, where a root was available, I measured that; otherwise, I took the alveolar measure.

*May be dp2 alveoli. **Possibly values of dp3. †With p3, is still encrypted.

††Edentulous jaw; alveolar measurements are provided for the incisors.

§PBI = present but indistinct.

TABLE 6. *Continued.*

	Washakie Basin, Washakie Formation, TWkA1					
	PM 38781††		PM 54801		PM 55174	
Item	L	R	L	R	L	R
m1						
L	—	—	2.57	—	2.47 (alv.)	2.35 (alv.)
AW	—	—	2.37	—	>1.40 (alv.)	1.74 (alv.)
PW	—	—	1.93	—	1.63 (alv.)c	1.64 (alv.)
m2						
L	—	—	3.23	—	3.66 (alv.)c	≤3.74 (alv.)
AW	—	—	2.89	—	2.09 (alv.)	1.91 (alv.)c
PW	—	—	2.39	—	2.04 (alv.)	—
m3						
L	—	—	Unerupted	>3.90	4.29 (alv.)c	4.14 (alv.)
AW	—	—	in crypt.	>2.50	2.45 (alv.)	2.22 (alv.)c
PW	—	—		>2.10c	2.12 (alv.)	2.14 (alv.)
dp2						
L	—	—	~1.75 (alv.)*	~1.80 (alv.)	—	—
AW	—	—	~0.60 (alv.)*	~0.90 (alv.)	—	—
PW	—	—	~0.70 (alv.)*	~1.10 (alv.)	—	—
dp3						
L	—	—	Note 1.		—	—
AW	—	—			—	—
PW	—	—			—	—
dp4						
L	—	—			—	—
AW	—	—			—	—
PW	—	—			—	—

*These are probably p2 alveoli.

Note 1. If these teeth or roots, dp3 and dp4, belong to p3 and p4 (as seems likely), then the deciduous teeth were long gone. If not, those values apply here. The case for the teeth and roots belonging to p3 and p4 is argued by the fully erupted but unworn condition of left p3 and right p4, but if left p4 is still unerupted, the timing of left and right eruption sequences is quite discrepant.

(This page continues reading vertically from previous page.)

TABLE 6. *Extended.*

	Washakie Basin, Washakie Formation, TWkA1							
	PM 55827		PM 56022		(*U. sp.* = *U. anceps*) DMNH EPV 1849		UFH 54015 v. 85.23.1§	
Item	L	R	L	R	L	R	L	R
L p2-m3	16.2	17.30 (alv.)	—	—	16.7	16.5		
L p3-m3	≥13.96	14.52	—	~16.0[e]	—	—		
L p4-m3	~11.20	12.02	—	—	—	—		
L m1-m3	~8.84	10.03	—	—	—	—		
L m1-m2	5.15	5.65	—	—	—	—		
L m2-m3	~6.50	~7.32	—	—	—	—		
L p2-m2	12.53	≥13.3 (alv.)	13.49 (alv.)	—	—	—		
L p2-m1	≥9.55	~10.12 (alv.)	—	—	—	—		
L p2-p4	7.36	~7.77 (alv.)	—	—	—	—		
L p2-p3	~4.83	~5.08 (alv.)	—	—	—	—		
L p3-m2	10.28	10.35	~11.75 (alv.)	11.1 (alv.)	—	—		
L p3-m1	≥7.43	7.56	—	—	—	—		
L p3-p4	5.22	5.07	—	—	—	—		
L p4-m2	7.42	7.8	—	—	—	—		
L p4-m1	≥4.55	4.89	—	—	—	—		
i/1								
Root/alv. L	—	—	—	—	—	—		
Mesial-distal L	—	—	—	—	—	—		
W	—	—	—	—	—	—		
Root/alv. W	—	—	—	—	—	—		
i/2								
Root/alv. L	—	—	—	—	—	—		
Mesial-distal L	—	—	—	—	—	—		
W	—	—	—	—	—	—		
Root/alv. W	—	—	—	—	—	—		
i/3								
Root/alv. L	—	—	—	—	—	—		
Mesial-distal L	—	—	—	—	—	—		
W	—	—	—	—	—	—		
Root/alv. W	—	—	—	—	—	—		
c								
Root/alv. L	—	—	—	—	—	—		
Mesial-distal L	—	—	—	—	—	—		
W	—	—	—	—	—	—		
Root/alv. W	—	—	—	—	—	—		
p2								
L	2.21	—	—	—	—	—	b	—
AW	>1.62	—	—	—	—	—	—	—
PW	≥1.63	>1.32	—	—	—	—	—	—
p3								
L	—	≥2.49	—	—	—	—	2.4	—
AW	—	1.94	—	—	—	—	1.7	—
PW	—	2.05	—	—	—	—	b	—
p4								
L	2.35	2.41	—	—	—	—	2.4	>2.3
AW	1.92	1.86	—	—	—	—	>1.9	—
PW	≥1.80	1.87[w]	—	—	—	—	1.5	—

Notes: [b]Broken, [e]estimated, [w]worn; L, left (for items) or length; W, width. For the incisors and canine, where a root was available, I measured that; otherwise, I took the alveolar measure.

§Probably = UFH 54515.

TABLE 6. *Continued.*

	Washakie Basin, Washakie Formation, TWkA1							
	PM 55827		PM 56022		(*U. sp.* = *U. anceps*) DMNH EPV 1849		UFH 54015 v. 85.23.1§	
Item	L	R	L	R	L	R	L	R
m1								
L	>2.15*	2.53	2.42	—	—	—	2.2*	>2.1*
AW	>1.65	1.68	2.37	—	—	—	1.8	~1.7
PW	≥1.73	1.72	2.08	—	—	—	1.5	~1.5
M2								
L	b	3.19	>2.95	3.26	—	—	3.2	>2.7
AW	b	>2.66	≫2.4	≥2.79	—	—	>2.2	>2.2
PW	>2.20	b	≫2.44	3.13	—	—	2.1	>1.8
m3								
L	≥4.04	≥4.44	≥4.29	≥4.42	—	—	3.8	4.1
AW	≥2.69	3.05	≥3.29	≫2.8	—	—	3.1	>3.0
PW	>2.15	≥2.71	>3.0	≫2.9	—	—	2.4	>2.7
dp2								
L	—	—	—	—	—	—	—	—
AW	—	—	—	—	—	—	—	—
PW	—	—	—	—	—	—	—	—
dp3								
L	—	—	—	—	—	—	—	—
AW	—	—	—	—	—	—	—	—
PW	—	—	—	—	—	—	—	—
dp4								
L	—	—	—	—	—	—	—	—
AW	—	—	—	—	—	—	—	—
PW	—	—	—	—	—	—	—	—

(This page continues reading vertically from previous page.)

TABLE 6. *Continued.*

	Bridger Basin and Fm.				
	(50 m above Sage Creek White Layer) UM 101209	Cast P 26233 (holotype, *D. laticeps* YPM 11039)		Cast PM 60171 (of specimen in Gunma Prefecture Mus. of Nat. Hist.)	
Item	**L**	**L**	**R**	**L**	**R**
L p2-m3	—	17.0 (alv.)#	17.56 (alv.)	14.6*	13.3*
L p3-m3	—	15.32 (alv.)	15.80 (alv.)	12.43*	11.35*
L p4-m3	10.06	12.54 (alv.)	13.31 (alv.)	10.18*	9.37
L m1-m3	7.91	9.59	10.65 (alv.)	7.68	7.13
L m1-m2	4.69	5.79	5.65 (alv.)	4.39	4.08
L m2-m3	5.9	7.11	8.34	5.62	5.42
L p2-m2	—	13.03 (alv.)	12.95 (alv.)	*	*
L p2-m1	—	10.10 (alv.)	9.51 (alv.)	*	*
L p2-p4	—	7.48 (alv.)	7.34 (alv.)	*	*
L p2-p3	—	4.33 (alv.)	4.42 (alv.)	*	*
L p3-m2	—	11.34 (alv.)	10.96 (alv.)	*	*
L p3-m1	—	8.27 (alv.)	7.51 (alv.)	*	*
L p3-p4	—	5.46 (alv.)	5.30 (alv.)	*	*
L p4-m2	6.77	7.11 (alv.)	833 (alv.)	*	6.36
L p4-m1	4.24	5.70 (alv.)	4.91 (alv.)	*	4.00
i/1					
Root/alv. L	—	~2.0 (alv.)	−1.84 (alv.)	3.42 (alv.)	3.0 (alv.)
Mesial-distal L	—	—	—	—	3.12
W	—	—	—	—	1.44
Root/alv. W	—	~1.5 (alv.)	—	1.5 (alv.)	1.6 (alv.)
i/2					
Root/alv. L	—	~2.4 (alv.)	2.70 (alv.)	2.94	2.16
Mesial-distal L	—	—	—	—	3.55
W	—	—	—	—	1.41
Root/alv. W	—	~1.5 (alv.)	—	1.72	1.46
i/3					
Root/alv. L	—	~1.95 (alv.)	~1.35 (alv.)	1.83	1.94
Mesial-distal L	—	*	**	—	—
W	—	*	**	—	—
Root/alv. W	—	~1.5 (alv.)	~1.45 (alv.)	2.12	1.89
c					
Root/alv. L	—	~1.5 (alv.)	~1.35 (alv.)	1.91	*
Mesial-distal L	—	—	—	—	—
W	—	—	—	—	—
Root/alv. W	—	~1.1 (alv.)	~1.25 (alv.)	~0.93	*
p2					
L	—	>1.75 (alv.)	~1.69 (alv.)	2.17*	1.05*
AW	—	>1.05 (alv.)	1.11 (alv.)	1.30*	1.12*
PW	—	>1.1 (alv.)	1.15 (alv.)	1.36*	1.42*
p3					
L	—	~2.5 (alv.)	2.33 (alv.)	2.24*	2.24*
AW	—	1.48 (alv.)	1.41 (alv.)	1.34*	1.39*
PW	—	1.48 (alv.)	1.60 (alv.)	1.89*	1.79*
p4					
L	2.16	2.60 (alv.)	2.52 (alv.)	2.61*	2.34
AW	1.8	1.48 (alv.)	1.58 (alv.)	1.55*	1.67
PW	1.66	1.52 (alv.)	1.61 (alv.)	1.50*	2.02

Notes: [b]Broken, [e]estimated, [w]worn.

TABLE 6. *Continued.*

	Bridger Basin and Fm.				
	(50 m above Sage Creek White Layer) UM 101209	Cast P 26233 (holotype, *D. laticeps* YPM 11039)		Cast PM 60171 (of specimen in Gunma Prefecture Mus. of Nat. Hist.)	
Item	L	L	R	L	R
m1					
L	2.07	2.51	2.33 (alv.)	2.12	1.95
AW	1.66	1.47	1.52 (alv.)	1.79	1.54
PW	1.61	1.58	1.49 (alv.)	2.04	1.66
m2					
L	2.64	3.2[e,w]	~3.5	2.34	2.39
AW	2.35	2.25[e,w]	2.11	1.85	1.95
PW	2.12	2.27[e,w]	2.60[e]	2.13	2.05
m3					
L	3.37	4.85[e]	4.78	3.46	3.14
AW	2.64	>2.37	2.81	2.51	2.38
PW	2.52	≫2.11	3.12	2.6	2.58
dp2					
L	—	—	—	—	—
AW	—	—	—	—	—
PW	—	—	—	—	—
dp3					
L	—	—	—	—	—
AW	—	—	—	—	—
PW	—	—	—	—	—
dp4					
L	—	—	—	—	—
AW	—	—	—	—	—
PW	—	—	—	—	—

#Wheeler's value of 17.1 for L p2-m3 is used in statistics

*This alveolus preceded antero-externally by a partly confluent smaller one (m-d L alv.0.7). The two thus are actually nos. 3 & 4.

**The extra alveolus is not present on right side.

*Not included in statistics. Although specimen looks great, it has problems—all premolars but R p4 look wrong. Wear does not match uppers, and two of them may be teeth of perissodactyls.

Note: The following measurs of cast P26977 (from ANSP 12607, holotype of *U. robustum*), not shown in the table because of space limitations, were included in the statistics: m2 length, 3.62 cm (alv., estimated); m3 length, 3.92 cm; m3 anterior width, 3.13 cm; m3 posterior width, 2.97 cm.

(This page continues reading vertically from previous page.)

TABLE 6. *Extended.*

Item	N	Range	Mean	s	Two specimens tentatively referred to *E.c.* PUM 11611	UFH 93002*
L p2-m3	7	15.00–16.70	15.91		Presumably *E. cornutus*; shown here to reveal its larger size for the few comparable measurements than those of range and mean for *U. anceps*. Measurements were made on Osborn's and Osborn and Speir's scaled photographs.	
L p3-m3	8	13.04–16.00	14.07	0.896		
L pr-m3	9	9.37–18.00	10.99	0.869		
L m1-m3	11	7.13–10.03	8.75	0.897		
L m1-m2	11	4.08–5.90	5.20	0.647		
L m2-m3	12	5.42–8.34	6.69	0.794		
L p2-m2	7	11.00–12.59	12.12			
L p2-m1	7	8.00–9.60	9.15			
L p2-p4	7	6.00–7.36	6.95			
L p2-p3	5	4.00–5.00	4.65			
L p3-m2	7	9.24–10.94	10.09			
L p3-m1	7	6.50–7.73	7.27			
L p3-p4	7	4.53–5.22	4.94			
L p4-m2	9	6.36–8.64	7.36	0.724		
L p4-m1	9	4.00–5.49	4.66	0.487		
i/1						
Root/alv. L	9	1.64–3.42	2.27	0.569	2.4 root	
Mesial-distal L	3	2.20–3.12	2.71		4.3	
W	3	1.10–1.74	1.43		1.7	
Root/alv. W	7	1.50–2.75	2.01		—	
i/2						
Root/alv. L	10	1.90–2.94	2.25	0.294	2.1 root	
Mesial-distal L	3	2.98–3.55	3.22		3.8	
W	3	1.41–1.62	1.55		1.6	
Root/alv. W	8	1.46–2.35	1.77	0.315	—	
i/3						
Root/alv. L	8	1.35–2.10	1.85	0.236	1.9 root	
Mesial-distal L	—	—	—		3.5	
W	—	—	—		1.4	
Roots/alv. W	8	1.30–2.12	1.66	0.269	—	
c						
Root/alv. L	6	1.20–2.50	1.73		1.9 root	
Mesial-distal L	—	—	—		3.5	
W	—	—	—		1.5	
Root/alv. W	7	0.93–1.25	1.1		—	
p2						
L	2	2.00–2.21	2.11			
AW	2	1.22–1.62	1.42			
PW	2	1.25–1.63	1.44			
p3						
L	5	2.26–2.49	2.39			
AW	6	1.61–1.94	1.77			
PW	4	1.48–2.05	1.84			
p4						
L	10	2.16–2.54	2.35	0.117		
AW	8	1.67–2.01	1.85	0.113		
PW	10	1.50–2.38	1.90	0.270		

TABLE 6. *Continued.*

Item	N	Range	Mean	s	Two specimens tentatively referred to *E.c.* PUM 11611	UFH 93002*
m1						
L	12	1.95–2.57	2.27	0.322		1.4b
AW	11	1.47–2.37	1.83	0.295		0.83
PW	11	1.50–2.08	1.75	0.204		0.96
m2						
L	13	2.34–3.50	2.97	0.360		1.72
AW	11	1.85–2.89	2.44	0.367		1.01
PW	11	2.05–3.10	2.01	1.057		1.11
m3						
L	16	3.14–4.78	4.02	0.471		1.95
AW	13	2.38–3.29	2.90	0.286		—
PW	9	2.40–3.30	2.86	0.318		1.29
dp2						
L	1		2			*UFH 93002 must be *Bathyopsis*. It is too small to be *U. anceps*.
AW	1		1.89 (alv.)			
PW	1		1.14			
dp3						
L	1		2.4			
AW	1		>1.87			
PW	1		1.84			
dp4						
L	1		2.53			
AW	2		1.96			
PW	2		2.09			

(This page continues reading vertically from previous page.)

This page intentionally left blank.

TABLE 7. *Uintatherium anceps*, rib measurements of PM 55423 (measurements in mm)

Rib no.	Left		Right	
	Arc length	Chord length	Arc length	Chord length
1	~317	298[c]	~315	301[c]
2	—	—	>335	>314[b]
3	≫210	≫191[b]	—	—
4–5	There are 8–10 rib pieces, each between 100 and 220 mm long, that cannot be assigned to any position.			
6–7		(head only)	?R6 or R7	
8–9		(head only)	?R8 or R9	
10	—	—	≫310 (float)	≫300 (?R10)
11	—	—	≫470 (float)	≫415 (?R11)
12	—	—	~730	~660[c]
13	—	—	≫630	≫620[b]
15	~775	>~630[c]	~770	~750[c]
15	~740	~585[c]	≫570 (exposed)	~680[c,e]
16	~665	~565[c]	—	—
17	>~540	530[c]	—	—
18	>290	>280[b]	~530	485[c]
19	>215	>210[b]	~260	>240[b]

Notes: [b]Broken, [c]calculated (partly covered in matrix), [e]estimated.

TABLE 8. Measurements of scapula and humerus, *Uintatherium anceps* and *Eobasileus cornutus* (in m).

	Uintatherium anceps						
	D. mirabile YPM 11215	Newborn PM 3896	PM 39915	PM 53921	PM 55423		DMNH EPV 493
SCAPULA	**L**	**R**	**R**	**L**	**L**	**R**	**R**
AP diameter of glenoid cavity	0.115	0.135*	—	>0.140	>0.146	0.155	0.14
Transverse diameter of glenoid cavity	0.09	0.062*	0.061	0.096	0.093	0.096	0.088
Greatest vertical diameter of scapula	0.575	0.266*	0.512	>0.433	—	0.59	0.51
Greatest horizontal diameter	0.48	0.239*	—	—	—	0.488	—
Length of coracoid border	0.57	0.18*	—	—	—	0.597	—
Length of suprascapula border	0.39	0.21*	—	—	~0.41	0.490	—
Length of glenoid border	0.35	0.135*	—	—	—	0.385	—
Height of acromion above glenoid cavity	0.12	0.043*	0.182	0.18	—	0.094	—
Greatest of diameter of prescapular fossa	0.14	0.08*	>0.136	—	—	0.161	—
Greatest diameter of postscapular fossa	0.31	0.171*	—	—	—	0.33	—

* No glenoid epiphysis; not included in statistics.

	Uintatherium anceps										
	D. mirabile YPM 11208	YPM 11212	YPM 11215	YPM 11245	PM 1458	PM 2079		PM 3894	PM 38781	PM 39393	PM 53935
HUMERUS†	**L**	**R**	**R**	**L**	**L**	**L**	**R**	**R**	**L**	**R**	**L**
Total length of humerus	—	—	—	0.555	0.58	—	0.61	≥0.613	—	0.57	—
AP diameter of head	—	—	0.14	0.136	0.13	—	0.132	>0.177	—	0.142	0.136
Transverse diameter of head	—	—	0.138	0.12	0.143	—	0.148	0.138	—	0.119	0.157
Greatest diameter of proximal end	—	—	0.22	0.22	0.244	—	0.23	—	—	0.221	0.229
Least AP diameter of shaft	0.064	0.058	—	0.07	0.077	—	0.065	≥0.075	0.061	0.07	—
Least transverse diameter of shaft	—	—	—	0.08	0.083	—	0.098	—	0.06	0.073	—
Transverse diameter, through condyles	0.184	0.183	—	0.2	0.204	0.202	0.221	—	≥0.159	0.178	—
Transverse diameter of trochlear surface	0.124	0.115	—	0.127	0.154	0.139	0.14	—	—	0.137	—
AP diameter of trochlear surface, ulnar side	0.1	0.098	0.116	0.109	0.119	0.108	0.085	—	—	0.108	—
AP diameter of trochlear surface, radial side	0.095	0.080	—	0.091	0.096	0.082	0.067	—	—	0.098	—
Least AP diameter, trochlear surface	0.08	0.072	—	0.078	0.086	0.081	0.084	—	—	0.083	—
Bone thickness between coronoid and anconeal fossae	0.018	0.014	—	0.016	0.016	0.017	<0.038	—	0.026	0.023	—

Notes: Data listings begin with Marsh's Yale University (YPM) specimens (Marsh 1886, pp. 91, 92).

* See notes in respective columns.

† YPM 11032 is part of the holotype of *U. anceps,* YPM 11030. It is only the distal end of a humerus and was not measured.

TABLE 8. *Extended.*

Uintatherium anceps								*Eobasileus cornutus*						
								PM 53934						
				N*	Range*	Mean*	s	L				N	Range	Mean
				3	0.115–0.155	0.137		(still unprepared)						
				6	0.061–0.096	0.087								
				4	0.510–0.590	0.547								
				2	0.480–0.488	0.484								
				2	0.570–0.597	0.584								
				3	0.390–0.490	0.43								
				2	0.350–0.385	0.368								
				4	0.094–0.182	0.144								
				2	0.140–0.161	0.151								
				2	0.310–0.330	0.32								
				* Includes only adults.										

Uintatherium anceps								*Eobasileus cornutus*						
PM 54676	PM 55423	PM 55920*	DMNH EPV 493					PM 1457	PM 1509	PM 1522	PM 53934			
R	R	L	R	N	Range	Mean	s	R	L	L	L	N	Range	Mean
0.586	0.524	—	—	11*	0.500–0.613*	0.568*	0.034*	—	0.64	≥0.500	—	3*	0.595–0.650*	0.628*
0.151	0.139	—	0.135	9	0.130–0.151	0.138	0.006	—	0.15	≥0.135	—	1	0.15	
0.123	0.129	—	—	9	0.119–0.157	0.135	0.013	—	0.118	≥0.130	—	1	0.118	
≥0.180	0.208	—	—	7	0.208–0.244	0.225		—	≥0.22	>0.168	—	1	0.22	
0.086	0.078	<0.104	—	10	0.058–0.086	0.07	0.009	<0.095	0.063	~0.095	0.086	3	0.063–0.095	0.081
≥0.094	0.088	~0.062	—	8	0.060–0.098	0.08	0.014	~0.076	0.076	0.09	0.08	4	0.076–0.090	0.081
0.192	0.243	≥0.209	—	10	0.178–0.243	0.202	0.02	0.154	0.209	0.245	0.22	4	0.154–0.245	0.207
≥0.137	0.197	≥0.168	—	10	0.115–0.197	0.144	0.024	—	0.147	—	0.153	2	0.147–0.153	0.15
>0.109	0.119	≥0.122	—	10	0.085–0.122	0.107	0.011	—	0.13	—	0.088	2	0.088–0.13	0.109
0.096	≥0.089	0.104	—	10	0.067–0.104	0.091	0.012	—	0.106	—	0.106	2	0.106	
0.08	0.077	0.084	—	10	0.072–0.086	0.081	0.004	—	0.099	—	0.081	2	0.081–0.099	0.09
<0.036	0.047	—	—	8	0.014–0.047	0.022	0.011	0.034	0.06	≤0.027	<0.053	3	0.034–0.06	0.022
	* Crushed diagonally.			* Includes Wheeler's values of 0.578 for YPM 11201, 0.50 for YPM 11238, 0.55 for AMNH 1658, and 0.583 for AMNH 1659.								* Includes Wheeler's values of 0.65 for YPM 11562 and 0.595 for AMNH 13153.		

TABLE 9. Measurements of radius and ulna, *Uintatherium anceps* and *Eobasileus cornutus* (in m).

	Uintatherium anceps							
	D. mirabile							
	YPM 11206	YPM 11208	YPM 11548	PM 2079A	PM 39393	PM 55396	PM 55423	PM 55540
RADIUS	**L**	**L**	**R**	**R**	**R**	**R**	**R**	**L**
Total length of radius	0.254	0.380	0.400	—	≥0.431	—	0.375	0.38
Greatest diameter of proximal end	0.116	0.098	0.112	0.097	0.107	≥0.107	0.172	>0.092
AP diameter of proximal end	0.071	0.061	0.070	≥0.060	0.059	0.065	0.084	≥0.058
Least diameters of shaft	0.062	0.032	0.063	—	0.055	0.064	0.063	0.067
	0.041	0.053	0.035	—	0.039	0.043	0.04	0.042
Transverse diameter, distal end	0.011	0.102	0.108	—	0.1	0.122	0.126	0.109
AP diameter, distal end	0.097	0.080	0.090	—	0.078	0.081	0.103	>0.067
Diameters of articulation for humerus	0.060	0.052	0.060	—	0.051	≥0.065	0.07	>0.048
	0.108	0.094	0.104	—	0.097	>0.100	0.172	≥0.083
AP diameter of articulation for scaphoid	0.065	0.055	—	—	0.06	≥0.057	0.061	>0.042
Transverse diameter of articulation for scaphoid	0.040	0.039	0.047	—	0.047	≥0.042	0.046	0.037
AP diameter of articulation for lunar	0.065	0.056	0.055	—	0.054	≥0.058	0.061	≥0.050
Transverse diameter of articulation for lunar	0.055	0.045	0.045	—	0.043	≥0.049	0.048	>0.05
Transverse diameter of distal articular surfaces	0.093	0.082	0.092	—	≥0.088	≥0.091	0.098	>0.085

	Uintatherium anceps							
	D. mirabile			New-born*				
	YPM 11038	YPM 11206	YPM 11232	PM 3896	PM 39393	PM 53931	PM 55408	PM 55423
ULNA	**R**	**L**	**R**	**R**	**R**	**R**		**R**
Total length of ulna	—	0.530	0.555	0.309*	0.505	>0.444	—	0.467
Diameters of proximal end	0.070	0.095	0.098	≥0.086*	0.128	0.139	≫0.085	0.139
	0.103	0.140	0.130	≥0.090*	0.183	0.141	≫0.109	0.16
Transverse diameter of shaft, behind humeral articular face	0.052	0.055	0.065	0.029*	0.048	0.066	−0.061	0.057
Diameter of shaft, through humeral articular face	0.088	0.097	0.103	−0.078*	0.094	0.089	—	0.141
Diameters of shaft, near middle	—	0.057	0.067	0.035*	0.057	0.044	—	0.058
	—	0.081	0.077	0.049*	0.067	0.05	—	0.071
AP diameter of shaft near distal end	—	0.085	0.095	0.072*	0.091	>0.063	—	0.109
Transverse diameter of shaft, near distal end	—	0.067	0.084	0.049*	0.107	0.086	—	0.131
Transverse diameter of humeral articulation, greatest	0.125	0.143	—	0.090*	0.126	0.139	≫0.109	0.138
Transverse diameter of humeral articulation, least	0.052	0.060	0.058	>0.039*	0.043	0.04	—	0.058
AP diameter of humeral articulation, at middle	0.090	0.085	0.086	0.081*	0.084	0.076	>0.078	0.091
AP diameter of humeral articulation, inner lobe	0.062	0.063	0.066	<0.068*	0.088	0.065	0.064	0.077
AP diameter of humeral articulation, outer lobe	0.038	0.045	—	<0.041*	0.036	−0.049	—	0.035
Transverse diameter of distal articular surface	—	0.076	0.073	<0.073*	0.068	—	—	0.098
AP diameter of distal articular surface	—	0.070	0.061	<0.052*	0.089	—	—	0.065
Least and greatest diameters of distal articular surface	—	0.067	—	0.052*	0.068	—	—	0.065
	—	0.097	0.090	—	0.091	—	—	0.098

* Not in statistics. Also without proximal epiphysis, but with distal.

Notes: Data listings begin with Marsh's Yale University (YPM) specimens (Marsh 1886, pp. 95, 98–99).
* See notes in respective columns.

TABLE 9. *Extended.*

Uintatherium anceps						*Eobasileus cornutus*					
PM 55927	DMNH EPV 493					PM 1452	PM 3211	PM 3212			
L	R	N	Range	Mean	s	R	L		N	Range	Mean
—	0.445	13*	0.254–0.445*	0.386*	0.046*	—	≥0.345	≥0.37	2*	0.424–0.508*	0.466*
>0.087	0.094	8	0.094–0.172	0.113	0.025	—	≥0.124	—	1	0.124	—
0.054	0.052	10	0.052–0.084	0.063	0.01	—	0.069	—	1	0.069	—
—	—	7	0.053–0.067	0.061		0.044	0.049	0.048	3	0.044–0.049	0.047
—	—	7	0.032–0.043	0.039		0.062	0.066	0.06	3	0.062–0.066	0.063
>0.089	—	7	0.100–0.126	0.111		≥0.126	—	≥0.126	2	0.126	0.126
>0.070	—	6	0.078–0.103	0.088		≥0.085	—	≥0.098	3	0.085–≥0.098	0.092
0.054	—	7	0.051–0.070	0.059		—	0.058	—	1	0.058	—
0.078	—	6	0.094–0.172	0.109		—	≥0.124	—	1	0.124	—
>0.048	0.045*	5	0.055–0.065	0.06		≥0.061	—	−0.063	2	0.061–0.063	0.062
0.038	—	8	0.087–0.047	0.042	0.004	0.047	—	−0.052	2	0.047–0.052	0.05
≥0.043	0.045*	7	0.050–0.065	0.057		≥0.058	—	0.072	2	0.058–0.072	0.065
0.042	—	7	0.042–0.055	0.047		≥0.053	—	−0.060	2	0.053–0.060	0.057
0.079	0.09	8	0.079–0.098	0.089	0.006	≥0.098	—	≥0.108	2	0.098–≥0.108	0.103

* Not in statistics. I took only this combined measure.

* Includes Wheeler's Values for AMNH 1667, 1668, 1675, and 12177 (0.368, 0.939, 0.408, and 0.375), YPM 11517 (0.393), and USNM 71-46 (0.41).

* Includes Wheeler's values for c.f. *E. cornutus*: YPM 11266 (~4.24) and AMNH 2333 (~0.508).

Uintatherium anceps							*Eobasileus cornutus*					
PM 55540	PM 56038	DMNH EPV 493					PM 1451	PM 1455				
R		R	N	Range	Mean	s	R	L		N	Range	Mean
—	—	0.506	10*	0.463–0.584*	0.512*	0.04*	≥0.518	≥0.534		1*	≥0.518–≥0.534*	0.526*
≥0.083	>0.136	—	6	0.070–0.139	0.112	—	≥0.095	0.123		1	0.123	—
−0.175	≥0.158	—	8	0.103–0.183	0.149	0.026	≥0.135	0.144		1	0.144	—
0.06	0.056	—	9	0.048–0.066	0.058	0.006	~0.071	0.059		2	0.059–0.071	0.065
—	≥0.142	—	7	0.088–0.142	0.108	—	—	0.108		1	0.108	—
—	≤0.058	—	6	0.044–0.067	0.057	—	0.052	0.055		2	0.052–0.055	0.054
—	≤0.072	—	6	0.055–0.081	0.07	—	0.074	0.057		2	0.057–0.074	0.066
—	—	—	4	0.085–0.109	0.095	—	≥0.087	0.085		2	0.085–0.087	0.086
—	—	—	5	0.067–0.131	0.095	—	>0.108	0.088		1	0.088	—
—	≥0.141	0.118	6	0.125–0.143	0.135	—	—	0.117		1	0.117	—
—	0.062	—	7	0.040–0.0623	0.053	—	—	0.046		1	0.046	—
—	0.092	—	7	0.076–0.092	0.086	—	—	0.079		1	0.079	—
—	0.074	—	8	0.062–0.088	0.07	0.009	—	0.064		1	0.064	—
0.057	0.047	—	7	0.035–0.057	0.044	—	—	0.03		1	0.03	—
—	—	—	4	0.068–0.098	0.079	—	0.058	0.066		2	0.058–0.066	0.062
—	—	—	4	0.016–0.089	0.071	—	0.097	0.089		2	0.089–0.097	0.093
—	—	—	3	0.065–0.068	0.067	—	0.059	0.066		2	0.059–0.066	0.063
—	—	*0.111	4	0.090–0.098	0.094	—	0.098	0.089		2	0.089–0.097	0.093

* Not in statistics. Measurement is of two distal facets combined (0.046 and 0.065).

* Includes Wheeler's values for ulna: AMNH 1669; 12177, and 12178 (0.463, 0.584, and 0.465); YPM 14324 (0.534); and USNM 71.46 (0.508).

* AMNH 12177 may belong here too. Wheeler gave it as 0.584, his largest value for *U.a.*, while the radius of the same specimen was 0.375 m, one of the smaller values for that species. I suspect the two to be unrelated, and that the ulna belongs to *E.c.*

TABLE 10. Measurements of pelvis and femur, *Uintatherium anceps* and *Eobasileus cornutus* (in m).

	Uintatherium anceps				
PELVIS	***Dinoceras mirabile* YPM 11036**	***Tinoceras ingens* YPM 11497**	**PM 3894**	**Newborn PM 3896**	**PM 37434**
				R	
Greatest transverse diameter, across ilia	1.120	1.180	1.158	—	—
Greatest transverse diameter, across blade of 1 ilium	—	—	~0.51	0.296*	0.4
Horizontal diameter of pelvic opening (approx.)	0.350	0.400	0.38	—	—
Vertical diameter of pelvic opening (approx.)	0.250	0.300	0.21	—	—
Diameter across acetabula	0.660	0.700	0.69	—	—
Diameters of acetabulum	0.110	—	0.125	0.079*	0.11
	0.125	—	0.145	0.085*	0.135
Diameters of thyroid foramen	0.075	0.060	—	—	—
	0.150	0.150	—	—	—
Length of public symphysis	0.140	0.140	~0.115	—	—
Length of four sacral vertebrae (approx.)	0.245	0.295	0.25	—	—
Extent of transverse processes of 1st sacral	0.330	0.355	~0.113	—	—
Horizontal diameter of anterior face at 1st sacral	0.110	0.117	—	—	—
Vertical diameter of anterior face of 1st sacral	0.075	0.072	—	—	—
Length of 1st sacral centrum	0.075	0.085	—	—	—
Length of 2nd sacral centrum	—	0.075	—	—	—
Length of 3rd sacral centrum	—	0.065	—	—	—
Length of 4th sacral centrum	—	0.067	—	—	—

* Ilium only (height of illium 0.258 m); not in statistics.

	Uintatherium anceps				
FEMUR	***D. mirabile* YPM 11036**	**PM 35943**	**PM 53921**	**PM 53931**	**PM 54407**
	R	**R**	**R**		**R**
Length	0.690	0.6590	0.684	(not found)	0.655
Diameters of head	0.123	~0.105	0.102		0.102
	0.126	0.1100	0.133		0.12
Distance from top of head to trochanter minor	0.200	—	0.192		~0.18
Height of trochanter minor	0.015	—	>0.009		~0.03
Transverse diameter through greater trochanter	0.215	0.2030	0.241		0.235
Least diameters of shaft	0.067	0.0710	0.064		0.099
(or minimum circumference)	0.093	>0.060	0.104		~0.057
Transverse diameter of distal end	0.170	—	0.196		0.188
Greatest AP diameter of distal end	0.160	≤0.110	0.129		0.103
Least AP diameter of distal end	0.100	0.0880	0.076		0.062
Transverse diameter of inner condyle	0.065	—	0.069		0.069
Transverse diameter of outer condyle	0.070	0.0750	0.075		0.076

Notes: Data listings begin with Marsh's Yale University (YPM) specimens (Marsh 1886, pp. 137–138, 141).
* See notes in respective columns.

TABLE 10. *Extended.*

Uintatherium anceps									
PM 53921	PM 54408			Univ. Colo. Mus. Bridger Fm. UCM 72519					
	R			L	R	N	Range	Mean	s
≥1.170	—					4	1.120–1.180	1.157	
~0.55	0.45					4	0.400–0.550	0.477	
0.37	—					4	0.350–0.400	0.375	
0.2	—					4	0.200–0.300	0.24	
0.72	—					4	0.660–0.720	0.69	
~0.11	~0.11					5	0.110–0.125	0.113	
0.124	0.136					5	0.124–0.145	0.133	
—	—					2	0.060–0.075	0.068	
—	—					2	0.15	0.15	
~0.115	—					4	0.115–0.140	0.128	
0.28	—					4	0.245–0.295	0.268	
0.15	—						(values extreme, not included*)		
—	—					2	0.110–0.117	0.114	
—	—					2	0.072–0.075	0.074	
—	—					2	0.075–0.085	0.08	
—	—					1	0.075	—	
~0.09	—					2	0.065–0.090	0.078	
−0.062	—					2	0.062–0.067	0.065	
							* I may misinterpret Marsh.		

Uintatherium anceps									
				Bridger UCM 72519*					
PM 54421	PM 55175	PM 55423	PM 55826	L	R	N	Range	Mean	s
0.66	—	—	0.702		0.71	16§	0.630–0.710§	0.67§	0.027§
0.108	—	—	0.116			6*	0.102–0.123*	0.109*	
0.129	—	—	0.126			6	0.110–0.133	0.124	
—	—	—	~0.190			4	0.180–0.200	0.191	
0.01	—	—	~0.013			4	0.010–0.030	0.017	
0.235	—	—	0.179			6	0.179–0.241	0.218	
0.09	—	—	0.056			6	0.056–0.099	0.075	
0.058	—	—	0.091			5	0.057–0.104	0.081	
0.178	—	0.179	0.152	~0.15	0.15	8	0.150–0.196	0.17	0.018
0.137	≥0.136	0.124	0.155			8	0.103–0.160	0.132	0.02
0.102	>0.086	>0.069	0.094			6	0.062–0.102	0.087	
0.074	0.053	0.076	0.052*			6	0.053–0.076	0.068	
0.082	0.056	0.073	0.068			8	0.056–0.082	0.072	0.008
			* Crushed; not in statistics	* University of Colorado Museum.		* Data for DMNH EPV 2603, proximal femur, are not included. Diameter of femoral head >0.108.			

§ Includes Wheeler's values for AMNH 1886, 1887, and 1888 (0.70, 0.709, and 0.69); YPM 11210, 11218, 11248, 11254, and 14327 (0.63, 0.659, 0.63, 0.69, and 0.655); and USNM 4742 (0.638). Another of Wheeler's values is for AMNH 12171 (0.541); it is not included as it may be juvenile.

TABLE 10. *Extended.*

Eobasileus cornutus

PM 1454	Juvenile without epiphyses PM 3212	PM 37434	Subadult (?)† P 12541 L	Subadult (?)† P 12541 R	Holotype AMNH 5040‡	N	Range	Mean
—	—	—	1.12[e]	1.15[e]	1.280‡	1*	1.280*	
—	—	0.41	0.564	0.560	—	3	0.410–0.564	0.511
—	—	≫0.4	—	—	—	0		
—	—	—	—	—	—	0		
—	—	—	~0.66	—	—	1	~0.66	
0.083	0.086	0.107	—	—	—	3	0.083–0.102	0.092
~0.11	0.118	0.133	≥0.115*	≥0.12*	—	5	0.110–0.133	0.119
—	—	—	—	—	—			
					—			
—	—	—	—	—	—			
—	—	—	—	—	—			
—	—	—	—	—	—			
—	—	—	—	—	—			
—	—	—	—	—	—			
—	—	—	—	—	—			
—	—	—	—	—	—			
—	—	—	—	—	—			

* Only widths.
[e] Estimated.

Eobasileus cornutus

PM 1453 L	Juvenile without epiphyses PM 3212 L	Juvenile without distal epiphysis PM 3224 L	Old female DMNH EPV 493 R	DMNH EPV 497	N	Range	Mean
—	≥0.564*	0.565*	0.6	—	3*	0.6–0.750*	0.699*
—	—	0.088	0.114	(0.16)*	2	0.114	0.101
—	—	0.106	0.131	(0.16)*	2	0.131	0.119
—	—	~0.19	—	—	1	0.19	
—	~0.01	<0.01	—	—	1	0.01	
—	>0.23	0.214	—	—	1	0.214	
0.051	0.053	0.052	—	—	3	0.051–0.053	0.052
~0.08	0.081	0.079	—	—	3	0.079–0.081	0.080
0.156	—	—	0.131	—	2	0.131–0.156	0.144
~0.135	—	—	—	—	1	~0.135	
~0.085	—	—	—	—	1	~0.085	
0.065	—	—	—*	0.078	2	0.065–0.078	0.072
0.066	—	—	—*	0.075	2	0.066–0.075	0.071
	* Not in statistics.	* Not in statistics.	* L inner condyle = 0.122 * L outer condyle = 0.101 * Not in statistics.	* Not in statistics; only one diameter recorded.		* Includes Wheeler's values for the holotype, AMNH 5040 (0.75), and YPM 14323 (0.747).	

† I think this specimen is subadult. One glenoid epiphyseal surface is off, i.e., was not well fused.
‡ Cope's (1873, p. 5) 4.5-foot estimate is suspect, probably a generous guess. The pelvis is not measurable in its present broken condition.

TABLE 11. Measurements of patella, tibia, and fibula, *Uintatherium anceps* and *Eobasileus cornutus* (in m).

	Uintatherium anceps							
	PM 2079	PM 3236	PM 39393	PM 54401	PM 54402	PM 54404	PM 55396	
PATELLA	R						L	R
Length of articular surface	0.112	0.1	0.109	0.108	0.106	—		
Width of articular surface	0.085	≥0.084	≥0.082	0.084	0.084	≥0.089		
Maximum thickness	0.057	0.057	0.055	0.051	0.057	0.049		

	Uintatherium anceps							
	D. mirabile YPM 11208	PM 2078	PM 2079B	PM 38782		PM 39393	PM 53921	
TIBIA†	L	R	R	L	R		L	R
Length	0.390	≥0.455	0.348	0.453	0.443	≥0.40	>0.395	0.442
Greatest diameter, proximal end	0.140	≥0.134	≥0.111	0.141	>0.120	≫0.116	0.158	0.165
AP diameter, below patella	0.096	>0.10	≥0.078	0.113	>0.105	—	≥0.077	0.081
AP diameter of inner proximal articular surface	0.080	>0.129	—	0.08	≥0.078	—	≥0.080	≥0.076
Transverse diameter of inner proximal articular surface	0.062	0.091	—	>0.068	0.07	—	0.08	0.077
AP diameter of outer proximal articular surface	0.070	>0.108	—	>0.069	—	—	≥0.077	≥0.071
Transverse diameter of outer proximal articular surface	0.075	—	—	>0.070	—	—	0.076	0.081
Greatest diameter of fibular articular surface	0.033	—	—	≥0.033	—	—	0.032	0.038
Least diameter of fibular articular surface	0.027	—	—	0.019	—	—	0.025	0.025
Least diameter of shaft	0.052	≥0.047	—	0.063	—	0.053	0.058	0.06
	0.057	≥0.049	—	0.063	—	0.068	0.074	0.07
Greatest diameter, distal end	0.107	>0.109	≥0.125	0.13	>0.091	~0.106	—	>0.129
AP diameter, distal end	0.093	>0.093	>0.078	0.104	0.091	≫0.066	—	0.091
Greatest diameter of astragalar surface (approx.)	0.095	>0.098	>0.089	>0.09	>0.081	>0.070	—	>0.108
AP diameters of astragalar surface	0.067	>0.081	>0.056	0.07	≫0.068	>0.040	—	—
	0.080	≫0.061	>0.054	0.075	—	—	—	—
AP diameter of distal fibular surface	0.035	—	—	—	—	—	—	—
Least diameter of distal fibular surface	0.015	—	—	—	—	—	—	—

	Uintatherium anceps					
	D. mirabile					
	YPM 11208	YPM 11210	PM 53921		PM 54866*	PM 55175
FIBULA			L	R		
Length of fibula (approx.)	0.350	—	0.392	≫0.33	0.373	—
Diameters of proximal end	0.040	—	0.033	—	0.046	—
	0.045	—	0.076	—	≥0.053	—
Diameters of proximal articular surface	0.028	—	0.025	—	>0.017	—
	0.033	—	0.044	—	≥0.035	—
Diameters of shaft	—	0.028	0.029	0.033	0.029	—
	—	0.020	0.024	0.023	0.019	—
Diameters of distal end	—	0.040	0.041	≫0.043	0.043	0.044
	—	0.070	0.073	≫0.054	0.078	0.071
Diameters of distal articular surface (approx.)	—	0.050	0.054	≫0.034	0.056	0.058
		0.045	0.044	0.027	≥0.040	≥0.036

* Specimen has a healed break.

Notes: Data listings begin with Marsh's Yale University (YPM) specimens (Marsh 1886, pp. 142–143).
* See notes in respective columns.
† Wheeler gives the length of YPM 11030, part of the holotype (restored tibia), as 0.34 m.

TABLE 11. *Extended.*

Uintatherium anceps					
PM 55407	PM 55423		PM 55577	DMNH EPV 2606	DMNH EPV 2652
	L	R			
≥0.090	≫0.087	≥0.105	>0.096	0.1	0.112
0.076	>0.077	0.088	≥0.067	0.07	0.094
0.053	0.055	0.059	0.051	—	—

Uintatherium anceps											
									Univ. Colo. Museum		
PM 35936	PM 54403	PM 54825	PM 55175	PM 55423	PM 55423	PM 58057	Old female DMNH EPV 493	DMNH uncat.	Bridger Fm. UCM 60871	Bridger Fm. UCM 72519	
	L			L	R	R	R		L	L	R
—	≥0.424	0.497	—	—	0.372¶	—	0.444	0.49	≥0.46	—	—
>0.12	≥0.152	0.151	≫0.124	—	0.179	≥0.174	>0.14	0.166	≥0.095	0.15	0.155
—	0.135	0.114	≫0.089	—	0.152	≥0.135	—	—	—	—	—
>0.07	>0.105	0.089	≫0.051	—	0.094	0.099	0.095	—	—	—	—
					0.092	≥0.073	0.072	—	—	—	—
>0.068	>0.074	0.074	>0.073	—	0.104	≫0.07	0.095	—	—	—	0.08
—	—	0.072	≫0.057	—	0.07	0.082	0.065	—	—	—	0.085
					<0.048	0.041	—	—	—	—	—
—	—	0.069	—	—	—	0.023	—	—	—	—	—
—	—	>0.026	—	—	0.07	>0.062	—	—	—	—	—
—	—	>0.014	—	—	0.073	>0.071	—	—	—	—	—
—	0.054	0.07	—	0.069	0.173	—	—	—	~0.145	—	~0.10
—	0.066	0.085	—	0.071	0.126	—	—	—	—	—	—
—	>0.127	≥0.118	—	0.15	0.127	—	0.085	—	—	—	—
—	≥0.106	>0.096	—	0.131	≥0.106	—	—	—	—	—	—
—	≥0.105	≥0.110	—	0.113	≥0.108	—	0.11	—	—	—	—
—	≥0.083	>0.086	—	0.086	~0.056	—	—	—	—	—	—
—	>0.087	—	—	0.087	<0.027	—	—	—	—	—	—
—	—	—	—	—							
—	~0.011	—	—	—							

Uintatherium anceps	
PM 55423	PM 55580
R	
0.342	—
0.052	—
0.068	—
0.035	—
0.039	—
0.023	—
0.022	—
0.047	0.039
0.078	0.071
0.059	0.060
0.036	0.032

¶ Telescoped; not included in statistics.

TABLE 11. *Extended.*

N	Range	Mean	s
9	0.090–0.112	0.105	0.007
11	0.067–0.094	0.082	0.008
10	0.049-0.059	0.054	0.003

				Eobasileus cornutus						Transitional zone specimens	
				Juvenile PM 1452 R	PM 3211	Juv. w/o epiphyses PM 3212				TWkA 1–2 PM 54865	TWkA2 PM 54866
N	Range	Mean	s	R			N	Range	Mean		R
28‡	0.300–0.497‡	0.426‡	0.045‡	—	—	−0.41	3§	0.410–0.500§	0.469§	—	—
14	0.095–0.179	0.148	0.023	—	—	—	—	—	—	≥0.165	—
9	0.077–0.152	0.109	0.028	>0.083	—	—	—	—	—	≥0.099	—
9	0.076–0.099	0.086	0.009	>0.062	—	—	1	0.095	—	>0.075	—
9	0.062–0.092	0.077	0.010	0.056	—	—	2	0.056–0.072	0.064	0.079	—
7	0.070–0.104	0.082		>0.062	—	—	1	0.095	—	—	—
8	0.065–0.085	0.075	0.007	≥0.055	—	—	1	0.055–0.065	0.06	—	—
5	0.032–0.038	0.035		—	—	—	—	—	—	—	—
5	0.019–0.027	0.024		—	0.044	—	1	0.044	—	—	—
10	0.047–0.070	0.06	0.008	0.046	0.047	0.059	3	0.046–0.059	0.051	—	—
10	0.049–0.085	0.068	0.010	0.061	0.065	0.069	3	0.061–0.069	0.065	—	—
9	0.100-0.173	0.128	0.024	—	~0.124	—	1	0.124	—	—	0.116
7	0.091–0.131	0.106		—	0.067	—	1	0.067	—	—	0.1
6	0.085–0.127	0.106		—	>0.082	—	—	—	—	—	(>0.089)
5	0.067–0.106	0.082		—	0.056	—	2	0.056–0.085	0.071	—	≥0.086
5	0.075–0.110	0.092		—	0.064	—	2	0.064–0.110	0.087	—	—
2	0.035–0.056	0.046		—	0.054	—	1	0.054	—	—	—
2	0.011–0.015	0.013		—	~0.037	—	1	0.037	—	—	—

N	Range	Mean	s
4	0.342–0.392	0.364	—
4	0.033–0.052	0.043	—
4	0.045–0.076	0.061	—
3	0.025–0.035	0.029	—
4	0.033–0.044	0.038	—
5	0.023–0.033	0.028	—
5	0.019–0.024	0.022	—
6	0.039–0.047	0.042	—
6	0.070–0.078	0.074	—
6	0.050–0.060	0.056	—
7	0.027–0.045	0.037	—

‡ Includes Wheeler's values for AMNH 1660, 1667, 1675, 1685, 2316, 5042, 5048, 12167, 12171 (0.453, 0.30, 0.408, 0.43, 0.436, 0.474, 0.396, 0.465, and 0.37); USNM 4740 and 4761 (0.416 and 0.42); and YPM 11243, 11252, 11558, and 11576 (0.448, 0.455, 0.451, and 0.416).

§ Includes Wheeler's values of 0.50 for YPM 11510 and 0.496 for YPM 11573.

TABLE 12. Measurements of astragalus and calcaneum, *Uintatherium anceps* and *Eobasileus cornutus* (in m).

	Uintatherium anceps			
	D. mirabile YPM 11210	*D. mirabile* YPM 11528	*D. laticeps* YPM 11197	*T. ingens* YPM 11209
ASTRAGALUS	**L**	**R**	**L**	**L**
Greatest AP diameter of astragalus	0.112	0.100	0.128	0.122
Greatest transverse diameter	0.121	0.108	0.128	0.147
Greatest vertical diameter	0.070	0.063	0.080	0.083
Greatest diameter of articular face for tibia	0.110	0.100	0.127	0.125
AP diameters of articular face for tibia	0.072	0.070	0.089	0.091
	0.066	0.060	0.080	0.082
	0.092	0.093	0.105	0.104
Transverse diameters of articular face for tibia	0.076	0.067	0.090	0.094
	0.071	0.067	0.085	0.096
	0.085	0.070	0.091	0.095
AP diameter of articular face for fibula	0.044	0.040	0.055	0.060
Vertical diameter of articular face for fibula	0.036	0.030	0.031	0.039
AP diameter of articular face for calcaneum	0.054	0.035	0.053	0.050
Transverse diameter of articular face for calcaneum	0.080	—	—	—
Transverse diameter of articular face for calcaneum, outer lobe	0.033	0.039	0.061	0.050
Transverse diameter of articular face for calcaneum, inner lobe	0.040	—	0.035	—
Diameter of band connecting lobes	0.018	—	—	0.018
AP diameter of united faces for navicular and cuboid	0.056	0.053	0.072	0.068
Transverse diameter of united faces for navicular and cuboid	0.107	0.093	0.113	0.130
Diameters of face for navicular	0.056	0.076	0.064	0.068
	0.082	0.053	0.091	0.105
Diameters of face for cuboid	0.035	0.026	0.031	0.042
	0.062	0.055	0.071	0.077
Minimum length of neck	0.014	0.015	0.016	0.019

	Uintatherium anceps		
	D. mirabile YPM 11208	*D. mirabile* YPM 11210	*D. mirabile* YPM 11225
CALCANEUM	**L**	**L**	**R**
Length from greater tuberosity to face for cuboid	0.093	0.096	0.107
Transverse diameter	0.086	0.090	0.086
Vertical diameter	0.074	0.070	0.074
AP diameter of inner face for astragalus	0.044	0.050	0.053
Transverse diameter of inner face for astragalus	0.042	0.043	0.037
AP diameter of outer face for astragalus	0.050	0.043	0.045
Transverse diameter of outer face for astragalus	0.032	0.039	0.037
Distance between faces for astragalus*	0.070	—	0.010
Transverse diameter of face for cuboid	0.035	—	—
Vertical diameter of face for cuboid	0.019	—	—

Notes: Data listings begin with Marsh's Yale University (YPM) specimens (Marsh 1886, pp. 150–151, 153).
* Either I misunderstand Marsh, or perhaps he meant 0.007 for this feature in YPM 11208.

TABLE 12. *Extended.*

Uintatherium anceps										*Eobasileus cornutus*
Field Museum TWkA1 specimens				DMNH specimens						
PM 39393	PM 53921	PM 55423		EPV 538	EPV 2605					PM 3212
L	R	L	R			N	Range	Mean	s	L
—	>0.094	0.132	0.135	0.105	≥0.09	6	0.100—0.135	0.122		0.134
≫0.097	0.12	0.141	0.143	—	>0.107	7	0.108–0.147	0.13		0.144
≥0.062	≥0.087	0.068	0.068	—	—	8	0.062–0.087	0.073	0.009	0.061
—	0.103	0.124	0.128	0.105	0.107	9	0.1–0.128	0.114	0.011	0.118
—	—	0.081	0.093	—	—	6	0.070–0.093	0.083		0.07
—	—	0.088	0.105	—	—	6	0.060–0.105	0.08		0.118
—	—	0.106	0.083	0.105	0.09	8	0.083–0.105	0.097	0.009	0.09
—	—	0.062	0.085	—	—	6	0.062–0.094	0.079		0.078
—	—	0.124	0.098	—	—	6	0.067–0.124	0.09		0.102
—	—	0.072	0.091	0.1	0.107	8	0.070–0.107	0.089	0.013	0.086
—	—	0.06	0.055	—	—	6	0.040–0.060	0.052		—
—	—	0.036	0.036	—	—	6	0.030–0.039	0.035		—
—	—	0.073	0.072	—	—	6	0.035–0.073	0.056		—
—	—	0.09	0.093	—	—	3	0.080–0.093	0.088		—
—	—	~0.0.48	0.04	—	—	6	0.033–0.061	0.045		—
—	—	−0.045	0.044	—	—	4	0.035–0.045	0.041		—
—	—	—	0.014	—	—	3	0.014–0.018	0.017		—
>0.047	—	0.074	0.067	—	—	6	0.053–0.074	0.065		—
>0.09	—	0.123	0.125	—	—	6	0.093–0.130	0.115		—
−0.049	—	0.074	0.105	—	—	6	0.049–0.105	0.07		—
−0.074	—	0.102	0.068	—	—	9	0.053–0.105	0.08	0.019	—
−0.03	—	0.041	≥0.041	—	—	7	0.026–0.042	0.035		—
>0.036	—	0.063	0.063	—	—	6	0.055–0.077	0.065		—
—	—	—	—	—	—	4	0.014–0.019	0.016		—

Uintatherium anceps				
PM 55423				
L	R	N	Range	Mean	s
0.123	0.125	5	0.093–0.125	0.109	
—	0.098	4	0.086–0.098	0.933	
0.069	~0.073	5	0.069–0.074	0.072	
≥0.063	~0.062	5	0.044–0.063	0.054	
≥0.040	—	4	0.037–0.043	0.041	
>0.045	—	3	0.043–0.050	0.046	
0.043	−0.04	5	0.032–0.043	0.038	
0.02	−0.022				
—	0.037	2	0.035–0.037	0.036	
—	0.022	2	0.019–0.022	0.021	

TABLE 13. *Eobasileus cornutus,* upper dentition (in cm).

Item	Uinta Basin, Uinta Fm.					Washkie Basin, Washakie Fm., TWkA2			
	AMNH	P 12170		P 12164		P 26234 (=YPM 11041)†		UW 13644*	
	5040	L	R	L	R	L	R	L	R
L									
P_2–M_3	16.8	18.5 alv.	17.2	>17.94 ~ 18.00	—	17.39	16.4 (W)	16.8	17.8
P_3–M_3		15.4	15.5	15.71	—	14.5	14.3	—	15.71
P_4–M_3		12.64	12.76	13.08	—	12.24	11.68	—	—
L									
P_2–P_4		8.00 (alv.)	7.02	>6.40	—	7.99	6.76	—	—
P_2–P_3		~5.45 (alv.)	4.18	>4.00	—	5.41	4.49	—	—
P_2–M_1		8.09 (alv.)	9.68	≫9.20	—	10.22	9.13	—	—
P_2–M_2		13.9 (alv.)	12.87	≫12.40	—	13.55	12.66	—	—
L									
P_3–P_4		5.16	5.04	5.22	—	5.38	4.44	—	—
P_3–M_2		10.48	10.71	11.59	—	11.07	10.34	—	—
P_3–M_1		7.76	7.76	8.19	—	7.86	7.11	—	—
L									
P_4–M_1		5.17	5.14	5.57	—	5.22	4.76	—	—
P_4–M_2		8.51	8.09	9.06	—	8.43	8.26	—	—
L									
M_1–M_3		10.33	10.42	10.64	—	9.7	9.53	—	—
M_1–M_2		5.73	5.59	6.57	—	5.84	5.5	—	—
M_2–M_3		8.01	8.14	8.07	—	7.44	7.64	—	—
C									
L (alv.)		—	5.46	—	—	6	5.68	—	—
W		—	2.96	—	—	—	2.97	—	—
L (alv.-tip)		—	18.61	—	—	—	—	—	—
P2									
L		—	2.23	—	—	2.76	2.35	2.38	2.19
AW		—	2.38	—	—	2.49	2.88	2.13	2.14
PW		—	2.45	—	—	2.52	2.38	2.29	1.94
P3									
L		2.77	2.73	2.77	—	2.63	2.36	2.77	2.33
AW		3.29	3.14	3.74	—	3.09	2.95	3.32	3.09
PW		3.18	3.05	>3.50	—	3.06	2.92	2.98	>3.04
P4									
L		2.66	2.89	>2.76	—	2.74	2.38	2.58	2.57
AW		3.44	3.28	>3.22	—	3.3	3.05	>3.08	3.21
PW		3.27	3.1	>3.10	—	3.25	2.9	>2.95	3.16
M1									
L		2.8	2.88	≥2.92[w,b]	—	2.73	2.66	2.33	>2.22
AW		3.48	3.27	≥3.42	—	3.36	>2.96	>3.35	>3.34
PW		3.17	2.97	>3.06	—	3.18	>2.54	3.04	>3.10
M2									
L		3.58	3.77	3.88	≫3.29	3.39	>3.6[e]	3.43	3.44
AW		4.58	4.4	>4.23	>4.07	4.48	3.93	4.16	4.14
PW		4	3.84	>3.48	4.21	4.02	3.58	3.53	3.68
M3									
L		4.46	4.55	4.75	≫4.37	4.37	4.37	4.89	4.44
AW		5.64	5.48	4.79	>4.57	4.82	4.63	5.04	5.02
PW		4.47	4.27	4.12	≫3.90	4.15	4	4.39	4.27

* All teeth P_2–M_3 are worn, especially M1.

* See notes in respective columns.
Notes: [b]broken, [e]estimated, [w]worn, W = width, or, in parentheses, Wheeler's value.
† Horizon uncertain; may be top of TWkA1.

TABLE 13. *Extended.*

Washkie Basin, Washakie Fm., TWkA2		Sand Wash Basin (TWkA2)						
YPM 11567‡	UWBM 59204	DMNH EPV 495		DMNH EPV 529				
L	L	L	R		N	Range	Mean	s
15.96	~17.88§	18.8 (W)¶		—	11*	15.96–18.80*	17.32*	0.89*
13.93	~15.61§	—	—	—	8	13.93–15.71	15.08	0.72
11.64	~13.13§	—	—	—	7	11.64–13.13	12.45	
6.7	~7.61	7.93	7.67	—	7	6.70–7.99	7.38	
4.74	~4.84	—	—	—	5	4.18–5.41	4.73	
9.33	—	—	—	—	4	9.13–10.22	9.59	
12.46	~14.12§	—	—	—	5	12.56–14.12	13.13	
4.63	~5.24§	—	—	—	7	4.44–5.38	5.02	
10.49	~11.77§	—	—	—	7	10.34–11.77	10.92	
7.31	—	—	—	—	6	7.11–8.19	7.67	
4.92	—	—	—	—	6	4.76–5.57	5.13	
8.12	~9.22§	—	—	—	7	8.09–9.22	8.53	
9.53	—	11.72	11.15	—	8	9.53–11.72	10.38	0.79
6.04	—	—	—	—	6	5.50–6.57	5.88	
7.18	~7.49§	—	—	—	7	7.18–8.14	7.71	
—	—	—	—	—	3	5.46–6.00	5.71	
—	—	—	—	—	2	2.96–2.97	2.97	
—	—	—	—	—	1	18.61		
2.13	2.23	2.59	2.5	2.71	10	2.13–2.76	2.41	0.22
2.11	2.21	—	—	>2.70	7	2.11–2.88	2.33	
2.18	2.18	2.41	2.46	>2.82	9	1.94–2.52	2.31	0.18
2.4	2.66	2.68	2.7	2.63	12	2.33–2.77	2.62	0.16
2.85	2.88	3.26	3.35	2.46	12	2.46–3.74	3.12	0.32
2.89	2.89	3.14	3.18	2.76	10	2.76–3.18	3.01	0.14
2.53	2.77	2.95	2.84	2.25	11	2.25–2.95	2.65	0.22
2.84	3.03	3.47	3.38	2.39	10	2.39–3.47	3.14	0.33
2.72	2.88	~3.13[b]	3.07	2.47	10	2.47–3.27	3	0.25
2.77	—	2.95	2.66	—	9	2.33–2.95	2.74	0.19
2.84	—	3.15	3.07[b]	—	6	2.84–3.48	3.22	
2.67	—	3.09	3.3	—	7	2.67–3.30	3.06	
3.65	3.55	3.98	4.11	4.01 ?	10	3.39–4.11	3.67	0.26
3.96	3.89	3.98	3.45	4.40 ?	10	3.45–4.58	4.1	0.33
3.55	3.49	3.78	3.89	4.04 ?	11	3.49–4.21	3.78	0.24
3.91	4.05	>4.98[b]	5.01	4.01 ?	10	3.91–5.01	4.48	0.34
4.85	>4.27	>4.08[b]	4.61	4.40 ?	9	4.61–5.64	4.99	0.36
4.28	~3.84	4.01	4.36	4.04 ?	11	3.84–4.47	4.2	0.19

? Position uncertain, M_2 or M_3, prob. M_2. Not included in statistics.

* Includes Wheeler's value of 18.4 for YPM 11043.

‡ PM 3944 is a cast of YPM 11567, *Tin. stenops* = *Teth. speirianus*. Wheeler's value is used in the statistics. My measurements, taken on the cast, varied between 16.4 and 19.09 cm.

§ This is a continuous tooth series, P_2–M_3. M_1 is highly altered, leading to the approximate measurements.

¶ Wheeler did not indicate which side was measured.

TABLE 14. *Eobasileus cornutus,* lower dentition (in cm).

	Washakie Basin, Washakie Fm., TWkA2 (All *Eobasileus cornutus*)							Sand Wash Basin, Washakie Fm. (All *Uintacolotherium blaynei* = *E. cornutus*)	
	PM 1674 A	PM 1737		YPM 11567*	YPM 11256*	PUM 11611	UCMP 81356	EPV 493	
Item	R	L	R	L	L	L	L	L	R
L									
p2–m3	—	>17.5, ~17.8	—	16.96	17.3 (W)	16.8 (W)*	alv. >18.17	—	—
p3–m3	—	>15.5, ~16.0	≫13.75	14.45	—	—	14.98w	—	—
p4–m3	—	>12.8, ~13.4	≫11.18	12.09	—	—	12.61w	—	—
L									
m1–m3	—	>10.0, ~10.5	≫8.65	9.79	—	9.4	9.96w	—	—
m1–m2	—	5.76	6.28	5.6	—	—	5.93w	—	—
m2–m3	—	>7.81, ~8.20	≫5.95	7.5	—	—	—	—	—
L									
p2–m2	—	13.3	—	12.34	—	—	—	—	—
p2–m1	—	9.97	—	9.01	—	—	—	—	—
p2–p4	—	7.6	—	6.71	—	—	—	—	—
p2–p3	—	4.93	—	4.37	—	—	—	—	—
L									
p3–m2	—	11.07	11.51	10.33	—	—	10.88w	—	—
p3–m1	—	7.74	8.01	7.15	—	—	7.51w	—	—
p3–p4	—	5.43	5.15	4.7	—	—	5.12w	—	—
L									
p4–m2	—	8.52	8.91	7.79	—	—	8.36w	—	—
L									
p4–m1	—	5.2	5.39	4.78	—	—	5.03w	—	—
p2									
L	—	2.34	2.62	2.19	—	2.3	—	2.08	—
AW	—	1.17	1.91	1.23	—	1.9w	—	1.32	—
PW	—	1.62	1.93	1.52	—	1.9w	—	1.38	—
p3									
L	—	2.72	2.67	2.25	—	—	2.49w	2.2	2.25
AW	—	1.89	2.14	1.82	—	—	1.88w	1.82	1.78
PW	—	2	2.11	2.03	—	—	2.07w	2.02	2.11
P4									
L	2.58*	2.66	>2.59	2.38	—	—	2.61w	2.12	2.42
AW	1.94*	2.17	>2.13	2.07	—	—	2.52w	1.89	1.78w
PW	2.01*	2.2	2.14	2.2	—	—	2.73w	2.05	1.59w
m1									
L	2.58*	2.41w	~2.85w	2.36	—	—	2.53w	2.17w	Shed
AW	1.94*	>1.9w	2.13w	2.04	—	—	2.16w	1.76w	Shed
PW	2.01*	>1.95w	>2.11w	2.03	—	—	2.13w	1.79w	Shed
m2									
L	—	3.43	3.44	3.2	—	—	3.45w	3	3.09
AW	—	2.87	2.84	2.89	—	—	2.82w	2.75	2.59
PW	—	2.71	2.72	2.62	—	—	2.71w	2.63	2.76
m3									
L	—	>4.5 ~4.9	—	4.41	—	4.7	4.45w	4.01	3.85
AW	—	3.56	3.58	3.65	—	3.8w	3.52w	>2.95	3.15
PW	—	3.46	—	3.04	—	3.8w	3.26w	2.92	3.17
	* Rp4 or m1; not included in statistics.			* PM 3944 cast (type *Tin. stenops*).	* P26235 cast (type *Tin. longiceps*).	* Osborne and Speir's measures are 16.5 and 16.6; not included in statistics.			

Notes: wWorn, (W) Wheeler's value; L, left (for items) or length; W, width.
* See notes in respective columns.

TABLE 14. *Extended.*

Sand Wash Basin, Washakie Fm. (All *Uintacolotherium blaynei* = *E. cornutus*)			Uinta Fm. (*E. cornutus*)							
EPV 496 type*		EPV 2604	UCM 51046 F*					PUM 11611		
L	R	R	L	R	N	Range	Mean	s			
18.72*	17.6*	—	—	—	7*	16.96–19.20*	17.77*				
—	—	—	—	—	3	14.45–16.00	15.14				
—	—	—	—	—	3	12.09–13.40	12.7				
									root L	2.4
								i1 Mesial-dist.	Length	4.3
10.97	11.48	—	—	—	6	9.40–11.48	10.35		W	1.7
—	—	—	—	—	4	5.60–6.28	5.89			
—	—	—	—	—	2	7.50–8.20	7.85			
									root L	2.1
—	—	—	—	—	2	12.34–13.30	12.82	i2 Mesial-dist.	L	3.8
—	—	—	—	—	2	9.01–9.97	9.49		W	1.6
7.64	6.31	—	—	—	4	6.31–7.64	7.07			
—	—	—	—	—	2	4.37–4.93	4.65			
									root L	1.9
—	—	—	—	—	4	10.33–11.51	10.95	i3 Mesial-dist.	L	3.5
—	—	—	—	—	4	7.15–8.01	7.6		W	1.4
—	—	—	—	—	4	4.70–5.43	5.1			
—	—	—	—	—	4	7.97–8.91	8.44		root L	1.9
								c Mesial-dist.	L	3.5
—	—	—	—	—	4	4.78–5.39	5.1		W	1.5
2.06	2.01	—	—	2.4	8	2.01–2.62	2.25	0.21		
1.96	1.64	—	—	1.7	8	1.17–1.96	1.51	0.33		
≥2.05	2.13	—	—	1.5	8	1.38–2.13	1.75	0.28		
2.67	2.31	—	—	2.3	9	2.2–2.72	2.43	0.21		
2.59	2.34	—	—	—	8	1.78–2.59	2.03	0.3		
2.77	2.32	—	—	1.9	9	1.90–2.77	2.15	0.26		
2.98	2.33	—	—	2.7	8	2.12–2.98	2.53	0.27		
2.75	2.44	—	—	>1.5, ~1.7	8	1.70–2.75	2.17	0.38		
2.37	2.51	—	—	1.9	9	1.59–2.73	2.19	0.33		
3	3.12	—	—	—	7	2.17–3.12	2.63			
2.88	2.94	—	~2.1	—	7	1.76–2.94	2.29			
2.92	2.96	—	—	—	5	1.79–2.96	2.37			
3.63	3.83	3.07*	~2.9	3	11	2.90–3.83	3.28	0.3		
3.21	3.28	2.77*	—	>2.5**	9	2.59–3.28	2.89	0.22		
3.86	3.48	2.96*	~2.7	~2.6	11	2.60–3.86	2.89	0.41		
4.77	4.63	—	~3.9	3.7	10	3.70–4.90	4.32	0.43		
3.77	3.48	—	~2.8	2.8	10	2.80–3.80	3.41	0.37		
3.91	3.87	—	~2.8	2.3	10	2.30–3.91	3.25	0.52		

* Wheeler measured 19.6 cm, based on a poor restoration.

* Not included in statistics

* Rio Blanco Co., Colorado. ** Not included in statistics.

* Includes Wheeler's 19.2 value for YPM 11043.

TABLE 15. Summary of table of upper dentitions, *Uintatherium anceps* and *Eobasileus cornutus,* compared with two of the specimens from the transition zone low within TWkA2, UW 13644 and U Wa 59204 (measurements in cm).

	Uintatherium anceps			UW 13644			U Wa 59204	*Eobasileus cornutus*		
Length	**Range**	**N**	**Mean**	**L**	**R**	**Average**	**L**	**Range**	**N**	**Mean**
P2–M3	13.26–17.78	14	15.51	16.80	17.80	**17.3**	**17.88**	15.96–18.80	10	**17.48**
P3–M3	11.49–14.20	9	12.71	15.71	15.71	**15.71**	**15.61**	13.93–15.71	8	**15.08**
P2	1.90–2.42	19	2.16*	2.38	2.19	**2.29**	2.23*	2.16–2.76	10	**2.41**
P3	1.90–2.74	21	2.42	2.77	2.33	**2.55**	**2.66**	2.33–2.72	12	**2.62**
P4	2.15–3.00	21	2.42	2.58	2.57	**2.58**	**2.77**	2.25–2.95	10	**2.65**
M1	1.89–2.73	20	2.33*	2.33	—	2.33*	—	2.33–2.95	9	2.74
M2	2.75–3.57	17	3.21	3.43	3.44	**3.44**	**3.55**	3.39–4.11	10	**3.67**
M3	3.01–4.50	18	3.70*	4.89	4.44	**4.67**	4.05*	3.91–5.01	10	**4.48**

Note: The **bolded** values for UW 13644 and U Wa 59204 suggest closer affinity with *E. cornutus* (whose corresponding values are also **bolded**). Values marked by an asterisk (*) suggest closer affinity to *U. anceps.* Overall, the *E. cornutus* fit is best.

Note that the University of Wyoming specimen, which is probably female with very worn teeth, has a skull length that is near to the norm for *Uintatherium anceps* (Table 1). Its individual tooth measures, however, especially those of M3 (and except for those of M1) clearly are much closer to *Eobasileus cornutus* (Tables 5, 13, and 15). The B/A cranial proportion ratio also is closer to the latter.

In fact, as those tables show, there is overlap in the ranges of measurements of all of the cheek teeth of the two species for each tooth position. In the case of the length of M1, the University of Wyoming specimen is near the middle of the range of *U. anceps,* but at the bottom end of that of *E. cornutus.* For the premolars, the reverse is true and the measures are all close to the means of *E. cornutus* and near to the upper limits of the ranges for *U. anceps.* With the multiple-teeth series, there is overlap of the ranges, but the Wyoming specimen is well within the range of *E. cornutus,* near its mean for P2–M3 or above it for P3–M3.

Inasmuch as the Wyoming specimen possibly came from high in the TWkA1 unit or more probably from low in the TWkA2 unit (i.e., near the base of the old Upper Washakie), I believe that the best interpretation is that we are here witnessing a stage in the evolution of *E. cornutus* from its predecessor, *U. anceps,* and that the dentition and cranial proportion ratio (B/A) preceded skull length during this transition.

The Burke Museum specimen presents a similar case; hence my assignment as cf. *E. cornutus.* It also comes from near the bottom of TWkA2, but there are fewer measurements to go on. In Table 15 a few more of its measures fall closer to *E. cornutus* than to *U. anceps* (lengths of P3, P4, and M2). For most of the others, they are in the upper part of the ranges of the latter taxon; i.e., they are always above the means of those measures (Table 5). All of the multiple tooth measures are larger, well beyond the range of *U. anceps,* and even above the means values of *E. cornutus* (Tables 5 and 13).

TABLE 16. Pelvic width measurements.

Taxon and specimen number	Sex	Greatest width across pelvis (cm)
Uintatherium (cf.) *anceps*		
PM 3984		116
PM 53921		>117
USNM		123
Loxodon africanus		
FMNH 18834 (subadult)		87
FMNH 53794 (juvenile)		63.5
Elephas maximus		
FMNH 49894	Male	123
FMNH 60601 (Ziggy*)		133
Mammuthus sp.		
P 12399		156
Mammut americanum		
P 25125		165
Ceratotherium simum cottoni		
FMNH 29174	Male	86
C. simum simum		
FMNH 125413		92
Diceros bicornis		
FMNH 57809		73
FMNH 127848		79
FMNH 127851		75
Rhinoceros unicornis		
FMNH 57639		85
FMNH 57822		84.5
Hippopotamus amphibius		
FMNH 22367		72
FMNH 127870		61.5
FMNH 127871		65

* One of the largest zoo animals.

TABLE 17. Skull, jaw, and cheek toothrow lengths (cm).

Specimen	Length (tip of premaxilla to rear of occip. condyle)	Skull, width of:		Other identity or teeth measured	Cheek teeth and lower jaws		
		Occiput	Condyles		Upper toothrow length: P2–M3 or as indicated	Lower toothrow length, p2–m3	Jaw length
Uintatherium anceps							
FMNH P 26232 (cast of YPM 11036?)	74	~24	~15	*D. mirabile*	16.17	—	—
FMNH P26233 (cast of YPM 11039)	77			*D. laticeps* type	—	>17.5	~52
FMNH PM 1667	—	31.5	19		—	—	—
FMNH PM3896 (juv.)	42.5				—	—	—
FMNH PM 3944 (cast of YPM 11567)	82				16.1	16.69	—
FMNH PM 8019 (juv.)	~50	~17.5	~14		—	—	—
FMNH PM 8089 (cast of PUM 10385)	—				—	15.43	—
FMNH PM 38781[a]	—				—	—	—
FMNH PM 53932	—				—	15.22	—
FMNH PM 53933[b] (young adult)	≥67.5	29+	16.0	*U. anceps*	14.8	—	—
FMNH PM 55174[c]	—				—	16.99	56
FMNH PM 55827[d]	—				—	17.57	est. 48
FMNH PM 60171	70	~25	14.5	(as restored)	~13.7	—	45.4
Eobasileus cornutus							
AMNH 5040, holotype (large adult)	91.5 (95)[e]				16.8	—	—
FMNH P 12164	57.5				18	—	—
FMNH P 12170[f]	85.0	28.4	20+		17.2 ~18.3	—	—
FMNH P12198[g]	—			(cf.) *Eobasileus*	cast 18.78		—
FMNH P12212 (as restored)	76.5				17.0	—	—
FMNH P 26234 (cast of YPM 11041)	92.0	33.5	~18.0	*T. ingens* type	18.02	—	—
FMNH PM 1737	—				—	18.39	—
FMNH PM 8088 (cast of PUM 10079) type	94		~17	*T. speirianus*	~16.90	—	—
UW 16344 (aged adult)	76.5	—	>14 ~16	transition spec.	(av) 17.3	—	—
UCMP 81356 (worn dentition)	—				alv. >18.7	(m1–3 = 10.0)	≥52.7
FMNH PM ? (cast of UWBM 59204)	—				17.88	—	—
DMNH EPV 495/496	94			*Uintacolotherium*	18.72	(m1–3 = 11.5 + 11)	18.7 + 17.6
Loxodon africanus							
FMNH 18843 (immature)	79.5		—	(P4–M1) ?	~30+	(p4–m1)? 27.+	62.5
FMNH 30345 (subadult)	71			(P3–P4) ?	26+	(p3–p4)? ~24	~60+
FMNH 34364 (mature adult)	98	79.5	23.5	(M2–M3)	32+	(p3–p4) 26+~30	75
FMNH 35115 (newborn ?)	27			(dP1–2)	~7	(dp1–2) ~6	~19
FMNH 53749 (juv.)	67			(P2–3) ?	~18.5	(p2–3)? 17+	48

TABLE 17. *Continued.*

Specimen	Length (tip of premaxilla to rear of occip. condyle)	Skull, width of:		Other identity or teeth measured	Cheek teeth and lower jaws		
		Occiput	Condyles		Upper toothrow length: P2–M3 or as indicated	Lower toothrow length, p2–m3	Jaw length
Elephas maximus							
FMNH (22257)	~64.5		16+	(M3) ?	~19	(m3)? >18.5	63
FMNH 49894 (male)	~84		22.0	(M3)	~21.5	(m3) >25.0	83
FMNH 57232 (juv)	~41			(P2) ?	6.3	(p2) ? ~6.5	—
FMNH 60601 (Ziggy, v.l. male)	~103	85.5	24	(M3)	>16.0	(m3) >21.0	~85
FMNH 68783 (juv., female)	>68		16	(P4) ?	≥12.5	(p4)? ~8.5	55
FMNH 104799 (2½ y female)	41.5			(P2) ?	7	(p2)? 6.5	—
FMNH 142008 (juv.)	~57.5			(P3 or P4)	>10.0	(p4)? ≥12.0	—
FMNH 166993 (adult)	100		23	(M2)	>23.5 est. 25	—	—
Mammuthus sp.							
FMNH UC 1733 *M. columbi*	~90[h] ~97	56.5	20	(M3) ?	21.5	(m1–2)? ~25	~63
FMNH P 12132 *M. boreas*	100		22	(M3)	worn 18	(m3) ~22	~63.4
FMNH P 12339[i] *M. primigenius*	~104.0		20.5	(M3)		(m3) ~25.0	64
FMNH P 12838 *M. columbi*	—			—		(m3) ~23.5	74
Mammut americanum							
FMNH UC ?[j]	—			—		(m2–3) 30.2	
FMNH P 12097	100[k] (107)		21	(M2–3)	29	(m3) 17.6	80
FMNH P13731 *Telobunomastodon*[l]	—			—		v. worn(m3) 21	~72
FMNH P25125[m]	103 (~140)	74.5	25.5	(M2–3)	~34	(m2–3) ~33	
FMNH PM 3945	122	est. 83.5	25	(M3)	18.	(m2–3) 30.3	97
FMNH PM 55468	—			—		(m2–3) ~34	~89
Ceratotherium simum							
C. s. cottoni							
FMNH 29174 (male, y. adult)	72.5	26.5	14.3	(P2–M2)	22.1	26.1	~60
FMNH 34363 (female, subad.)	70.4	24.6	14.4	(P2–M2)	23.7	—	—
C.s. simum							
FMNH 51471 (subadult)	65.5	27.1	14.3	(P2–M2)	24	27.2	55
FMNH 125413 (subadult)	70.5	27.2	16	(P2–M2)	25.3	28.5	60
Diceros bicornis							
FMNH 51868 (subadult)	—			—		(p2–m3)? 22	—
FMNH 57809 (young adult)	52.8	26.2	13	(P1–M3)	24.8	24	47
FMNH 60784 (young adult)	55.7		14.8	(P1–M3)	28	(p1–m3) >28.0	~47
FMNH 121646 (female)	56.7			(P1–M3)	27.2	(p2–m2)? 25.6	—
FMNH 127848 (female subad)	>58.0	25.6	~13.9	(P1–M3)	>28.0	(p2–m2)? 29	49.5
FMNH 127851 (adult)	58		~13	(P1–M3)	26.8	25	50

TABLE 17. *Continued.*

Specimen	Length (tip of premaxilla to rear of occip. condyle)	Skull, width of:		Other identity or teeth measured	Cheek teeth and lower jaws		
		Occiput	Condyles		Upper toothrow length: P2–M3 or as indicated	Lower toothrow length, p2–m3	Jaw length
Rhinoceros unicornis							
FMNH 57639 (adult)	66.3		14	(P2–M3)	25.8	24.1	~56
FMNH 57822 (adult)	66		14.2	(P1–M3)	28.4	26.5	56
FMNH 140833 (adult)	61.5		~15	(P2–M3)	26	26.5	56.5
R.u. indicus 14823 (adult)	≥54.0	23.5	13.2	(P1–M3)	26.1	24.5	46
Hippopotamus amphibius							
FMNH 22367 (male, adult)	68	30.5	16	(P2–M3)	29.2	29	57
				(P3-M3)	23.9	(p3–m3) 24.8	
FMNH 34927 (adult)	63.5		16	(P3–M3)	22.3	(p3–m3) 25	~54
FMNH 34928 (female, y. adult)	58.5			(p3–m3)	>23.3	(p3–m3) 24.7	~46
						p1 or 2–m3 >27.4	
FMNH 34929 (male, adult)	62		16.5	(P3–M3)	22	(p3–m3) >24.0	~52
FMNH 104085 (male)	57		13.5	(dP2–M3)	26.2	(dp2–m3) 26.5	~56
FMNH 105018	60.8		16.5	(P2–M2)	23.2	(p2–m2) 23.4	~52
FMNH 127869 (male, juv.)	—			—		(dp1–m1) 17	
FMNH 127870 (female, adult)	58.8		14.5	(P3–M3)	>23.5	(p3–m3) 26	52
FMNH 127871	—			—		(p3–m3) 24.7	53

[a] Mental foramen to jaw tip = 14+.
[b,f] Best adult skull of this species in FMNH collection.
[c] Condyle to front of flange = 43.5.
[d] Condyle to mental foramen = 39: to front of flange = 43.5.
[e] Given as 95 cm by Wheeler (p. 53), but shown as 91.5 cm on his chart 3 (p. 78)
[f,i,k,m] On exhibit.
[g] Dubious restoration, teeth may be cast or model of P 12170.
[h] Left value = premaxillary tip to rear of occipital condyles; right value = premax. tip to rear of occiput.
[j] Specimen number lost.
[l] As restored.

TABLE 18. Long bone dimensions (cm).

Horizon/specimen	Humerus				Femur			
	Length	Max. diam.	Min. diam.	Min. circum.	Length	Max. diam.	Min. diam.	Min. circum.
Uintatherium anceps								
TWkA1 FMNH PM 1458	**57.3**	9.63	6.1	**29.2**	—	—	—	—
TWkA1 FMNH PM 2079	**60.4**	9.22	7.18	**29**	—	—	—	—
TWkA1 FMNH PM 38781	—	6.71	6	**20**	—	—	—	—
TWkA1 FMNH PM 53921[a]	—	—	—	—	**68.2**	10.2	6.09[b]	**27.6**
TWkA1 FMNH PM 53934	—	—	—	**28**	—	—	—	—
TWkA1 FMNH PM 54407	—	—	—	—	**66.1**	9.94	61.2	**26.5**
TWkA1 FMNH PM 54421	—	—	—	—	**65.8**	8.88	6.58	**24.3**
TWkA1 FMNH PM 54676	**57.2**	8.05	6.78	**28.5**	—	—	—	—
TWkA1 FMNH PM 55423[c]	**53**	9	8	**29.8**	—	11	4	est. **27.5**[b]
TWkA1 FMNH PM 55826	—	—	—	—	**69.6**	9.06	6.13	**25.5**
TWkA USNM[d]	~**61**	—	—	—	~**72**	—	—	—
TWkA USNM 4742	—	—	—	—	**63.7**	—	—	**23**
Eobasileus cornutus								
TWkA2 FMNH PM 1453	—	—	—	—	—	8.44	5.57	**23.5**[b]
TWkA2 FMNH PM 1457	—	~8.04	~7.77	**28.5**	—	—	—	—
TWkA2 FMNH PM 1509	**63.1**	7.62	6.81	**25**	—	—	—	—
TWkA2 FMNH PM 1522	—	9.64	9.21	**32.8***	—	—	—	—
TWkA2 FMNH PM 3212 (juv.)	—	—	—	—	≫**56**[c]	7.97	5.22	**22.9**
TWkA2 FMNH 3224	—	—	—	—	≫**59**	7.85	5.17	**22.9**[b]
TWkA2 FMNH PM 3894	—	—	—	**28**	—	—	—	—
Loxodon africanus								
FMNH 18843	85.2	7.86	~6.90	**23.19**	102.2	9.88	6.29	**25.4**
FMNH 53749	**61.8**	5.93	5.43	17.18	77.2	7.64	5.5	**20.64**
Elephas maximus								
FMNH 49894	90.7	11.81	~10.44	**34.95***	111.2	13.52	7.5	33.02
FMNH 60601 (ziggy)	96	11.48	9.47	**32.91***	118.7	12.96	8.38	33.52
FMNH 142008 (juv.)	52	5.31	5.05	19.27	64.8	6.18	4.89	17.39
FMNH	47.1[g]							
FMNH	40.9[e]				53.8[e]			
Mammuthus sp.								
FMNH PM 1716	~90	~14	10.1	~44.5				
FMNH PM 1719	84.5	12.5	9	**31.5***	~107	~13	~8.5±	35.5
FMNH PM 39231					≫89[f]	~13.5	~8.7	~38.4
FMNH PM 39394	~74	~11.2	~8.5	~**34.7***				
Mammut americanum								
FMNH PM 3945	93	13.9	11.3	48	116.4	16.7	8.9	~43
FMNH PM 26267	85.5	12.7	11.9	45	—	—	—	—
FMNH PM 26632					≫80[g]	~12.8	~8	~33.8
FMNH PM 39404	>80[h]	14.3	11.5	38.5	—	—	—	—
FMNH P 12828					103	17.6	8.6	46.3
Ceratotherium simum								
C. s. cottoni FMNH 29174	**47.7**	7.77	6.85	**22.97**	54.2	7.74	5.38	**20.61**
C. s. simum FMNH 125413	**48.6**	8.33	6.31	**23**	53.6	8.53	5.51	**22.05**
Diceros bicornis								
FMNH 57809	40.7	6.2	6	19.16	44.4	7.05	5.03	18.98
FMNH 60784	44.4	6.21	5.23	17.97	47.7	6.45	5.19	18.28
FMNH 127848	**46.9**	7.05	6.17	**20.77**	49.1	7.75	5	**20.03**
FMNH 127849	43.9	6.33	5.35	18.35	48	6.61	5.14	18.46
FMNH 127851	>**45.4**	5.8	5.68	18.03	47.7	6.42	4.96	17.88

TABLE 18. *Continued.*

Horizon/specimen	Humerus				Femur			
	Length	Max. diam.	Min. diam.	Min. circum.	Length	Max. diam.	Min. diam.	Min. circum.
Rhinoceros unicornis								
FMNH 57639	**50.6**	7.64	7.47	**23.73**	57	8.45	5.82	**22.42**
FMNH 57822	**49.5**	7.29	5.81	**20.58**	54.6	8.17	5.48	**21.44**
Hippopotamus amphibius								
FMNH 22367	**45.9**	6.33	5.25	18.19	49.1	6.41	6.18	19.78
FMNH 127870	40.6	6.96	5.41	19.43	44.4	6.36	6.05	19.48
FMNH 127871	41.6	7.6	5.51	**20.59**	47	7.6	6.44	**22.05**

Note: Comparable length and minimum circumference measurements are shown in **boldface** type.
* An exceptional feature in which *E. c.* compares with elephants.
[a] From Daniels' Lombardi area in Sec. 27, T16N, R95W, N side of Shallow Creek, Salazar Butte Quadrangle.
[b] Crushed.
[c] Flynn's specimen.
[d] Composite skeleton on exhibit, I could find no number on humerus or femur.
[e] Without epiphyses.
[f] Lacks head.
[g] Lacks distal epiphysis.
[h] Lacks head and trochanter.

TABLE 19. Head-Body length measures of mounted specimens (m).*

Specimen	HBL (M)
USNM 16662	3.205†
AMNH 1692	3.110†
Average	3.158
UFH (mounted cast)‡	3.550
Overall average	**3.288**

* It is my considered opinion that the limb bone data are sufficient for my purpose here. Although I would have liked to get HBL for the full suite, that would have been difficult, and I did not make the attempt. However, since apparently Damuth and I are the only ones to have those measurements for any uintatheres, I give these data here.

† Data from Damuth (pers. commun.).

‡ Measured with the help of S. Bilby and A. H. Hamblin.

Field Museum of Natural History
1400 South Lake Shore Drive
Chicago, Illinois 60605-2496
Telephone: (312) 665-7055